

# Early Developments of an Intervertebral Disc Model Using Bovine Coccygeal Discs

Bernice Jim

Doctor of Philosophy

Department of Biomedical Engineering  
Orthopaedic Research Laboratory, Department of Surgery

McGill University

Montreal, Quebec, Canada

June 2012

A thesis submitted to the Faculty of Graduate Studies and Research in partial fulfillment of the requirements of the degree of Doctor of Philosophy

Copyright © Bernice Jim, 2012

## DEDICATION

To my wonderful loving family.

## ABSTRACT

**Early developments of an intervertebral disc model using bovine coccygeal discs.**

Degeneration of the lumbar disc, which frequently leads to low back pain, is an age related disease that often diminishes a patient's quality of life. Despite the continued efforts of research in this area, biological understanding of the disease remains unclear. The treatment strategies are few, with the gold standard being fusion of the motion segment, which permanently prevents any motion at the treated level of the spine. Although there are several new treatments available that attempt to recover some mechanical function of the motion segment, such as arthroplasty, they all remain unsatisfactory in doing so. The biggest challenge that researchers face in this area is the lack of tools to increase the understanding of disc degeneration etiology in order to develop better treatment strategies. The long-term goal of the research conducted in this thesis is to develop an in-vitro intervertebral disc organ culture model using bovine coccygeal discs as an experimental platform to advance disc degeneration understanding and treatment.

This thesis begins with the development of a culture environment for the in-vitro culture model and ends with early work on the biological validation of a cultured bovine coccygeal tissue model. A comprehensive introductory chapter, with information reviewing current research in the area, is included to help readers to familiarize themselves with the topic. This is followed by a description, in technical terms, of the in-vitro organ culture system that was developed and its validation and application

towards the development of the organ culture. To follow is the largest contribution, presentation of a new harvest method to isolate intervertebral disc tissue for culturing. The results of the investigation provide insight on the nutritional and mechanical aspects of the disc preserved in an in-vitro organ culture. Experimental studies are developed and analysis methods are considered, determining the best method to validate an in-vitro organ culture model. Preliminary investigations to establish culturing up to two weeks is presented, as well as the beginnings of an induced injury model.

The early works in the development of a bovine in-vitro organ culture model that is presented in this thesis research will hopefully mark the beginning of a useful tool to further understand intervertebral disc degeneration and more importantly become a platform to develop and test new treatment strategies. The text aims to provide a reference source for researchers, orthopaedic surgeons, and orthopaedic manufacturers, stimulating further advances in disc degeneration understanding and treatment.



## ABRÉGÉ

### **Debuts d'un modèle de culture d'organe appliqué au disque inter-vertébral avec tissu coccygien bovin.**

La dégénération des disques lombaires, qui conduit fréquemment à la lombalgie, est une affection liée au vieillissement qui diminue souvent la qualité de vie du patient. Malgré une recherche continue dans ce domaine, la compréhension biologique de cette maladie demeure limitée. Il existe peu de stratégies de traitement, la référence dans ce domaine étant la fusion d'un segment articulaire, qui empêche tout mouvement du niveau traité de la colonne vertébrale de manière permanente. Bien qu'il existe quelques nouveaux traitements qui permettent de récupérer une partie des fonctions, telle que l'arthroplastie, ceux-ci n'ont mené à rien de concluant. Le plus gros challenge que les chercheurs affrontent dans ce domaine est le manque d'outils qui augmenteraient la compréhension de l'étiologie de la dégénération du disque, ceci afin de développer de meilleures stratégies de traitement. Le but à long terme de la recherche conduite dans cette thèse est de développer un modèle in vitro de culture de disque utilisant des disques bovins coccygien comme plateforme expérimentale pour améliorer la compréhension et le traitement de la dégénération de disque.

Cette thèse commence avec le développement d'un environnement de culture pour le modèle in vitro et se termine avec une validation biologique du tissu coccygien bovin cultivé. Un chapitre d'introduction passant en revue les informations concernant la recherche actuelle dans ce domaine aidera les lecteurs à se familiariser avec ce domaine. Ce chapitre est suivi d'une description, en termes techniques, du

système de culture in vitro qui été développé, sa validation et son application pour le développement de la culture d'organe. S'ensuit une investigation des différentes méthodes de récolte proposées et évaluées pour isoler le tissu de disque intervertébral utilisé pour la culture. Les résultats de cette investigation apportent des informations sur les aspects mécaniques et nutritionnels d'un disque préservé dans une culture d'organe in vitro. Des études expérimentales sont développées et des méthodes d'analyses sont considérées, afin de déterminer la meilleure méthode pour valider le modèle de culture d'organes in vitro. Une investigation préliminaire examinant les effets de la simulation mécaniques dans une expérience de culture de deux semaines et validant les conditions de culture est présentée ainsi que les débuts d'un modèle avec lésions.

Le modèle bovin de culture d'organe in vitro présenté dans cette recherche de thèse marque les débuts d'un outil utile pour mieux comprendre la dégénération du disque intervertébral et avant tout pour développer et tester des nouvelles stratégies de traitement. Le texte apportera une source de référence pour les chercheurs, les chirurgies et les entreprises orthopédiques, et encouragera des avancées dans le traitement et la compréhension de la dégénération du disque.

## ACKNOWLEDGEMENTS

I was very lucky to receive the assistance of many people during the course of this thesis and it would be impossible to list them all. I am particularly indebted to my supervisor, Thomas Steffen, who gave me many opportunities to enrich my knowledge in both the theoretical and application foundation of my research. I am infinitely grateful for his mentorship, which helped shape this final thesis.

I am very proud to be part of the Orthopaedic Research Lab, whose members (importantly, Naomi Jackson, Scott McGrail and Demetri Giannitsios) created a warm and stimulating place to conduct research. In particular, I would like to thank Lorne Beckman who shared with me his wisdom in experimental research. Without his guidance, the development of the in-vitro organ culture environment would have been impossible.

For technical assistance I am indebted to Ophelie Arlet and Sarina Thoeni and I would also like to thank Ladina Ettinger and Janet Moir who both spent countless hours introducing me to the world of cell culturing and biochemistry.

For their expert advice during the course of this research, I would like to thank Peter Roughley, Mauro Alini, Stephen Ferguson and Lisbet Haglund, who joined our lab in 2007. They have been pivotal in broadening my understanding of disc research.

This research was conducted primarily at the Orthopaedic Research Lab, McGill University, Montreal, Canada and in part at the former MEM Research Institute, Bern, Switzerland.

## CONTRIBUTION OF AUTHORS

All of the research presented in the thesis for chapters 3 to 6 was planned, executed and analysed by the candidate with guidance from Prof. T. Steffen. For the published manuscript introduced in chapter 7, “Development of an intact intervertebral disc organ culture system in which degeneration can be induced as a prelude to studying repair potential,” the candidate is listed as first author because the tissue-injury model that is introduced is based on the work presented in chapters 3 to 6. Prof. T. Steffen is listed as second author in recognition of his contributions to all aspects of this study and as the thesis supervisor. J. Moir is listed as third author due to her involvement with the experimental work and data analysis. Prof. P. Roughley is listed as the fourth author along with Prof. L. Haglund as the final author because of their major contributions to the development of the injury and repair model, which included establishing the experimental protocol and conducting the analysis of the results.

## ORIGINAL CONTRIBUTIONS

Chapter 3 presents a customised bioreactor that was built on user specifications to culture intervertebral disc organs. The bioreactor was designed to be modular to culture bovine to human disc organs. Furthermore the system was cost optimised to allow for scalability.

Chapter 4 introduces a novel harvest method to isolate bovine coccygeal discs which led to the development of a self-confined organ disc model. This method allows for the largest disc organ to be cultured successfully for two weeks.

Chapter 5 offers a method to isolate tissue for analysis that maintains the full sagittal profile of the disc organ to be examined. With this isolation method, spatial correlation of live/dead images can be conducted.

Chapter 7 proposes a degeneration/regeneration disc organ culture model. The feasibility of disc organ culture is confirmed. Furthermore, the proof-of-concept of a degeneration/regeneration is established.

## TABLE OF CONTENTS

DEDICATION . . . . .	ii
ABSTRACT . . . . .	iii
ABRÉGÉ . . . . .	v
ACKNOWLEDGEMENTS . . . . .	vii
CONTRIBUTION OF AUTHORS . . . . .	viii
ORIGINAL CONTRIBUTIONS . . . . .	ix
LIST OF TABLES . . . . .	xiv
LIST OF FIGURES . . . . .	xv
1 Introduction . . . . .	1
2 Background . . . . .	6
2.1 The Intervertebral Disc . . . . .	6
2.2 Disc Degeneration . . . . .	12
2.3 Diagnosis and Treatment . . . . .	17
2.4 Intervertebral Disc Models . . . . .	26
2.5 Tables and Figures . . . . .	30
3 Design of a Bioreactor System to Culture Intervertebral Disc Tissue . . .	42
3.1 Strategy . . . . .	44
3.2 Embodiment . . . . .	46
3.3 Verification . . . . .	49
3.4 Validation . . . . .	51
3.5 Discussion . . . . .	54
3.6 Summary . . . . .	55
3.7 Tables and Figures . . . . .	56

4	Harvesting Method Development . . . . .	71
4.1	Tissue Source . . . . .	71
4.2	Endplate Preparation Methods . . . . .	71
4.3	Bony Endplate Harvesting Method . . . . .	73
4.4	Cartilaginous Endplate Harvesting Method . . . . .	73
4.5	No-Endplate Harvesting Method . . . . .	74
4.6	Sample Preparation . . . . .	74
4.7	Mechanical Stability . . . . .	75
4.8	Solute Transport . . . . .	80
4.9	Swelling Analysis . . . . .	82
4.10	Discussion . . . . .	82
4.11	Conclusion . . . . .	85
4.12	Tables and Figures . . . . .	86
5	Short-Term Organ Culture . . . . .	92
5.1	Disc Preparation and Culture . . . . .	93
5.2	Viability . . . . .	93
5.3	Cell Proliferation . . . . .	95
5.4	Glycosaminoglycans and DNA . . . . .	96
5.5	Discussion . . . . .	99
5.6	Summary . . . . .	103
5.7	Tables and Figures . . . . .	103
6	Mechanical Stimulation for Long-Term Culture . . . . .	107
6.1	Preliminary Studies . . . . .	108
6.2	Methods and Materials . . . . .	108
6.3	Mechanical Loading . . . . .	109
6.4	Preparation of Disc Tissue for Analysis . . . . .	109
6.5	Tissue Viability . . . . .	110
6.6	Protein Analysis . . . . .	110
6.7	Glycoaminoglycans Analysis . . . . .	112
6.8	Histological Evaluation . . . . .	112
6.9	Statistical Analysis . . . . .	113
6.10	Results . . . . .	113
6.11	Discussion . . . . .	116
6.12	Summary . . . . .	124
6.13	Tables and Figures . . . . .	124

7	Development of an intact intervertebral disc organ culture system in which degeneration can be induced as a prelude to studying repair potential . . . . .	139
7.1	Abstract . . . . .	140
7.2	Introduction . . . . .	141
7.3	Materials and methods . . . . .	144
7.4	Results . . . . .	149
7.5	Discussion . . . . .	153
7.6	Acknowledgments . . . . .	157
7.7	Conflict of interest . . . . .	157
7.8	Figures . . . . .	157
8	Discussion and Concluding Remarks . . . . .	168
8.1	Bioreactor Design . . . . .	168
8.2	Harvest Methods . . . . .	169
8.3	First Steps to an In-vitro Organ Culture . . . . .	171
8.4	One Application of the New Harvest Method . . . . .	175
8.5	Clinical Significance . . . . .	176
8.6	Future Work . . . . .	177
8.7	Epilogue . . . . .	179
9	Conclusion . . . . .	180
9.1	Summary . . . . .	180
9.2	Future Work . . . . .	183
A	Bioreactor: Labview Code and Bill of Materials . . . . .	185
A.1	Labview Code . . . . .	185
A.2	Bill of Materials . . . . .	193
B	MATLAB Routines . . . . .	194
B.1	Routine 1 . . . . .	196
B.2	Routine 2 . . . . .	198
B.3	Routine 3 . . . . .	199
B.4	Routine 4 . . . . .	200
B.5	Routine 5 . . . . .	204
B.6	Routine 6 . . . . .	205



B.7	Routine 7 . . . . .	208
C	Preliminary Experiments for Long-Term Culture . . . . .	212
C.1	Preliminary Studies . . . . .	213
C.2	Tissue Preparation . . . . .	213
C.3	Mechanical Stimulation . . . . .	214
C.4	Measurement of Cell Viability . . . . .	215
C.5	Discussion . . . . .	216
C.6	Summary . . . . .	217
References	. . . . .	218

## LIST OF TABLES

<u>Table</u>		<u>page</u>
3-1	Design and functional requirements of the organ culture system . . . .	58
4-1	Calculated variables based on fit of mechanical data . . . . .	89
5-1	Measured values comparing BEP and CEP harvesting method . . . . .	104
6-1	Block randomized assignment of discs for each loading condition and control . . . . .	125
6-2	Summary of quantified data . . . . .	125

## LIST OF FIGURES

<u>Figure</u>	<u>page</u>
2-1 Schematic view of the spinal segment and the intervertebral disc . . .	31
2-2 Example of a change in collagen fibre bundle angle orientation . . . .	32
2-3 Schematic of the interface between the collagen fibres . . . . .	32
2-4 Vascularization and enervation, adapted from [178]. . . . .	33
2-5 NP cells and surrounding extracellular matrix, adapted from [164]. . .	34
2-6 Typical stress profiles for healthy and degenerated disc . . . . .	35
2-7 MRI schematic view of the routes supplying nutrients . . . . .	36
2-8 Schematic view of the physical environment of disc nucleus cells . . .	37
2-9 Pfirrmann algorithm of different grades I-V . . . . .	38
2-10 Thompson grading scale . . . . .	39
2-11 Disease progression; current and future treatments . . . . .	39
2-12 Relative sizes of discs in different species . . . . .	40
2-13 Median range of motion (ROM) . . . . .	41
3-1 Initial design constraints sketch for the bioreactor . . . . .	56
3-2 Schematic diagram of the bioreactor . . . . .	59
3-3 Cross section view of the culture chamber . . . . .	60
3-4 Bioreactor chamber in loading frame in the incubator . . . . .	61
3-5 Electrical schematic diagram of the organ culture system . . . . .	62
3-6 Screen shot of bioreactor program . . . . .	63

3-7	Mechanical validation of the bioreactor system . . . . .	64
3-8	Validation of the linear variable displacement transducer . . . . .	65
3-9	Diagram of the bioreactor force control transfer function model . . . .	66
3-10	Magnitude plot of the system . . . . .	67
3-11	Phase plot of the system . . . . .	68
3-12	$R^2$ values of load input versus output of the organ culture system . .	69
3-13	Experimental set up for the wet test . . . . .	70
4-1	Harvest methods shown on bovine coccygeal tail radiography . . . . .	86
4-2	Example of experimental data . . . . .	87
4-3	Example of experimental compressive creep consolidated data . . . . .	88
4-4	Measured diffusion of $^{35}\text{S}$ into the discs . . . . .	90
4-5	Swelling analysis of discs prepared with CEP and NEP . . . . .	91
5-1	Sample images showing live/dead cell viability for BEP and CEP methods . . . . .	105
5-2	DNA content of the bovine coccygeal IVDs; tissue weight . . . . .	106
5-3	DNA content of the bovine coccygeal IVDs; dry weight . . . . .	106
6-1	Sample image of dynamically loaded bioreactor chambers . . . . .	126
6-2	Sample images of disc specimen preparation for biological analysis . .	127
6-3	Schematic diagram of CHAD and FM at molecular level . . . . .	128
6-4	Schematic of the isolation of intervertebral disc tissue . . . . .	129
6-5	Sample plot for cell viability quantification . . . . .	130
6-6	Sample stacked image obtained from confocal microscopy. . . . .	131
6-7	AF cell viability staining representative areas of discs . . . . .	132
6-8	NP cell viability staining representative areas of discs . . . . .	133

6-9	Quantified cell viability determined using CLSM . . . . .	134
6-10	Western blot analysis for the presence of FM and CHAD levels . . . .	135
6-11	GAG content of annulus and nucleus tissue . . . . .	136
6-12	Histological staining examples of the AF tissue . . . . .	137
6-13	Histological staining examples of the NP tissue . . . . .	138
7-1	Appearance of the IVDs isolated by three different methods . . . . .	158
7-2	Comparison of swelling capacity and deformation of CEP and NEP isolated discs . . . . .	159
7-3	Cell survival in the NP of BEP and NEP isolated discs . . . . .	160
7-4	Cell survival in the NP of CEP isolated discs . . . . .	161
7-5	Glycosaminoglycan content in CEP discs with or without trypsin treatment . . . . .	162
7-6	Hematoxylin-Safranin O-fast green stained disc sections . . . . .	163
7-7	Cell viability in trypsin and buffer injected CEP discs . . . . .	164
7-8	Cell viability in trypsin and buffer injected CEP discs . . . . .	165
7-9	ECM and proteoglycan degradation caused by a single trypsin injection	166
7-10	Proteoglycan synthesis in trypsin and buffer-injected CEP discs following TGF $\beta$ injection . . . . .	167
B-1	Illustration of polynomial fit on data set to interpolate y0 for y shift .	205
B-2	Figure generated by routine with cross-hair function to select and de-select data point outliers. . . . .	209
B-3	Data fit of one creep cycle with fitted variables tau, delta0 and Deltat returned with figure plot. . . . .	210
B-4	Plot of fit variables . . . . .	211
B-5	Variable output in MATLAB workspace . . . . .	211

## **CHAPTER 1**

### **Introduction**

Degeneration of the lumbar disc, which is frequently indicated by low back pain, is an age related disease that often diminishes a patient's quality of life. Despite the efforts of ongoing research in this area, the biology of the disease remains poorly understood. Treatment strategies are few, with the gold standard still being a fusion, which permanently prevents any motion at the treated level of the spine. Although alternative treatments, such as arthroplasty, which attempt to recover some of the mechanics, have increased in popularity, a recent review comparing arthroplasty and fusion have found the overall success of arthroplasty to be very small [36].

The intervertebral discs, which separate the vertebrae, function as both shock absorbers and springs, providing flexibility to the spine and head. The discs in the spine are demarcated by the longitudinal ligaments and the cartilaginous endplates of the vertebrae [70]. Most of the nutrition to the disc is through the cartilaginous endplates, which may become compromised with age from bony endplate calcification [153]. With no vasculature in the disc, the nutrients and waste products are required to diffuse over large distances [42, 126]. This slow process of nutrient and waste exchange is believed to be a contributing factor leading to disc degeneration [21, 69].

The intervertebral disc itself can be divided into two distinct zones: the outer, fibrous annulus fibrosus and the inner gel-like nucleus pulposus [72]. The annulus fibrosus is rich in collagen and its fibres are arranged in concentric lamellae forming

the outer ring of the disc. The nucleus pulposus, enclosed in this ring, has collagen fibres which are arranged in a more random fashion, entrapping highly anionic proteoglycan aggregates which provide swelling properties, allowing the disc to resist compression [217]. It is currently thought that the degradation of the extracellular matrix of the intervertebral disc has a detrimental effect on disc function. The accumulation and slow removal of extracellular matrix degradation products further exacerbates this phenomenon [188]. However, the rate at which extracellular degradation occurs may vary between individuals and this may be the reason that accelerated disc degeneration occurs in some compared to others.

The continued effort to both understand the disease and develop better treatment strategies relates to the ongoing work in developing different models, ultimately to derive better treatment strategies and approaches to preventative care. Using different models to gain better understanding and to reduce experimental cost has always played a critical role in human research.

Animal studies have been useful in studying disc degeneration [5]. Large animal models, such as ovine and porcine, have long been accepted as suitable models for studying disc structure, geometry, biochemistry and biomechanics [24, 28, 32, 94, 136, 233]. Small animal models, such as rabbits, rats and mice, have been useful to answer metabolic questions [37, 59, 77, 117, 122, 194, 230]. While large animals have a disc structure similar to the human, they undergo degeneration slowly and are expensive to use. In contrast, small animals are relatively cheap and undergo degenerative changes rapidly, but their disc structure is different to the human, particularly in the maintenance of notochordal cells within the nucleus pulposus

throughout life [73, 74]. An organ culture model using discs from larger animals is a seemingly attractive approach, allowing for the entire disc to be studied in an environment under strict controlled conditions [16]. Furthermore, in-vitro models allow for controlled biomechanical, bioelectrical or biochemical stimulation while measuring its effect at the cellular or tissue level. Understanding the relationship between mechanobiology, disc composition and metabolism is crucial in order to first understand the underlying cause of disc degeneration and secondly to be able to study how possible it is to regenerate the degenerate disc [199, 200].

When developing an in-vitro model, the design of the system is critical. The system relies on replicating an in-vivo environment, in order for the model to sustain cell viability for the term of culture. Not only is developing such a model a complex undertaking, the methods to analyze the results must also be developed in conjunction. Finally accurate interpretation of the results derived by a model is essential. Regardless of the model, whether animal or human, whether in-vivo or in-vitro, limitations are inevitable, therefore awareness of which results are transferable and those that are not should be clearly recognized.

The work that will be presented in this thesis was conducted between 2003 and 2007. The decision made at each step was based on the knowledge and understanding of the field at the time. Several groups endeavoured to develop a large sized intervertebral disc organ culture model with the same intention, to develop better tools to further the understanding of the intervertebral disc. At the onset of the organ culture development, only small tissue models, with a diameter of less than approximately 15 mm, were successfully cultured for more than two weeks [48, 59, 115].



The limitation to culturing larger sized discs was attributed to insufficient nutrition supply, progressive calcification of the cartilaginous endplates, and the post-mortem formation of blood clots blocking the transendplate nutrition path. Although some of these models systemically treated the animals with anticoagulant prior to slaughter to overcome blood clotting and promote nutrient supply [48], it still did not overcome the nutritional barrier. Some groups removed bone and cartilage endplates to maintain transport of nutrients to the centre of the disc [105, 106]. Although by using this method disc nutrition was maximized, it was at the expense of sacrificing disc integrity since all naturally confining collagen fibres that connected the disc to its adjacent endplate were severed.

There was a natural goal to develop an organ culture system that would eliminate the endplate barrier while still maintaining disc integrity. Early culture attempts with bovine coccygeal discs using static and diurnal loading were only marginally successful and suggested that a system capable of dynamic loading would improve the nutrition transport by mimicking a more physiological loading environment [115]. Since 2007 not only was the work, which was begun in this thesis, continued and successful in producing a dynamic loadable intervertebral disc organ culture model, several other groups were equally successful in this endeavour [81, 93, 106]. The following thesis presents the early work in the development of an intervertebral disc organ culture model using bovine coccygeal discs. During the development of this model the largest efforts were made in three areas:

1. Establishing the culture environment
2. Deriving the optimal tissue harvesting method

### 3. Establishing protocols to validate the organ culture

The thesis will begin with a discussion on the current understanding of the intervertebral disc and the clinical problem that is driving the need for better tools such as organ culture models to understand and treat the disease. Furthermore, the chapter will cover current and past models used for studying intervertebral disc tissue, their purpose and limitations. The main body will be separated into three sections addressing the different efforts made in the development of the organ culture model. Firstly the development of the physical culturing environment, the bioreactor, will be discussed, followed by evaluating the optimal tissue harvesting method, and finally the preliminary endeavours to culture intervertebral disc tissue will be presented. In the discussion, the findings from each development area will be summarized; furthermore, the state of the model development as well the remaining work left to be done will be addressed. The conclusion will bring to the table the major contributions of this thesis work as they relate to the clinical issues that motivated the research.

## **CHAPTER 2**

### **Background**

#### **2.1 The Intervertebral Disc**

The human intervertebral disc is a complex tissue. Its structure can neither be seen as homogeneous, nor be seen as static. It has the stiffness to connect the adjacent vertebral bodies so that the continuous load transfer for the spinal column is provided while providing sufficient elasticity to allow for spine mobility in flexion/extension, side-bending and rotation. Disc tissue connecting vertebral bodies contributes to 25 to 30 % of the human spine. The spine can be separated into four distinct regions: the cervical, the thoracic, the lumbar and the sacral. There are six discs in the cervical spine, twelve in the thoracic and six in the lumbar spine. In the lumbar region, discs are approximately 7 to 10 mm thick and measure 4 cm in diameter [184, 213]. Structurally, the disc can be separated into three distinct parts (Figure 2-1): the nucleus pulposus (NP), the annulus fibrosus (AF), and the cartilaginous endplates (CEP) [222]. Each disc is attached to the adjacent vertebrae with AF fibres and the CEP.

##### **2.1.1 Development**

The vertebral column develops in the fourth week of an embryo. The disc, even in these early stages, develops in an environment of few blood vessels. The spinal column originates from the central notochord and surrounding mesenchyme [72, 180, 216]. The NP is formed by the notochord, whereas the lamellae of the AF are formed

from mesenchymal tissue. The demarcation between NP and AF is distinctive, both in structure and composition. The NP is composed of notochordal cells and proteoglycan, whereas the AF is composed of fibroblast-like cells and collagen. Above and below these embryonic discs, mesenchymal cells form bone and cartilaginous endplates. Notochordal cells in the nucleus begin to disappear after birth and are gradually replaced with chondrocyte-like cells of mesenchymal origin. At age ten, notochordal cells have completely disappeared for humans; however, this is not true for all other species [22, 229]. This aspect plays an important role when using animal models to study disc degeneration. Notochordal cells have been identified as playing a role in disc regeneration and do not exist in adult human discs [188]. When using the disc of animals which still have notochordal cells in the nucleus, such as rabbit and fetal calf, the results from these studies, depending on the research question, may not correctly reflect the behaviour in mature human discs since the composition of the model disc is no longer the same. In the presence of new chondrocyte-like cells, the NP becomes firmer, due to collagen fibril accumulation [188]. The inner AF increases in proteoglycan content and the distinctiveness between AF and NP becomes less pronounced.

The disc with adjacent vertebral bodies and associated ligaments constitutes a motion segment. The motion segment is a fundamental unit, particularly in biomechanical experimental studies of the disc. Longitudinal ligaments can be found in both the front and the back of vertebral bodies. The anterior longitudinal ligament is attached firmly to the periosteum of the vertebral bodies, but is loose over the

intervertebral discs [180]. The posterior longitudinal ligament, on the other hand, is firmly attached to the IVDs.

### 2.1.2 Composition

The nucleus pulposus, located in the centre of the disc tissue, is composed of randomly oriented collagen fibrils, embedded in an abundant interfibrillar matrix rich in proteoglycan [188]. It is the anionic proteoglycan aggrecan in this matrix which establishes the swelling properties that are important for resistance to compression [217]. The gel has a low cell density of chondrocyte-like cells of approximately  $4 \times 10^6$  cells/cm<sup>3</sup> at maturity [188].

The annulus is composed of approximately 15 to 25 concentric rings of lamellae. The collagen fibres within each lamella are parallel with a reported 60-degree orientation to the vertical axis [164, 188] with the orientation alternating from lamella to lamella, forming a cross-woven reinforced structure [71]. This is however a generalization; detailed study of the annulus fibrosus structure found that fibre bundle orientations can vary within a layer by as much as 35 degrees, with bundles being curved as shown in Figure 2-2 [125]. Moreover, at the posterior location, the fibre bundles of the peripheral layers can be nearly vertical with an angle as high as 70 degrees and at locations where the laminae is interrupted, the fibres can be inclined at any angle between 0 and 90 degrees.

More recent work has confirmed a localized interconnectivity existing between lamellae. By using a technique of oblique sectioning and thin slice micromechanical destruction, bridging elements within the compartmental divisions of the lamellae which were anchored back into the collagenous array of the adjacent lamellae could

be shown [160]. An immunologic staining study by Yu found a presence of elastin in these bridging elements for both human and bovine discs, which was suggested to give the AF the ability to return to its initial form after bending, flexion or extension movement [244, 245]. A later study by Melrose identified collagen I and IV in these bridging fibres [137]. This is further supported by microscopic studies, showing that the bridging fibres exhibit a crimp which is inherent with collagen [195]. Furthermore, a more intricate and complex structure was found; not only did the fibres show localized branching between lamellae, a radial bridging network which both branched and weaved across the disc wall was also found [195]. Based on the data found in this study, the strength and stiffness of the bridging system was attributed to the collagen component with the elastin functioning to aid the restoration of collagen fibre crimp at low stresses.

There are two types of cells in the adult intervertebral disc. The cells in the outer region of the AF are described as fibroblast-like, elongated, thin and in parallel to the collagen fibres [162]. The cells in the inner AF and nucleus are more oval and are characterized as chondrocyte-like, being rounded and enclosed in a capsule [181]. The fibroblast-like annular cells synthesize mostly collagen type I. Synthesis is believed to be a response to deformation. The chondrocytes-like cells synthesize mostly proteoglycans and fine collagen type II fibrils. The latter synthesis is believed to be a response to hydrostatic load [199, 223]. Some cells in both AF and NP have cytoplasmic projections with lengths that can be larger than 30  $\mu\text{m}$  [20, 39]. These kinds of cells has not been found in articular cartilage. The function of these

projections is unknown but there is a suggestion that they may be sensors and communicators of mechanical strain within the tissue [39].

The cartilaginous endplates are composed of thin (usually less than 1 mm), hyaline cartilage (Figure 2-3 — showing close-up of cartilage and nutrient transport routes [164]) and act as an interface between the disc and the adjacent vertebral bodies [164, 182]. Collagen fibres in the cartilage run in both parallel and perpendicular directions to the vertebral bodies, with fibres extending into the disc tissue [184].

The disc is the largest avascular tissue of the body. In a healthy mature disc, there are few, if any, blood vessels and only a few nerves, which appear only in the outer lamellae (Figure 2-4 [178]). The mechanical function of the disc is made possible by the composition and structure of the extracellular matrix. The macromolecular components making up the extracellular matrix, collagen fibre, elastin and aggrecan, control its mechanical responses. The collagen network is composed of type I and type II collagen fibrils, making up 70 % of the AF and 20 % of the NP dry weight [41]. It functions to provide the disc with tensile and shear strength and to anchor disc tissue to bone (Figure 2-5 of collagen and aggrecan [164]). Aggrecan is the most prominent proteoglycan of the disc, and is responsible for rehydrating tissue using osmotic pressure created by the anionic charge chondroitin and keratan sulfate chains [91, 215]. The combined proteoglycan and water contents of the nucleus are 95 % (15 % and 80 %, respectively, of its wet weight). In the annulus the contents are 75 % of wet weight (5 % and 70 %, respectively).

### 2.1.3 Function

The extracellular matrix has three major functions: (1) to provide structural support, tensile strength and elasticity to the tissues; (2) to provide a substrate for the cells to adhere and migrate and (3) to regulate cellular differentiation and metabolism [17, 166].

The intervertebral disc allows the spine to be mobile. With an intervertebral disc positioned between two vertebrae, it allows the spine to move. The ability of the disc to provide this mobility is attributed to its unique structure. The gel-like NP develops a hydrostatic pressure and is contained by the strong lamellae of the annulus. The loads are distributed uniformly through the disc and also transmitted evenly to the adjacent inferior vertebrae, as illustrated in Figure 2–6 [43].

In their physiological environment, the cells of the IVD are continuously subjected to a complex array of physical stimuli: compressive, tensile and shear stresses and strains, fluid flows, hydrostatic and osmotic pressures and electrokinetic effects. This is the combined effect of body weight and muscular activity. The extracellular matrix in the nucleus pulposus of the disc is affected with each cycle of load and unload. Under load, the matrix and cells deform, hydrostatic pressure is increased and fluid is expressed. All these changes are dependent on the magnitude and duration of the load. This hydrostatic pressure is considerable, at 0.1 to 0.12 MPa in a relaxed lying down position, but can reach pressures up to 2.3 MPa for heavy lifting [237]. In 1984 there was a suggestion that the cells of the annulus fibrosus, under normal loading conditions, could behave similarly to bone according to Wolff’s law, the applied stress affects the cellular activity causing the disc to remodel and rebuild



the extracellular matrix to reduce the stress [19]. Although Wolff’s law was originally used to describe cancellous bone behaviour, Brickley-Parsons suggested that there is no a priori reason why the same mechanical principles cannot be applied to structural tissues such as the annulus fibrosus, whose major function is also of mechanical nature. However, when the load is abnormal, such as exposure to heavy machinery or vibrations, it has been suggested to lead to disc degeneration. The responses of the cells to these biophysical stimuli can vary greatly, dependent on their anatomic region and cell origin [118, 219].

## **2.2 Disc Degeneration**

Defining disc degeneration has been a controversial issue. There is no standard definition of disc degeneration because the phenomenon is not well understood. In 2006 Adams and Roughley proposed the following definition [1]: ‘The process of disc degeneration is an aberrant, cell-mediated response to progressive structural failure. A degenerate disc is one with structural failure combined with accelerated or advanced signs of aging. Early degenerative changes should refer to accelerated age-related changes in a structurally intact disc. Degenerative disc disease should be applied to a degenerate disc that is also painful.’ Fundamentally disc degeneration is a natural process of aging, a lifelong degradation as with all other parts of the human body. Constant remodelling of the discs and neighbouring vertebrae include adapting of the tissue structure to physical loading and responses to injury. There is a general consensus that there is not a single factor that can be attributed to the complex process but that there are rather many exogenous and endogenous factors, each contributing individually to the progress of degenerative changes in the disc.

These factors however can be divided into three main groups: mechanical load, genetic predisposition and nutritional effects [158].

Early epidemiological studies have attributed disc degeneration to insults and injuries, related to physical abnormal loading. For many decades, back problems were seen as the result of work-related injuries. It was believed that these injuries initiated a pathway for disc degeneration to develop and ultimately resulted in clinical symptoms and back pain [8]. On the other hand, intense physical exercise does not appear to be damaging to discs and has actually been shown to promote proteoglycans synthesis [163]. Recent work suggests that the influence of genetics plays a more important role in disc pathology than previously anticipated.

Hereditary factors can influence not only size and shape of the spinal structure, but also the regulation of biological processes, such as the breakdown and synthesis of the biochemical components [1]. The above mechanisms, combined with external environment contributions such as heavy loading or obesity, may be the reason for accelerated degenerative changes in some individuals.

### **2.2.1 Nutrition Deficit**

In 1970 Nachemson suggested that the primary cause of disc degeneration is limited nutrient supply to the disc cells [146]. However in 2004 Urban stated that there is only strong evidence that a fall in nutrient supply is associated with disc degeneration but whether it is the cause is not proven [223]. The intervertebral disc is the largest avascular tissue in the body. Inadequate nutrition to its centre, the nucleus pulposus, has long been tied to disc degeneration. In the adult disc the blood vessels extend at most to the outmost layers of the annulus. Cells located in the outer

annulus receive nutrients from these peripheral blood vessels. But nutrients from this source do not reach the rest of the disc, the nucleus and the inner annulus, which depend upon longer paths for their supply of nutrients and removal of metabolic wastes.

The essential nutrients for matrix production such as oxygen, glucose, amino acids and sulphate can only be supplied to the disc through the endplates. Metabolite transport relies solely on diffusion for smaller molecules, and convection (bulk fluid flow) for larger molecules [42, 223]. The transport route is shown in Figure 2–7 [223]. For nutrients such as oxygen and glucose which are required for energy metabolism, or for amino-acids which are required as building blocks for protein synthesis, the principle means of transport is by diffusion from the capillaries, across the cartilaginous end plate, and through the dense disc matrix ultimately to the cells. Nutrients must travel through dense fibrous tissue to the cells that potentially are located at the centre of the disc, up to 8 mm away from the nearest blood vessel and up to 5 mm away from the vertebral endplate.

Due to the low oxygen tension in the nucleus, anaerobic metabolism is prevalent and results in a high concentration of lactic acid and a low pH (Figure 2–8 [219]). Studies have shown that continuous lack of oxygen only diminishes nucleus cell activity, whereas continuous lack of glucose can eventually kill nucleus cells [69]. This underlines the critical influence of metabolic transport on both nucleus pulposus cell density and activity.

The disc also has a limited ability to recover from any mechanical or metabolic injury. Unfortunately, as the disc degenerates, even with natural aging, endplate

permeability decreases and as a result disc metabolite transport also decreases. The limitation of nutrients to be available to the disc is attributed to this problem. Interestingly in the presence of disc degeneration and following endplate damage, metabolite transport increases [165]. Based on the complex link of proper cell function to adequate nutrition to the innermost cells of the disc it is not difficult to support the idea that disc degeneration is triggered by a fall in nutrient supply.

### **2.2.2 Biochemical Changes**

There are several biochemical changes that mark disc degeneration. The most significant biochemical factor to occur in disc degeneration is the increased fragmentation of proteoglycans leading to an overall decrease in proteoglycan and water especially in the nucleus pulposus [1]. However the loss of proteoglycans is a slow process, due to the entrapment of the nucleus by the fibrous annulus and cartilage endplates of the vertebrae [222] and because of its large geometrical size and structure [188]. Although fragmented, these non-aggregated proteoglycans still continue to function similarly to intact aggregated proteoglycan [1]. When the non-aggregated proteoglycan fragments are finally removed from the disc, the overall anionic charge which is created by the glycosaminoglycan chains is reduced, thereby affecting the disc's ability to maintain the osmotic pressure of the disc matrix [164]. This in turn leads to a more rapid loss of disc height and fluid under axial load, changing the load distribution across the disc.

A less obvious change than the loss of proteoglycans is the loss of collagen fibres. Although the total amount of collagen remains approximately the same, the type and distribution of collagens present in the extracellular matrix can be altered.

Furthermore, collagen type II, a fibrillar collagen, becomes more denatured from increased enzymatic activity present during disc degeneration [11, 67]. Although fibronectin increases in degenerated tissue, it becomes more fragmented [154]. Collagen populations similarly become increasingly fragmented. This increased fragmentation strongly suggests that enzymatic activity is contributing to degenerative disc disorder. Enzymes such as cathepsins, MMPs and aggrecanases all are capable of breaking down matrix molecules of the disc.

Changes observed in cell morphology are not specific to disc degeneration. Most frequently reported changes such as the decrease in cell density or increase in necrotic cells are observed in the both degenerated and aged nucleus pulposus and are not specifically linked to disc degeneration [16]. Some animal models have shown that disc degeneration may be associated with a decline in cell density; however these were short studies. In humans this process occurs over a long time, therefore it is difficult to directly implicate these findings to the human disc [68, 117].

There are other findings that suggest that human intervertebral disc cell density has a more cyclic rather than linear variation over the whole degenerative course [21, 224]. Loss of cell density in the nucleus pulposus is correlated with the onset of disc degeneration [21, 224]. But after this initial decrease in cell population, the disc shows a recovery and gradual increase in cell density. This cell density decrease is found however to occur in the inner annulus fibrosus [84, 126]. Moreover there are other studies that confirm a higher cell density for severely degenerated, discs in both the nucleus and the inner annulus fibrosus than for less degenerated, discs [60].

Many investigations have noted an increase of cell proliferation of chondrocytic cells in clusters adjacent to tissue clefts and tears [16, 151, 193]. These clusters of cells have also been found to increase with age in human lumbar discs and have been looked upon as an indicator of disc degeneration. In-vitro studies have shown that the increased proliferation of the disc cells is related to elevation of serum and deprivation of glucose [53, 211, 246]. Despite the overall lack of nutrition for the disc, the structural degradation of the tissue forms clefts and tears, which host focal points for increased nutrient supply. Neovascularization within the disc, which also occurs as a result of degeneration, also becomes sites of increase proliferation [13, 99, 135].

Despite the increased proliferation of cells, cell senescence is also another symptom of disc degeneration. Cells isolated from degenerative discs, when cultured in-vitro, exhibit a lower proliferating potential than cells isolated from non-degenerated discs [112]. Another important finding is the increased number of other cell types and tissue found in the degenerated disc tissue that includes nerve fibres, Schwann cells, endothelial cells and fibroblasts. Their occurrence is attributed to the increased vasculature, which permits these other cells to migrate into the disc [16, 90].

## **2.3 Diagnosis and Treatment**

### **2.3.1 Disc Grading**

Diagnostically, there are many different methods for grading disc degeneration. In 2006 a study of lumbar disc degeneration grading found twenty-two different grading systems! The study recommended four preferred scales, each for a different type of imaging media: Thompson et al. for macroscopic anatomy [210], Boos et al. for histology [16], Lane et al. for plain radiography [110] and Pfirrmann et al.

for magnetic resonance imaging [100, 161]. For patient diagnosis, with recent and continuing improvements in imaging techniques, magnetic resonance imaging (MRI) has become the most important method for the clinical assessment of intervertebral disc pathology. The algorithm of Pfirrmann is illustrated in Figure 2–9 [161]. However, to visualize the progression of disc degeneration, the Thompson grading scheme (Figure 2–10) is a better tool. Recently Wilke et al. established a new grading system that was suggested to be even more comprehensive for radiography. It is a grade 0 (no degeneration) to 3 (severe degeneration) system using postero-anterior and lateral radiographs [240]. The new grading system attempted to gain a more objective observership on the degree of degeneration for both cervical and lumbar disc degeneration.

### **2.3.2 Pain Occurrence**

Degeneration of the disc does not necessarily correlate with actual pain [86, 227]. On the other hand, degenerative spinal segments are found in almost all patients that suffer from severe back and leg pain [202]. The pain can be from various sources. Motion beyond physiologic constraints, which causes compression or stretching of neural elements, can be a pain source. Abnormal deformation of ligaments, joint capsules, annular fibres or vertebral endplates can also be a source, since nociceptors can be found in these areas. Lastly, in-growth of nerves and blood vessels into degenerated annulus fibrosus sometimes even penetrating the nucleus pulposus, can be a pain source.

Back and leg pain is a frequent reason for physician consultation. Since pain is also influenced by psychosocial factors, treatment decisions are multifactorial, complex and crucial for the outcome. The initial treatment course of action is pain management without resorting to surgery, such as rehabilitation exercises. For most individuals pain management produces acceptable relief, but for a few, back pain remains intrusive and imposes unacceptable functional restrictions. Surgery then becomes the next course of action.

### **2.3.3 Current Surgical Treatment Strategies**

Traditionally the gold standard is fusion of the affected spinal segment. Spinal fusion was first used in the early 1900's to treat spinal infection; it was later extended to treat fractures and tumours and then to correct spinal deformity. The purpose for fusion is to eliminate pain, restore segmental stability, and sometimes, spinal alignment. The degenerated disc is removed and replaced with a metal cage or polymer spacer (Figure 2–11). In most cases, harvested autologous bone from the pelvis is used to fill the spacer. The constructs implanted are temporary until natural in-growth of bone is achieved. Using spinal fusion for degenerative disc disease has become established only by default, in the absence of other viable alternatives. It is expensive and a major surgical procedure that requires a several day hospital stay. Furthermore, complication rates are quite high with considerable morbidity. Recovery for the patient can be lengthy.

The largest concern for fusion is the alteration of spine mechanics. With rigid fusion, stress is transferred to the adjacent segments, that has a high likelihood to cause degeneration in the adjacent discs [40, 51]. Furthermore, approximately 20 % of



patients require revision surgery within two years and the number increases to 37 % a decade after successful lumbar fusion [50]. Given the complications and risks it is not surprising that various non-rigid stabilisation techniques, such as arthroplasty, dynamic stabilization, inter-spinous spacers and others have been developed.

Arthroplasty, also known as total disc replacement, is the replacement of a degenerated disc by a prosthetic device. Artificial discs are marketed by companies as a revolutionary new treatment option that relieves pain, preserves motion at the operated level and protects against degeneration at the adjacent levels. In 2007, over one hundred different disc prostheses were marketed [169]. Amongst the 100, the Charité III and the ProDisc are implanted most [101]. Both implants are designed with low friction sliding surfaces with metal endplates and a polyethylene core. The prostheses are fit into the prepared disc space between the vertebral bodies with fixation to the adjacent vertebra improved by teeth or fins.

Arthroplasty was first performed in 1988 [23]. Despite the long existence of such devices, today there still remains a lack of clinical investigations demonstrating the advantage of these implants over segmental fusion or even over non-surgical care. Concerns are voiced over the high complication rates, especially vascular complications during revision surgery. A study performed on a collective of patients that underwent Charité lumbar disc replacements concluded that only 57 % were successful [139]. Therefore, fusion is still recognized as the standard treatment, particularly for full medical reimbursement, despite the high surgical failure rate, because alternative treatment strategies such as disc prostheses have not proved to be more effective, but are definitely more costly [45]. Other treatment options such as nucleus

pulposus replacements and dynamic stabilization constructs, which are screw-based interspinous devices [18, 33, 150, 225, 241], may potentially prevent adjacent disc disease, but to date there are no long-term clinical outcomes documenting the benefits of these devices.

Future disc treatment options are aiming to be more biological, minimally invasive and at an earlier stage of degeneration. Figure 2–11 illustrates disc disease progression and indicates current or future the treatment strategies. The goal is to introduce biological treatments that will slow down the natural course of degeneration, stop further degeneration, or even start regenerating the disc.

#### **2.3.4 Future Treatment Solutions**

Biological treatments in the past have been more commonly used as a supplement to interbody fusions or discectomies [120]. Recent advances in molecular biology, cell biology and material science have created an emerging field of new stand-alone techniques for the treatment of musculoskeletal disorders including the disc. However, most of these emerging techniques have not reached the clinical stage. Unfortunately the unique properties of the intervertebral disc and the rapid alterations that the disc undergoes during degeneration limit the range of suitable approaches. Furthermore, the limited knowledge and often contradictory findings on disc cell biology challenge biological treatments [158].

Regenerative treatment refers to generating healthy disc tissue or functional surrogate tissue to stop or reverse disc degeneration. Most experimental studies for regenerative treatments have used animal models either in-vivo or in-vitro. Cell based therapies were first tested when an intact allogenic disc, including the vertebral

endplates, was transplanted in a dog. The surgery was unsuccessful, with the transplant rapidly degenerating [46, 98]. A later study in rhesus monkeys only showed minimal disc degeneration and partial recovery of disc height after twelve months [119]. Others cultured autogenic nucleus pulposus cells and re-implanted the cells in rats and rabbits. They could demonstrate a deceleration of degeneration when compared to a control group [149, 155]. One of these studies performed by Nomura involved first aspirating the nucleus of Japanese white rabbits to induce degeneration followed by replacement with allogenic intact or partial nucleus pulposus tissue [151]. The rabbits were examined every sixteen weeks [151]. The group found reduced degeneration in rabbits which received an entire nucleus pulposus transplant [151]. The most successful study so far was cultured allogenic canine nucleus pulposus cells injected in degenerated canine IVD [47]. The labelled cells could still be detected after six months. Disc height and proteoglycan content were both increased but complete restoration of a normal disc structure was not achieved.

The use of mesenchymal stem cells (MSC) as a regenerative treatment strategy has been successfully performed, predominantly by Sakai's group using a induced degeneration rabbit animal model where after twenty-four weeks of implant with MSC cells, 91 % of original disc height was regained [191–193, 248]. Harvesting MSC is a less invasive procedure than harvesting nucleus pulposus cells, and also may avoid allogenic rejection in animals and ultimately humans [61, 62]. MSC can be isolated from bone marrow, cultured and differentiated in-vitro into mesenchymal tissue. A study with rats using MSC showed that cells exhibited similar expression profiles to those of nucleus pulposus cells when cultured in a disc-like environment

with low oxygenation and high osmolarity [173]. Nonetheless, studies using cell-based strategies so far only were short-term and in most cases the original height of the disc was not restored. Furthermore, studies have been limited to small animals such as rats and rabbits, and it is not clear if results can be reproduced in larger animal models and for long-term.

Using bioactive factors, also commonly referred to as growth factors, is another regenerative treatment strategy. Factors such as fetal calf serum and plasma-derived equine serum were found to increase proteoglycan synthesis in-vitro up to 300 % [209]. Another growth additive is platelet-rich plasma, which has shown to increase proteoglycan and collagen type II synthesis [4, 27, 147]. Isolated growth factors in-vitro have shown proteoglycan synthesis, most significantly from fibroblast growth factor (by 300 %) and TGF-beta (by 500 %) [209]. BMP-2 injected in human disc cells (at 1500 ng/ml) were found to enhance proteoglycan synthesis by 200 % and increase gene expression of aggrecan and collagen type I and II. In degenerated disc, however, although BMP-2 increased the synthesis of proteoglycan by 560 %, increased collagen synthesis was not achieved [3]. BMP-7 compared to BMP-2 showed even more success in animal models. BMP-7 injected into a degenerated rabbit disc completely restored the initial disc height after six weeks [128, 140]. Histological analysis at twenty-four weeks showed, when compared to healthy control, increased proteoglycan content in the nucleus and annulus as well as a higher collagen content in the nucleus pulposus. Biomechanical properties, when comparing elastic moduli and viscosity, were restored after eight weeks.

The most common concern is whether cell-based or bioactive factor regenerative treatments have only a time-limited effect and are dosage dependent. Genetic strategies would be another regenerative treatment idea which could provide a permanent solution [226]. The objective would be to modify the genetic code so that cells within the IVD could (a) enhance their expression of matrix components, (b) express anabolic growth factors, (c) express inhibitory factors against catabolic enzymes or inflammatory cytokines or (d) benefit from a combination of the aforementioned. This treatment could be potentially accomplished by injecting vector-mediated genetic elements directly targeting cells in-vivo or indirectly via precursor cells such as MSC that are cultured and transduced in-vitro and then introduced in-vivo.

One of the initial studies for genetic therapy incorporated TGF-beta1 gene encoding with adenoviral vectors that was injected into the IVD. Increased levels of TGF-beta1 and proteoglycan were found which encouraged further studies [168, 235]. A later study using Sox9 (SRY (sexdetermining region Y)-box) gene encoding demonstrated increased collagen type I secretion [159]. From twelve different BMPs and Sox9 adenoviruses tested [247], BMP-4 and BMP-14 were most effective to stimulate collagen synthesis while BMP-2 and BMP-7 were the most effective to stimulate proteoglycan. Yet other studies have shown a slowdown of the matrix degradation processes by transducing gene encodings for TIMP-1, a matrix metalloproteinase inhibitor [228].

Yet another derived regenerative treatment strategy is to introduce a combination of cells embedded in carrier materials, known also as scaffolds, into the disc. In-vitro studies demonstrated that nucleus pulposus cells can proliferate and express

proteoglycans and collagen type II within a range of carrier materials such as alginate beads [104, 123], collagen sponges and gels [54], collagen type I/hyaluronan composites [6, 7] gelatin/chondroitin-6-sulfate/hyaluronan tri-copolymers [243], atelocollagen [187] and chitosan [7, 187]. There are different approaches for using scaffolds. One approach is to construct a matrix scaffold and grow in-vitro a complete IVD. Past groups which have tried this approach have only managed to accumulate only 50 % of proteoglycan and collagen compared to that of native tissue and only 15 % of the collagen content in the nucleus pulposus [141, 142].

Finally another idea is to perform a partial disc replacement with cell-loaded scaffolds. The scaffold would be either implanted surgically or injected as a gel that cures in-situ. MSC embedded in a 15 % hyaluronan gel injected into rat coccygeal discs showed proliferation, viability and a trend of increased disc height suggesting a regenerative processes took place [29]. Pure hyaluronan (without cells) injected in pig discs following a nucleotomy showed no disc degeneration at six months [170].

There are numerous different and promising regenerative techniques that have been developed, however they have only been thus far in-vitro tested and in small live animal models. These regenerative treatments however do not overcome or eliminate the common obstacles such as insufficient nutrient supply of the degenerated disc, pain mediating factors and functionally impaired donor cells which have been associated to disc degeneration. There are still many unanswered questions regarding intervertebral disc degeneration. Better tools are needed so that the trigger mechanisms of disc degeneration can be identified and better treatments can be developed. Disc organ culture systems can be a very useful tool in such cases.

## 2.4 Intervertebral Disc Models

### 2.4.1 Animal Models

Because of the difficulty in obtaining human intervertebral disc tissue for studies, animal disc models are commonly used as a tool to understand disc degeneration and to test treatment strategies. The range of animals that have been used to study disc degeneration include mouse [117], rat [77, 122], rabbit [107, 140, 155, 159, 191, 192], dog [47], pig [68, 170], sheep [48, 135] and baboon [31, 156]. Each of these models has their own advantages and disadvantages. For instance, small animal models such as rats and rabbits are inexpensive models whereas larger animal models, which exhibit closer disc morphology to human, such as primates, are extremely expensive, not to mention raise ethical questions.

Although animal models are invaluable tools to further our understanding of disc biology, the differences between species must be taken into consideration. One difference is in the cell morphology [74]. Notochordal cells that are present in the mature nucleus of mouse, rat, rabbit, dog, and pig discs are not found in the mature human nucleus [22]. On the other hand, larger animals such as cows and sheep, like humans, have notochordal cells in the nucleus at birth, but these cells diminish rapidly during growth and disappear in adulthood [74]. Notochordal cells are able to produce a large amount of hyaluronan [203] and influence the metabolism of proteoglycans by fibrochondrocytes within the NP [2, 154]. A recent study by Kim [102] found that migration of cartilaginous endplate chondrocytes was facilitated by soluble factors produced by notochordal cells in the nucleus pulposus.

Another variation between some animal and human discs is the ossification centres. The primary ossification centres generally stem from the centre of the vertebral body for mammals with a secondary ossification centre at the endplates [5]. In humans the secondary ossification centre only exists on the circumferential parts of the vertebral endplate, forming an epiphyseal ring at the outer edge of the vertebral column which fuses after the age of approximately 25 [5]. This means that the base of the cartilage endplate in humans act as the growth region for the vertebral body, whereas for most other species, including sheep and cows, the epiphyseal plate remains within the vertebral body [5].

The geometrical differences between species are also another factor to consider when using an animal model. The size and shape can influence both the biomechanics and the transport of nutrients to the cells of the disc. The size and shape differences between different animal disc models are shown in Figure 2–12. The sizes of adjacent vertebrae also vary. The ratio of annulus to nucleus, or the thickness of the cartilaginous endplate can all contribute to the cells' response and metabolism [79, 104, 167, 234]. These size and shape differences influence a variety of properties such as the biomechanical, morphological and cellular between regions within the disc itself.

Another limitation to consider with the use of animal models is the difference in load distribution in the spine. Studies have found that biomechanical differences can also play an important role in affecting degeneration and regeneration process. A more flexible lumbosacral segment could be one factor responsible for reduced proteoglycan production in the disc [208]. In humans the weight of the upper body



acts on the lumbar spine differently than that on quadrupeds. The distribution of load to the different spinal levels vary as well as range of motion as shown in Figure 2–13 [236, 239]. In smaller quadrupeds such as rabbit, mouse or rat, smaller muscle and ligament forces are required to stabilize the spine, therefore the loads on the spine are much lower than that of human. However the intradiscal pressure remains similar, due to the smaller diameter of the discs [5]. Therefore, the appropriate animal model is much dependent on the scientific question that is being asked.

There are three different types of animal models that have been developed: cadaveric [24, 28, 94], live animal [37, 77, 117, 122] and more recently in-vitro organ culture models [59, 105, 115]. Cadaveric large animals and humans have been useful as a tissue source for the understanding of the gross anatomy, histology and biomechanics of the disc. It is limited in its scope to study mechanical responses, and perhaps short-term biological responses. Obtaining fresh tissue of such species is usually expensive, if not impossible. Furthermore, maintaining viability of large disc models is an added difficulty.

Small animals have been beneficial as live animal models particularly to answer biological questions. The facilities required for small animal testing to produce a reasonable sample size are relatively low in cost when compared to using large animals. However, the limitation to such models is clear. The differences in both anatomy and tissue morphology between rats, rabbits and mice to humans are large. In Alini’s review on intervertebral disc models he pointed out that animal studies may miss the vital importance of genetics which is now believed to be responsible for up to 75 % of disc degeneration in humans [5].

### 2.4.2 Culture Models

In-vitro animal culture models have been a more economical and controlled approach to study disc degeneration and repair. Using an in-vitro model gives more control over the culture environment and avoids the high cost and ethical issues of in-vivo animal models. The models can be separated into two areas: cell cultures [243] and whole disc cultures [5]. Growing disc cells is a useful technique to study disc cells. Cells can be cultured in different environments that mimic insults or the effect of various interventions. Although the cell response is interesting from these studies, heavy caution must be used to interpret the results. In the absence of the disc matrix and the natural structure of the disc, it is only a simple model. These cells sit in a monolayer with many cells together which is very different from cells in the disc, which sit in an extracellular matrix with negligible cell contact. Support materials such as scaffolds have also been used in cell culture models; however, the environment still does not mimic the in-vivo environment correctly, and therefore caution must still be taken in result interpretation.

Most recently animal models include in-vitro whole disc organ culture models. This has become an important alternative to in-vivo studies. The entire disc is cultured under controlled in-vitro conditions to mimic in-vivo conditions. The main advantage of whole disc culture models is that cells are not removed from their highly intricate extracellular matrix, whose effect on cell behaviour is still poorly understood. Bovine coccygeal discs have been strongly suggested as the most appropriate biological model for the study of lumbar discs [32]. Anatomically they are close in size to human lumbar discs and the musculature of the bovine tail maintains

an in-vivo pressure on the disc that is similar to that of the human lumbar spine in prone position which is 0.1 to 0.3 MPa [237]. Studies have shown that cell viability and biosynthetic activity was maintained up to one week and have suggested that applied cyclic load could lead to a longer culture term [115]. More recent studies have produced a bovine culture model without mechanical loading for a culture term of three weeks [183]. However, cell viability of the tissue was never measured. A larger sized organ culture model using ovine tissue has also been successfully developed [48, 81, 93], but with this particular model the animals were systemically treated with anticoagulant prior to slaughter to overcome blood clotting and promote nutrient supply. Other models remove bone and cartilage endplates to maintain the transport of nutrients to the centre of the disc [105, 106, 157, 231]. In this method, disc nutrition is maximized, but at the expense of sacrificing disc integrity, since all naturally confining collagen fibres connecting the disc to its adjacent endplate are severed.

The development of an entire IVD organ culture of large dimensions is believed to have a high impact on future research on disc degeneration and regeneration [7, 183]. Such an organ culture will be an invaluable tool to further progress the development of biological regenerative treatments as mentioned previously. Furthermore, fewer animal experiments would be needed to perform in-vivo tests, reducing the use of live animals in research to a minimum.

## **2.5 Tables and Figures**

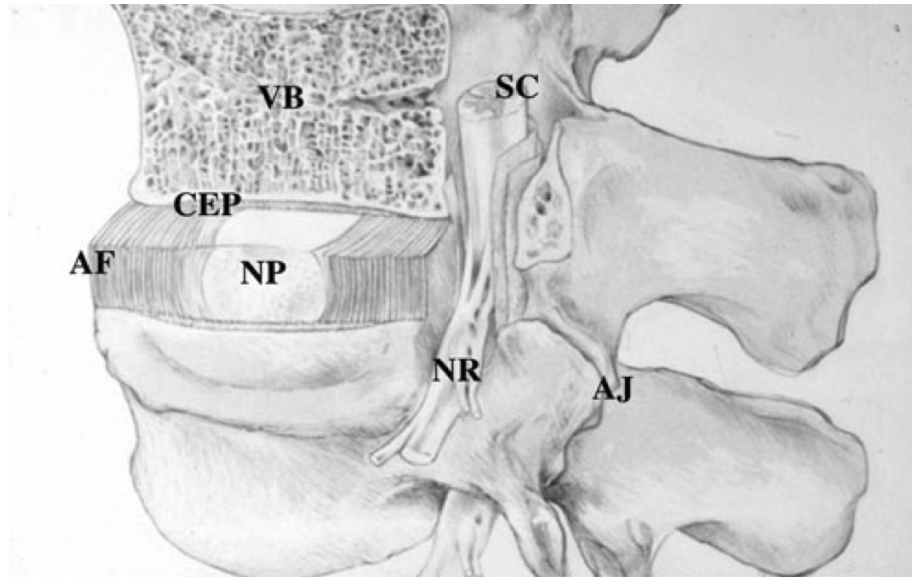


Figure 2-1: Schematic view of the spinal segment and the intervertebral disc. The figure shows the organization of the disc with the nucleus pulposus (NP) surrounded by the lamellae of the annulus fibrosus (AF) and separated from the vertebral bodies (VB) by the cartilaginous end-plate (CEP). The figure also shows the relationship between the intervertebral disc and the spinal cord (SC), the nerve root (NR), and the apophyseal joints (AJ) adapted from [216].

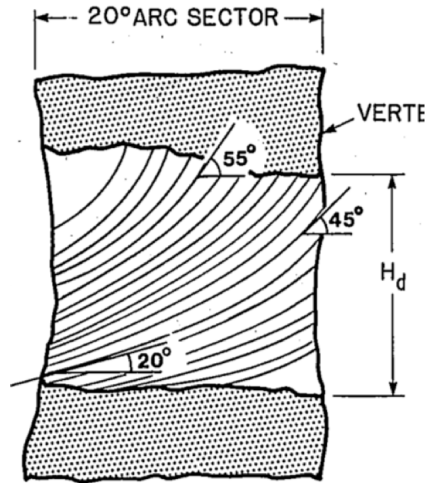


Figure 2-2: Example of a change in collagen fibre bundle angle orientation in one individual lamellae, where  $H_d$  represents the disc height. The fibre angles are not only curved but may vary as much as  $35^\circ$  adapted from [125].

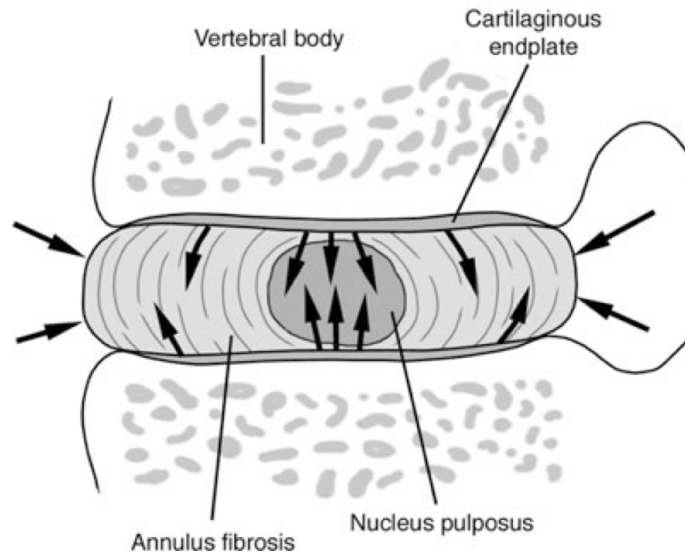
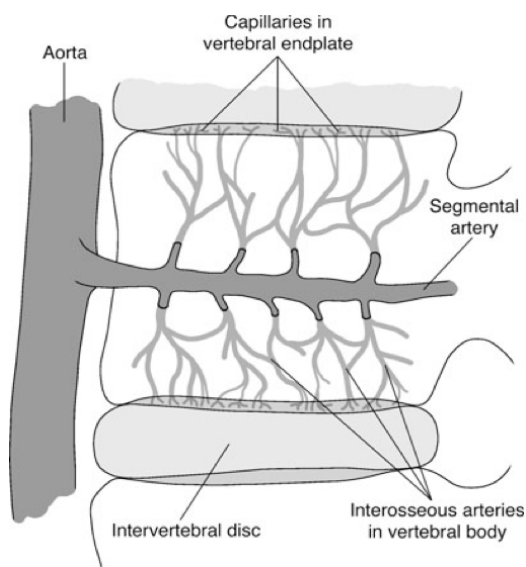
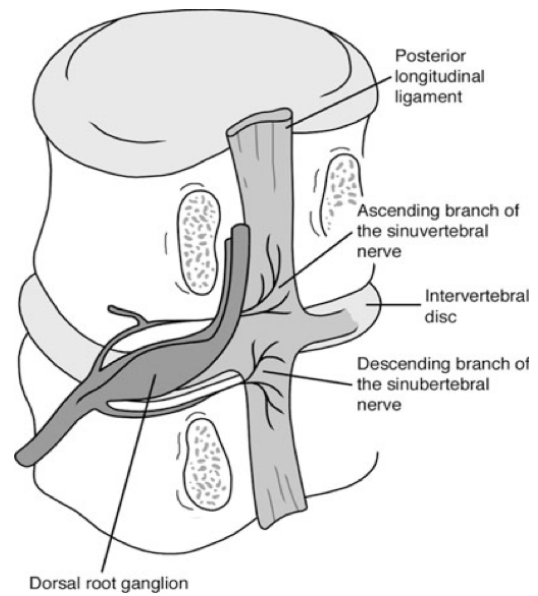


Figure 2-3: Schematic of the interface between the collagen fibres of the annulus, the nucleus, and the hyaline cartilage which is bonded to the perforated cortical bone of the vertebral body of the intervertebral disc. The arrows indicate the routes for nutrient transport from the adjacent vertebral body to the centre of the disc, adapted from [164].



(a) Vascularization



(b) Ennervation

Figure 2-4: Vascularization and ennervation, adapted from [178].

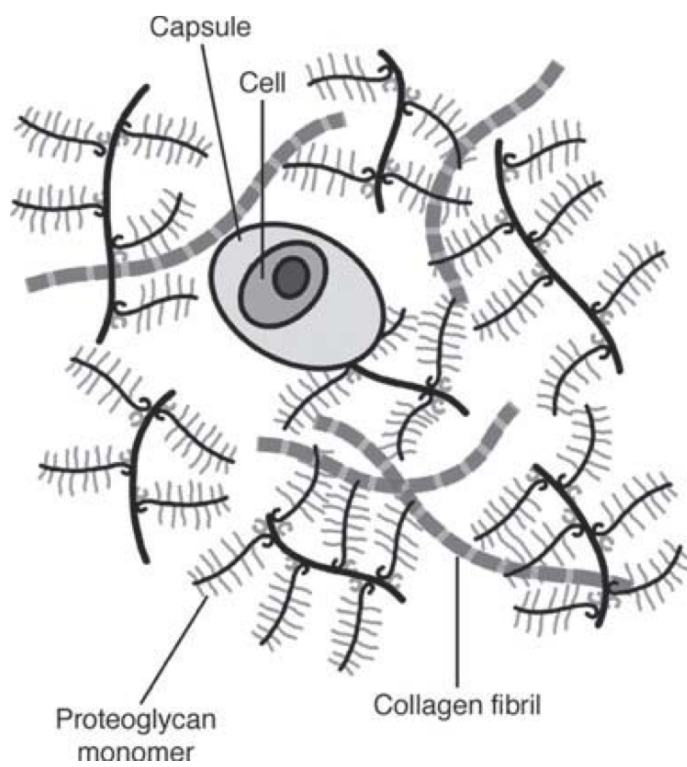


Figure 2-5: NP cells and surrounding extracellular matrix, adapted from [164].

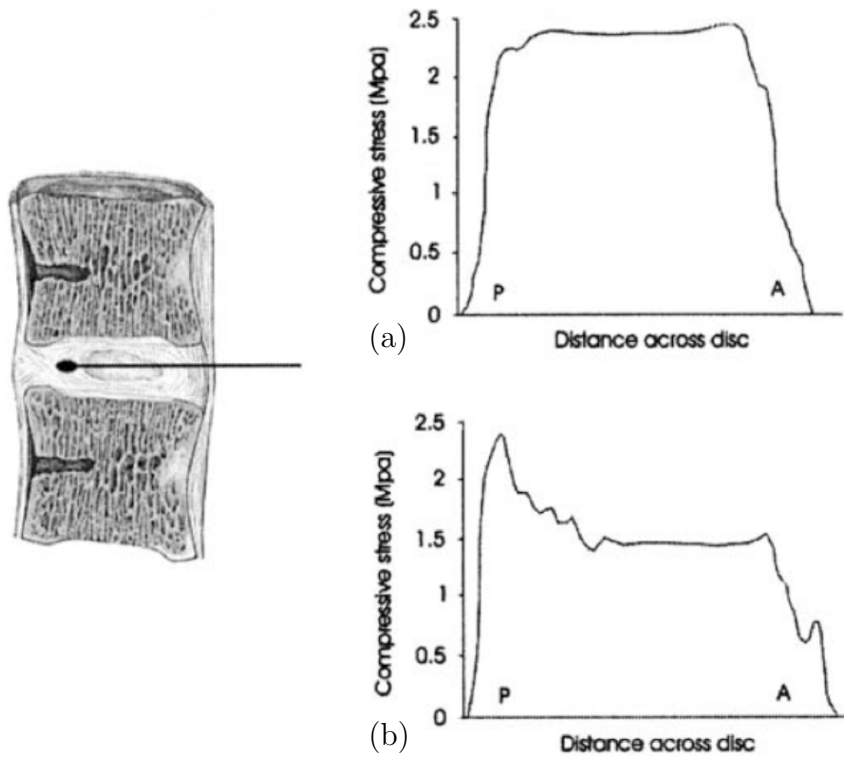


Figure 2-6: Typical stress profiles for healthy (grade-1) disc (a) and degenerated (grade-4) disc (b) adapted from [133] and featured in [43].



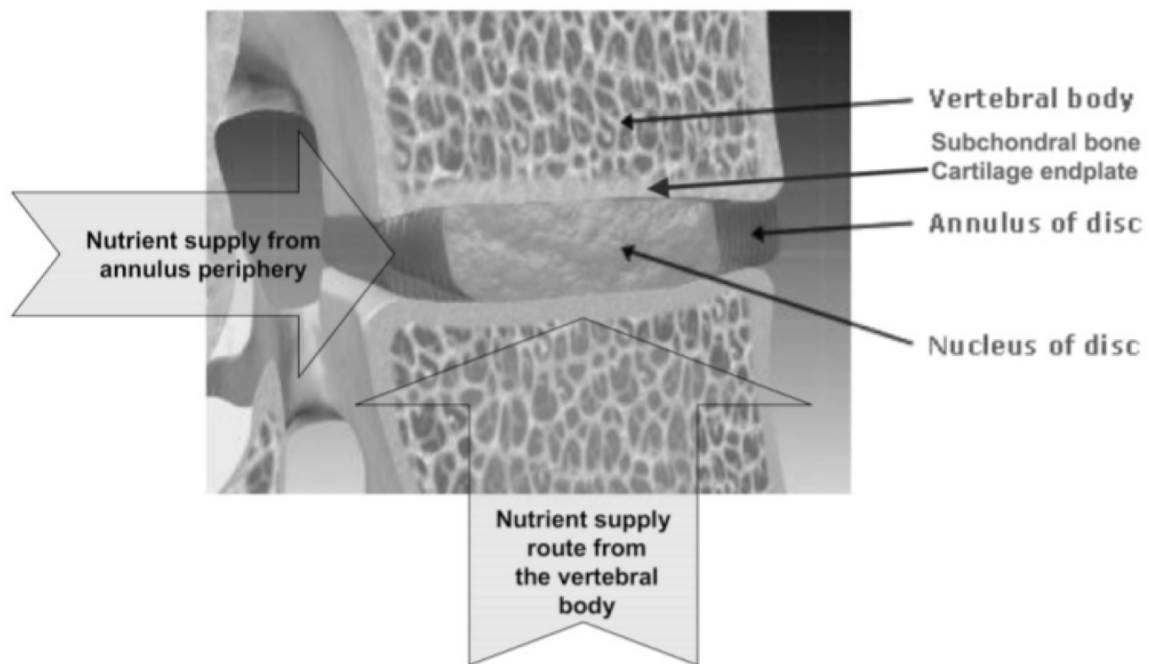


Figure 2–7: Magnetic Resonance Imaging Studies Schematic view of the routes supplying nutrients to the avascular intervertebral disc, adapted from [223].

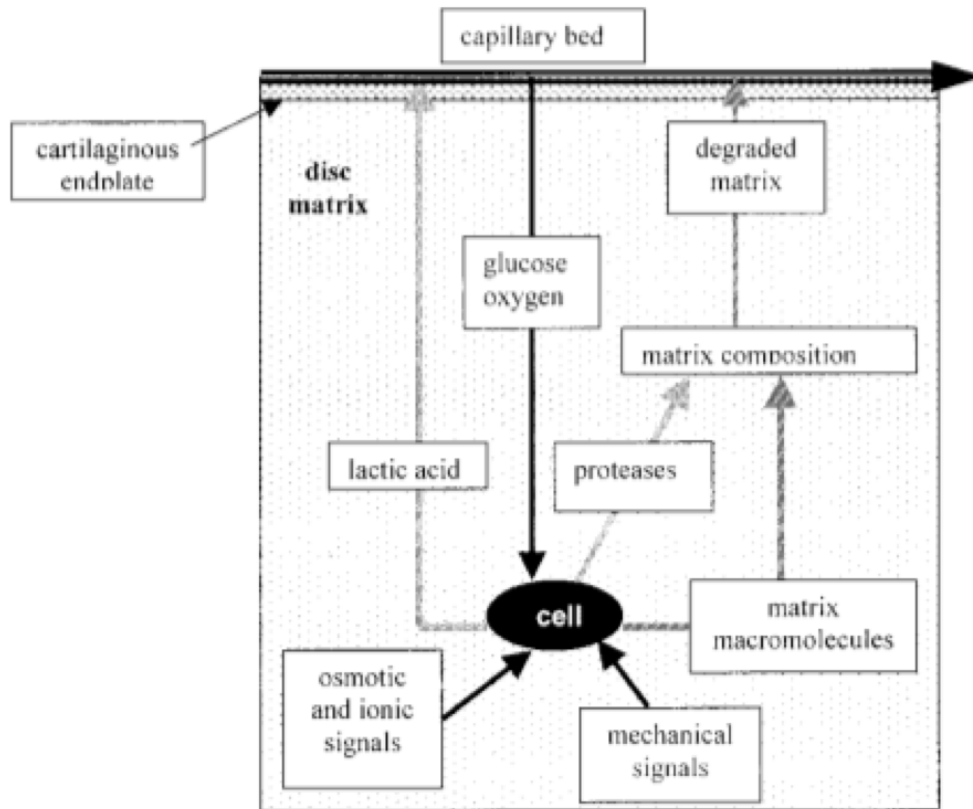


Figure 2-8: Schematic view of the physical environment of disc nucleus cells. The cells are embedded in the avascular disc matrix. Glucose and oxygen diffuse from the blood supply through the matrix to the cell; lactic acid produced by the cell diffuses back to the blood supply. The extracellular osmolarity and ionic composition depend on glycosaminoglycan content and disc hydration. Mechanical signals (pressure, deformation, fluid flow) arise with every movement. The cell integrates these signals to produce matrix macromolecules and proteases and hence determines matrix composition, adapted from [219].

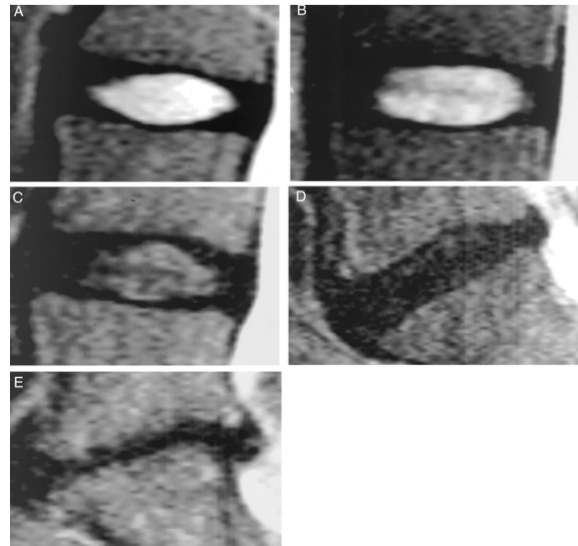
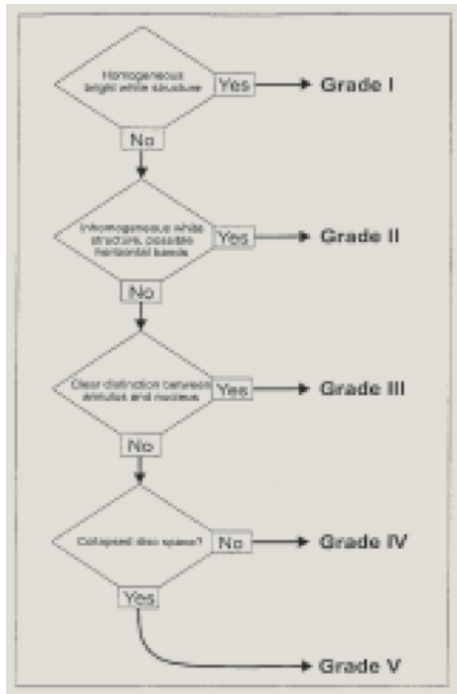


Figure 2–9: Pfirrmann algorithm of different grades I–V, adapted from [161]; a grading system for the assessment of lumbar disc degeneration. (A) Grade I: The structure of the disc is homogeneous, with a bright hyperintense white signal intensity and a normal disc height. (B) Grade II: The structure of the disc is inhomogeneous, with a hyperintense white signal. The distinction between nucleus and annulus is clear, and the disc height is normal, with or without horizontal gray bands. (C) Grade III: The structure of the disc is inhomogeneous, with an intermediate gray signal intensity. The distinction between nucleus and annulus is unclear, and the disc height is normal or slightly decreased. (D) Grade IV: The structure of the disc is inhomogeneous, with an hypointense dark gray signal intensity. The distinction between nucleus and annulus is lost, and the disc height is normal or moderately decreased. (E) Grade V: The structure of the disc is inhomogeneous, with a hypointense black signal intensity. The distinction between nucleus and annulus is lost, and the disc space is collapsed. Grading is performed on T2-weighted midsagittal (repetition time 5000 ms / echo time 130 ms) fast spin-echo images.

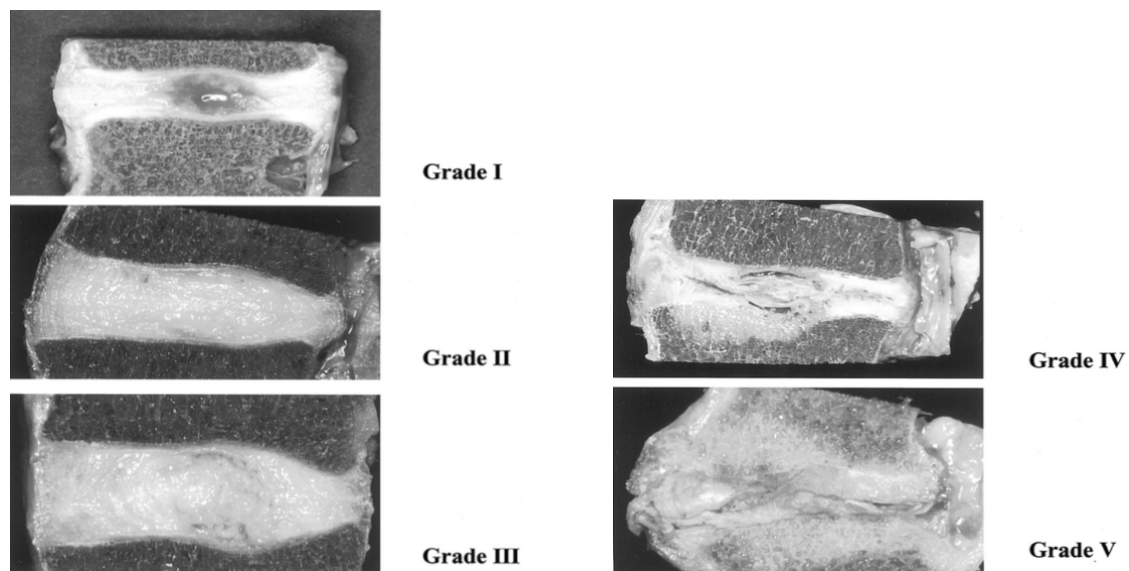


Figure 2-10: Thompson grading scale, macroscopic grading of age-related disc alterations, adapted from [210].

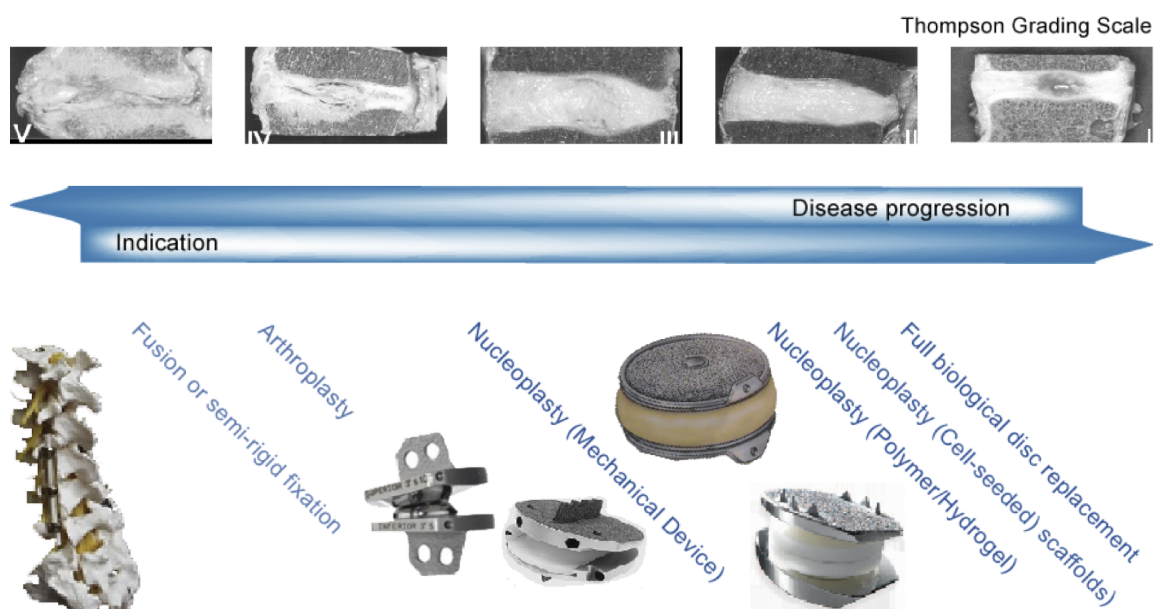


Figure 2-11: Disease progression; current and future treatments

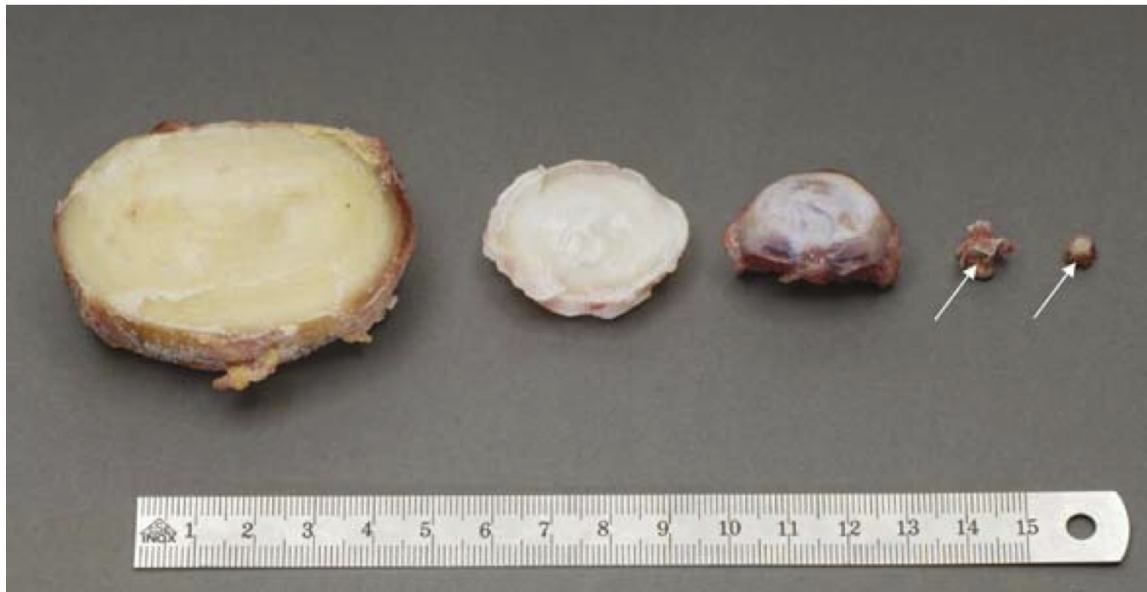


Figure 2-12: Relative sizes of discs in different species. From left to right: human lumbar, L4-L5; bovine tail, C1-C2; sheep thoracic, T11-T12; rat lumbar and tail (arrows show the intervertebral disc location), adapted from [5].

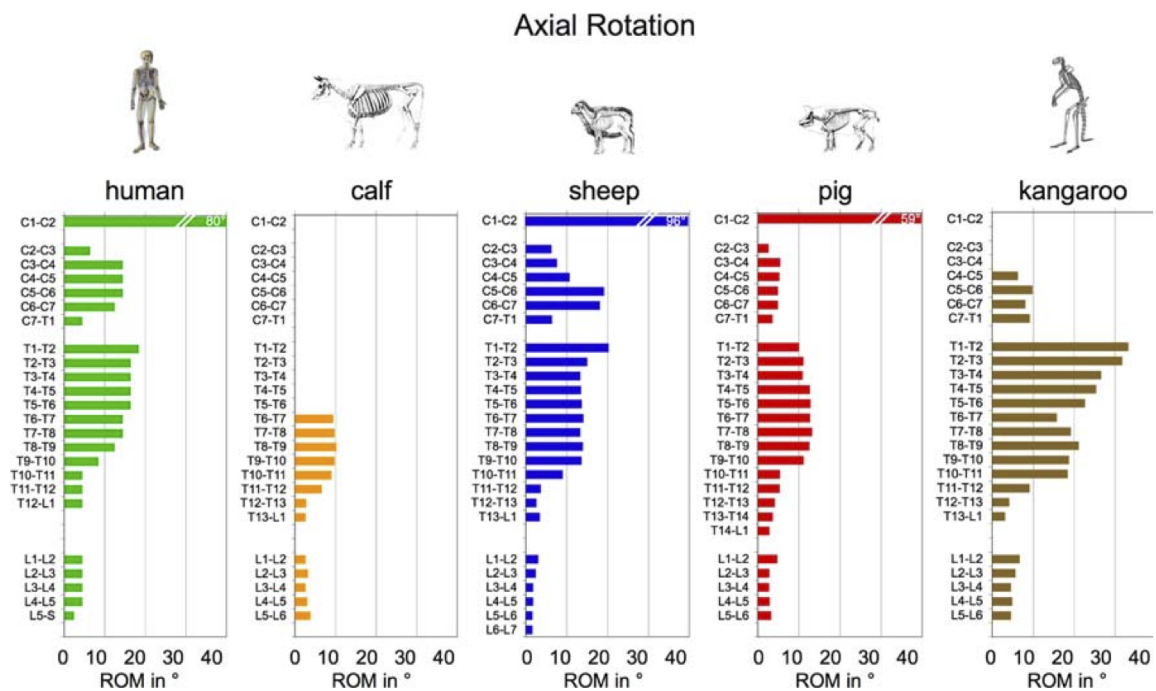


Figure 2–13: Median range of motion (ROM) in degree in left plus right axial rotation for each single segment of the calf, sheep, pig and kangaroo spine compared to the human, adapted from [236].

### CHAPTER 3

#### Design of a Bioreactor System to Culture Intervertebral Disc Tissue

Live animals, depending on the experimental set up and scientific question asked, have been accepted as good models to study disc degeneration [5]. However, controlling the biochemical and mechanical environment is extremely difficult in live animal models, and many studies involve high costs and raise ethical questions. For such reasons the development of in-vitro organ culture systems and models has received attention [10, 48, 56, 59, 81, 88, 89, 93, 105, 106, 115, 171, 174, 183, 231]. In-vitro organ culture models can be seen as a tool that will bridge the gap between cadaveric and live animal models, particularly for the study of the intervertebral disc [5]. They also may play a principal role in advancing the understanding of disc degeneration and for studying potential regenerative treatments such as growth-factors.

Our limited understanding of the intervertebral disc, the intertwined relationship between its extracellular matrix and the macroscopic environment, has made establishing an organ culture system difficult, particularly large organ disc cultures. Only one group has managed to create a successful biomechanical organ culture, allowing for dynamic loads, with a culture term of more than eight days [93]. However, this model used ovine caudal discs that are reported to have a major diameter of  $10.5 \pm 1.2$  mm and a minor diameter of  $9.5 \pm 1.2$  mm [48], which are much smaller than human lumbar discs. Furthermore, to create the model, administration of an anticoagulant to the animal, prior to slaughter was required [48]. This was done to

reduce or possibly eliminate blood clots that would develop, with this harvesting method, in the endplates which created a barrier for nutrition flow. While this procedure enhanced disc nutrition, it did not overcome the nutritional barrier imposed by the calcified cartilage endplate. Furthermore, although this procedure was possible for sheep, it would not be a financially and ethically viable possibility for larger sized animals, which have closer geometric sized discs as to that of humans, such as cows.

The human intervertebral disc is exposed to compressive (up to 2.3 MPa) loads during normal daily activities such as sitting, standing and lifting [237]. Early studies have suggested that mechanical stimulation affects in-vivo cell metabolism and gene expression in the intervertebral disc [76, 77, 83, 121, 122]. Two types of mechanical stimulation have been modeled in the past: hydrostatic on intervertebral disc cells and static diurnal compression on whole intervertebral disc organ cultures. In these studies, isolated monolayer cells found in the annulus fibrosus, chondrocytes, have shown to respond to both frequency and duration of loads [116, 130, 218]. Intervertebral disc nucleus pulposus cells have shown, however, to respond primarily to the magnitude of hydrostatic load [96, 97]. Despite these findings, the variability in culture models, method of load application and cellular phenotypes of the species have made it difficult to cross apply these results. A current study on a whole organ culture model, used a physiological load defined as static diurnal loading with eight hours at 0.2 MPa and sixteen hours at 0.6 MPa load [81]. In addition, two four-hour cycles of dynamic load were applied during the sixteen hour, high-load period at



0.2 Hz;  $\pm 0.2$  MPa to simulate high activity. This study showed that at a high frequency (10 Hz) mechanical load was detrimental to cells in a seven-day culture, but neither the loads nor the variation in nutrition stimulated changes in the extracellular matrix. Prior to this study, previous studies on whole organ disc cultures, have shown that the cells cultured in the absence of stimulation (whether an osmotic or a mechanical load) have not replicated their normal in-vivo cellular response [7].

The first step toward developing an organ culture model was to establish the culture environment, a bioreactor able to mechanically stimulate intervertebral disc tissue under long-term culture conditions. Furthermore, the bioreactor should allow for the control of culture parameters, such as the mechanical stress and strain while monitoring various properties of the disc tissue (Figure 3-1). The initial design constraints included both basic requirements such as controlled nutrition, sterility/clean ability and biocompatibility and additional requirements such as low operation cost, controlled dynamic axial loading with data recording and modularity.

### **3.1 Strategy**

The basic principle in the design of this bioreactor was to construct a small-scale mechanical testing platform so that several units could be housed in a standard laboratory incubator. Two types of controls that have commonly been used for mechanical stimulus are displacement and load control. Poroelasticity of the intervertebral disc, which implies creep, makes using displacement control difficult; therefore load control will be used. Furthermore, intervertebral disc studies are discussed in terms of pressure and force. Previous research on disc tissue has found mechanical loading in a physiological range (0.1 to 1.0 MPa for human lumbar intervertebral discs) to

have an effect at the cellular level [121]. The ability of this bioreactor platform to deliver cyclic dynamic axial load was thought to be a critical component to achieve successful culturing of the intervertebral disc. Earlier in-vitro organ cultures were limited to either using a disc which was less than 15 mm diameter in size, or culturing without dynamic cyclic loading. The present chamber design follows a similar design to one presented by Lee et al. in 2006 [115], however the method of load control and data acquisition is different.

Two distinct solutions for the efficient setup of organ culture systems have been previously employed to maintain in-vivo temperature and CO<sub>2</sub> levels. The first uses a standard mechanical loading frame, such as an MTS, and incorporates a closed, dedicated environmental chamber maintaining CO<sub>2</sub> and temperature levels. This setup limits the specimens either to be tested sequentially or concurrently with the same loading scheme. The cost to expand the system for concurrent specimen testing with different stimulation schemes is substantial. Such solutions to culture a range of different tissues are commercially available. They may cost thousands of dollars, and generally have a large foot-print because of the elaborate and proprietary mechanical actuators and environmental control components. The second approach uses low cost, small foot-print, mechanical loading units with single culture chambers housed in a single standard laboratory incubator that provides the stable CO<sub>2</sub> and temperature levels. For our system, we wanted a compact system that can be duplicated at a low cost and allows for running many concurrent experiments with different stimulation protocols.

Running multiple experiments in parallel is essential for conducting long-term culture experiments within a reasonable time. To conduct a six-week culture experiment with two different testing conditions plus a control group, with a group sample size of eight, requires three bioreactors running in parallel and continuously for one year to complete an experiment. With six systems the experimental time is reduced to six months and with twelve systems, to three months. One of the design requirements was a minimum of three culture experiments running concurrently, but otherwise fully independently (loading protocol, media, etc.) in a single incubator and for relatively low cost.

The details of the design and functional constraints for the culture system are presented in Table 3–1. Each of the design constraints was either validated or verified as listed in the table.

## **3.2 Embodiment**

The bioreactor system was designed to culture intervertebral disc tissue ranging from bovine caudal discs, with a diameter ranging from 14 to 22 mm [5] to human lumbar discs, with a diameter ranging from 30 to 50 mm [9]. The chamber and load delivery part of the bioreactor was designed using Catia and Solidworks software (Dassault Systems SA, Concord, Massachusetts). The overall schematic of the bioreactor is presented in Figure 3–2.

### **3.2.1 Culture Chamber**

The culture chamber was manufactured from polycarbonate with an inlet and outlet machined into the chamber to enable media circulation. Within the chamber, the specimen was held between two Polytetrafluoroethylene (PTFE) platforms fitted

with porous hydrophilic polyethylene platens as the contact surfaces. Fresh sterilized platens were used for every new experiment to prevent contamination or compromised fluid flow from clogged platen pores.

The PTFE platforms had six radial holes at the level of the porous plates to direct radial flow of media from the centre of the platen to the periphery (Figure 3–3). The top PTFE platform was connected to a polycarbonate piston arm in-line with an axial loading actuator. The culture chamber was closed with a sterile latex hose (Figure 3–4). All components of the culture chamber were designed with materials that would withstand steam sterilization carried out during the preparation stage of a culture experiment.

### **3.2.2 Media Circulation**

The entire disc tissue was surrounded by culture medium, the nutrition supply for the disc. New media was pumped to the porous platens in contact with the disc from both top and bottom, simulating the in-vivo nutrient supply. Side ports in the chamber allowed for fluid to continuously circulate using a peristaltic pump (Masterflex, Cole-Parmer Instrument Company, Illinois, USA) with individual cartridges (Masterflex, Cole-Parmer Instrument Company, Illinois, USA) allowing for the chambers to be easily removed for fresh media exchange. The pump connected to the system provided an adjustable flow in the range of 1.3 to 130 ml/min, which translates to a blood flow rate of 50 to 200 beats/minute. The non-toxic, non-hemolytic, silicon tubing used in media circulation is UV impermeable to protect the light sensitive media. The tubing also has a CO<sub>2</sub> gas permeability of  $1200 \times 10^{10} \text{ cm}^2 \cdot \text{s} \cdot \text{cm Hg}$

allowing the 5% CO<sub>2</sub> from the incubator to buffer media in the enclosed culture chamber.

### **3.2.3 Axial Loading and Data Collection**

An axial force was applied to the intervertebral disc during culture with an pneumatic rolling diaphragm actuator (Uni-block cylinder, 1.7 DAS, Illinois Pneumatics, IL, USA). A rolling diaphragm pneumatic actuator kept friction to a minimum. Air pressure was supplied to the rolling diaphragm actuator with a proportional pressure control valve (VP50, Norgren, USA) controlled numerically with an interfaced computer. The 100 psi supply air for the proportional valve was fitted with an in-line contaminant filter, with a pore size of 90 µm. The exhaust from the valve was directed to the outside of the incubator to not contaminate the incubator.

Piston displacement was recorded using a linear variable differential transformer (LVDT) displacement transducer (LD400-5, Omegadyne, USA) mounted to the frame of the bioreactor system. The magnetic rod of the LVDT displacement transducer rested on a polycarbonate plate attached to the piston arm. Axial displacement of the piston arm was coupled to the movement of the magnetic rod in the LVDT displacement transducer. The magnitude of the output voltage of the displacement transducer was proportional to the displacement of the magnetic rod. The magnetic rod sat freely without contacting the inner tube surface and could therefore slide without friction. The function of the displacement transducer did not require any sliding and rotating contacts and was therefore sealed from the effects of incubator environment that could affect its function. Load values were collected using a load cell (LC703-300, Omegadyne, USA) in line with the rolling diaphragm actuator and

the piston of the loading chamber. All devices were interfaced to a data acquisition board (Labjack U12, Labjack, Colorado, USA) connected to a desktop computer and controlled and monitored through a custom program written with Labview (National Instruments, Texas, USA). Details of the control program is illustrated in Appendix A. Simple electronics were used to amplify input and output signals with the use of instrument amplifiers (INA114AP, Texas Instruments, Texas, USA) as shown in Figure 3–5. The custom program was designed to allow dynamic cyclic load ranging from 0.01 to 1.0 Hz. It was also designed to deliver ramp, square wave, sinusoidal and triangle wave loading patterns. A screen shot of the user interface of the program is shown in Figure 3–6. A sample of collected data for 0.1 Hz, 0.5 Hz and 1.0 Hz with load amplitude of 1.0 MPa is shown in Figure 3–7.

### **3.3 Verification**

#### **3.3.1 Drawings**

Drawings of the organ culture chambers and axial loading interface were done in Solidworks (Dassault Systems SA, Concord, Massachusetts). The drawings were reviewed to verify lines 1–7 of the Design and Functional Requirements table presented in Table 3–1.

1. The chamber diameter has an inner diameter of 56 mm, large enough to accommodate the maximum 50 mm diameter requirement based on morphological knowledge of human lumbar intervertebral discs.
2. The top and bottom interfaces in contact with the disc have a diameter of 45 mm, which is lower than the maximum lumbar disc range stipulated as

required, but sufficient when the reported maximum lumbar disc diameter presented in Roberts study was no more than 40 mm [184].

3. A latex hose as illustrated in Figure 3–4 encloses the chamber unit. Furthermore, media change is conducted through a filtered (2  $\mu\text{m}$ ) luer connection.
4. The frame, which houses three units, has dimensions of 360 mm  $\times$  100 mm  $\times$  300 mm, which is well within the 0.25 m<sup>3</sup> volumetric limitation.
5. The culture chamber utilizes a 1/8 NPT (pipe thread) inlet and outlet to facilitate the circulation of media.
6. A 3D model interference study was conducted on the parts of the chamber with the frame to verify that all parts fit together before machining.
7. The components of the culture chamber are made of known biocompatible, cleanable and sterilizable materials: polycarbonate, polyethylene and Teflon. The mechanical strength of the materials used surpasses the load will be imposed on the organ culture.

### **3.3.2 Pump and Tubing Specifications**

An 8-roller, 12-channel peristaltic pump (Masterflex L/S 12-Channel, 8-Roller Pump Head, HV-07519-25 with Masterflex L/S Standard drive system, HV-07553-70) was selected. The specifications of the system allowed for an adjustable flow range of 1.3 to 130 ml/min volumetric rate, which surpasses the 0.3 ml/s requirement in line 10 of the Design and Functional Requirements in Table 3–1. Matching tubing and a cartridge system (Masterflex tubing cartridge, L/S 14, 07519) compatible with the system was also selected. The tubing was non-toxic, non-haemolytic silicone

with UV impermeable properties to protect the light sensitive media. It was also permeable to CO<sub>2</sub>, allowing the 5 % CO<sub>2</sub> in the incubator to buffer media.

### **3.3.3 Materials**

All materials that were used in the organ culture system were reviewed, as required in lines 13–15 of the Design and Functional requirements matrix presented in Table 3–1. All materials that were used in the organ culture chamber in contact with the tissue culture or media are of known biocompatible, cleanable and sterilizable material, polycarbonate, PTFE, polyethylene, silicon and latex. The electrical and mechanical instruments and transducers have no direct contact with the tissue culture. The remaining components, housing frame, chamber interfacing components as well as the fasteners, are not oxidative or ferromagnetic. The frame of the culture system is also fabricated from a known biocompatible material, stainless steel.

## **3.4 Validation**

### **3.4.1 Form, Fit and Function**

The form, fit and function of the system was tested first outside the incubator. The complete system as illustrated in Figure 3–2 was assembled. Saline was used as circulating media. A rubber disc of 20 mm in diameter and 15 mm in height was used as the tissue sample. The following was checked:

1. Organ culture chamber could be assembled along with the axial piston arm.  
The piston arm could interface with the axial loading arm, the linear variable displacement transducer, and the load cell.
2. The fluid circulation components were compatible with each other.



3. The computer interface could control the system and could read and record data.

4. Axial displacement could be produced.

The system could function as planned with no issues in the form and fit of all the components of the system. Measurements characterising the performance of the system were carried out to validate the system.

### **3.4.2 Displacement**

The linearity of the linear variable differential transformer was validated with feeler gauges (McMaster Carr, Cleveland OH). The feeler gauge set had 15 sizes ranging from 0.051 to 0.630 mm. The interest was to see the performance of the displacement transducer at small displacements. Each of the 15 gauges was used and the displacement of the LVDT was recorded using the organ culture system setup with data values recorded by the interface program. Tests were repeated four times. The input versus output values were plotted with an  $R^2$  value of 0.998,  $n=60$ . The plot is shown in Figure 3–8. The validation test showed that the displacement transducer could cleanly distinguish increments of 25  $\mu\text{m}$ .

### **3.4.3 Input/Output**

The performance of the system was characterized using a rubber sample with a diameter of 20 mm, height of 15 mm, and a known stiffness of 5 MPa. The organ culture system was installed into the incubator and varying sinusoidal cyclic loads (load between 0.1 MPa and 1.0 MPa and frequency between 0.1 Hz and 1.0 Hz) was loaded onto the sample. Loads and displacements of the sample were recorded. A simplistic illustration of the system transfer function is presented in Figure 3–9.

The performance of the system was quantified studying the input values versus the actual output values. First, the input magnitude for different loading frequencies was compared with the output magnitude (Figure 3–10). Then the lag of the system calculated, represented as a phase shift in degrees, was studied (Figure 3–11). Finally, the  $R^2$  value of the input versus the output, was computed (Figure 3–12).

#### **3.4.4 Wet Test**

The media delivery to the disc surface by the interfacing platens, as illustrated in Figure 3–3, was verified using a wet test. The interface bottom block along with the hydrophilic platen was placed against a glass plate with a dry paper towel sandwiched in between (Figure 3–13). Phosphate buffered saline was delivered through the inlet of the interface bottom using the peristaltic pump. This set up required the fluid to be forced through the interface against gravity, which was the worst case scenario for the organ culture chamber system set-up. Visual inspection of the paper towel wetting verified that fluid was delivered to the surface of the platen. This was repeated ten times, yielding the same result. This was a simple test to verify that fluid was reaching the surface of the platen, but it did not indicate whether fluid distribution was uniform.

#### **3.4.5 Cleanability, Sterilization and Incubation**

The cleanability and sterilizability of the system was validated with media. The full functioning culture system was installed into the incubator. The organ culture chambers and interfaces were cleaned with detergent and steam sterilized. The culture chambers were then filled with standard culture media (DMEM with 5% fetal bovine serum and  $1 \times P/S$ ) and left in the bioreactor chamber for one week

with continuous media circulation. The media was checked for contamination after the experimental period with a microscope. The same culture equipment was then cleaned and steam sterilized. The remaining parts of the organ culture system were washed with 70 % ethanol and left in the incubator. This protocol was repeated three times. No bacterial or fungal contamination was detected. The culture chambers and interfaces were inspected for cracks and fissures, and none were found. As well, there was no visible corrosion on the external components such as the loading frame, proportional valve, actuators and measurement devices.

### **3.5 Discussion**

In this chapter the development of the organ culture environment was presented. The design of the chamber bears resemblance to that presented by Lee et al. [115]. However, the components used to deliver the controlled dynamic load as well as the measuring instruments differ. The dynamic load is delivered using a 100 psi air line, which can be supplied using an air compressor. The system uses a rolling diaphragm actuator that is known for its low friction and hysteresis free performance. Furthermore, the electronics of the control system include a simple USB interface and computer graphical user interface to deliver controlled dynamic axial loading for a range of 0.1 to 1.0 MPa and 0.1 to 1.0 Hz with reasonable performance.

At load values of 0.1 MPa or smaller, the input load reading was not within the 10 % error range that was deemed acceptable. The accumulated friction force of the system could be one source of the error. A second source of the error could be the error in the load cell in correctly reading at low force values. For a cross-sectional area of 20 mm a force of approximately 31.4 N would be required to reach

0.1 MPa. The load cell in the system has a full scale performance of 1333 N, with a zeroing error of  $\pm 1\%$  and a linearity and hysteresis error of  $\pm 0.15\%$ . Therefore the accumulated error for a load of 31.4 N is approximately  $\pm 15.4$  N which is almost 50 % of the input load value. The effect of this was not as noticeable at higher loads, but more apparent at lower loads.

The biggest contributor to this error is the fact that the control system is an open loop system without a closed loop feedback to regulate the output. It is suggested that additional programming to incorporate a closed loop feedback into the system will greatly overcome the limitations of the system at these low loads and would furthermore improve the overall system performance up to 1.0 Hz. In addition, the system's performance could benefit from more accurate sensors, which would particularly benefit the system's performance at low loads; however, this would in turn increase the overall cost of the system. For instance, if the zero error of the load cell could be reduced from 1 % to 0.1 %, it may be possible to achieve better performance in low load situations. Although the actuator and other mechanical components have been selected with the goal to reduce friction as much as possible, perhaps higher accuracy components, obviously also at a higher price, may allow to further reduce friction.

### **3.6 Summary**

An in-vitro environment designed for intervertebral disc organs has been developed. The design of the culturing system entailed controlled, measured and recorded axial mechanical stimulation. The system was designed to be compact, allowing nine units to fit into a standard laboratory incubator and easily replicable, with simple

off-the-shelf components. To reduce differences in results contributed from different tissue sources and the lifetime of organ culture experiments, a total of three units were built. Validation of the system showed that the bioreactor could operate at 0.1–1.0 Hz and 0.1–1.0 MPa, which was sufficient for bovine coccygeal discs. The system did experience limitations at the low loads of 0.1 MPa and at 1.0 Hz. The difficulty to deliver low amplitude loads was most likely a limitation of the control system design which was an open loop system. At low loads, the friction in the system reduced the axial load to the specimen and could not be corrected. In short, the system would benefit from a closed loop control system to improve the performance at low loading values.

### 3.7 Tables and Figures

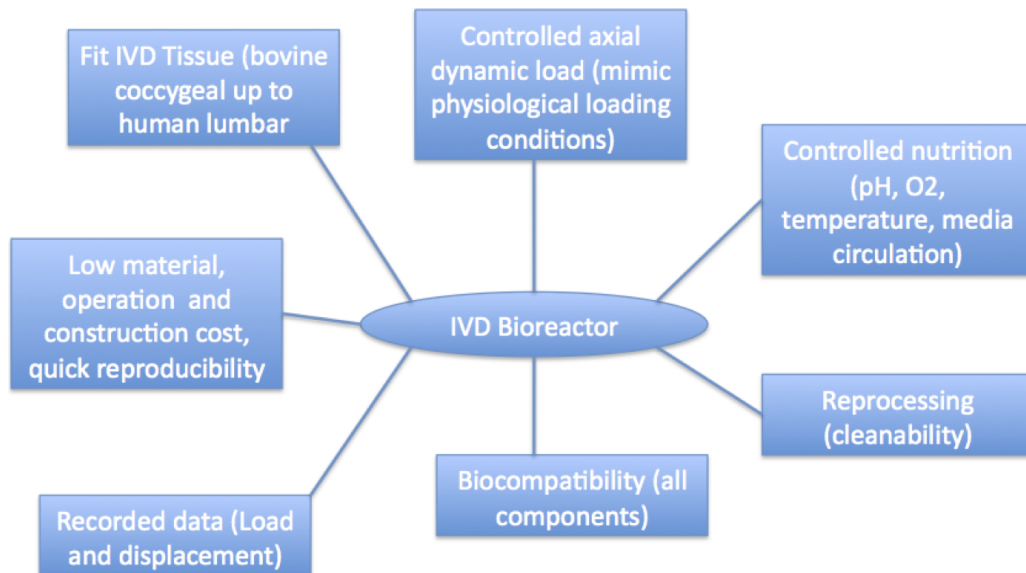


Figure 3–1: Initial design constraints sketch for the intervertebral disc organ culture bioreactor

#	Requirement	Quantification	Required?	Verification/Validation Method	Verification	Validation
<b>Design (functional properties, geometry, ergonomics, shape etc.)</b>						
1	Bioreactor chambers to house disc tissue for bovine coccygeal upto including human lumbar disc tissue	Morphological study: disc size 175 to 500 mm <sup>2</sup>	×	Drawing review	×	
2	Interface platens for disc tissue — bovine coccygeal up to and including human lumbar disc tissue	Morphological study: disc size 175 to 500 mm <sup>2</sup>	×	Drawing review	×	
3	Entire bioreactor with a minimum of 3 units to fit into incubator	Incubator interior 0.25 m <sup>3</sup>	×	Drawing review	×	
4	Enclosed bioreactor chamber to prevent contamination	Openings $\leq 2 \mu\text{m}$ to prevent bacteria infiltration	×	Drawing review	×	
5	Inlets and outlets to allow for media exchange	Standard connection to pump tubing	×	Drawing review	×	
6	Compatibility of components with each other		×	Drawing review Form/Fit/Function	×	×
<b>Mechanical/biomechanical properties</b>						
7	Mechanical strength of bioreactor chamber and pistons to accommodate loading force	Walking 0.53–0.65 MPa, Jogging 0.35–0.85 MPa and Resting 0.1–0.24 MPa [238]	×	Drawing review Incubation Test	×	×
8	Control system to deliver controlled axial load with range of 0.1–1.0 MPa and 0.001–1 Hz	Walking 0.53–0.65 MPa, Jogging 0.35–0.85 MPa and Resting 0.1–0.24 MPa [238]	×	Input/Output test		×
9	Displacement measurement difference with range 0.05–7.2 mm	Morphological study: human lumbar disc height 7.2 mm Max [108] Minimum caudal disc thickness 5 mm [5], 1 % of min disc thickness and max disc thickness	×	Displacement test		×
10	Circulation system to provide nutrition to the organ culture at disc interface $> 0.3 \text{ ml/s}$	Circulation capability of volume $> 0.3 \text{ ml/s}$ [223]	×	Pump and tubing specifications review Wet test	×	×
11	Controlled physiological environment — 5 % CO <sub>2</sub> , 37 °C, 95 % humidity	Early disc organ culturing environment [115]	×	Incubators, yearly inspection, automatically controlled	×	
12	Recorded load and displacement data	Recorded data of output load, actual load and displacement	×	Input/Output test		×

#	Requirement	Quantification	Required?	Verification/Validation Method	Verification	Validation
<b>Raw material / Biocompatibility</b>						
13	Chamber system (interface, tubing, media reservoir) must be biocompatible	Known biocompatible material to be used with all components	×	Material review	×	
14	All components of bioreactor surface must be non-oxidative to a 95 % humidity, 5 % CO <sub>2</sub> and 37 °C environment	Known non-oxidative materials to be used with all components	×	Material review Incubation test	×	×
15	Design of chamber system (interface, tubing, media reservoir) must be compatible with the media	Known biocompatible material to be used with media (DMEM with 10 % fetal bovine serum and 100 U/ml penicillin, 100 µg/ml streptomycin)	×	Material review Incubation test	×	×
<b>Hygienic reprocessing requirements (dis-/assembling, wash-/disinfecting, functional testing)</b>						
16	Bioreactor frame and components cleanable	Known materials that can be washed down with 70 % etOH	×	Material review Cleanability test	×	×
17	Chamber system (interface, tubing, media reservoir) must be sterilizable	Known steam sterilizable material to be used with all components	×	Material review Sterilization test (repeated sterilisation cycles followed by visual observation of materials)	×	×

Table 3–1: Design and functional requirements of the organ culture system

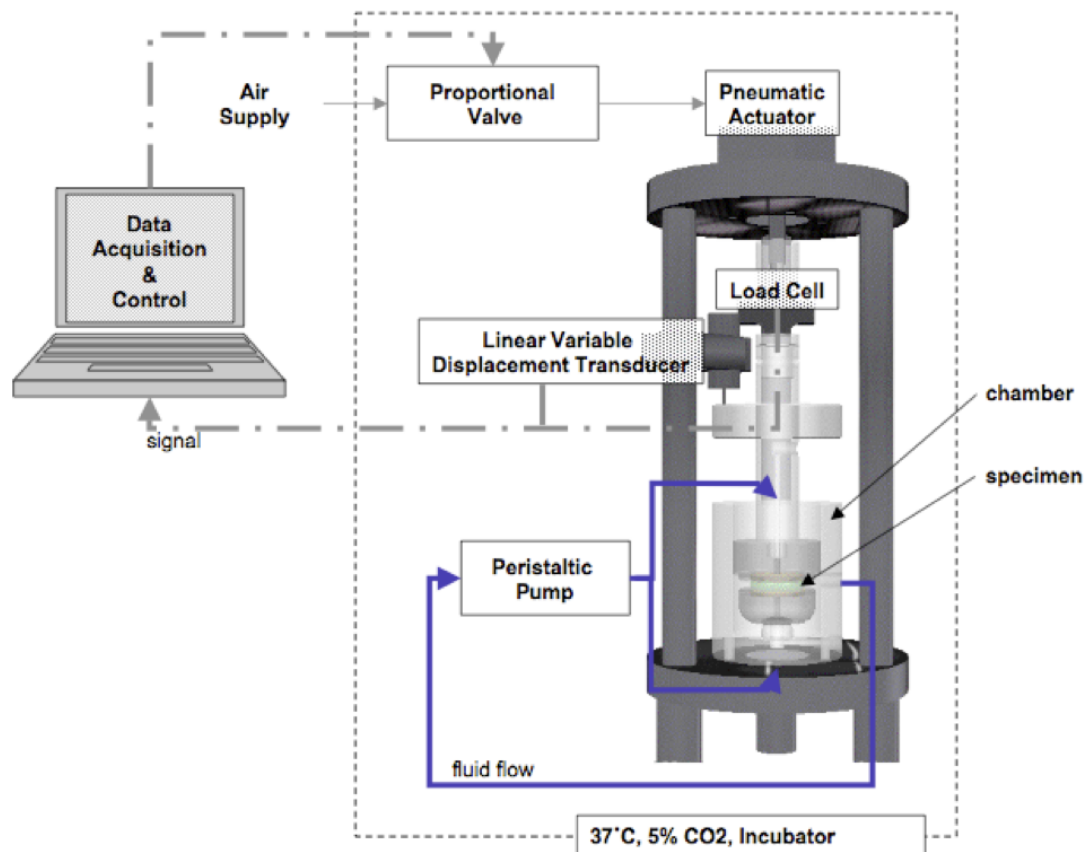


Figure 3–2: Schematic diagram of the bioreactor. The specimen is placed inside the culture chamber. A load cell is mounted to the top piston, in-line with a pneumatic actuator. An airline connects the computer controlled proportional valve to the actuator, generating controlled compression. A linear variable displacement transducer is mounted to the frame of the bioreactor. Load and displacement is acquired with a computer. A peristaltic pump is used to circulate media to top and bottom of the specimen. The whole unit, other than the computer, power supply and airline, is housed in a standard laboratory incubator.



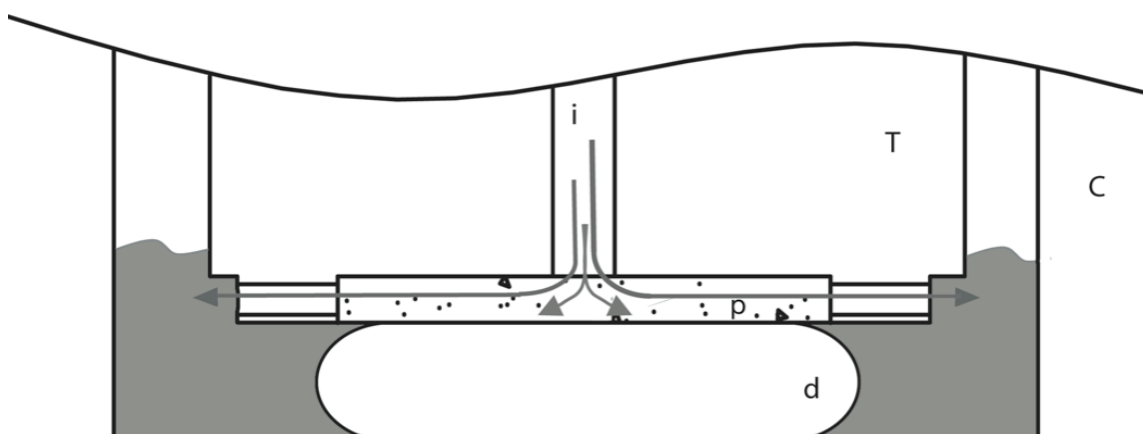


Figure 3-3: Cross section view of the culture chamber. Media is directed through the inlet (i) of the Teflon loading platform (T) to the porous platen (p). The design of the piston creates a flow path where media first arrives at the centre of the disc (d) and flows outwards to the periphery, collecting in the culture chamber (C).

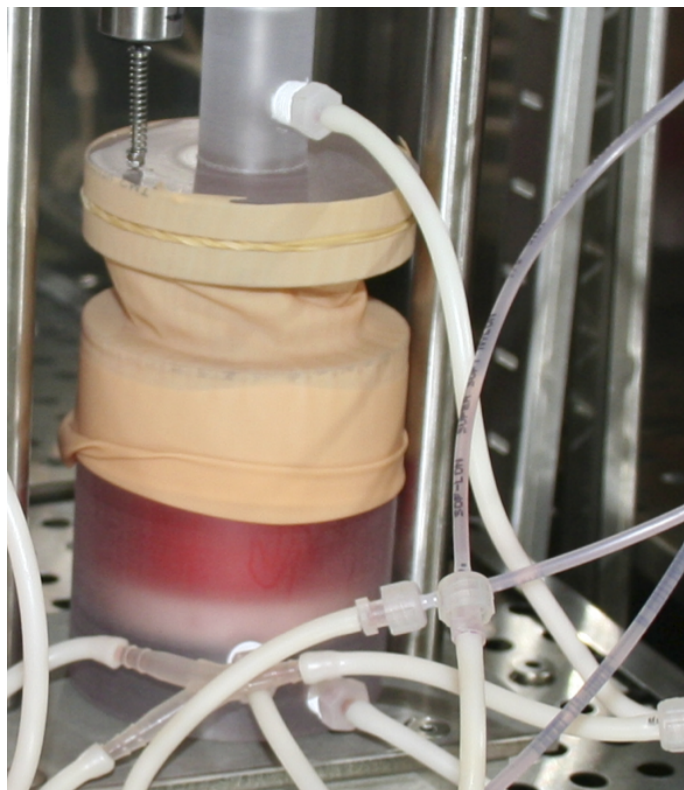


Figure 3-4: Bioreactor chamber in loading frame in the incubator

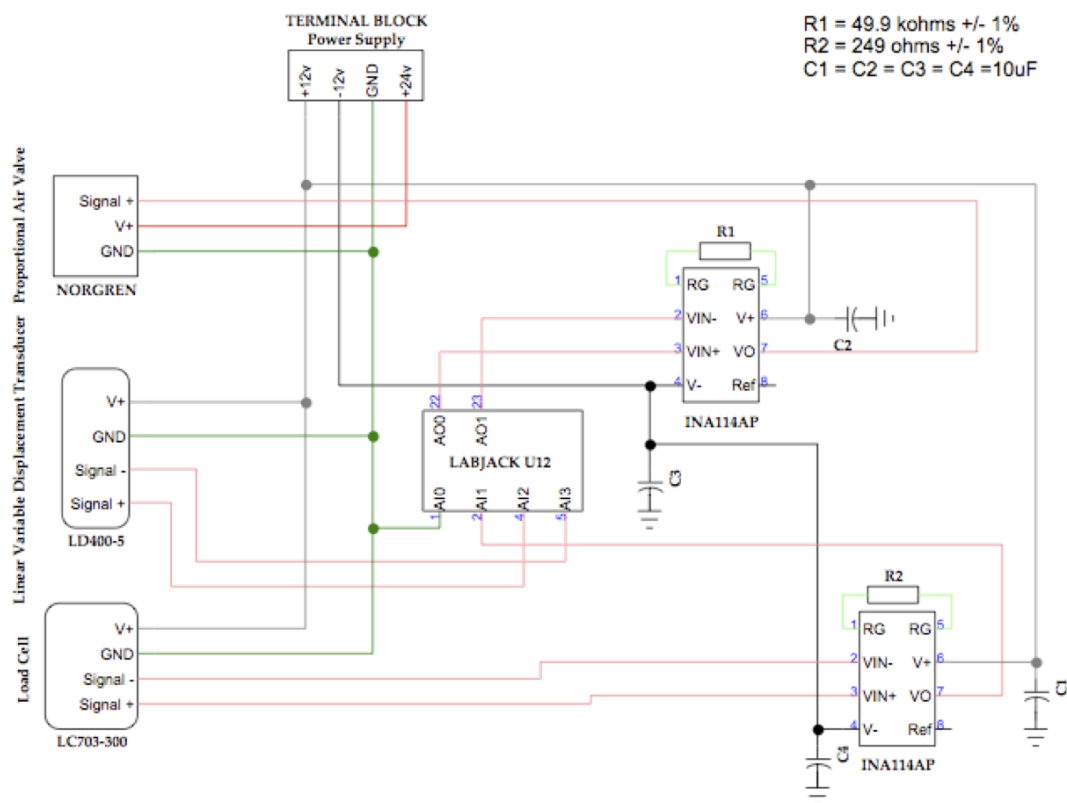


Figure 3-5: Electrical schematic diagram of the organ culture system

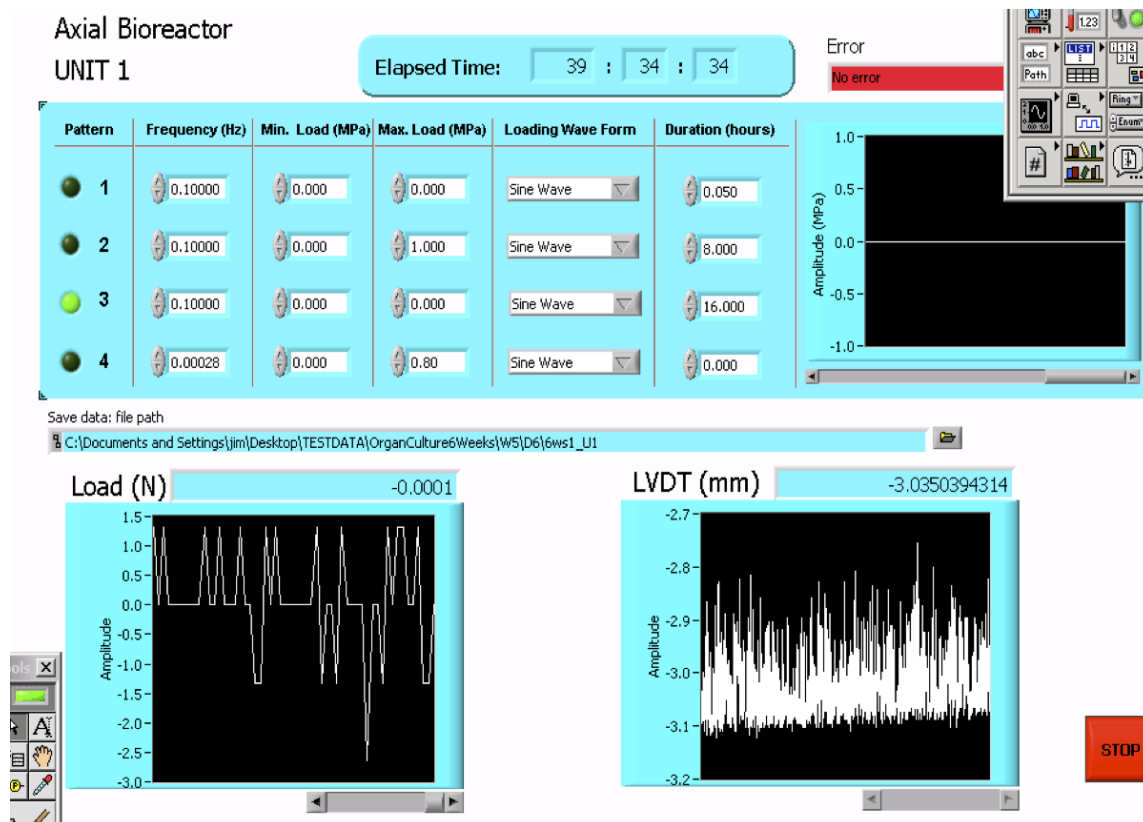


Figure 3-6: Screen shot of bioreactor program

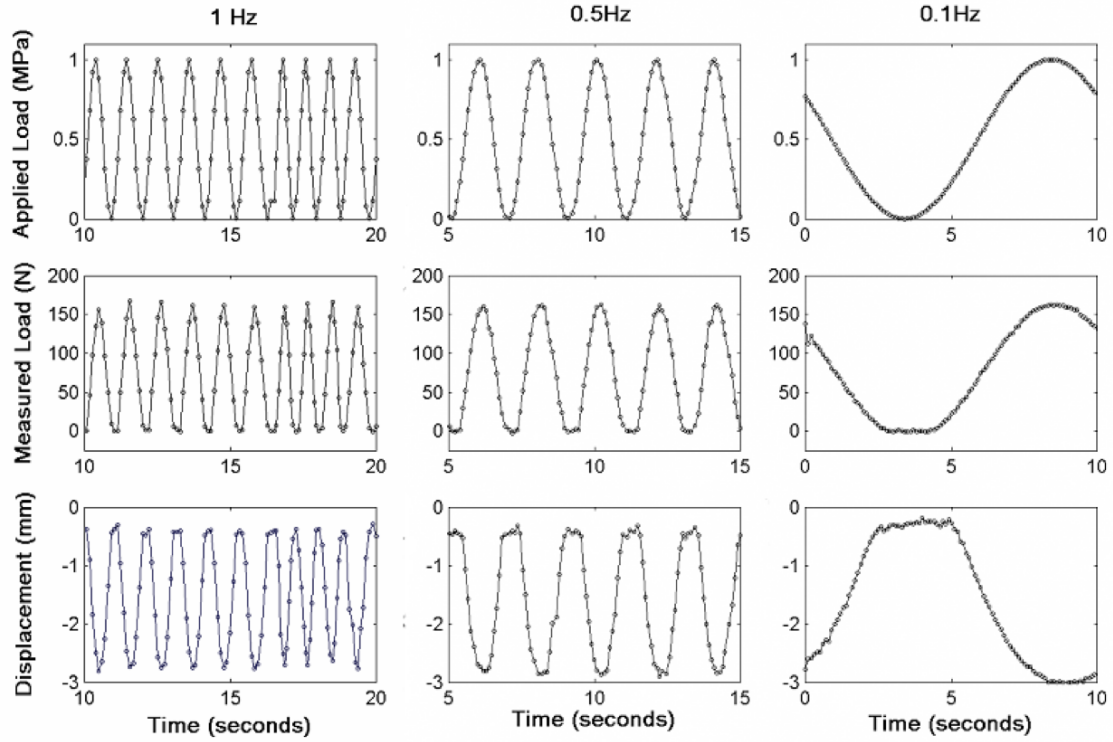


Figure 3-7: Mechanical validation of the bioreactor system. Sample data of applied load on a test specimen and measured results of load and displacement for frequencies of 1 Hz, 0.5 Hz and 0.1 Hz is shown. The experimental data points are shown with  $\circ$  and connected by a solid line —.

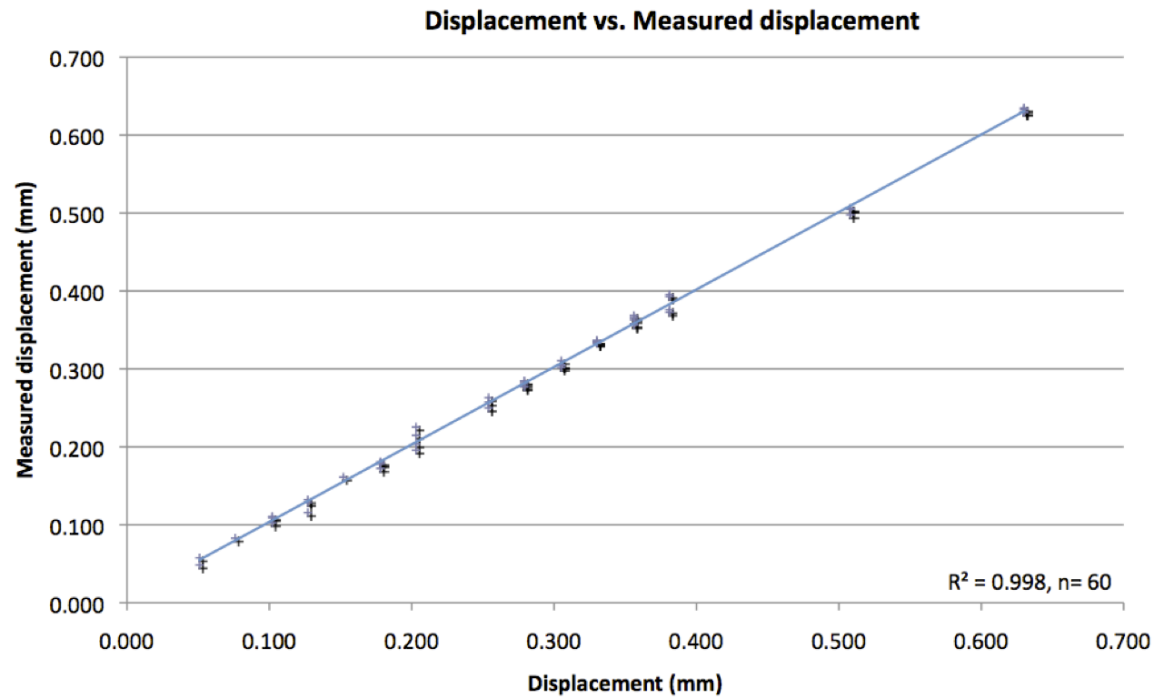


Figure 3-8: Validation of the linear variable displacement transducer: input versus output measurements. Input values were known thickness of different feeler gauges and output was the displacement measured by the linear variable displacement transducer.

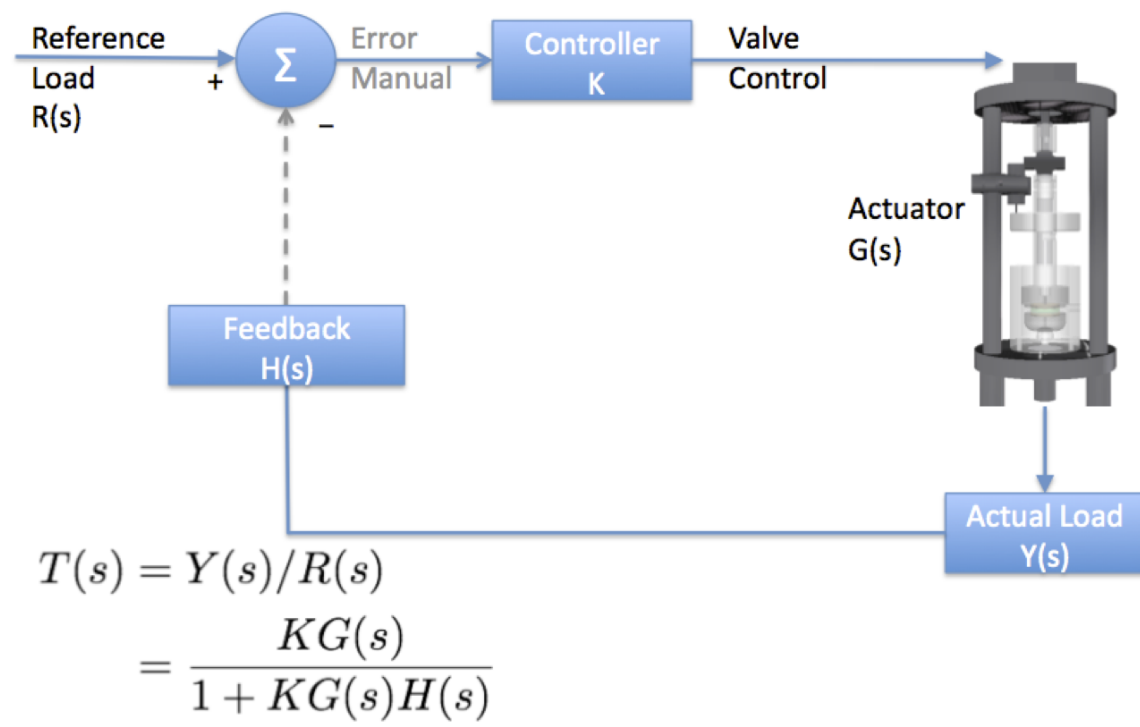


Figure 3–9: Diagram of the bioreactor force control transfer function model

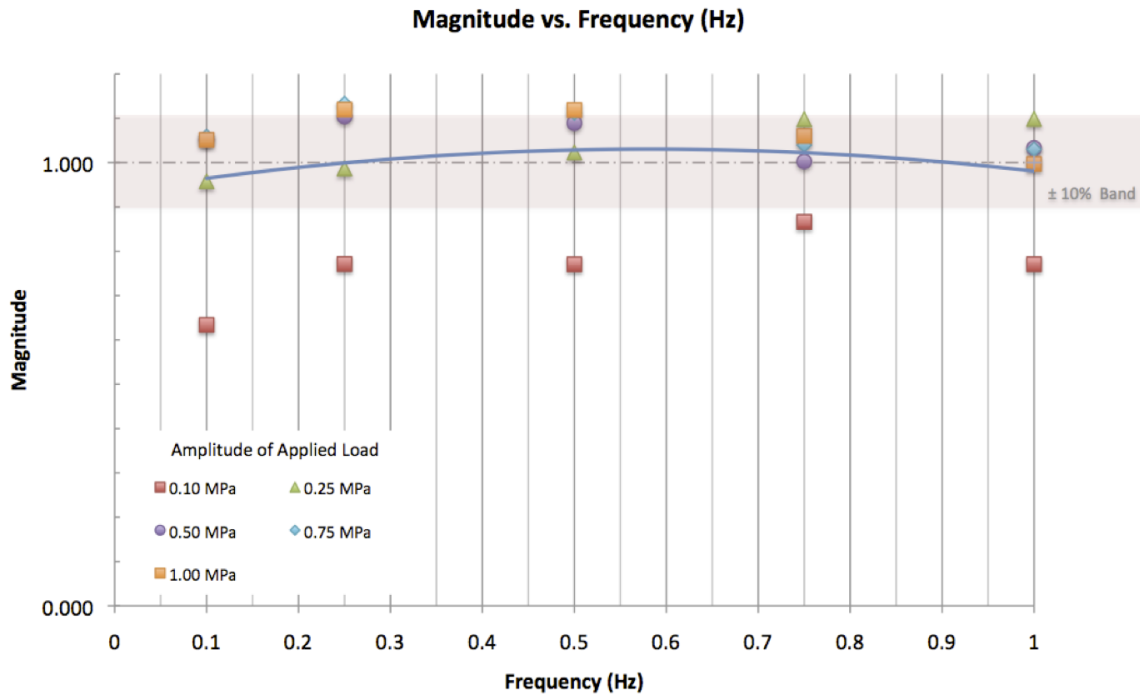


Figure 3–10: Magnitude plot of the system. The magnitude which is plotted in the y-axis and the frequency is shown on the x-axis in Hz. The magnitude is a measure of the actual force delivered and measured by the system over the intended input force. The solid blue line represents the moving average value of magnitude for all tested amplitudes. The different markers show the different amplitudes of sinusoidal load that was tested at the different frequencies. The shadowing shows a 10 % error band, which we considered as the range for acceptable performance.



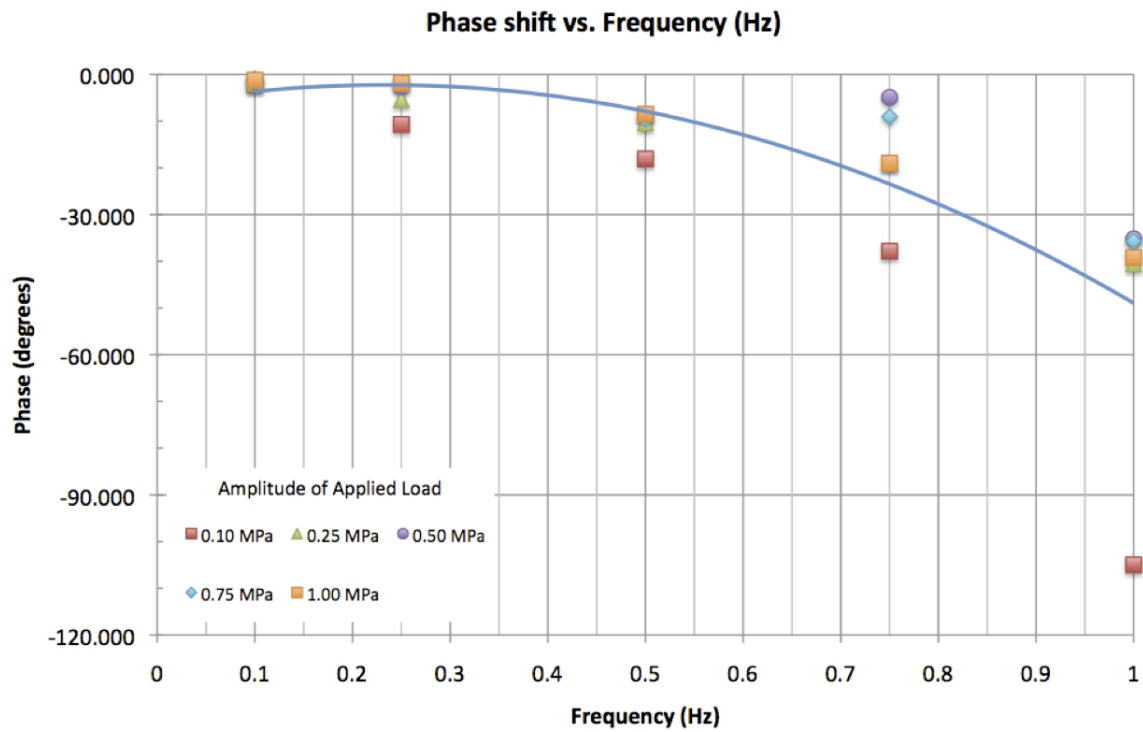


Figure 3–11: Phase plot of the system. This chart plots the lag performance of the system. The phase shift between the intended output versus the actual output is shown on the y-axis in degrees. The various frequencies are represented in Hz on the x-axis. The solid blue line represents the moving average value of the phase shift. The different markers show the different amplitudes of sinusoidal load that was tested at the different frequencies.

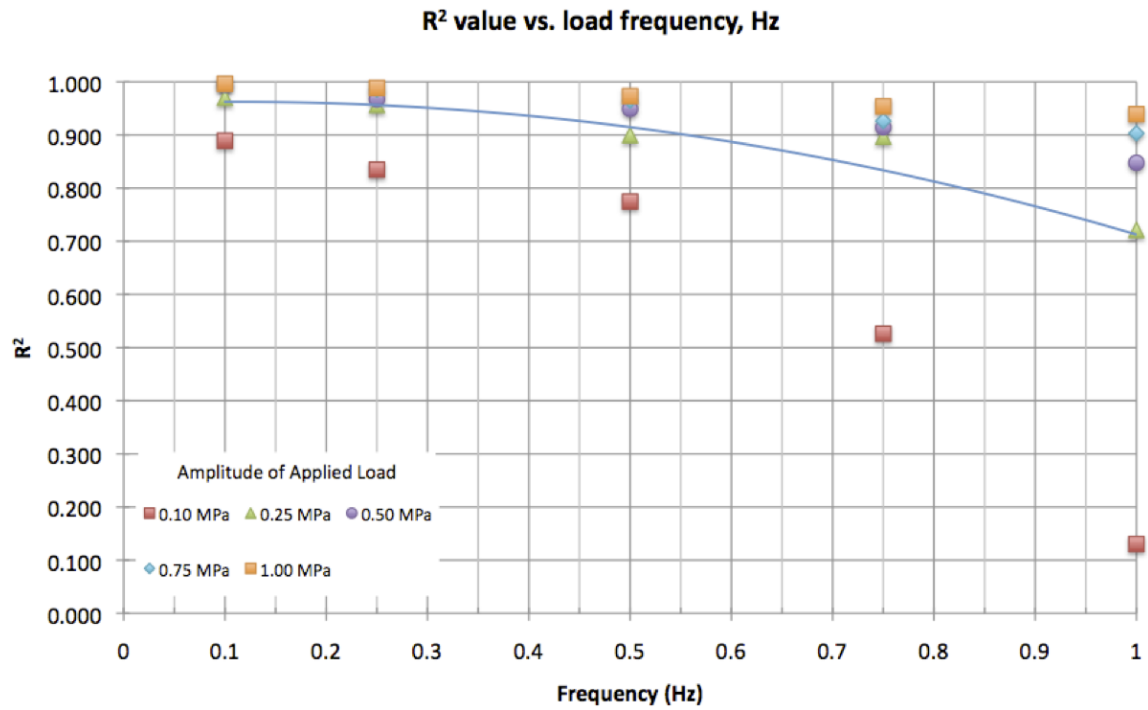


Figure 3-12: R<sup>2</sup> values of load input are shown on the y-axis and were calculated based on the intended intended output forces versus the actual output force. The R<sup>2</sup> values are plotted against the various loading frequencies in Hz. The different markers show the different amplitudes of sinusoidal load that was tested at the different frequencies.

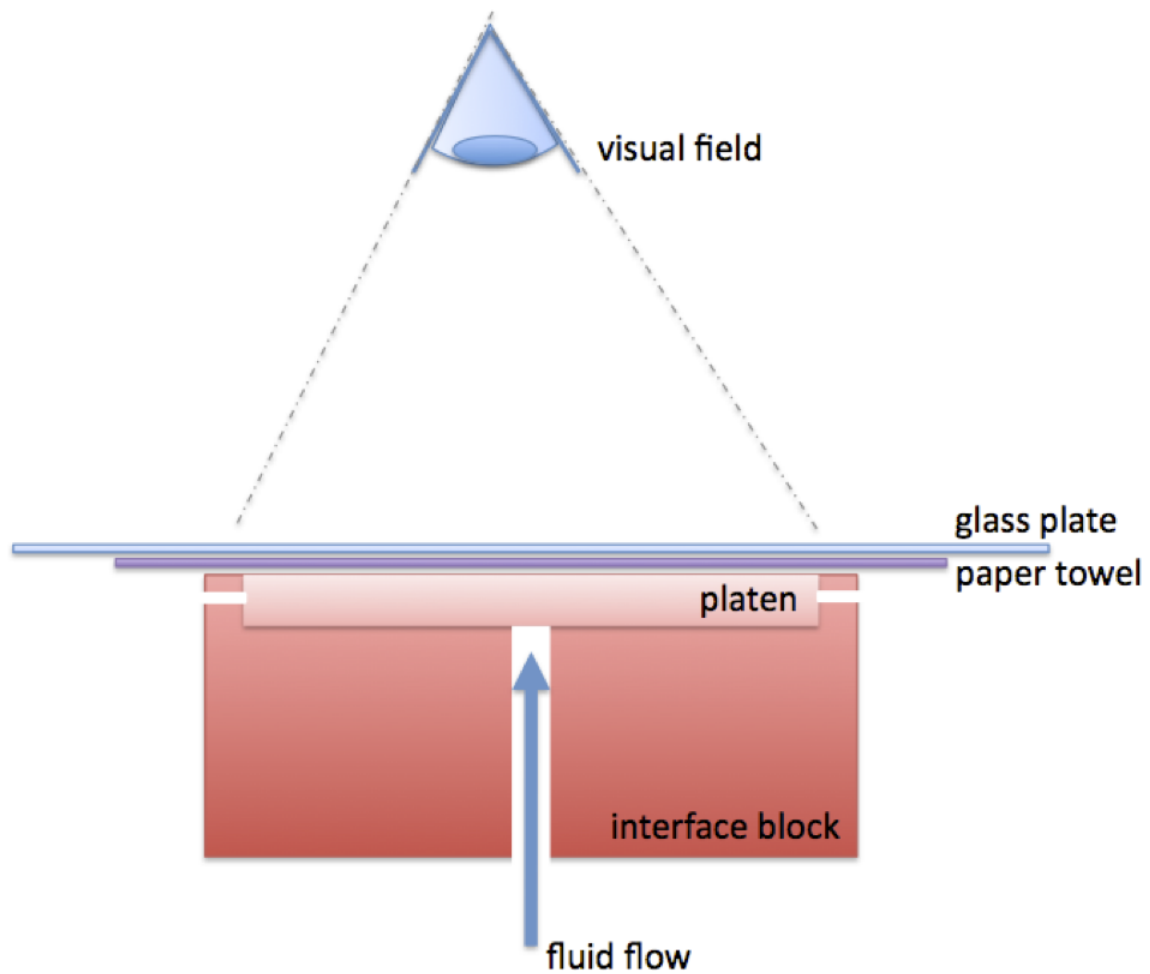


Figure 3-13: Experimental set up for the wet test. Phosphate buffered saline was pumped through the bottom of the interface block. Wetting of the sandwiched paper towel verified that fluid was reaching the platen surface, where the organ culture tissue would be seated.

## **CHAPTER 4**

### **Harvesting Method Development**

A component of an in-vitro organ culture model is the method used to isolate discs for culture. The structure of the removed disc (with or without endplates) affects the biomechanics and the path of nutrient supply, which are both important aspects for mimicking the in-vivo environment. This chapter presents an investigation into three harvesting methods that were examined and compared. Disc mechanical stability, solute transport and the amount of tissue swelling were used to measure the suitability of the harvest methods.

#### **4.1 Tissue Source**

The in-vitro organ culture model was developed using bovine coccygeal intervertebral discs. Bovine coccygeal intervertebral discs have been widely accepted as a suitable animal model since they have a composition and biochemical profile similar to human lumbar discs [32, 157]. Furthermore, the large size, width-to-depth aspect ratio, diffusion distances and disc intrinsic swelling pressure of 0.1 to 0.3 MPa of bovine discs all compare favourably to those of humans [152, 157]. In addition, bovine tails have the added advantage of being readily available, fresh from local slaughterhouses.

#### **4.2 Endplate Preparation Methods**

Mimicking similar disc biomechanics and maintaining adequate nutrition diffusion are two interrelated aspects that have considerable influence over the success

of a harvested disc in in-vitro organ culture. The ideal harvested disc would mimic physiological biomechanics. In order to establish such a model, most or all of the surrounding support tissue such as the vertebral endplates, muscle and ligaments would need to be retained. Furthermore the same availability of nutrients to the disc would need to be reestablished. This is a hurdle to accomplish. Any injury to bone causes the natural formation of blood clots at the injury surface. In the in-vitro case, blocking the nutritional pathway from the culture media to the cells of the disc. Even if the blood clots could be cleared, the in-vivo nutrient source, pressurised, circulating blood in the adjacent vertebral bodies, would be difficult to replicate. Furthermore, the risk of bacterial contamination is increased as excess muscle, fat and ligament tissue creates an environment that is prone to harbour bacteria in culture conditions. Considering these limitations, the final harvest method used to develop the in-vitro model would need to consider and carefully balance these aspects.

In the beginning three harvest methods were considered for the in-vitro organ culture model: (1) the bony endplate harvesting method which produced a disc with the most structural stability but also a more complex route for nutrition diffusion [48, 81, 93, 115], (2) the no-endplate method that had been used prior where no endplates are intact which meant a shorter diffusion distance gained at the expense of structural stability [105, 106, 115, 231], and (3) a harvesting method that compromises between the two, the cartilaginous endplate method where a thick layer of cartilaginous tissue is kept [56, 89]. In each case all excess ligament, fat and muscle tissue were removed to minimize the risk of infection during culture.

### **4.3 Bony Endplate Harvesting Method**

For the Bony End Plate (BEP) harvesting method, the bony endplates are left intact. This method is most realistic for an organ culture, fully respecting the natural biomechanics of the disc. Lee et al. [115] first presented the BEP harvesting method in an early study of a statically loaded culture system. For the BEP harvesting method, parallel cuts close to the disc were made with a table band saw through the adjacent vertebral bodies (Figure 4–1). The bone thickness varied from 3 mm at the centre of the disc to 0.5 mm at the periphery. The convex shape of the endplate of the bovine coccygeal vertebrae was the reason for this large range of bone thicknesses. After cutting out the disc, the freshly cut bony surfaces were rinsed with a phosphate-buffered saline solution (PBSS) to wash off debris. The disc was further soaked in an anti-coagulate solution (sodium citrate) to dissolve blood clots at the bone surface. The washing of the freshly cut bony surface continued with sodium citrate PBSS until the solution ran clear.

### **4.4 Cartilaginous Endplate Harvesting Method**

The cartilaginous endplate (CEP) harvesting method, which only preserves a thin layer of the cartilaginous endplate, was a novel method that was developed as a result of the exploration of different harvest methods for the organ culture [56, 87, 89]. Similar to the BEP harvest method, parallel cuts were made with a table band saw through the adjacent vertebral bodies. Then using a commercially available high-speed (up to 30 000 rpm) Dremel tool (Racine, WI, USA), fitted with a 6 mm diameter burr drill bit (Figure 4–1), the bony endplate was gradually removed until

only cartilaginous endplate was left. To prevent tissue overheating and wash away debris, drilling was conducted with the specimen frequently dipped in 4 °C PBSS.

#### **4.5 No-Endplate Harvesting Method**

The no-endplate (NEP) harvest method removes both the cartilaginous and the bony endplates. It has been used previously in the organ cultures of bovine coccygeal discs subjected to static and diurnal loading and was reported to be able to maintain cell viability for up to eight days [105, 115].

The NEP method for disc organ culture [105] is expected to provide the cells with adequate nutrients. However, by removing the endplates, this method eliminates the anchoring structural support of the annulus fibrosus fibres and therefore would alter the mechanical function of the disc as a load-bearing structure [115]. Since the disc is an organ that functions responding to mechanical stimulations, this change in the disc biomechanics may affect the disc not only at the macroscopic physical level but also at the cellular level [118, 178].

For the NEP harvest method the intervertebral disc was removed using two thin parallel histological sectioning blades. Cuts were made closest to the endplates through the disc (Figure 4-1), but no further preparation was required.

#### **4.6 Sample Preparation**

Young steers (8-20 months of age) obtained from a local abattoir (Abbattoir z'Billette, Montreal, Canada) were used in this study. The bovine coccygeal discs were isolated within eighteen hours after animal slaughter. Only the first four discs of each tail, numbered from proximal (CC1) to distal (CC4), were used in the experiments.

The intervertebral discs were harvested with one of three methods: with the bony endplates (BEP), with a thin layer of the cartilaginous endplates (CEP), and with no endplates (NEP). Four discs were harvested from one bovine coccygeal tail, three using one of the three harvesting methods and a baseline, day 0, control disc. A total of twenty-four discs were harvested, producing six discs for each harvest method and six day 0 discs. The order of harvest in each tail was deliberately varied by random assignment. In each case, all skin, pedicles, muscle and ligaments were removed from the tail for four levels from proximal to distal.

All discs were rinsed with a concentrated 10x penicillin-streptomycin (P/S; 10x = 1000 U/mL penicillin, 1000 µg/ml streptomycin) phosphate buffered saline solution (PBSS), followed by a 1x P/S PBSS. The specimens were then placed into the polycarbonate culture chambers of the bioreactor system with media (DMEM with 5 % fetal bovine serum and 1x P/S). The media was exchanged every two to three days.

#### **4.7 Mechanical Stability**

Each bioreactor containing a culturing chamber was set on a dynamic loading program: twelve hours of sinusoidal dynamic load at 0.1 to 1.0 MPa, 0.3 Hz and a static load for twelve hours at 0.1 MPa which is within the range of previously used protocols to simulate physiological loads [26], although we know that a physiological load for humans is closer to eight hours of rest with sixteen hours of activity. A longer recovery load time was set to optimize tissue recovery after the compression cycle. A static load of 0.1 MPa was chosen to counteract the natural swelling pressure of the intervertebral disc that is reported to be in the range of 0.06 to 0.22 MPa [221]



while sleeping. The compressive force was calculated from the the measured disc diameter. The disc diameters were measure from radiographs of each tail that was taken before harvest. This diameter was entered into the system control interface and the displacement and loading measured by the bioreactor was recorded and collected during the six-day culture period.

The intervertebral disc mechanical behaviour was modelled using a one-dimensional linear biphasic model. The biphasic theory models a soft hydrated tissue as a composite material with a fluid phase and a solid phase, where both mass and momentum are conserved within each phase [109]. The solid phase is assumed to be incompressible, porous and elastic; the fluid phase intrinsically incompressible and inviscid [144, 205]. Although acknowledging that the intervertebral disc is a more complex tissue, with the annulus fibrosus and nucleus pulposus having different material properties, a more simplified model was used to compare the harvest methods on the mechanical behaviour of the intervertebral disc tissue. The goal was not to characterise the material properties of the intervertebral disc but to compare each of the harvest methods. A one-dimensional model that includes permeability and osmotic potential as functions of strain has been shown to be able to model the time-dependent deformation of a lumbar motion segment in a multiple compression-expansion loading regime [172, 205]. The aggregate modulus and permeability were found to be similar to previously published data. The model eliminated the initial elastic deformation of the intervertebral disc, stating that the initial large elastic deformation was to be associated with the initial lateral bulging of the nucleus pulposus into the vertebral endplate and lateral bulging of the annulus fibrosus [172].

After removing these large elastic deformations, the fit of the model retained results close to that previously published [172].

The following assumptions were taken for the model that was used to fit the data:

- The intervertebral disc is homogenous, uniform soft tissue with a solid and fluid phase.
- The disc tissue was fully saturated at the onset of loading.
- The structural part of the disc tissue and water are incompressible.
- The compression and flow are one-dimensional (vertical).
- Strains are relatively small.
- Darcy's law is valid at all hydraulic gradients.
- The coefficient of permeability,  $\kappa$ , and the coefficient of volume compressibility, in this case, the aggregate modulus,  $H_A$ , remains constant throughout the process.
- There is a unique relationship, independent of time, between void ratio and effective stress.
- The disc itself, ignoring the initial lateral bulge, has a confined structural shape.

Reducing the linear biphasic equations of Mow [144] to a parabolic partial differential equation [205] for the displacement of the solid matrix, the equation becomes

$$\frac{du}{dt} - H_A \kappa \frac{d^2 u}{dz^2} = 0 \quad (4.1)$$

where  $H_A$  is the aggregate compressive modulus.

The initial and boundary conditions for cyclic compressive loading were:

$$u(0, t) = 0, \quad t \geq 0 \quad (4.2)$$

$$u(z, 0) = 0, \quad 0 \leq z \leq h \quad (4.3)$$

$$H_A \frac{du}{dz} \Big|_{z=h} = -\sigma_0(1 - \cos \omega t), \text{ at } z = h \quad (4.4)$$

where  $h$  is half of the initial tissue thickness,  $\sigma_0$  is the median magnitude of the cyclic load and  $\omega$  is the loading frequency. The solution for the equation then becomes

$$\begin{aligned} u(z, t) = & -\frac{\sigma_0}{H_A} z(1 - \cos \omega t) \\ & + \frac{2\sigma_0}{H_A h} \sum_{n=1}^{\infty} \left[ \sin \mu_n h \sin \mu_n z \frac{\omega}{\mu_n^2(\alpha_n^2 + \omega^2)} \right. \\ & \left. \times \{ \omega \exp(\alpha_n t) - \alpha_n \sin \omega t - \omega \cos \omega t \} \right] \end{aligned} \quad (4.5)$$

where

$$\mu_n = (n - 0.5) \frac{\pi}{h} \quad (4.6)$$

and

$$\alpha_n = -\mu_n^2 H_A \kappa. \quad (4.7)$$

The characteristic diffusion time of the tissue can be quantified as

$$\tau = \frac{4h^2}{\pi^2 H_A \kappa}. \quad (4.8)$$

At the equilibrium of tissue displacement to the exerted load, the fluid flow out of the tissue has reached a steady state and therefore the applied stress  $\sigma_0$  is carried entirely by the solid matrix of the tissue. The aggregate modulus  $H_A$  represents

the intrinsic confined compressive modulus of the tissue's solid skeleton and can be calculated as

$$H_A = \frac{\sigma_0 h}{z_\infty} \quad (4.9)$$

where  $z_\infty$  is the median equilibrated displacement of the tissue.

Using this model the tissue mechanical strain and recovery behaviour was analysed following each change from a 0.1 to 1.0 MPa dynamic cyclic compression (creep) to a 0.1 MPa static compression (relaxation). A sample of the raw data that was collected is presented in Figure 4–2. The first creep-relaxation cycle was used as a conditioning cycle equilibrating the disc to the test environment. The temporal development of the creep strain for the compressive phase of each (subsequent) cycle was fit using Matlab (The Mathworks Inc., Natick, MA, USA). The Matlab codes and process is enclosed in Appendix B. The variables that were derived from this fit were used to compare the mechanical stability of the tissue between the different harvest methods. A sample fit is shown in Figure 4–3.

The compressive properties that were obtained are presented in Table 4–1. The mean compressive aggregate modulus of the intervertebral disc specimens was  $H_A = 0.71 \pm 0.20$  MPa. There was a consistent increase of the aggregate modulus value after each cycle for all harvest methods. Using a two-way ANOVA analysis with the loading cycles and harvest methods as factors and Tukey's HSD posthoc test, a significant difference was found between the loading cycles ( $p$ -value of  $< 0.05$ ), where values of cycle 1 were significantly different from cycles 2–5, further confirming this finding. Using the loading cycles as a co-factor, the Tukey HSD posthoc test showed

a significant difference in the aggregate modulus was found between the NEP harvest method and that of the BEP and CEP methods.

The mean hydraulic permeability coefficient, with respect to each harvest method, also exhibited small differences in value, with  $\text{BEP} < \text{CEP} < \text{NEP}$  (Table 4–1). The mean value was  $\kappa = 0.59 \pm 0.21 \times 10^{-15} \text{ m}^4/\text{Ns}$ . However, the values showed no statistical difference between the harvest methods. The loading cycles showed a larger influence on the permeability coefficient, with cycle 1 showing a significant difference from cycles 2 to 5, in the Tukey HSD posthoc test. However, taking the loading cycles as a co-factor, the Tukey HSD posthoc test did not show any statistical differences between the different harvest methods on the hydraulic permeability.

The  $R^2$  value representing the fit of the mechanical data to the model was also calculated (Table 4–1). Both the BEP and CEP groups obtained a good fit with the model with  $R^2$  values of  $0.98 \pm 0.13$  and  $0.92 \pm 0.01$ . The mechanical data for discs harvested with the NEP method ( $0.76 \pm 0.29$ ) did not fit as well to the model. Furthermore there were large standard deviations between the samples. Using a Tukey HSD posthoc test, a significant difference was found, where the fit was significantly different for the NEP group from the BEP and CEP groups.

#### 4.8 Solute Transport

The use of  $^{35}\text{S}$ -sulfate to measure the diffusion rate of intervertebral tissue is an accepted methodology [220]. The facilities and methodology was well established [220] with the marker substance being less time sensitive for handling and did not require a laser confocal microscope, which was not available at the time. Using a method such as fluorescent marked dextran would have given more illustrative results

[48], however, since the aim of the study was to compare the diffusion between the different harvest methods, the methodology was sufficient.

At end of day 5 (and at day 0 for the control), 2.5  $\mu\text{Ci}$   $^{35}\text{S}$ -sulfate was introduced into the culture chamber as a solute transport marker. The radioactive sulphate particles had twenty-four hours, one complete creep-relaxation cycle to propagate into the disc. After the culture, 6 mm diameter samples were punched from the disc in a superior to inferior direction with a biopsy punch. A total of five samples were collected for each disc, four annulus fibrosus (AF) samples taken evenly distributed over the annulus tissue circumference and one nucleus pulposus (NP) sample taken from the centre. The samples were further sliced into 1 mm sections from superior to inferior using a jig and razor blades. The radio-labelled samples were lyophilized, weighed for dry weight, and digested in proteinase-K (0.5 mg/ml, overnight at 60 °C). The radioactivity of the dialysed samples was measured using a beta-scintillation counter and the measured values were then normalised to the dry tissue weight.

The mean  $^{35}\text{S}$ -sulfate diffusion, for the different harvest methods, normalised to a molar equilibrium distribution coefficient as presented by Urban et al. in 1982 [220] is presented in Figure 4–4. The control showed an almost even distribution of radioactivity counts, indicating saturation of the tissue. For both the CEP and NEP harvest methods radioactivity counts increased from the annulus to the nucleus, 75 % to that of the control saturation. The radioactivity count of  $^{35}\text{S}$ -sulfate for the BEP discs were overall significantly lower (shown statistically  $p$ -value of  $< 0.05$ ), no more than 25 % saturation when compared to the control.

## 4.9 Swelling Analysis

As the NEP isolation technique severs the attachment of collagen fibrils between the disc and the cartilage endplates, it was predicted that NEP discs would be prone to swell to a greater extent than the CEP or BEP discs when maintained in culture. The swelling capacity of discs prepared with the CEP method was therefore compared to discs isolated using the NEP method, under conditions with no external load applied. Increase in disc weight as an indicator of swelling was measured over a thirty-hour period (Figure 4-5a). In both cases weight increase occurred rapidly during the first four hours of culture, and then gradually over the next twenty-six hours. Weight increase was limited to about 20 % using the CEP method. In contrast, discs isolated using the NEP method increased between 60 to 100 % of the initial weight when cultured unconfined. The CEP discs maintained their morphology throughout the experiment, whereas the NEP discs were already deformed after one hour and were severely deformed after thirty hours (Figure 4-5b, c).

## 4.10 Discussion

This chapter focused on the examination and comparison of three different harvesting methods. Two previously used methods (the bony endplate (BEP) and no endplate (NEP) method) were examined along with a novel method (cartilaginous endplate (CEP) leaving only a thin layer of cartilaginous endplate intact). The cultured discs using one of the three harvesting methods were measured on both mechanical stability and the ability to transport  $^{35}\text{S}$ -sulfate as well as the swelling capacity of the tissue.

From the biomechanical analysis, only small differences were found between harvesting methods in calculated mechanical properties when looking at the mean values. In each case, the loading cycle had a statistically significant influence on the calculated variables, which follows the findings from previous studies [172]. Although acknowledging that the intervertebral disc is a more complex tissue, with the annulus fibrosus and nucleus pulposus having different material properties, a more simplified model was used to compare the harvest methods on the mechanical behaviour of the intervertebral disc tissue. The goal was not to characterize the material properties of the intervertebral disc but to compare each of the harvest methods. When eliminating the influence of the loading cycle, the calculated aggregate modulus for the BEP and CEP harvested tissue, was significantly different from that of the NEP group. Furthermore, it was difficult to obtain a good fit of the NEP data to the model. These differences can be explained by the harvest method themselves. The poor fit could be logically linked to the structure of the explants, with the biomechanics of CEP-harvested discs behaving more similar to BEP harvested discs, both having some form of endplate as opposed to that of NEP-harvested discs, which have no endplates. Furthermore, obtaining a perfect parallel cut of the tissue was difficult because of the convex nature of bovine coccygeal endplates.

The transport of small molecule nutrients was analysed using  $^{35}\text{S}$ -sulfate radio-labelling. The results showed that BEP-harvested discs were not able to obtain the same levels of diffusion as those harvested with the CEP and NEP method. This deficiency might be due to blood clots that formed in the endplate at the time of harvest, despite the use of anti-coagulants to dissolve them. Another contributing



factor to inadequate nutrition diffusion could be the increased diffusion distance for nutrients to the nucleus of the disc that is created with the presence of the bony endplates. On the other hand, the CEP harvest method showed diffusion of nutrients at similar levels to the NEP harvest method after the twenty-four hour period.

Swelling analysis showed that intervertebral discs harvested with the CEP method swelled about 20 % from the initial weight. Whether this amount of swelling has a significant influence on cell behaviour and biomechanical function needs to be further examined. However, human discs loose and regain 20-25% of its fluid throughout the course of a day [219]. It is clear, that without endplates, the disc tissue swells significantly and deforms. Discs harvested using the NEP method will always need to be confined to prevent excessive swelling and deformation. This is an added complication for harvesting disc tissues with this method.

Organ cultures of whole bovine discs have been reported previously using the BEP and NEP methods [115]. The discs were maintained under a constant load to negate the effects of swelling, and cultures were maintained for seven days. At the end of this time the majority of cells in the BEP disc were dead, whereas good cell viability was obtained for the NEP discs. The difference between the two isolation techniques presumably reflects the decreased nutrition to the discs when the bony endplate remains intact. The work also illustrates that the NEP method of isolation may be of value if the resulting discs are maintained under load, however additional studies have shown that the type of loading is important if cell death is to be avoided [105]. The BEP isolation method has been shown to be of use for viable organ culture when the discs were obtained from sheep that were heparinized prior to slaughter

[48, 93]. Presumably, heparinization prevented blood clot formation in the capillary channels that are present in the endplate, and so improved nutrient flow. This technique would not however be a feasible option for bovine discs obtained from the abattoir, and this is by far the most convenient source for large animal discs in large quantity. The use of the CEP isolation technique avoids the need for heparinization to improve nutrient supply to the disc, and also avoids the need for the use of loading devices to prevent excessive swelling that is inherent to the NEP method.

With the CEP harvesting method the internal arrangement of nucleus pulposus and annulus fibrosus is not affected. The outer ring of fibro-cartilaginous endplate tissue, which anchors the oblique circumferential annulus fibrosus fibres, is namely unaltered, thus better mimicking the contained in-vivo disc structure. Meanwhile the problem of a compromised nutritional pathway to the organ due to blood clots, as found with the BEP method, is eliminated.

#### **4.11 Conclusion**

The novel harvest method of keeping the cartilaginous endplates is a promising method to isolate intervertebral disc. This method allowed the disc to maintain a mechanical stability similar to the physiological environment (using the BEP method as the benchmark). Furthermore, the transport of small molecule nutrients into the nucleus was accomplished after twenty-four hours and the distribution of nutrients expressed a profile and count levels that were similar to that of the NEP method. However, thus far, the harvest method has been examined only at a macroscopic level. Achieving cell viability of the cultured harvested discs in the bioreactor system is logically the next step in the development of the in-vitro organ culture model.

#### 4.12 Tables and Figures

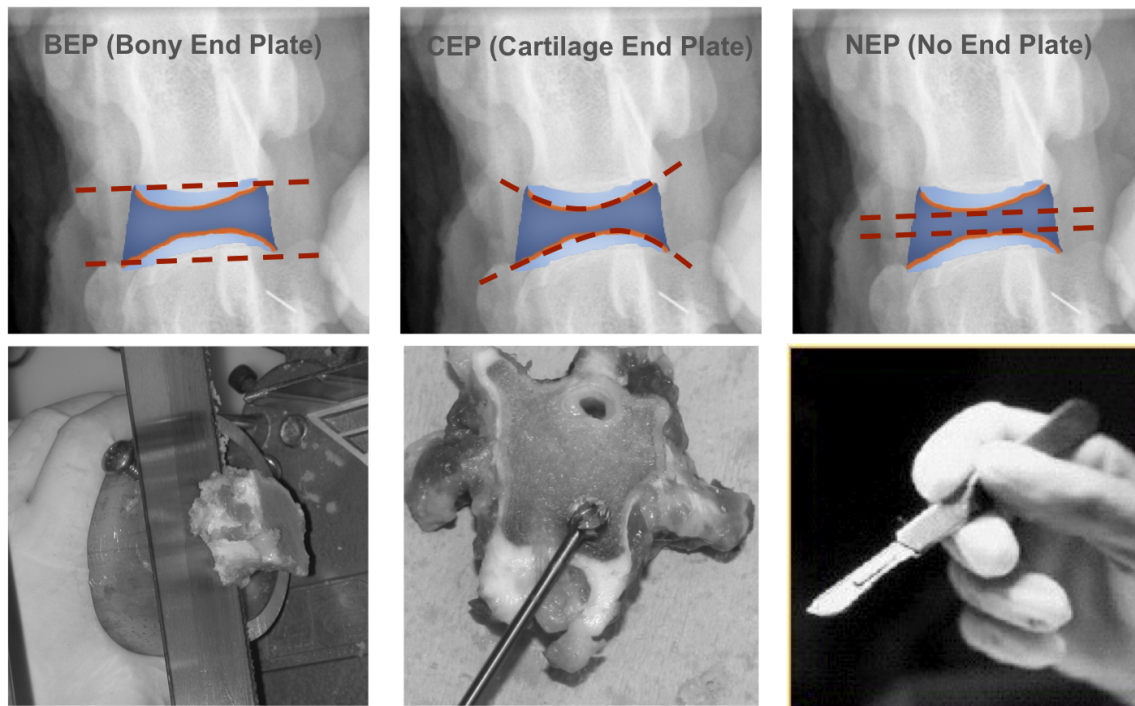


Figure 4-1: Harvest methods shown graphically on bovine coccygeal tail radiography. The intervertebral disc is shown in blue, the cartilaginous endplate in orange, the vertebral endplate in light blue. Parallel sagittal cuts, with mitre saw for BEP and CEP method and with scalpel with the NEP method, are shown with a - - - line.

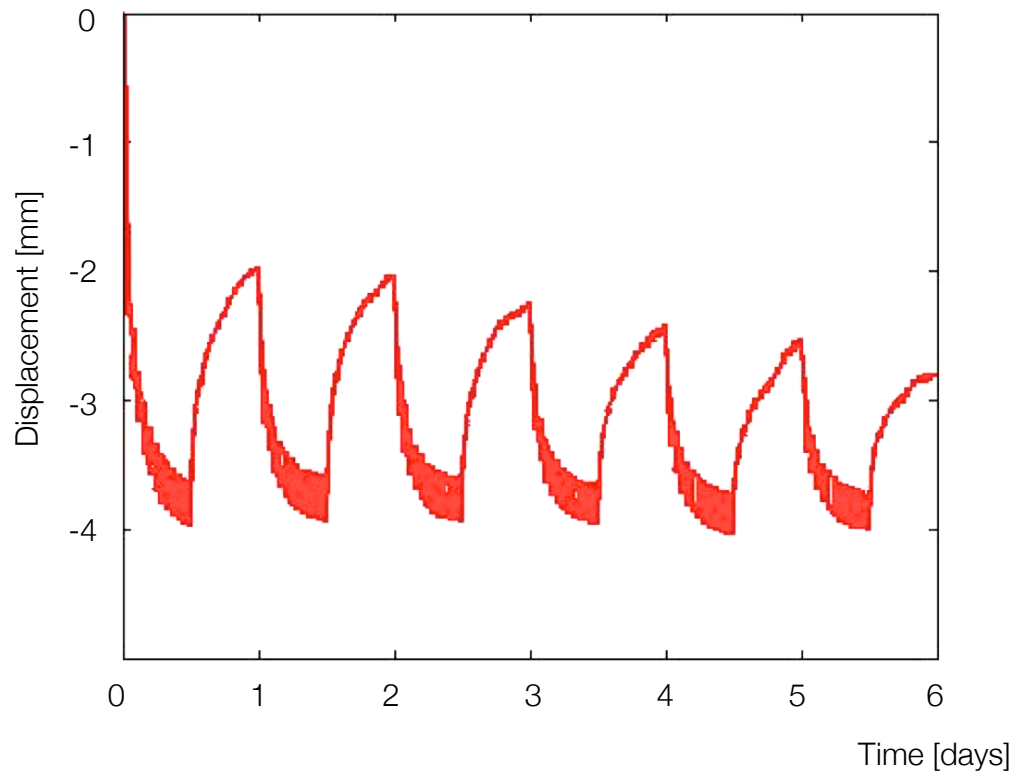


Figure 4-2: Example of recorded experimental displacement data over the six days of 12 hours sinusoidal load followed by 12 hours of static load.

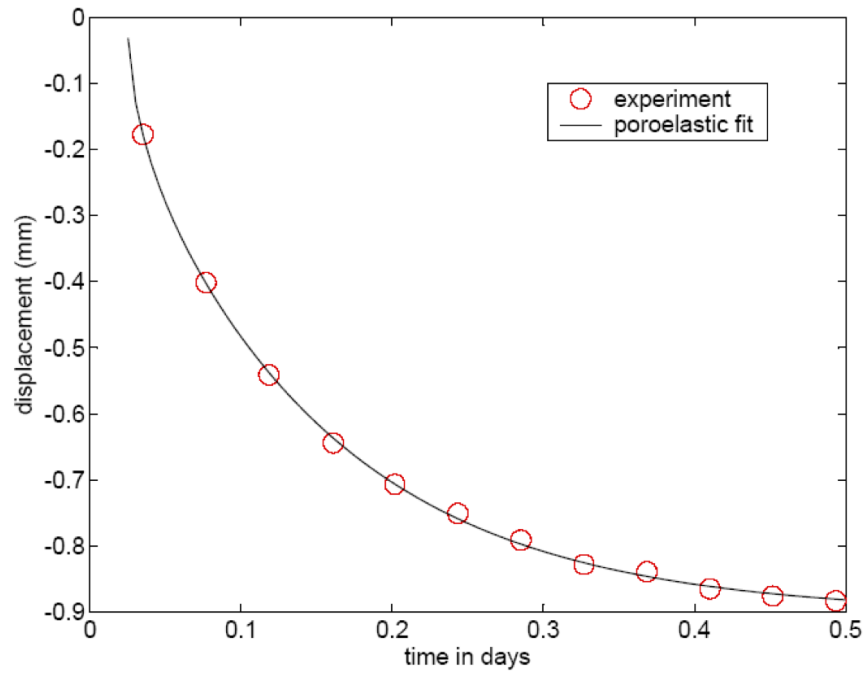


Figure 4–3: Example of experimental compressive creep consolidated data during one cycle compared with the poroelastic model fit. There is a good agreement of the experimental values to the model fit for the initial slope and equilibrium displacement.

Harvest method	Cycle	Compressive modulus, $H_A$ (MPa)	Hydraulic permeability, $\kappa$ ( $\times 10^{-15}$ ) $m^4/Ns^{-1}$	Model fit, $R^2$
BEP	1 (n=5)	$0.70 \pm 0.03$	$0.35 \pm 0.09$	$0.96 \pm 0.03$
	2 (n=5)	$0.72 \pm 0.01$	$0.45 \pm 0.09$	$0.97 \pm 0.02$
	3 (n=5)	$0.75 \pm 0.01$	$0.58 \pm 0.06$	$0.96 \pm 0.01$
	4 (n=5)	$0.76 \pm 0.01$	$0.65 \pm 0.02$	$0.99 \pm 0.01$
	5 (n=5)	$0.78 \pm 0.02$	$0.69 \pm 0.03$	$0.97 \pm 0.03$
mean	(n=25)	$0.74 \pm 0.04$	$0.52 \pm 0.15$	$0.98 \pm 0.13$
CEP	1 (n=5)	$0.69 \pm 0.01$	$0.44 \pm 0.11$	$0.92 \pm 0.01$
	2 (n=5)	$0.70 \pm 0.01$	$0.54 \pm 0.08$	$0.93 \pm 0.01$
	3 (n=5)	$0.72 \pm 0.01$	$0.61 \pm 0.08$	$0.93 \pm 0.01$
	4 (n=5)	$0.73 \pm 0.01$	$0.67 \pm 0.07$	$0.92 \pm 0.01$
	5 (n=5)	$0.77 \pm 0.03$	$0.84 \pm 0.11$	$0.93 \pm 0.01$
mean	(n=25)	$0.73 \pm 0.04$	$0.59 \pm 0.18$	$0.92 \pm 0.01$
NEP	1 (n=5)	$0.24 \pm 0.11$	$0.30 \pm 0.21$	$0.62 \pm 0.16$
	2 (n=5)	$0.51 \pm 0.16$	$0.45 \pm 0.22$	$0.80 \pm 0.21$
	3 (n=5)	$0.64 \pm 0.27$	$0.65 \pm 0.20$	$0.67 \pm 0.23$
	4 (n=5)	$0.84 \pm 0.15$	$0.74 \pm 0.20$	$0.57 \pm 0.31$
	5 (n=5)	$1.10 \pm 0.24$	$0.89 \pm 0.22$	$0.67 \pm 0.26$
mean	(n=25)	$0.71 \pm 0.31$	$0.62 \pm 0.30$	$0.76 \pm 0.29$
mean $\pm$ SD				

Table 4–1: Calculated variables based on fit of mechanical data, comparing intervertebral discs harvested with three different methods.

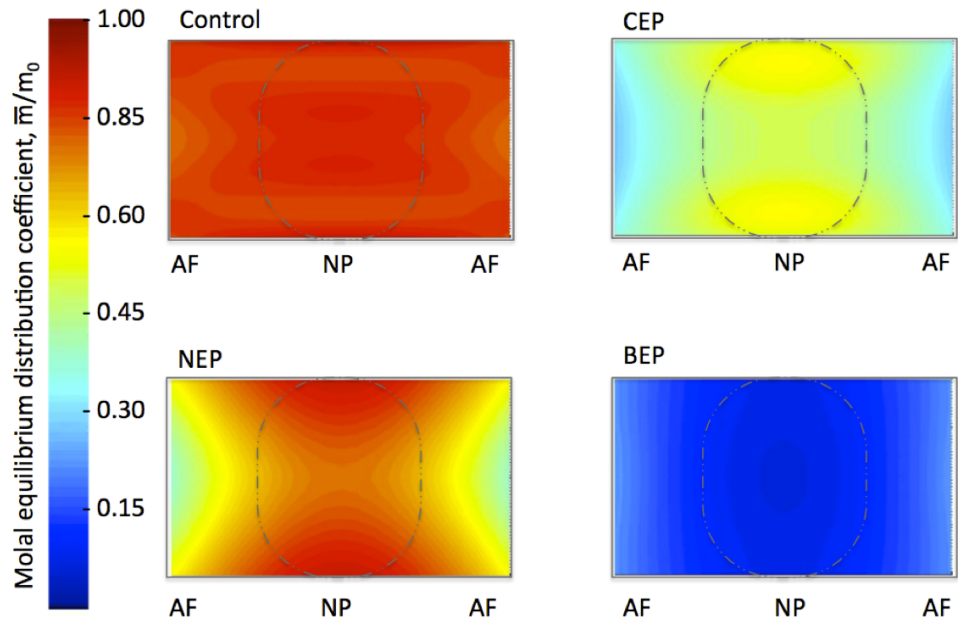


Figure 4–4: Measured diffusion of  $^{35}\text{S}$  into the discs normalized to a molal equilibrium distribution coefficient as used by Urban et al. 2004. The images represent a mid-sagittal cross-section with the  $-\cdot\cdot-$  line indicating the nucleus pulposus region and the remaining area, the annulus fibrosus region.

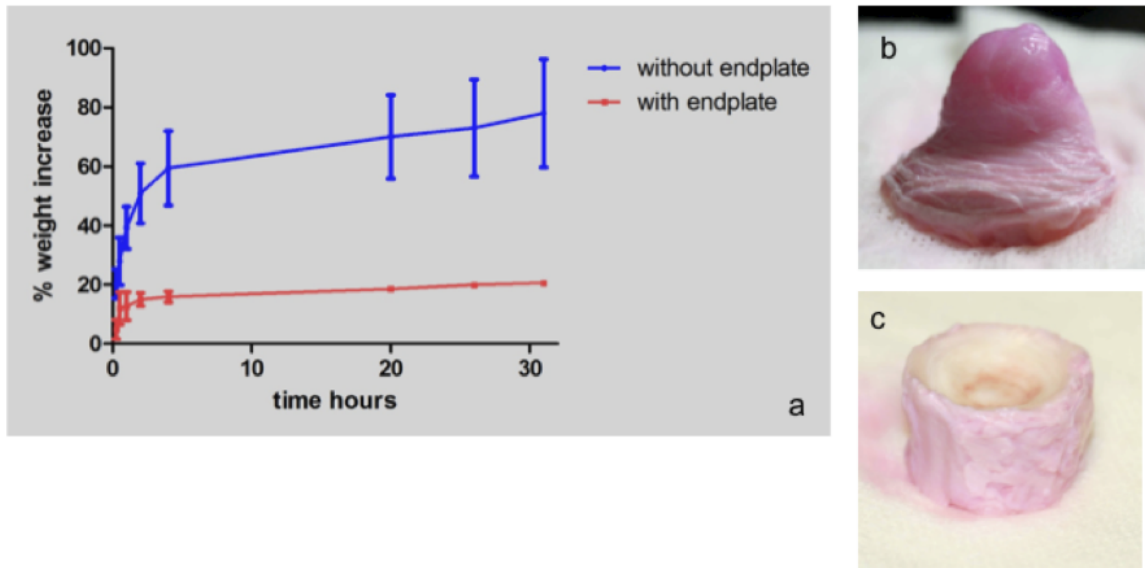


Figure 4-5: (a) Swelling analysis of discs prepared with CEP and NEP shown in % of weight increase. Disc harvested (b) without endplate (NEP) and (c) with cartilaginous endplate (CEP).



## **CHAPTER 5**

### **Short-Term Organ Culture**

In the previous chapter, different possible harvesting methods were evaluated based upon small molecule nutrient transport and mechanical stability. A disc harvested without endplates (NEP) uncontrollably swelled up to double its original weight when left without physical constraint in saline. In contrast, the new harvest method, with intact cartilaginous endplates, could retain the disc's shape in saline without physical constraint despite its 20 % increase of weight over time. Furthermore, small nutrient transport to the center of the disc suffered only a little (75 % compared to control) unlike the discs isolated with endplates (25 % compared to control).

Although the small nutrient transport rate for discs harvested with full endplates was slower, previous groups have shown the possibility of its culture [48]. The hypothesis was that under axial loading culture conditions the waste products and nutrition of the organ could be circulated into the tissue and overcome the slow transport rate, making this endplate method still viable. Therefore in the next steps in the development of the organ culture model, a six-day culture of intervertebral discs isolated with the two different harvesting methods, with a thin layer of cartilaginous endplate (CEP) or with the bony endplates (BEP), was conducted. In this study, measurements of cell viability and metabolism were used to confirm the suitability of the harvest method for our culture system.

## 5.1 Disc Preparation and Culture

Fresh bovine coccygeal discs were harvested from young steers (3 to 6 months of age) freshly obtained from the local abattoir (Reber, Langnau, Switzerland). From each bovine tail four discs were removed consecutively using either the bony endplate or cartilaginous endplate harvesting method. Four different time points were examined for the study: 0, 2, 4 and 6 days. A total of forty-eight discs were analysed, twenty-four for each harvest method, giving six discs for each time point. The harvested discs were rinsed three times in Hanks solution containing 100 U/ml penicillin and 100 µg/ml streptomycin. The disc height and diameter was measured and recorded. The discs were then placed into the polycarbonate culture chambers and into the bioreactor system. Although the aim was to simulate a physiological environment for the disc tissue, as there is no data available for the biomechanics and load of bovine coccygeal tissue, we followed a similar but slightly modified protocol of Lee [115]. A static compressive load of 0.1 MPa for sixteen hours followed by a load of 0.75 MPa for eight hours was used. The longer, low loading period of sixteen hours was used to encourage disc tissue recovery from the high loading conditions. The nominal stress of 0.1 MPa was selected to counter the reported internal swelling pressure of human disc tissue (0.06 to 0.22 MPa) [221].

## 5.2 Viability

After culturing, cell viability and metabolic activity was evaluated. The endplates were removed from the disc with a scalpel blade and the disc was segmented into six annulus fibrosus (AF) and six nucleus pulposus (NP) pieces. The disc was first cut in half across the diameter of the disc. From each disc half, the nucleus was

separated from the annulus, a half-circular piece for the nucleus and a semi-circular strip for the annulus. These pieces were each split pie-like into three additional pieces, giving both the nucleus and the annulus six samples. The isolated tissue segments were weighed. Every second pie piece was taken and digested in 0.1 % pronase for one hour. This was followed by overnight (sixteen hours) 0.025 % collagenase digestion. The digestive enzymes were removed and the cells were isolated with a combination of using Hanks to wash the solution and centrifuging. The isolated cells were counted using a haemocytometer Neubauer chamber (Superior, Bad Mergentheim, Germany) and Trypan blue staining. Four counts per sample were averaged and used to seed cells into a 96-well microassay plate. Each well contained 100  $\mu$ l of media and 20 000 cells. The assay plate was incubated at 37 °C for thirty minutes, allowing cells to settle to the bottom of the well plate.

After the incubation, 50  $\mu$ l of Ethidium Homodimer-1/Calcein-AM (EthD-1, 2  $\mu$ M/calcein AM, 1.6  $\mu$ M) from a Live/Dead® cell viability kit (Invitrogen, Basel, Switzerland) was administered to each well. This was followed by a thirty minute incubation period. The stained samples were imaged with an inverted confocal microscope (Leica, DM Ill filters: IS S450–490 nm and N2.1 S515–560 nm). Five high-resolution digital photographs were taken from each well, using both filters, at five set points distributed over the well. Total live/dead cell counts were extracted using image analysis software (Quantity One®, Bio-Rad, Hercules, CA).

A sample of the live/dead cell viability staining is shown in Figure 5–1. Live cells were visible for specimens harvested using the CEP method after two, four and six days with very few dead cells. The cell viability for specimens harvested using

the CEP method in both the annulus fibrosus (AF) and nucleus pulposus (NP) was maintained over six days with  $62 \pm 22\%$  (annulus) and  $84 \pm 14\%$  (nucleus) for the control and  $74 \pm 18\%$  and  $91 \pm 5\%$  at day 6 (Table 5–1). However, the BEP method, despite showing similar AF viability, had only a NP viability of  $37 \pm 5\%$  at day 6. This low cell viability found in BEP discs confirms the suspicion concluded in the previous chapter, that the lower rate of small nutrient transport found with the BEP method could be inadequate to maintain nucleus pulposus viability for long-term culture in our culture system.

### 5.3 Cell Proliferation

Live/dead staining is a quick method to determine disc viability. However, it is not possible, with this method, to distinguish whether live viable cells are healthy active, stagnant, or dying. Therefore another intermediate step was used to determine the level of activity of the cells with the use of a salt-reduction kit [59]. With salt reduction, the number of active cells in proliferation corresponds directly to the amount of tetrazolium salt reduced, therefore giving an indication of cell activity. The reduction is measured with an enzyme-linked immunosorben assay-plate reader.

In this study, a CCK-8 kit of Dojindo’s tetrazolium salt (WST-8, 2-(2-methoxy-4-nitrophenyl)-3-(4-nitrophenyl)-5-(2,4-disulphophenyl)-2H-tetrazolium, monosodium salt) was used to assess the cell activity over three hours. WST-8 is cleaved to formazan by a complex cellular mechanism that occurs primarily at the cell surface. This reduction depends mostly on glycolytic NAD(P)H production of viable cells and the amount of formazan dye formed would directly correlate to the number of metabolically active cells in the culture.

Isolated cells (20 000/well) were distributed into the wells of a 96-well microassay plate containing 100  $\mu$ l of media. The plate was incubated overnight to allow for cells to settle. 10  $\mu$ l of WST-8 solution was added to each well and the plate was incubated for three hours to allow for cellular dehydrogenase reduction of WST-8 to orange formazan. Photometric analysis was performed using an ELISA plate reader (Spectra Max 190, Molecular Devices, Sunnyvale, CA).

The metabolic activity of the disc cells harvested with the BEP method dropped over the six days for both the AF and NP regions (Table 5–1). The 0% values for the BEP at day 6 was attributed to the low number of remaining cells so that the test could not be properly conducted. The CEP metabolic activity in the Nucleus remained steady but decreased visibly in the annulus.

## **5.4 Glycosaminoglycans and DNA**

### **5.4.1 Sample Preparation**

In the study, the remaining samples, three pieces from the AF and three pieces from the NP from each disc were processed to determine glycosaminoglycans (GAG) content and total DNA. The pieces were weighed and cut into 2 mm by 2 mm sized pieces. They were then digested overnight with papain (Sigma, St. Louis, MO, 60°C, 125  $\mu$ g/ml dissolved in 5 mM L-cysteine HCl, 5 mM Na-citrate, 150 mM NaCl, 5 mM EDTA, pH 6.0).

### **5.4.2 GAG Content**

Glycosaminoglycans (GAG) are one of the major macromolecular components forming the cellular environment. GAGs are found covalently bonded to protein cores to yield proteoglycans, which are present in both the extracellular matrix and

at the cell surface [12]. One of their functions is to provide structural integrity to cells and passageways between cells, allowing for cell migration. Loss of GAG in the intervertebral disc is an early sign of disc degeneration. By comparing the levels of GAG content in the disc over the culture period a marked change in disc composition can be observed.

The use of Alcian blue binding assay to detect GAG content has been previously reported in intervertebral disc cultures [59]. Alcian blue is a tetravalent cation with a hydrophobic core that contains a copper atom, hence its blue color [95]. The four charges allow Alcian Blue to bind to GAGs. The intensity of Alcian blue binding imaged photometrically can be used to quantify the amount of GAGs present.

Prepared papain digested tissue sample solutions were mixed with an equal volume of 8 mM guanidine-HCl. The solution was then precipitated with H<sub>2</sub>SO<sub>4</sub> and Triton X-100 (Sigma), 1 % Alcian blue (8GX, Fluka, Milwaukee, WI), 0.25 % Triton X-100 and 0.5 M guanidine-HCl overnight at 5°C. Samples were washed with 40 % DMSO and the precipitate was dissociated with 4 M guanidine-HCl and 33 % propanol. Optical density was determined using photometrical methods at a wavelength of 600 nm with an ELISA plate reader (Spectra Max 190, Molecular Devices, Sunnyvale, CA).

No significant increase in proteoglycan (GAG) concentration was found after six days in the annulus fibrosus for discs harvested with a thin layer of cartilaginous end plate (CEP) (Table 5–1). However, the value for GAG found in the nucleus was  $847 \pm 469$  mg/g at day 0 and  $1120 \pm 394$  mg/g at day 6. In contrast, the GAG content

in the nucleus of the BEP group were  $933 \pm 740$  mg/g day 0 and  $415 \pm 277$  mg/g at day 6.

#### 5.4.3 DNA Content

DNA analysis gives the total number of cells present in tissue. This method of DNA quantification does not differentiate between live and dead cells. The method merely quantifies the total amount of DNA in a disc and therefore both intact and fragmented DNA is quantified. However, large differences in DNA content between specimens can indicate early cell death during the culture.

In this study, DNA quantification was determined with a bisbenzimidol fluorescent dye (Hoescht 33258, Sigma) [59]. A standard curve was created using known concentrations of calf thymus DNA (Sigma). The samples, previously prepared with papain digestion, were diluted 1:50 with 10 mM tris(hydroxymethyl) aminomethane (Fluka), 1 mM Na<sub>2</sub>EDTA dehydrate, and 100 mM NaCl. The fluorescence of the samples was enumerated with a Hoefer DyNaQuant 200 (Amersham Biosciences, San Francisco, CA) where all readings were performed in triplicate and the mean DNA value was normalized to wet tissue weight.

The results of DNA quantification showed a slight increase in DNA/tissue weight for both the nucleus pulposus and the annulus fibrosus of the CEP harvested specimens over the 6 days (Figure 5-2). On the contrary, specimens harvested with the BEP method showed a slight decrease of DNA/tissue weight in both the annulus fibrosus and the nucleus pulposus over the six days of culture. The main source of deviation of the calculated DNA values was attributed to differences between sample source. This was also reported in Demers' study on the suitability of bovine

coccygeal discs as an intervertebral disc model [32]. Demers showed large varying values of DNA/tissue weight that occurred between disc levels and between different animal sources. Furthermore, the values derived from this study are within the range reported by Demers (Figure 5–3).

Using an independent t-test with Levene’s test for Equality of variances the statistical differences between BEP and CEP DNA values for the respective days and regions was determined. No statistical significant difference was found between the two groups for the DNA in the annulus fibrosus for all culture terms. In the nucleus pulposus, a significant difference was found between CEP and BEP at day 4 ( $M=111 \pm 41$ ,  $t(8)=2.402$ ,  $p < 0.05$ ) and 6 ( $M=229 \pm 94$ ,  $t(8)=2.429$ ,  $p < 0.05$ ). In addition, a one-way ANOVA with a post-hoc Tukey test was used to analyze whether significant differences existed between the length of culture and between experiments within each harvest method for the respective disc regions. A significant difference was found between experiments for the CEP annulus  $p < 0.05$ . A significant difference was also found between both experiments and culture term for CEP nucleus. These differences between the experiments can be used to explain the large standard deviation value of the DNA content.

## 5.5 Discussion

In this study live cells could be found in static diurnal loaded intervertebral discs after six days using both the BEP and CEP harvesting methods. Cell viability of the nucleus suffered using the BEP harvest method, with cell viability dropping below 50 % after 6 days. Furthermore, the low number of remaining cells found in the nucleus pulposus of BEP discs prevented quantification of the cell activity using



salt-reduction methods. In contrast, discs that were cultured with CEP exhibited no significant decrease in nucleus pulposus cell activity.

Cell-isolation has been traditionally the method of choice to quantify cell viability. The method stems from establishing cell lines of biological tissue. The tissue is broken down with digestive enzymes and the freed cells are isolated and stained with a live/dead kit to reveal cell viability. It is a low cost method that allows for visual counting of live and dead cells. Previous studies of intervertebral disc culture have successfully relied on this method to measure both cell viability and metabolic activity [59]. A limitation to this method is that it requires a large number of intact cells, in the order of millions, to be available and isolated from the disc to reliably quantify the live to dead cell ratio. Therefore the process depends largely on the technician performing the isolation. Typically only 50 % of the cells are retained. Furthermore, information on the exact location of where the live or dead cells were in the tissue is lost. Sampling could originate from an area of the disc with low viability therefore misrepresenting the actual cell viability of the total tissue. Another limitation to this method is that only the ratio of live to dead cells can be quantified, not the absolute numbers of live or dead cells.

Laser-confocal microscope on disc sections is another method previously used to determine viability in in-vitro organ culture studies [115]. Thin slices of intervertebral disc tissue are similarly stained with fluorescence chemicals identifying live or dead cells. The tissue is scanned under laser confocal microscopy, layer by layer, with micrometer increments in depth, ultimately producing a three-dimensional image of the disc tissue. One of the advantages of this method is that cells are imaged directly

in the tissue and therefore can immediately convey the number of cells in the tissue as well as the cell distribution. The ability of the microscope to image “into” the tissue is vital. Imaging at the surface may not be representative of cell viability for the total tissues as apoptotic cells can be formed at the surface as a result of the cutting of the tissue. A limitation to the method is that only a limited amount of light can penetrate into the tissue, therefore a thin layer of tissue must be prepared. With the disc’s natural propensity to swell, the imaging must be done quickly after tissue sample isolation and staining as there is a risk that the piece becomes too thick to be visualised properly.

Confocal microscopy is a more expensive method and not all research groups have access to such facilities. Moreover, the cell-isolation method gave enough information to adequately answer the questions posed in the previous study. However, it was during the analysis of the current study that the difficulty of obtaining the appropriate number cells to properly quantify the metabolic activity and cell viability of discs cultured using the BEP isolation method was experienced. It was decided that both the isolation method and the measurement method could no longer be used.

Despite CEP discs maintaining cell viability during the six days, a drop in cell numbers over this period was apparent when preparing cells to administer the live/dead kit. This drop, however, was not seen when DNA/tissue weight was quantified. This difference could be attributed to the methods used to isolate the cells for live/dead analysis and for DNA determination. Fragmented DNA of dead cells that is quantified with DNA analysis would not be accounted for when using live/dead kit

analysis. This discrepancy can be avoided with confocal laser scanning microscopy imaging of tissue, directly labelled with a live/dead kit. The distribution and viability of the cells would therefore be imaged in-situ giving a better indication of tissue viability and cell density. This method was applied to our later studies.

It was clear that the drop for DNA/tissue weight, in the BEP group, was attributed to the early loss of cell viability, as early as day 2. The previous studies have shown that culture of bovine coccygeal with BEP would be difficult due to blood clotting in the endplates that would be developed during the harvest. The work of one group has shown to be successful in this method by administering heparin to the animal prior to slaughter, which in our case, was not possible [48, 93].

Bovine discs are of similar structure to the human and possess the same barriers to nutrient diffusion, but have the advantage of being readily available and not having variable degrees of degeneration [32]. In the previous chapter bovine discs were isolated using three different techniques, and were cultured without external load. Discs isolated without any cartilaginous or bone endplates showed enormous swelling and severe deformation which made them unsuitable for studying repair. On the other hand, discs cultured with both cartilaginous and bone endplates preserved their integrity and shape, but small nutrient transport was compromised. In the current study this was confirmed by the high percent of dead cells after six days in culture, also making it impossible to study repair in this system. In contrast, discs isolated with intact cartilaginous endplates overcame these shortcomings, as both disc integrity and cell viability were maintained. It is likely that with the bone endplate present nutrient supply to the cells in the center of the disc is severely impaired,

but that retention of only the non-calcified cartilaginous endplate allows adequate nutrition to be maintained. While the discs maintained their gross morphology with the cartilaginous endplates present, their weight did increase by up to 20 %. However, the expected increase in disc height with such limited swelling is within the reported diurnal variation range [175]. This may be a major contributor to the retention of cell viability, and may ensure that normal cell metabolism is maintained.

## **5.6 Summary**

The study presented in this chapter has helped define a promising harvesting method to further develop the organ culture model. With the novel CEP harvesting method a six-day culture with good cell viability was shown with diurnal loading. It has been suggested that dynamic loading stimulation would be beneficial for the cells in intervertebral disc organ cultures [105, 115], which was the intention in the development of the organ culture system.

## **5.7 Tables and Figures**

Location	Harvest method	Day	Cell viability (% alive)	Dehydrogenase (activity %)	DNA/ tissue weight (ng/mg tissue)	GAG/ tissue weight (mg/g tissue)
Annulus	BEP (n=6)	0	60 $\pm$ 10	100 $\pm$ 139	0.60 $\pm$ 0.14	166 $\pm$ 80
		2	58 $\pm$ 9	14 $\pm$ 15	0.80 $\pm$ 0.23	114 $\pm$ 68
		4	57 $\pm$ 22	3 $\pm$ 2	0.58 $\pm$ 0.25	196 $\pm$ 94
		6	72 $\pm$ 21	0 $\pm$ 0	0.49 $\pm$ 0.24	354 $\pm$ 159
	CEP (n=6)	0	62 $\pm$ 22	100 $\pm$ 90	0.90 $\pm$ 0.39	295 $\pm$ 79
		2	82 $\pm$ 11	140 $\pm$ 111	1.04 $\pm$ 0.39	371 $\pm$ 211
		4	74 $\pm$ 3	37 $\pm$ 17	1.22 $\pm$ 0.48	271 $\pm$ 96
		6	74 $\pm$ 18	53 $\pm$ 23	1.06 $\pm$ 0.53	311 $\pm$ 177
	BEP (n=6)	0	81 $\pm$ 13	100 $\pm$ 46	0.24 $\pm$ 0.10	933 $\pm$ 740
		2	67 $\pm$ 15	34 $\pm$ 16	0.26 $\pm$ 0.08	431 $\pm$ 278
		4	60 $\pm$ 11	21 $\pm$ 7	0.19 $\pm$ 0.05	654 $\pm$ 593
		6	37 $\pm$ 5	0 $\pm$ 0	0.13 $\pm$ 0.04	415 $\pm$ 277
Nucleus	CEP (n=6)	0	84 $\pm$ 14	100 $\pm$ 78	0.29 $\pm$ 0.10	847 $\pm$ 469
		2	89 $\pm$ 9	79 $\pm$ 27	0.30 $\pm$ 0.16	663 $\pm$ 141
		4	93 $\pm$ 3	102 $\pm$ 27	0.39 $\pm$ 0.07	1124 $\pm$ 277
		6	91 $\pm$ 5	88 $\pm$ 12	0.50 $\pm$ 0.09	1120 $\pm$ 394

Table 5–1: Measured values for the six-day diurnal loading study comparing BEP and CEP harvesting method. Values measured at day 0, 2, 4 and 6 for both the annulus fibrosus and nucleus pulposus.

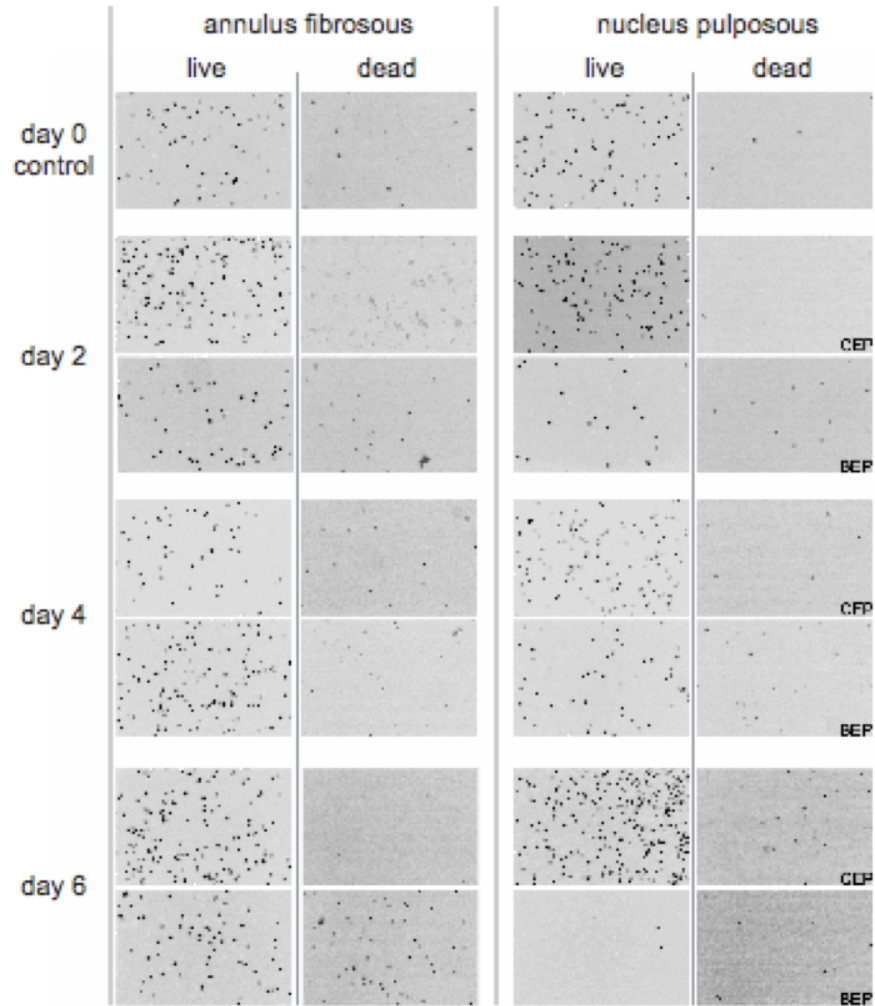


Figure 5–1: Sample images from one experiment showing live/dead cell viability for the disc specimens harvested with BEP and CEP methods for day 2, 4 and 6 in comparison to the control at day 0. CEP shown in the top row for each day and BEP shown below.

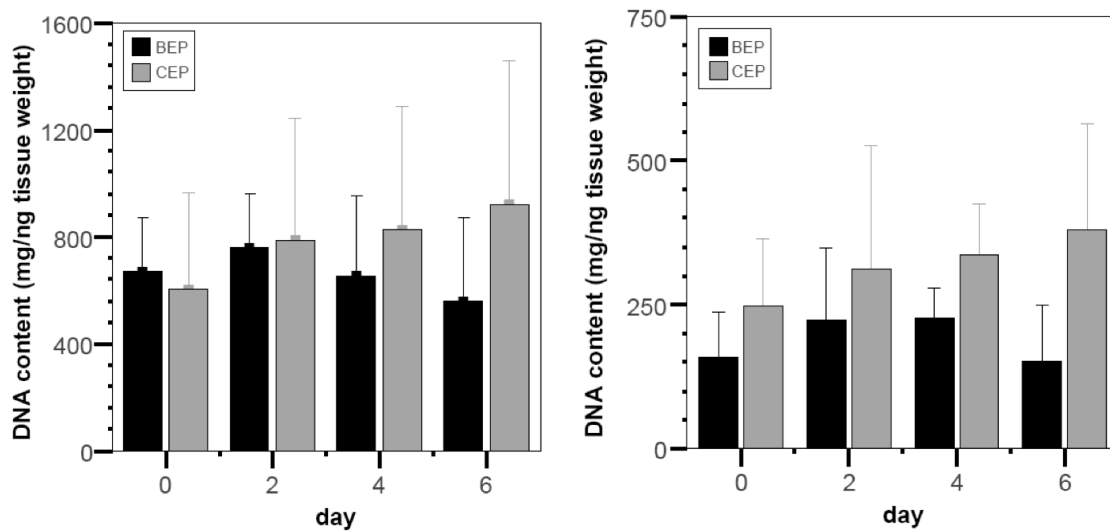


Figure 5-2: DNA content of the bovine coccygeal IVDs. The DNA content in the annulus fibrosus (A) and the nucleus pulposus (B) was measured by the bisbenzimidazole Hoescht H-33258 fluorometric assay. Results are reported per the tissue weight of the respective regions of each disc  $\pm$  standard deviation.

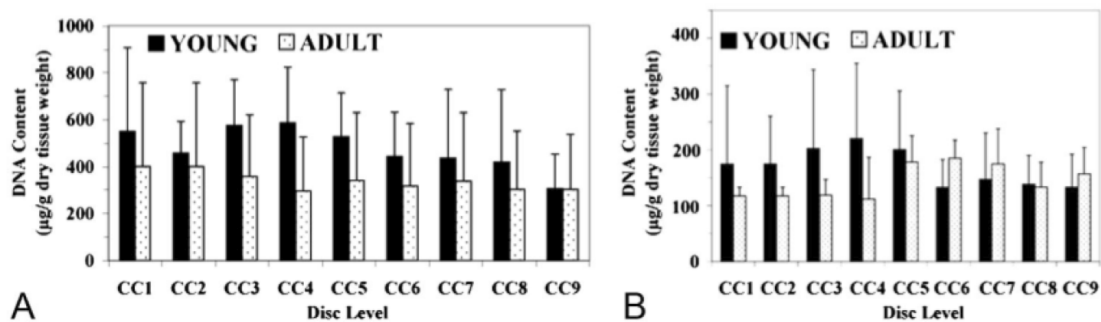


Figure 5-3: DNA content of the bovine coccygeal IVDs. The DNA content in the annulus fibrosus (A) and the nucleus pulposus (B) was measured by the bisbenzimidazole Hoescht H-33258 fluorometric assay. Results are reported per the dry weight of the respective regions of each disc  $\pm$  standard deviation [32].

## **CHAPTER 6**

### **Mechanical Stimulation for Long-Term Culture**

In the previous chapter, the culture of intervertebral disc explants for a period of six days was established and the a harvesting method for our culture system was determined. However, an organ model with a validated culture viability period of six days is not sufficient as a bridging model between cadaver and in-vivo animal models that can be used as a tool to test and develop biological regenerative techniques. Such a model would require discs to be cultured in the range of two to six weeks. With a six-week model, for example, degeneration of the disc can be induced in the first two weeks and the regenerative treatment can be studies in the following four weeks.

Delivering adequate nutrients to the cells of the intervertebral disc is the common difficulty in developing large disc organ culture models [69]. Without external mechanical stimulation, the disc is supplied primarily by small molecule nutrients and only through diffusion, as the disc is avascular [223]. When the disc is small, the diffusion distance is much shorter and therefore this difficulty is overcome. However, for large discs additional stimulation to induce convection of nutrients becomes critical [42, 230], especially for large molecule nutrients such as glucose [42, 223]. This chapter presents a study that extends the culture period of the organ culture model with the use of mechanical stimulation, which has been shown to be effective in increasing nutrient transport to the disc [42, 230]. The study examines the effects



of three different mechanical stimulations: static loading, dynamic loading and naturally confined loading through swelling. Organ culture cell viability was followed for two weeks. The objective of the study was to test the hypothesis that appropriate load could affect, possibly extend the culture period of bovine coccygeal disc in-vitro, while maintaining proper disc cell metabolism. The effects of the different mechanical stimuli were compared using cell viability, GAG content and total DNA analysis. Furthermore, the effect of the loading conditions on chondroadherin and fibromodulin was also explored and the histology examined.

### **6.1 Preliminary Studies**

Prior to this study, preliminary pilot studies were conducted on freshly harvested CEP disc tissue, cultured with the bioreactor system with naturally confined loading conditions through swelling for two weeks to determine feasible culture periods. The cultured discs were able to survive after two weeks in these culture conditions. Based on these positive results the same culture period was used for this study.

### **6.2 Methods and Materials**

Fresh bovine coccygeal discs were harvested with cartilaginous endplates intact from young steers (8–20 months of age) from a local abattoir (Abattoir Bernard Poirier Inc., Montreal, QC). A stainless steel high-speed cutter was used to remove the bony endplates leaving a thin cartilaginous layer preserving the annulus fibrosus and nucleus pulposus tissue underneath. Previous work by us has demonstrated this to be an acceptable isolation technique for intervertebral disc whole explants for culture [87, 88] Freshly harvested control discs underwent the same isolation and analysis. The process of block randomized assignment of discs to the control group

and to the three different culture conditions is illustrated in Table 6–1. A total of thirty-six discs were harvested, nine discs to each loading condition group and the control group.

The isolated discs were rinsed three consecutive times in Hanks solution containing 100 U/ml penicillin, 100 µg/ml streptomycin and 500 µg/ml fungizone. The discs' height and diameter were measured under an equilibrating compressive load of 50 N, applied between parallel platens, which is for a disc diameter of 25 mm approximately 0.1 MPa load. Weights for the isolated discs were also recorded. The discs were cultured in Dulbecco's modified Eagle medium, containing HEPES buffer, 5 % fetal calf serum, 0.1 % ascorbic acid, 250 µg/ml fungizone, 1 % glutamax I, 100 U/ml penicillin and 100 µg/ml streptomycin.

### **6.3 Mechanical Loading**

Three different loading conditions were used: (1) static diurnal load with a constant load of 0.2 MPa for sixteen hours followed, by a high load of 0.8 MPa for eight hours, (2) dynamic: diurnal load of 0.2 MPa static load of sixteen hours followed by a  $0.5 \pm 0.3$  MPa sinusoidal load of 0.3 Hz for eight hours, (3) naturally self-confining load (without additional external load). The discs were placed into sterile culture chambers with continuous media circulation and subjected to one of the three loading conditions. The control discs were analyzed immediately after harvest.

### **6.4 Preparation of Disc Tissue for Analysis**

The discs were removed from the culture chambers and again, the weights, heights, and diameters were measured. A custom designed cutting tool with three parallel histological blades was used to isolate concurrently two cross-sectional slices,

being 1 mm and 3 mm thick respectively as shown in Figure 6–4. The 1 mm slice was used to determine cell viability. The 3 mm slice was used for protein analysis, histological evaluation and proteoglycan quantification.

## **6.5 Tissue Viability**

The 1 mm thick slice of the disc was further divided into nucleus pulposus and annulus fibrosus pieces (3 mm×3 mm×1 mm). Samples were incubated for thirty minutes in serum free medium containing fluorescent dyes (Live/Dead® viability kit, Invitrogen, Basel, Switzerland) according to manufacturer’s instructions, using 1 mM each of calcein (green fluorescence, 494/517 nm) and ethidium homodimer-1 (red fluorescence, 528/617 nm, in the presence of DNA). The pieces were then transported for imaging. Using an inverted confocal laser scanning microscope (Zeiss LSM 510) twenty consecutive images were scanned, starting from the surface, at 6 µm intervals. The confocal laser scanning microscope image stack was split into single images. The first image to be analysed was chosen approximately five images into the stack to avoid artefacts from the cut surface. A total of ten consecutive images split into single colour red or green images were saved into JPEG file formats for each tissue sample. The labelled cells were quantified separately using CellC® (Matlab based software developed by Tampere University of Technology).

## **6.6 Protein Analysis**

### **6.6.1 Extraction of ECM Proteins and Proteoglycans**

Nucleus pulposus and annulus fibrosus tissue were isolated and finely diced. The proteins were extracted at 4 °C under continuous agitation for forty-eight hours. The wet weight was measured, and then the pieces of tissue were frozen and lyophilized.

Extraction was conducted on a wet weight per volume basis using 15 volumes extraction buffer (4 mol guanidine hydrochloride, 50 mmol sodium acetate, pH 5.8, 10 mmol EDTA) [64]. The extracts were then cleared by centrifugation at 16 000 *g* for thirty minutes. 40  $\mu$ l portions of GuHCl extracts of the samples were precipitated with a final concentration of 90 % (v/v) ethanol. Proteins from the precipitate was recovered with 10 000 *g* centrifugation and washed twice with 750  $\mu$ l of cold 80 % (v/v) ethanol.

### **6.6.2 Fibromodulin and Chondroadherin**

For fibromodulin and chondroadherin analysis using the Western blot method, 15  $\mu$ l of protein suspension each was electrophoresed on 7.5 % (fibromodulin) and 10 % (chondroadherin) SDS-polyacrylamide gel, respectively. Proteins were transferred onto nitrocellulose membranes with electrophoresis at 40 V for ten minutes, then at 30 V overnight. The membranes were blocked with 3 % (w/v) skim milk in Tris-buffered saline, pH 7.4, containing 0.05 % (v/v) Tween 20 for sixteen hours at 4 °C. A rabbit polyconal antiserum specific for either fibromodulin (1:1000) or chondroadherin (1:2000) was used as first antibody. The polyclonal rabbit antibody recognizing human chondroadherin was a kind gift from Dr. Dick Heinegård, Lund University, Sweden [111]. The second antibody was a horseradish peroxidase (HRP) conjugated anti-rabbit antibody (Santa Cruz Biotechnology) diluted in a 1 % (w/v) skim milk in Tris-buffered saline/Tween solution. Chondroadherin and fibromodulin were visualized by chemiluminescence detection (GE biotechnology).

## 6.7 Glycoaminoglycans Analysis

In the previous experiments, an Alcian blue assay was used to determine glycoaminoglycans (GAG). However dimethylmethylenblue (DMMB) assay is a more sensitive test to detect GAG, requiring 10 times smaller sample volumes [92]. A 1:500 dilution of a prepared solution of dry weight tissue extracted with 30 volumes 4 mol GuHCL, 50 mmol NaOAc, 10 mmol EDTA, pH 5.8 was used for DMMB assay to determine glycoaminoglycan content. A volume of 20  $\mu$ l for each well was taken from each sample of diluted mixture and distributed in duplex to 96 well plates. Absorbance was measured with a Bio-TEK ELx absorbance microplate reader ELx 800 (VT, USA). Samples were diluted to fall in the middle of the linear range of the standard curve.

## 6.8 Histological Evaluation

A cross-sectional 2 mm thick slice was cut from the centre of the previously isolated intervertebral disc tissue and fixed in 4 % buffered para-formaldehyde, 3 samples were processed for each loading condition. The slices were further separated into annulus fibrosus and nucleus pulposus sections. The sections were serially dehydrated in ethanol and subsequently infiltrated and embedded in paraffin. Sagittal 6  $\mu$ m sections were prepared using a microtome. The paraffin was removed with xylene and rehydrated through graded alcohol. Specimens were stained with alcian blue (glycoaminoglycans), hematoxylin (nucleus and cytoplasmic structures) and eosin (cellular proteins).

## 6.9 Statistical Analysis

Nucleus pulposus and the annulus fibrosus regions were analyzed separately. Only three somewhat similarly geometrically sized discs could be obtained from each tail, which were used for the three loading conditions. Control discs were harvested with the same isolation method but were analyzed immediately.

SPSS statistical software was used to analyze the raw data. Mean  $\pm$  1 standard deviation was used to present all results. Significant differences between culture conditions were determined for the DMMB assay using a one-way ANOVA and Fishers PLSD posthoc test to detect differences between groups with a  $p$  value of  $< 0.05$ .

## 6.10 Results

### 6.10.1 General Observation

Initially nine discs were assigned to each group. However, three discs from both the static diurnal and dynamic diurnal loading group were contaminated leaving only six specimens for analysis.

Macroscopic changes could be seen for the specimens subjected to the different loading conditions when compared to freshly harvest control discs. The outer annulus for both the dynamic diurnal and static diurnal loaded specimens were stiffer and appeared significantly compressed. The disc culture under naturally self-confined loading conditions showed an increase in volume and a slight bulge in the nucleus pulposus region when compared to fresh discs. Quantified data of disc geometry, GAG and cell viability is presented in Table 6–2.

### 6.10.2 Cell Viability

Figure 6–6 shows a composite stack of ten images capturing a 60  $\mu\text{m}$  thick tissue slice, 50  $\mu\text{m}$  from the exposed surface. Representative images of a single live/dead image taken from each loading condition are also shown in Figures 6–7 for the annulus fibrosus and 6–8 for the nucleus pulposus.

Cell viability showed a drop in both nucleus pulposus and annulus fibrosus cell viability for static diurnal and dynamic diurnal loaded discs (Figure 6–9). Under naturally self-confined loading culture conditions, cell viability showed similar levels compared to fresh control discs. In the static diurnal culture group, three out of six discs were completely absent of viable cells after two weeks. For the dynamic diurnal culture group only two out of six discs had only dead cells in both the annulus and the nucleus. Cell death was much higher in the annulus than the nucleus in both diurnal-loading groups.

### 6.10.3 Protein Analysis

#### **Fibromodulin and Chondroadherin**

Annulus fibrosus and nucleus pulposus samples of the control and the three different loading conditions were analyzed for both fibromodulin (FM) and chondroadherin (CHAD). FM was found in all specimens and in both nucleus pulposus and annulus fibrosus around the 50 kDa marker (Figure 6–10a), which is plausible for the size of FM, reported at 59 kDa [66]. In the nucleus, the FM quantity appeared lower in all three culture-conditions compared to freshly harvested discs. The static diurnal loaded had the greatest number of specimens that had little to no FM.

In the annulus fibrosus, FM quantity did not appear to differ between groups, however two out of nine specimens in the naturally self-confined loading group had an absence of FM signal whereas a strong signal for FM was found in both the static diurnal and dynamic diurnal loaded groups. No secondary band was found below 50 kDa, which would indicate degradation fragments of FM.

CHAD was found in the nucleus and annulus for all specimens with higher intensity in the nucleus and lower in the annulus (Figure 6–10b). CHAD was expressed at the 36 kDa marker, which is consistent to its reported size [169]. All cultured groups showed a similar intensity of the protein in the nucleus pulposus in comparison to the control. Prominent secondary bands, which indicate the presence of degradation fragments, were not found. In the annulus, CHAD intensity was weaker for some samples for the cultured groups when compared with others on the same gel. Furthermore, the abundance of CHAD seemed less in the naturally confined loading group, however since each culture condition was run on a different gel, this difference may only be an artifact.

### **Glycoaminoglycans**

The data is expressed in percentage of wet tissue weight in Table 6–2. A normalized value of GAG with respect to control discs is presented in Figure 6–11. The average GAG content of the fresh control discs was  $104 \pm 30$  mg/g for the annulus and  $602 \pm 41$  mg/g tissue for the annulus. After two weeks of culture under the different loading conditions, all discs showed a drop of GAG in both the nucleus and the annulus. The drop for annulus GAG contents were however not significant. Static diurnal loaded specimens dropped by 10 % in annulus GAG content, dynamic



diurnal loaded specimens by 70 % and naturally self-confined discs by 50 %. A most significant ( $p < 0.05$ ) decrease in GAG content was found for the nucleus with static diurnal loaded specimens dropping by 50 %, dynamic diurnal loaded specimens by 25 % and naturally self-confined cultured specimens by 75 %.

#### **6.10.4 Histological Evaluation**

Qualitative morphologic changes were apparent between the groups. Proteoglycan was found in both annulus fibrosus and nucleus pulposus regions of all samples. However, the intensity varied (Figures 6–12, 6–13). The number of cells, cell shape and distribution also differed between the different groups in the nucleus pulposus. Most notably the presence of cell clusters of more than twenty cells could be seen in the nucleus pulposus for both, the dynamic loaded and naturally self-confined groups (Figure 6–13). In the outer annulus fibrosus similar fibroblasts-like-cells were found distributed evenly along the lamellae with clusters of more than twenty cells found for all groups (Figure 6–12).

#### **6.11 Discussion**

The initial objective of this study was to evaluate the effect of different mechanical stimulations on the culture of bovine intervertebral discs in order to maintain its in vitro culture. The investigation of static, dynamic and self-confined loads on intervertebral disc explants have only been briefly studied on short term organ culture models. Furthermore most studies on larger organ culture have focused on short-term cultures of less than one week as the development of organ culture models have proven to be a complex undertaking [105, 115]. At the end of the two-week culture period it was clear, macroscopically, that the cultured discs were different

in appearance than that of freshly harvested discs. It was most prominent in the static and dynamic stimulated specimens that the outer annulus suffered from excessive mechanical load. Furthermore the discs cultured under self-confined conditions showed bulging in the nucleus region.

Imaging live and dead cells to a depth of more than 100  $\mu\text{m}$  from the surface is difficult especially in the annulus due to the density of the fibres. The first 30  $\mu\text{m}$  contained a majority of red (dead) cells resulting from cutting tissue pieces in preparation for staining. Live/dead cell counts from the ten consecutive images showed a gradual decrease of dead cells along with a gradual increase of live cells (Figure 6–5). The cutting artefact could not be eliminated due to the imaging limitations. Assuming that dead cells are either the result of cutting artefact (depth-sensitive parameters) or the result of non-suitable culture conditions (non depth-sensitive uniform parameter) the highest percentage of the cells was chosen to represent cell viability resulting from culture.

The cell viability results indicate that discs cultured under self-confined unloaded conditions are able to retain close fresh disc cell viability after two weeks. In contrast, dynamic and static diurnal loaded discs experienced severe losses particularly in the annulus fibrosus. This finding is consistent and can be attributed to the severely compressed outer annulus. The cell viability results also suggest the sensitivity of intervertebral discs to mechanical load. Despite identical dynamic loads, discs in the dynamic stimulated group exhibited two extremes. Discs were found to have a high cell viability in the both the nucleus and annulus or completely void of live cells. Static diurnal loaded discs performed even worse, which supports the belief

that dynamic load may be beneficial in the maintenance of cell viability but static load causes a decrease in metabolic activity of articular chondrocytes in vitro and can lead to alterations in the histological and biochemical properties of intervertebral disc in vivo.

Despite the consistent presence of live cells for discs cultured in self-confined unloaded conditions, glycosaminoglycans content analysis showed a more than 50 % loss of initial GAG over the two weeks. This result could suggest that although the viability of the cells was maintained, the metabolic activity of the cells decreased. Slightly higher values of GAG content found in the dynamic and static loaded groups may support the role of mechanical stimulation in GAG production [26]. The timeline for the loss of GAG was not clear. In retrospect, measuring the amount of GAG in the media could have been useful to determine whether the loss was immediate from the harvest or if it was progressive over the two-week culture period.

So far our studies have looked at the macroscopic behaviour of the cultured disc tissues and have only begun to take a look at the cellular response of the disc tissue in culture. It is through looking at the biochemistry of the disc that the state of the organ culture can be assessed. The measure of GAG shows whether the disc maintains proteoglycans over the culture period. It is known that a drop of proteoglycan content occurs in a degenerated disc. Studies have shown different indicators of disc degradation through the analysis of metalloproteinase (MMPs) [15, 44, 78, 81, 106], cytokines [232] as well as the abundance and fragmentation of certain proteins such as fibronectin [154], fibromodulin [190, 206] and chondroadherin [57] have been shown to be linked with good and poor mechanical loading stimulation

as well as age related disc changes. Therefore whether the disc is synthesizing the same combination of these components as to healthy control discs, becomes a good indicator for the validity of the in-vitro organ culture model.

The extracellular matrix is understood as the steady structure in the intervertebral disc that facilitates cell attachment, dictates disc architecture, form and function. Recent evidence suggests that the extracellular matrix also plays an instructive role [25, 154, 189, 190], providing structural information or cues to integrins and other cell surface molecules. This allows the cell to sense mechanical alterations in its microenvironment. Studying proteins that interact either with cells of the intervertebral disc or with the extracellular matrix may possibly measure effects of mechanical stimulation to the explants in culture.

Two such proteins, fibromodulin and chondroadherin, have previously been examined in cartilage tissue [25, 138, 148, 173] and furthermore fibromodulin has also been examined in intervertebral disc tissue [138, 173]. The above proteins' known roles in cartilage were summarized in Figure 6–3.

Fibromodulin is the most abundant member of the leucine-rich repeat protein family, a 59 kDa collagen binding protein [65]. It is known to interact with both, types I and II collagens, and is thought to have an important role for fibre formation [65]. Degraded fragments of the core protein have been reported to be present in rheumatoid and osteoarthritic cartilage, as well as with age [30, 190]. Furthermore, fragmentation of fibromodulin in experimentally injured ovine intervertebral discs has been found to correlate temporally and spatially with annulus fibrosus remodelling [138].

Chondroadherin is a cartilage protein with cell binding properties and also a member of the leucine-rich repeat family of the extracellular matrix proteins [148], with a mass of 36 kDa. Chondroadherin has been shown to bind cells via the integrin  $\alpha 2\beta 1$ , which does not induce spreading of cells [25]. A high expression of this cell binding protein in a dynamic region of cartilage suggests the importance of the protein in the regulation of chondrocyte growth and proliferation [201]. As chondroadherin may play a role in promoting matrix homeostasis, changes in its abundance or structure might be expected to lead to pathological changes in the tissue.

It is commonly thought that the degradative changes in the extracellular matrix are detrimental to disc function, a property that is exacerbated by the accumulation and slow removal of the extracellular matrix degradation products. While the rate at which these changes occur could vary between individuals, they are thought to form the basis of the tissue loss associated with disc degeneration. Changes in the abundance and structure of fibromodulin and chondroadherin along with aggrecan can help determine whether disc degeneration is evident in the organ culture disc model.

Lower amounts of fibromodulin were found in some samples of the nucleus pulposus region for all cultured groups compared when compared to the control. This was most apparent in the static loaded group. This could suggest that all of the discs suffered degradation changes similar to that experienced with aging [206]. The increase of chondroadherin in all cultured discs in both annulus and nucleus can be linked to the stiffening of all cultured explants after two weeks as cartilaginous

cells express chondroadherin [201]. The presence of chondroadherin has been found to indicate major change in the properties of the territorial matrix immediately surrounding the cells [201]. However since the different culture condition samples were not run on the same gel with the control, this claim can not be clearly made.

Previous groups have shown marked degeneration of the disc through measuring the abundance matrix metalloproteinase (MMP) [177, 207], the fluctuation in MMP quantities can occur in both healthy disc remodelling as well as in unrecoverable degradation of the tissue. The abundance of FM and structure of the protein is linked to the age-related changes of the disc [206]. Indications such as fragmentation of FM would suggest the disc structure to exhibit an aging degeneration. CHAD is a protein that has been linked to interacting with collagen, influencing the generation of collagen fibres. An increase of CHAD is another indicator of age-related degeneration [57, 201], suggesting a potential increase of collagen fibres in the cultured disc tissue, leading to a more fibrous disc.

Cell viability alone could not be used to study the effects of mechanical stimulation on cultured discs. The influence of mechanical stimulation on structure such as the extracellular matrix and the distribution of cells within the disc must also be studied. Histological analysis of the disc tissue after the mechanically stimulated culture was thus necessary.

The ideal histological section is a cross-section including the outer and inner annulus fibrosus as well as the nucleus pulposus. A cutter was developed using histology cutting blades so that a cross-sectional 3 mm slice of intervertebral disc tissue could be isolated (Figure 6–2) to be fixed (a standard step in histological methods).

However, cutting such a large piece of fixed tissue using a microtome and with only a few micrometers in thickness is not easy. We discovered that the tissue had to be clamped down during paraformaldehyde fixing to counter the natural swelling of intervertebral disc tissue so that the structure of the disc tissue could be preserved. After the specimens were fixed and embedded in paraffin, uniform cuts were still difficult to obtain because of the differences in stiffness between cartilaginous endplates and disc tissue. Decalcification of the tissue prior to sectioning became necessary to avoid such differences in stiffness.

Histological analysis showed no noticeable change in the organization of lamellae in the annulus fibrosus of all loaded discs when compared to fresh discs. However the magnitude, frequency and duration of the load and a longer culture terms is required to determine if macroscopic structure is truly maintained. In the nucleus of the cultured discs, clusters of cells were found in both the self-confined unloaded and dynamic loaded specimens. The presence cell clusters have been linked early osteoarthritic degeneration in disc tissue [176].

The result of over compression on the outer annular ring of static and dynamic loaded disc tissue is an artefact of the organ culture system. The initial design of the system was based on a future migration to load human intervertebral discs that have parallel flat endplates. The system did not account for the concave nature of bovine coccygeal discs, which was introduced with our novel harvest method. In the early validation of disc cell viability after one week of culture this artefact was not noticed. When this artefact was first noticed a study to determine the minimal amount of load that was required for full contact of the disc tissue to the axial loading

platens was determined. A load of 0.1 MPa was found to be sufficient to overcome this. A 0.1 MPa load that is initially concentrated on 2–3 mm of the outer annular ring can become a 1.0 MPa load for the outer disc tissue to bear. Initially it was thought that since the disc was loaded with a minimal load of 0.1 MPa at all times to counter disc swelling pressure, the concentrated load to the outer rim of the disc would be alleviated. However, this experiment clearly shows that perhaps the altered biomechanics had a negative effect on the outer annulus causing the cells to die over the two-week culture period. A modification to the porous platen of the bioreactor system must be made to accommodate to the concave nature of bovine coccygeal disc tissue. With the natural variation of biological tissue there will be no perfect adaptation to the concave curvature of all discs therefore a study to test different porous platen shapes while measuring the distributed inner pressure across the disc would be required to determine the optimal platen shape. This method of intradiscal pressure measurement has been developed by McNally using a transducer attached to a needle of 1.3 mm thickness [134]. The slim design of the instrument would be suitable for measuring the intradiscal pressures of bovine coccygeal disc and would be a valuable tool to help improve the bioreactor system to overcome over compression of the outer annulus ring and validate bovine coccygeal disc mechanics which have not previously studied in detail.

The discs left to self-confined loading showed similar levels of cell viability as freshly harvested disc tissue. However the level of GAG measured was markedly less than 30% in the nucleus pulposus when compared to the control. Furthermore, a decrease in fibromodulin was also found. These findings show, despite the maintenance



of viable cells, this disc tissue was exhibiting early degeneration behaviour with a rapid decrease of cell activity. This loading condition could be a beginning to the development of an age-related degeneration disc model.

### **6.12 Summary**

In this study bovine coccygeal intervertebral discs were used to evaluate the influence of mechanical load for a two-week culture term. This was the first step towards developing an organ culture model that can be mechanically stimulated for long-term culturing. Although there were promising results in the early study for a one-week culture term, for two-weeks, comparing different loading conditions, overloading of the disc causing loss of cell viability and GAG was the end result. The expected outcome of maintaining disc metabolism and cell viability through dynamic loading was not realized. Further work is needed to understand the factors which led to this result. The mechanical loading protocol, despite being similar to previously reported loads might not have been delivered to the disc as intended because of the concavity of bovine endplates.

Furthermore, improvement in the culturing method is still required to eliminate the occurrence of tissue infection. The failure of the experiment to produce a two-week organ culture model with consistent results led to two conclusions:

1. The bioreactor needed to improve, i.e. optimising the disc interface with stress-profilometry.
2. The culturing protocol needed to be validated i.e. repeating the experiment with only the natural, self-confining loading condition for two weeks.

### **6.13 Tables and Figures**

Tail	1	2	3	4	5	6	7	8	9	10	11	12
CC level 1	D	S	U	C	C	U	D	S	C	D	S	U
CC level 2	U	D	S	C	C	S	U	D	C	U	D	S
CC level 3	S	U	D	C	C	D	S	U	C	S	U	D

Control = C , Static = S , Dynamic = D , Unloaded = U

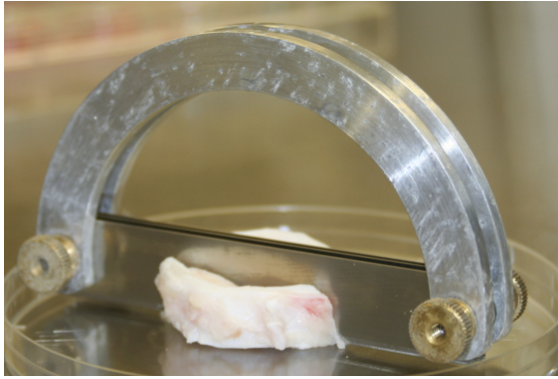
Table 6–1: Block randomized assignment of discs for each loading condition and control. A total of thirty-six discs were harvested, nine discs for each group.

Location	Condition	Diameter (mm)	Height (mm)	Weight (g)	GAG/DW (mg/g tissue)	Cell Viability (%)
Annulus	Control (n=9)	24.66 ± 2.18	9.67 ± 1.31	6.29 ± 1.56	104 ± 30	75 ± 14
	Static (n=6)	23.71 ± 1.15	10.59 ± 1.34	6.79 ± 1.78	95 ± 46	38 ± 43
	Dynamic (n=6)	24.12 ± 1.42	10.16 ± 1.15	6.45 ± 1.77	34 ± 15	51 ± 39
	Unloaded (n=9)	24.55 ± 2.61	9.42 ± 1.32	6.11 ± 1.63	50 ± 17	76 ± 9
Nucleus	Control (n=9)	24.66 ± 2.18	9.67 ± 1.31	6.29 ± 1.56	602 ± 41	74 ± 12
	Static (n=6)	23.71 ± 1.15	9.97 ± 1.34	6.79 ± 1.78	315 ± 63	45 ± 49
	Dynamic (n=6)	24.12 ± 1.42	9.63 ± 1.15	6.45 ± 1.77	426 ± 31	68 ± 35
	Unloaded (n=9)	24.55 ± 2.61	9.42 ± 1.32	6.11 ± 1.63	141 ± 28	79 ± 13
Data is presented ± SD						

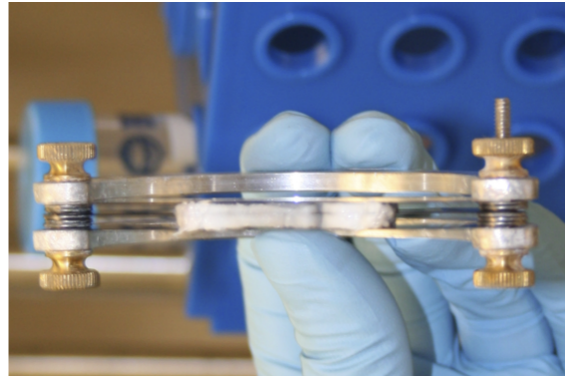
Table 6–2: Summary of quantified data: disc geometry, GAG and cell viability for the control and the different culturing conditions.



Figure 6-1: Sample image of dynamically loaded bioreactor chambers



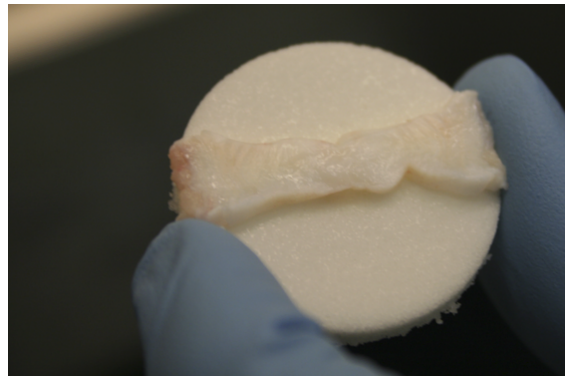
(a)



(b)



(c)



(d)

Figure 6-2: Sample images of disc specimen preparation for biological analysis. Isolation of slices with a custom jig fixture (a) can produce samples with a thickness of 2 mm and 3 mm in parallel (b). Disc slices are further separated with a scalpel blade (c). A 3 mm slice was used for histological analysis (d), placed between porous platens and fixed in 4 % paraformaldehyde.

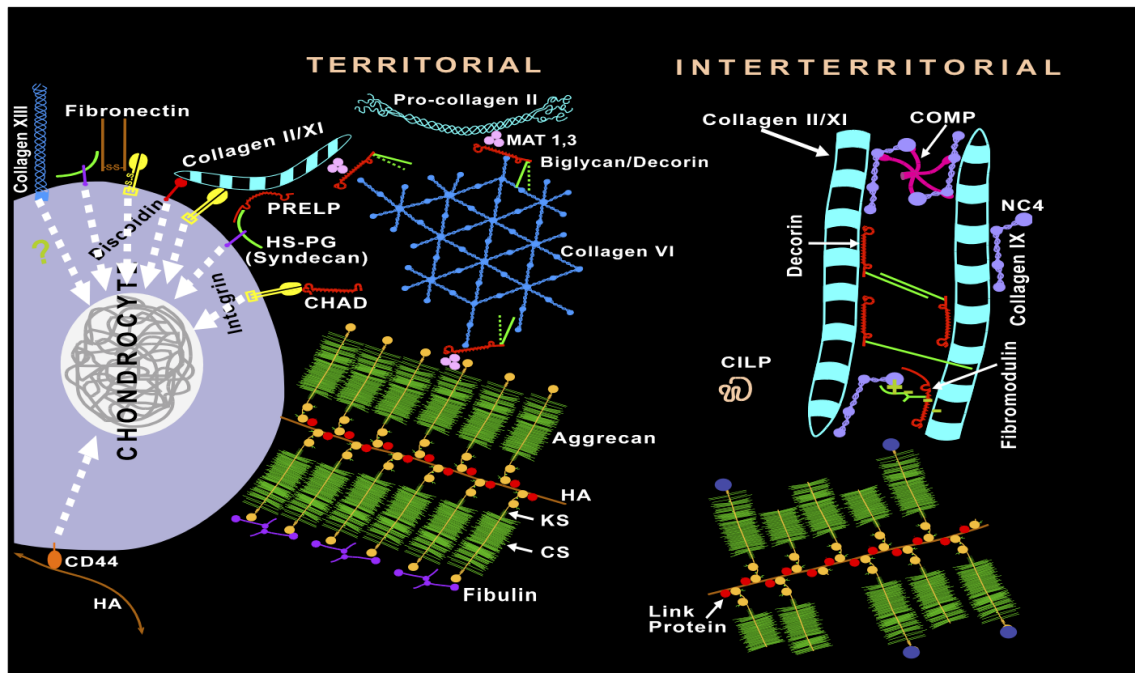
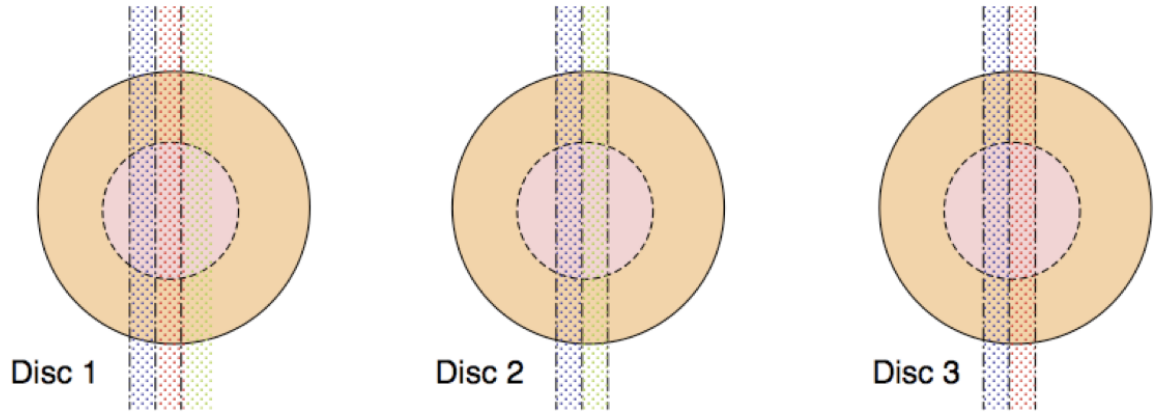


Figure 6–3: Schematic diagram of territorial, chondroadherin (CHAD) and interterritorial, fibromodulin as seen at the molecular level. CHAD can be found to interact with integrin and bound to the surface of chondrocyte. Fibromodulin can be found to be attached to collagen fibres of the extracellular matrix, involved in protein linking.



(a) Three discs from one loading condition



(b) Live/dead slice  $3\text{ mm} \times 3\text{ mm} \times \text{disc height}$

Figure 6–4: Schematic of the isolation of intervertebral disc tissue for biological analysis. From each experimental set of three discs from one culture condition, 1–2 mm section and 1–3 mm section was removed laterally across the disc. Live/dead and protein analysis was performed on all three specimens. A histological sample of 3 mm was taken from the first disc of the set. The annulus and nucleus pieces sectioned from the 2 mm slice is illustrated in (b).

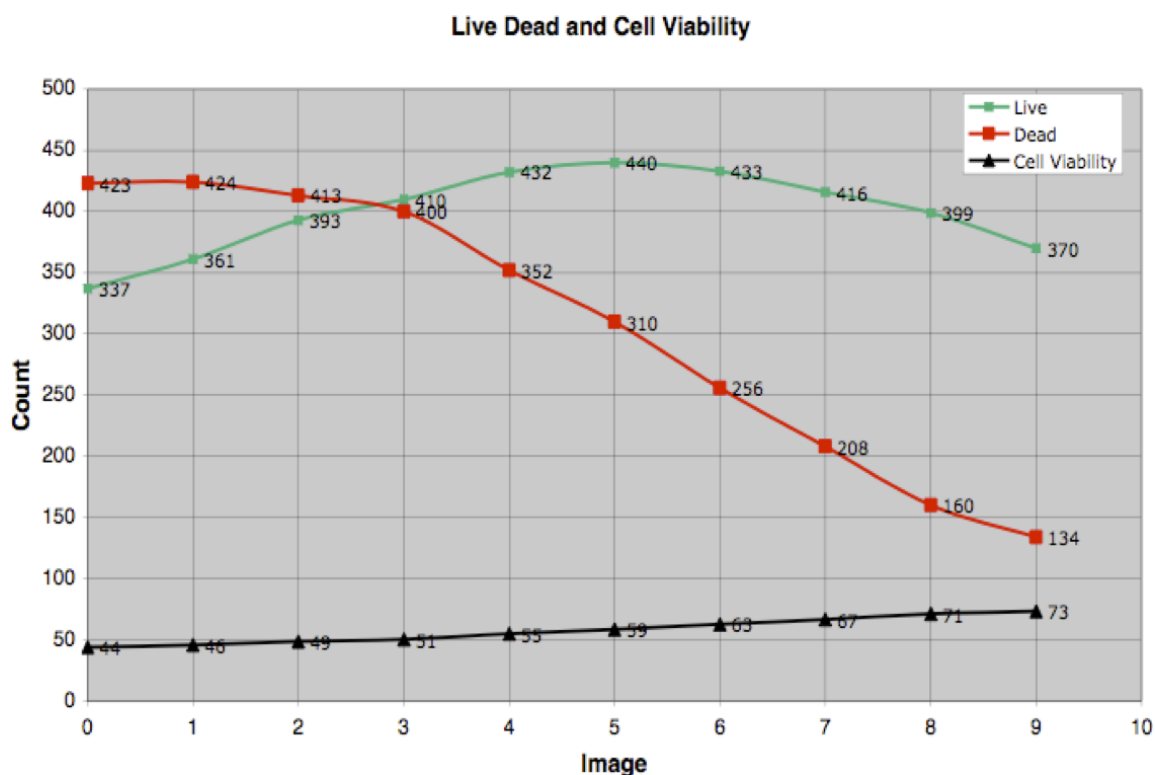


Figure 6–5: Sample plot for cell viability quantification. Maximum cell viability was taken as the true cell viability value. High numbers of dead cells at cut layer can be seen in the first three slices. As the slices progress away from the cut layer, the numbers of dead cells decrease. However this artifact can not be completely eliminated as the clarity of the images decreases progressively as imaging depth increases (a limitation of the confocal laser scanning microscope to image a depth of 200  $\mu\text{m}$ , at best).

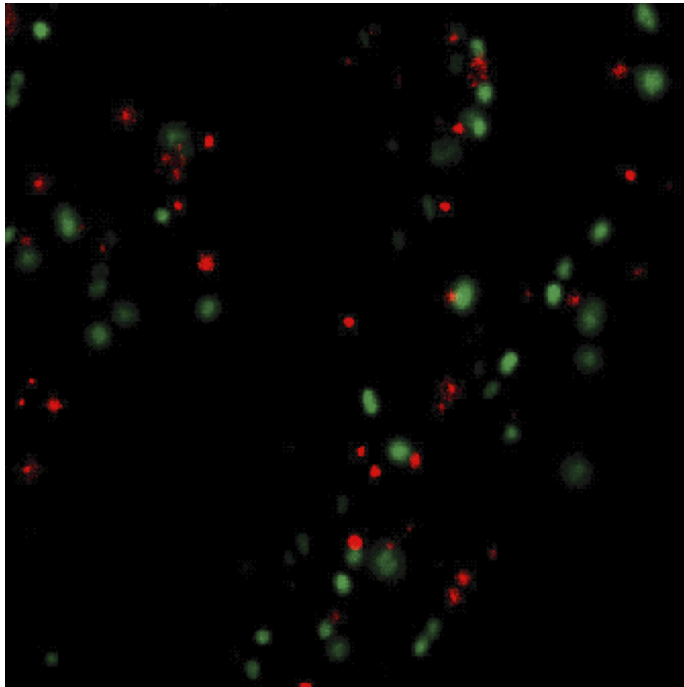


Figure 6–6: Sample stacked image obtained from confocal microscopy.



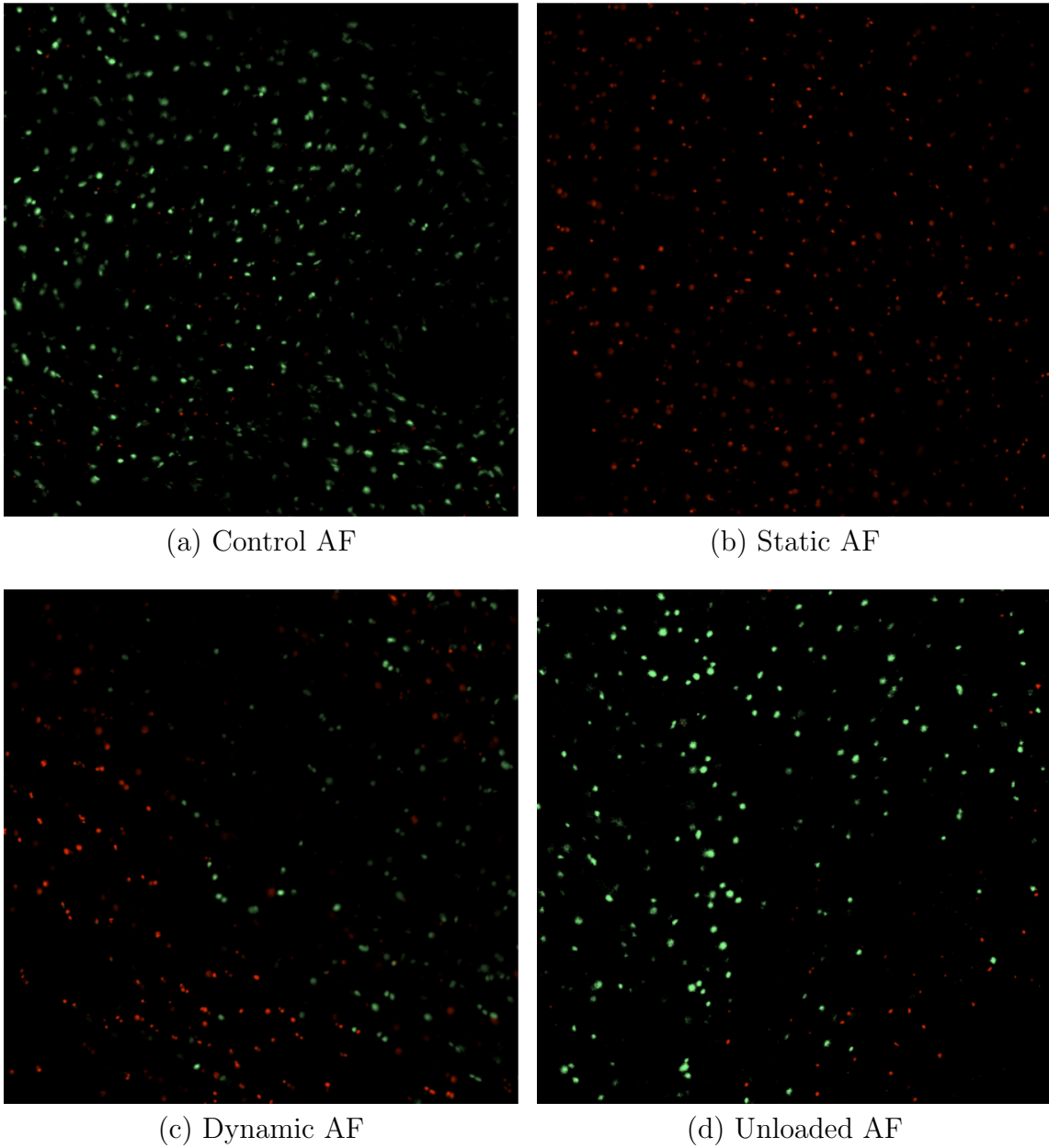


Figure 6–7: Annulus fibrosus cell viability staining representative areas of fresh harvested control and culture discs in different conditions: dynamic, static and free-swelling. Live cells fluoresce green and dead cells fluoresce red. Images show cells in a 6  $\mu\text{m}$  slice of the tissue.

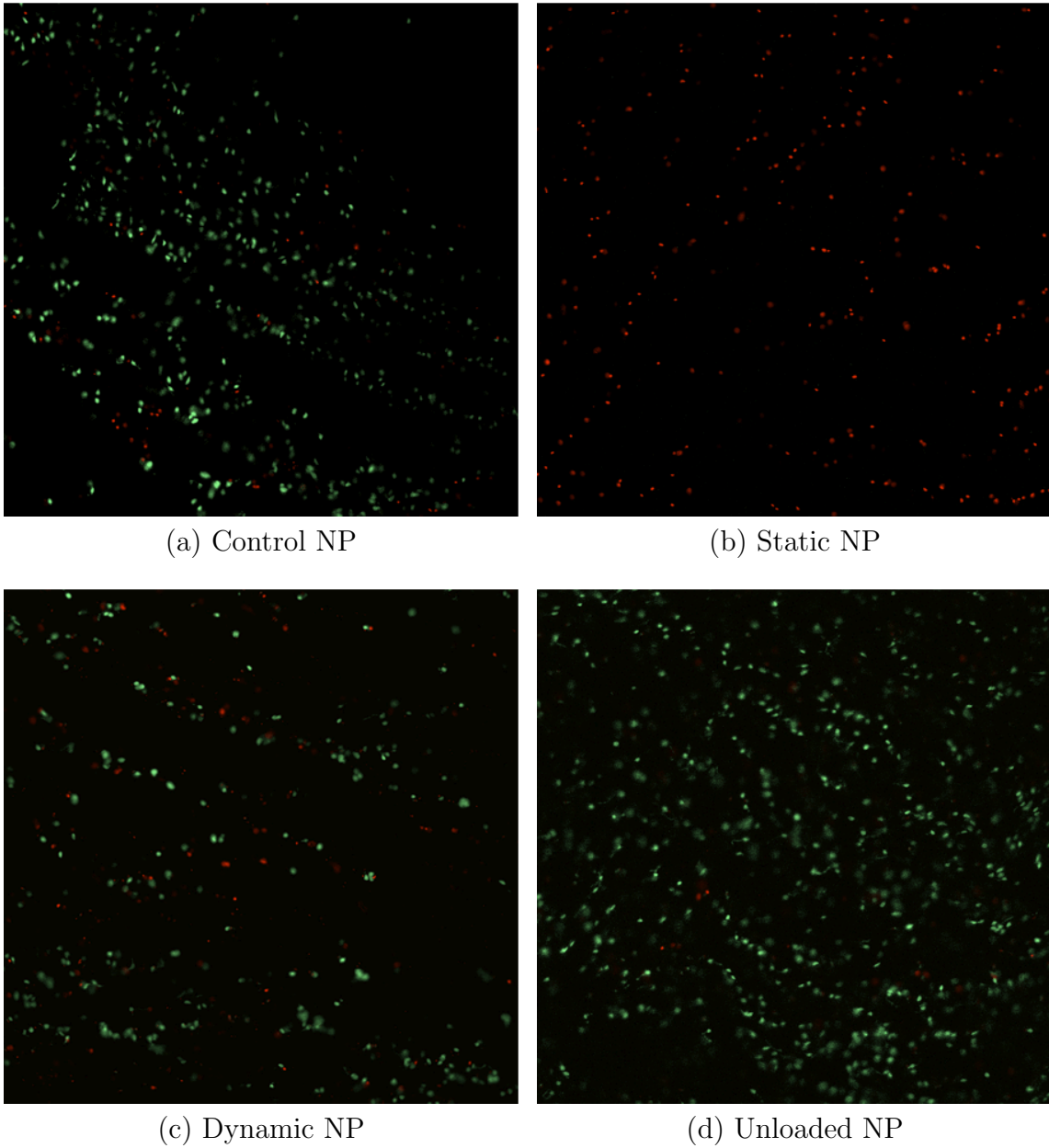


Figure 6–8: Nucleus pulposus cell viability staining representative areas of fresh harvested control and culture discs in different conditions: dynamic, static and free-swelling. Live cells fluoresce green and dead cells fluoresce red. Images show cells in a 6  $\mu\text{m}$  slice of the tissue.

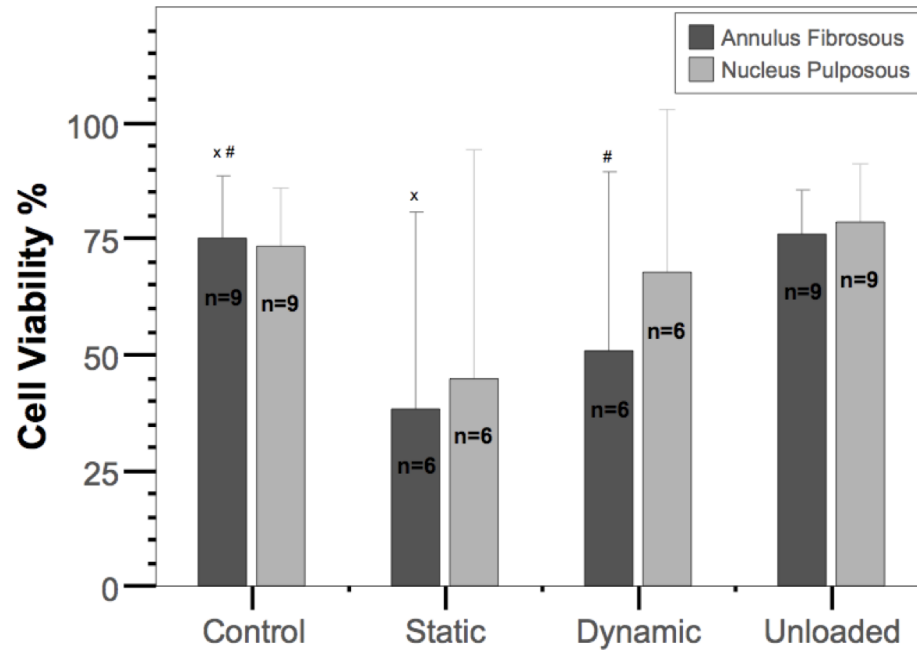
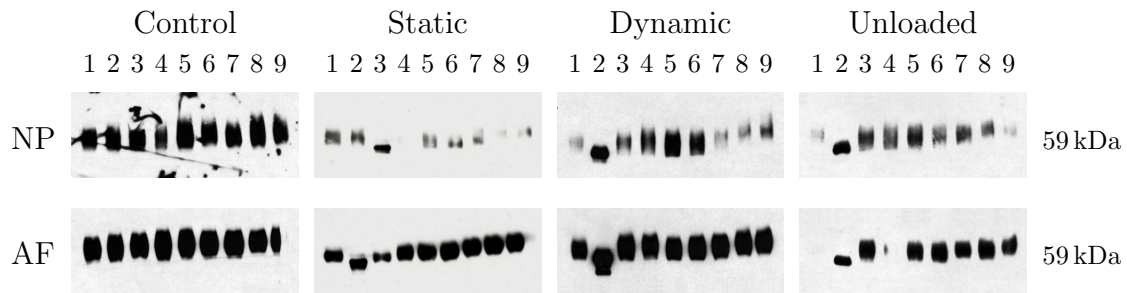
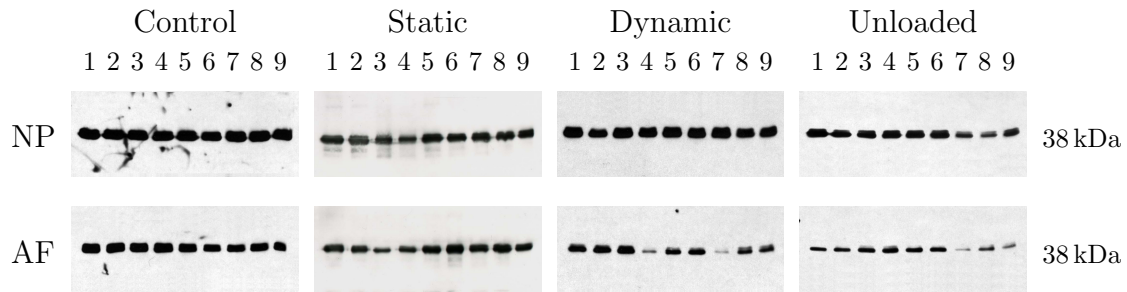


Figure 6-9: Quantified cell viability determined using laser scanning confocal microscopy and live/dead staining. Values are presented normalized to fresh harvested control discs  $\pm$  SEM (standard error of the mean). Statistical difference tested with one-way ANOVA and Fisher PLSD posthoc testing ( $p < 0.05$ ) is indicated with x and # common symbols.



(a) FM



(b) CHAD

Figure 6–10: Samples of extract analysis for the presence of fibromodulin (a) and chondroadherin (b) levels using western blot method for pooled values of nucleus and annulus for the different loading, culture conditions. Chondroadherin and fibromodulin were detected by chemiluminescent detection with matching antiserum.

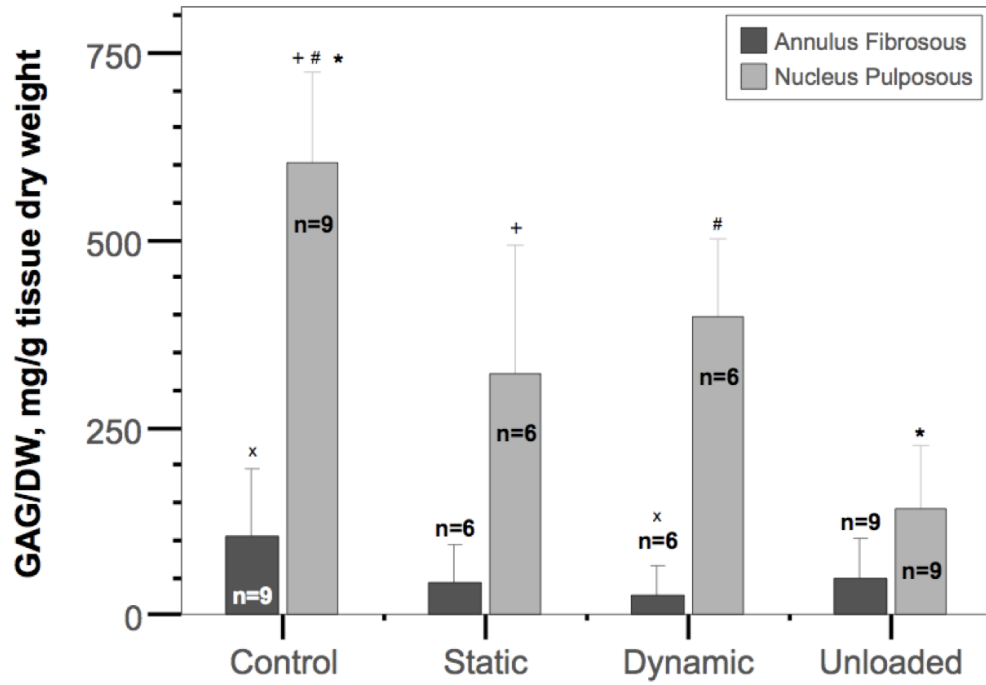
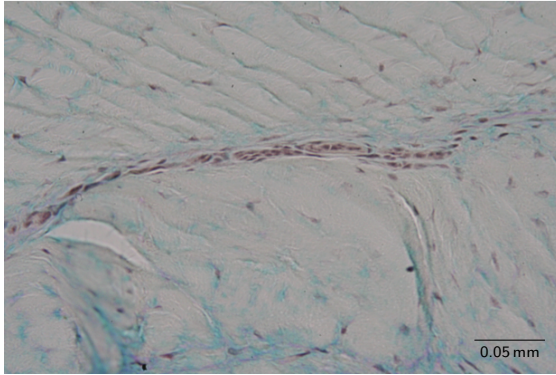
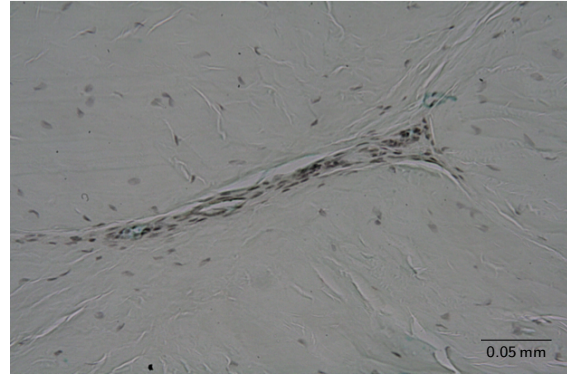


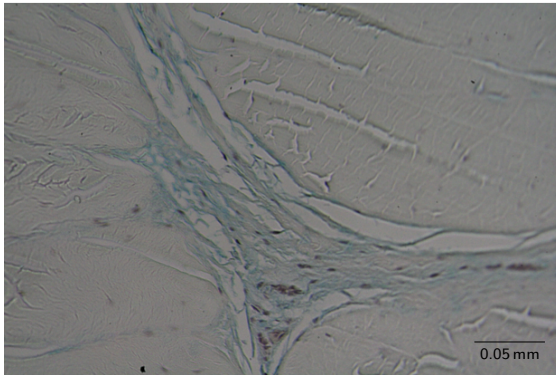
Figure 6–11: GAG content of annulus and nucleus tissue of fresh (control) and cultured bovine coccygeal discs for each loading group: dynamic diurnal, static diurnal and free swelling ( $n = 9$  for all groups). Data is presented as mean  $\pm$  standard deviation. Common +, x, #, \* symbols indicate significant differences  $p < 0.05$  between the control and the different loading groups.



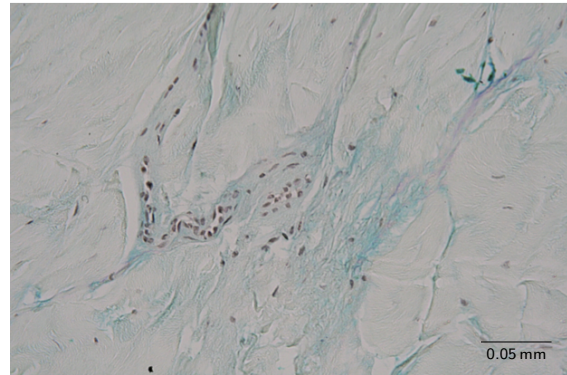
(a) Control AF



(b) Static AF



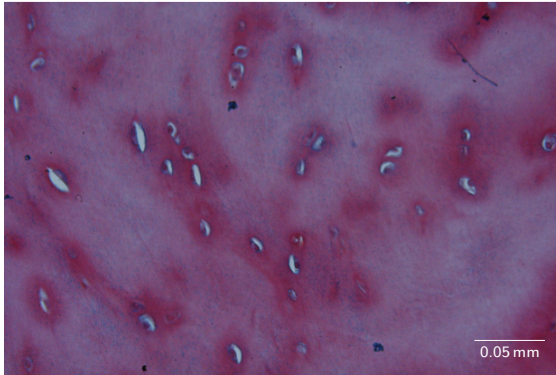
(c) Dynamic AF



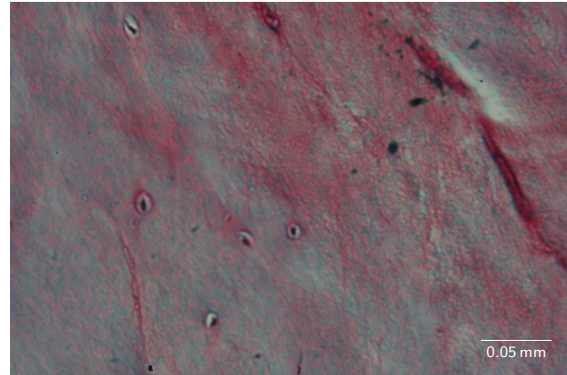
(d) Unloaded AF

Figure 6-12: Histological staining examples of the annulus fibrosus tissue imaged with a 20x/0.50;  $\infty$ /0.17 magnification, comparing freshly harvested discs with the three different culture conditions: dynamic diurnal load, static diurnal load and unloaded.

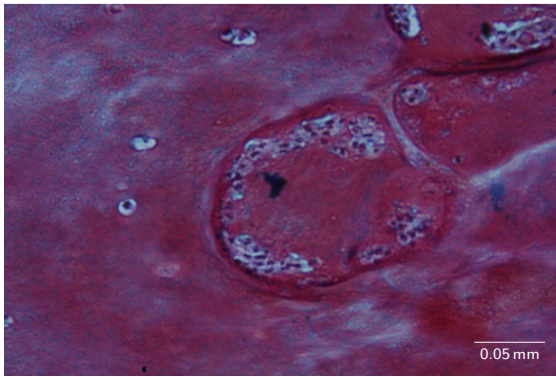




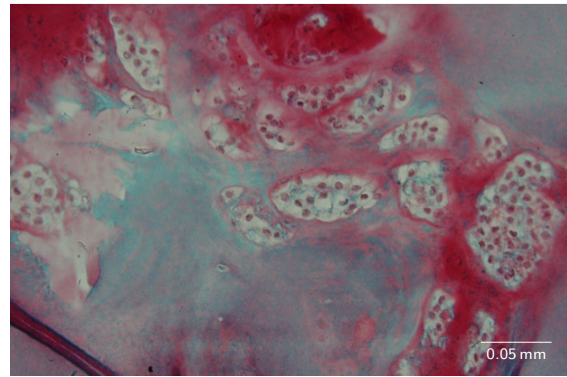
(a) Control NP



(b) Static NP



(c) Dynamic NP



(d) Unloaded NP

Figure 6–13: Histological staining examples of the nucleus pulposus, imaged with a 20x/0.50;  $\infty$ /0.17 magnification, comparing freshly harvested discs with the three different loading groups: dynamic diurnal, static diurnal and unloaded.

## CHAPTER 7

### **Development of an intact intervertebral disc organ culture system in which degeneration can be induced as a prelude to studying repair potential**

The goal of the thesis was to begin the developments of an organ culture model of the intervertebral disc. The method to harvest the intervertebral disc tissue was one of the aspects of the model that was studied. During the exploration of different harvest methods, a new harvest method was developed. Isolating the intervertebral discs with intact cartilaginous endplates (CEP) allowed the tissue to be self-confined. In other words, unlike disc tissue harvested without endplates, discs harvested with the CEP method could retain their form when placed in media without external physical constriction. Although the disc tissue did swell 20 % in weight, short-term culture of the tissue under self-confined loading conditions showed the maintenance of cell viability. Furthermore, the human disc is known to lose and regain 20 to 25 % of its fluid in a day through compression and rehydration [219].

With this new development, a new question arose. Could this new harvest method allow for a different type of organ culture model to be established — one that does not look at the influence of mechanical loads on the disc tissue but could still serve as a viable disc model for the intervertebral disc? The reasoning behind pursuing this model is that all types of disc models can be useful to understanding the intervertebral disc as long as the limiting factors of the model are identified and the



results are correctly interpreted. Furthermore, clearly from our initial culture of the intervertebral disc, using similar loading schemes of that previously reported [114] we were unsuccessful at maintaining cell viability of the organ in vitro. Whether this was because of our bioreactor design or the culturing conditions required further consideration. This next study was to take a step back in the development of the organ culture environment, determining whether the tissue cell viability can be maintained outside of the bioreactor system. It then took the study a step further, when it was realized that the disc culture can be a model in itself, allowing for a degeneration repair model to be developed. With the new harvest method a new organ culture with long-term maintenance of cell viability could be established without mechanical loading stimulation.

The following is the manuscript of this new model that was published by The European Spine Journal, February 2011.

### **7.1 Abstract**

The present work describes a novel bovine disc organ culture system with long-term maintenance of cell viability, in which degenerative changes can be induced as a prelude to studying repair. Discs were isolated with three different techniques: without endplates (NEP), with bony endplates (BEP) and with intact cartilage endplates (CEP). Swelling, deformation, and cell viability were evaluated in unloaded cultures. Degeneration was induced by a single trypsin injection into the center of the disc and the effect on cell viability and matrix degradation was followed. Trypsin-treated discs were exposed to  $TGF\beta$  to evaluate the potential to study repair in this system. NEP isolated discs showed  $> 75\%$  maintained cell viability for up to 10 days but were

severely deformed, BEP discs on the other hand maintained morphology but failed to retain cell viability having only 27 % viable cells after 10 days. In CEP discs, both cell viability and morphology were maintained for at least 4 weeks where > 75 % of the cells were still viable. To mimic proteoglycan loss during disc degeneration, a single trypsin injection was administered to the center of the disc. This resulted in 60 % loss of aggrecan, after 7 days, without affecting cell viability. When TGF $\beta$  was injected to validate that the system can be used to study a repair response following injection of a bio-active substance, proteoglycan synthesis nearly doubled compared to baseline synthesis. Trypsin-treated bovine CEP discs therefore provide a model system for studying repair of the degenerate disc, as morphology, cell viability and responsiveness to bio-active substances were maintained.

## **7.2 Introduction**

One of the major causes of low back pain is degeneration of the intervertebral discs (IVDs). A contributing factor leading to IVD degeneration is the absence of vasculature entering the disc [21, 69], leading to slow exchange of nutrients and waste products across the endplates. The cartilaginous endplate is often calcified with age [185], which might further compromise nutrient flow into the disc. The IVD is only sparsely populated with cells, which are surrounded by a vast extracellular matrix (ECM). Cell number decreases and cell senescence increases with age and degeneration, especially with disc herniation, and the exposure to cytokines [63, 113, 179]. This is also likely a contributing factor to the disc cell's difficulty in maintaining the integrity of the extracellular matrix and the onset of degeneration [153].

The IVD is divided into two distinct zones, the outer fibrous annulus fibrosus (AF) and the central cartilaginous nucleus pulposus (NP) [72]. The AF forms a fibrous outer ring that encloses the more gelatinous NP. The highly anionic proteoglycan aggrecan is entrapped in the collagen fibril network of the NP, and provides the swelling properties important for resistance to compression [217]. Aggrecan fragmentation and loss is one of the hallmarks of disc degeneration and occurs early in the degenerative process, but also in normal ageing, and has commonly been used as a marker of disc degeneration [34, 85]. Loss of aggrecan can be due to either an increase in proteinase production or a decrease in aggrecan synthesis. The disc also possesses a variety of leucine-rich repeat (LRR) proteins, including chondroadherin (CHAD) [111, 143, 201], which interacts with both the collagen fibrils and the cells, so regulating cell metabolism and ECM structure [25, 111, 124]. CHAD has been associated with premature degeneration in scoliotic discs [14, 57], but there is no published data regarding CHAD and degenerative disc disease. In articular cartilage, CHAD has been shown to be associated with collagen fibers, where it is thought to maintain the integrity of the collagen network [124, 148, 201]. Although currently no information is available on CHAD function in the disc, it is likely to have a similar function to that in articular cartilage. As CHAD may play a role in promoting matrix homeostasis, changes in its abundance or structure might be expected to contribute to pathological changes in the tissue. It is commonly thought that the degradative changes in the ECM are detrimental to disc function, a property that is exacerbated by the accumulation and slow removal of the ECM degradation products. The rate

at which these changes occur may vary between individuals, but they are thought to form the basis of the tissue loss associated with disc degeneration.

Numerous animal models have been used to study IVD degeneration. Large animal models using ovine and porcine discs have been accepted as good models for studying disc structure, geometry, biochemistry and biomechanics [136, 233], whereas small animal models using rabbits and rats have in general been used to answer metabolic questions [80]. While the large animals have a disc structure analogous to humans, they undergo degeneration slowly and are expensive to use. In contrast, the small animals are relatively cheap and undergo degenerative changes rapidly, but their disc structure is different to humans, particularly in the maintenance of notochordal cells throughout life [74, 75]. An organ culture model using discs from large animals would be an ideal system to study both disc degeneration and repair. Organ culture models described to date have two important gaps: optimization of dissection techniques and development of a model of degeneration. Lee et al. [115], removed vertebral endplates to retain NP cell viability for 1 week, while other studies retained vertebral endplates through heparinization and cleaning to maintain live cells for 3 weeks [48, 93]. Yet optimal dissection procedures of large animal organ culture are still being developed and there are also very few IVD explant models of degeneration. The present work describes a bovine disc organ culture system, which permits the maintenance of cell viability for at least 4 weeks using a novel dissection technique, and in which degenerative changes can be induced as a prelude to studying repair.

## **7.3 Materials and methods**

### **7.3.1 Source of reagents**

The polyclonal rabbit antibody recognizing human chondroadherin was a kind gift from Dr. Dick Heinegård, Lund University, Sweden [111]. The polyclonal rabbit antibody recognizing the G1 region of human aggrecan was raised against synthetic peptides, as described previously [207]. The horseradish peroxidase (HRP)-conjugated anti-rabbit antibody was from Santa Cruz Biotechnology. The enhanced chemiluminescence (ECL) detection system was from GE Healthcare. Keratanase II and chondroitinase ABC were purchased from BioLynx Inc.

### **7.3.2 Disc isolation**

The largest first 4 caudal discs were isolated from the tails of 24- to 30-month-old steers within 18 h after slaughter. The tails were dissected free of skin, muscles and ligaments, and pedicles for each segment were removed. Whole discs were isolated using one of three techniques: with bony endplates (BEP), without endplates (NEP) or with cartilage endplates (CEP) (Fig. 7–1). For BEP and CEP, parallel axial cuts were made through the vertebral bodies close to the cartilage endplates. The CEP discs were then further processed so that the bone and the adjacent calcified part of the cartilaginous endplate were removed using a surgical round end boring bit on a high-speed drill (Racine, WI, USA). The discs were processed until the surface of the tissue was soft and flexible without detectable calcified tissue. NEP discs were isolated by parallel cuts using a straight edged microtome blade to fully remove both bone and cartilage endplates. The processed discs ranged from  $27.6 \pm 2.8$ ,  $29.5 \pm 2.3$

and  $7.6 \pm 1.5$  mm in diameter and  $4.4 \pm 1.2$ ,  $16.2 \pm 3.1$  and  $7.0 \pm 1.0$  g in weight for NEP, BEP and CEP discs, respectively.

### **7.3.3 Disc organ culture**

BEP discs were washed extensively with phosphate-buffered saline (PBS) containing 50 mM citrate to eliminate any blood clots and then followed the general procedure. BEP, NEP and CEP discs were rinsed in PBS supplemented with 1000 U/ml penicillin, 1000 µg/ml streptomycin (Gibco) and 0.25 µg/ml fungizone (Gibco), then placed in culture chambers (sterile 80 ml specimen containers, STARPLEX Scientific) containing 50 ml culture medium (Dulbecco's Modified Eagle Medium with 2 mM Glutamax and 25 mM Hepes, supplemented with 5 % fetal bovine serum, 500 U/ml penicillin, 100 µg/ml streptomycin, 50 µg/ml L-ascorbate). To evaluate cell viability the discs were cultured without external load applied for up to 4 weeks ( $n = 8$  per time point). Medium was aspirated and replenished using a pipet-aid with a 25 ml pipet every 3 days over the entire culture period. To evaluate tissue swelling, discs isolated using the NEP or CEP method were placed in culture medium and weights were recorded after 15 min, 30 min, 1, 2, 4, 20, 25 and 30 h ( $n = 4$  per group were tested).

### **7.3.4 Induced disc degeneration**

Degeneration was induced by a single injection of trypsin (Sigma, 2.5 µg/50 µl PBS) into the center of the CEP disc using a 28-G needle after a 48 h pre-culturing period. Control discs were injected with the same volume of PBS.

### 7.3.5 Cell viability

A 1 mm section was taken through the center of the discs using an in-house designed cutting tool consisting of two microtome blades placed 1 mm apart. This gives a 1-mm- thick slice though the entire disc that is about 3 cm wide (disc diameter) and 1 cm high (disc height). The 1 mm tissue section was incubated in serum-free medium containing fluorescent dyes (Live/Dead<sup>®</sup>, Invitrogen) according to the manufacturer's instructions, using 1 mM each of calcein (494/517 nm) and ethidium homodimer-1 (528/617 nm, in the presence of DNA). The cells were visualized using an inverted confocal laser scanning microscope (CLSM, Zeiss LSM 510). 20 consecutive 6  $\mu$ m sections were imaged. CLSM stacks were split into single images. The first image to be analyzed was chosen approximately five images into the stack to prevent artefacts from the cut surface and then extending another four images. The selected five images were merged, saved as single color JPEG files (red and green separate), and the labeled cells were quantified separately using the CellC software (Matlab) [198]. The live to dead cell ratio was then calculated from the proportion of green and red cells.

### 7.3.6 Extraction of ECM proteins and proteoglycans

NP and AF tissue ( $n = 8$  per group) was excised separately and sliced thinly. Proteins and proteoglycans were extracted at 4 °C under continuous agitation for 48 h on a wet weight per volume basis using 15 volumes extraction buffer [4 M guanidinium chloride, 50 mM sodium acetate, pH 5.8, 10 mM EDTA, COMPLETE<sup>®</sup>(Roche)]. The extracts were then cleared by centrifugation at 16 000 g for 30 min.

### 7.3.7 GAG analysis

Sulfated glycosaminoglycans (GAGs) were quantified ( $n = 8$  per group) from tissue extracts by a modified dimethyl methylene blue (DMMB) dye-binding assay [12]. Samples were diluted to fall in the middle of the linear range of the standard curve.

### 7.3.8 Western blot analysis

Proteins and proteoglycans in 5  $\mu$ l aliquots of disc extracts were precipitated by the addition of 9 volumes of ethanol, washed twice in 95 % ethanol, and finally lyophilized. Samples for analysis of CHAD were re-dissolved in SDS sample buffer. Samples for analysis of aggrecan were digested with keratanase II (Seikagaku) at 0.1 mU per 5  $\mu$ l extract for 6 h. The solution was then adjusted to 100 mM Tris, 100 mM sodium acetate, pH 7.3, and digested overnight with chondroitinase ABC (Seikagaku) at 1 mU per 5  $\mu$ l extract and then mixed with SDS sample buffer. Samples were separated by SDS-PAGE (10 % or 4 to 12 % NOVEX<sup>®</sup> gels) under reducing conditions. Separated proteins were transferred to nitrocellulose membranes [212], and western blotting was performed using antibodies recognizing chondroadherin and aggrecan. The membranes were blocked with 3 % skim milk powder in 10 mM Tris-HCl, pH 7.4, 0.15 M NaCl, and 0.2 % Tween (blocking buffer), and then incubated with the primary antibodies at a 1:1000 dilution in blocking buffer containing 3 % BSA, followed by the secondary antibody conjugated with HRP (1:1000 dilution) in blocking buffer containing 1 % dried skim milk. The bound antibody was visualized by chemiluminescence (GE Healthcare).



### 7.3.9 Proteoglycan synthesis

CEP discs (7 days after trypsin-induced degeneration) were injected with 50  $\mu$ l PBS containing 20  $\mu$ l soya bean trypsin inhibitor (Sigma), 25  $\mu$ Ci  $^{35}$ S (Perkin-Elmer), with or without 30 ng TGF $\beta$ 1 (PreproTech Inc). NP tissue was collected 72 h after treatment and digested with proteinase K [52]. Aliquots of the proteinase K digests were dialyzed against 1 mM sodium sulfate in distilled water (BRL micro dialysis chamber, with SpectraPor 12–14 kDa molecular weight cut off dialysis membrane) to remove unincorporated  $^{35}$ S-sulfate. Incorporated radioactivity was measured by scintillation counting and normalized to tissue wet weight ( $n = 7$  per group).

### 7.3.10 Histology

A 1 mm section was taken through the center of the disc as described above. The intact slice was fixed between porous platens in 4 % paraformaldehyde, lysine, periodate as described by McLean and Nakane [132] for 24 h before transferring to decalcifying solution (10 % EDTA in 0.1 M Tris-HCL, pH 7.4) for 12 days with solution changes twice daily. Samples were then embedded in paraffin wax and 5- $\mu$ m-thick sections were cut and stained with hematoxylin and Safranin O-fast green [186].

### 7.3.11 Statistical analysis

An unpaired  $t$  test was used to calculate significance in Figs. 7–2, 7–3, 7–4 and 7–10. In Figs. 7–5, 7–7 and 7–8, multivariate linear models were used to assess the effects of treatment (trypsin vs. buffer injection) and time (4, 8 and 14 days, respectively). The value at time zero of native discs for DMMB and % live cells was used as an internal comparison to normalize all subsequent values. A  $p$  value

of  $< 0.05$  was used as the criteria for a significant difference. Where multiple tests were performed, Bonferroni corrections were applied.

## 7.4 Results

Three isolation methods were compared to find a protocol allowing for long-term culture of IVDs which maintained cell viability, morphology and integrity of the tissue. The discs were cultured without external load, as optimal loading conditions will vary for discs prepared by each isolation technique and this would further complicate the comparison. As the NEP isolation technique severs the attachment of collagen fibrils between the disc and the cartilage endplates, it was predicted that NEP discs would be prone to swell to a greater extent than the CEP or BEP discs when maintained in culture. The swelling capacity of discs prepared with the CEP method was therefore compared to discs isolated using the NEP method. Increase in disc weight as an indicator of swelling was measured over a 30-h period (Fig. 7–2a). In both cases weight increase occurred rapidly during the first 4 h of culture, and then gradually over the next 26 h. The difference in swelling was already significant after 15 min ( $p < 0.002$ ) and remained significant at all subsequent time points. Weight increase was limited to about 20 % using the CEP method. In contrast, discs isolated using the NEP method increased between 60 and 100 % of their initial weight when cultured unconfined. The CEP discs maintained their morphology throughout the experiment, whereas the NEP discs were already deformed after 1 h and were severely deformed after 30 h (Fig.7–2b).

As excessive swelling of the disc, as occurs following the NEP isolation procedure, or impaired nutrient flow, as expected following the BEP procedure, may be

detrimental to disc cell viability; cell survival in culture following the different disc isolation techniques was investigated. Discs prepared by the NEP and BEP methods were cultured for up to 10 days and cell viability was measured using the live/dead fluorescent system in combination with confocal microscopy. Although the NEP discs were severely deformed, cell survival was maintained with more than 75 % viable cells in the NP throughout the culture period (day 6,  $88 \pm 28\%$  and day 10,  $84 \pm 19\%$ , this was not significant and gave  $p$  values of 0.7 and 0.6, respectively compared to freshly isolated discs). In contrast, while the morphology was retained in BEP discs, cell survival was compromised after 6 days of culture ( $43 \pm 28\%$ ,  $p = 0.04$  compared to freshly isolated discs) and the majority of the cells were dead after 10 days ( $27 \pm 23\%$  viable cells in all areas,  $p = 0.004$  compared to freshly isolated discs) (Fig. 7–3). Because of these limitations, experiments with NEP and BEP isolated discs were not perused past day 10. Using the CEP method, which also allows maintenance of disc morphology but lacks the impediment to nutrition caused by the bony endplates, cell survival of the disc was maintained for up to 4 weeks ( $80 \pm 7\%$  in freshly isolated,  $80 \pm 13\%$  at 2 weeks and  $75 \pm 12\%$  at 4 weeks in all areas, this gave  $p$  values of 1 and 0.5 when compared to freshly isolated discs) (Fig. 7–4).

As the CEP method preserved both cell viability and morphology, it was chosen to develop a proteinase-induced model of disc degeneration. Trypsin was chosen for this purpose as it will degrade most ECM proteins but not the collagen fibrils. It also has very precise cleavage specificity and is readily inactivated by inhibitor treatment. In preliminary experiments, 0 to 5  $\mu\text{g}$  of trypsin was injected into the center of CEP discs to determine the dose needed to deplete aggrecan from the NP

to about 60 to 80 % of its initial level. 2.5 µg trypsin per 50 µl buffer was selected for further study. When a single 2.5 µg trypsin injection was delivered to the center of the NP, GAG levels in the NP were depleted by about 40 % after 4 days and by about 70 % after 14 days (Fig. 7-5). Slow GAG loss also occurred in the control discs with a 25 % depletion after 14 days. DMMB dropped significantly over time for both treatment groups ( $p = 0.0006$ ). Trypsin-injected discs however were losing proteoglycans much faster. This was highly significant ( $p < 0.0001$ ). Post hoc  $t$  tests comparing individual group means for proteoglycan concentrations with the native control at time zero were significantly lower (all  $p < 0.01$ ), except for the buffer-injected discs at 4 days ( $p = 0.74$ ). As expected GAG content in AF tissue was initially lower than in the NP. However, GAG loss in the AF of control and trypsin-treated discs occurred at a similar rate to that observed in the NP, indicating diffusion of the trypsin throughout the disc (data not shown). Safranin O staining of histological sections showed similar proteoglycan levels in freshly isolated and control discs cultured for 14 days and a loss of Safranin O staining in trypsin-treated discs at day 14 (Fig. 7-6), thus confirming the results obtained by the GAG assay. This method is only able to detect a significant difference in proteoglycan concentration and is not able to detect low levels of proteoglycans [186].

As trypsin treatment and the consequent extracellular matrix depletion has the potential to adversely affect cell viability, the proportion of live to dead cells was compared in trypsin-treated and control discs at different times in culture (Fig. 7-7). Of the cells present in the tissue, an average cell survival rate greater than 75 % was measured at all time points independent of manipulation (Fig. 7-8), and no

decline was observed with time in culture. The multivariate linear model failed to demonstrate any effect (adjusted  $r^2 = 2\%$ ) for either treatment or time ( $p = 0.40$  and  $0.23$ , respectively). There was also no interaction found between treatment and time (treatment  $\times$  time cross product  $p$  value =  $0.33$ ). Individual  $t$  tests comparing the group means for % live cells with the native control at time zero and applying Bonferroni corrections for multiple tests, all showed no significant differences. Individual  $t$  tests comparing the group means for % live cells with the native control at time zero, and applying Bonferroni corrections for multiple tests (i.e., the  $p$  level of  $0.05$  was corrected for  $6$  concurrent  $t$  tests, resulting in a more strict  $p$  level of  $0.0500/6 = 0.0083$ ) all showed no significant differences. Thus, trypsin treatment is not detrimental to cell survival.

To determine the influence of trypsin on the extent of ECM proteoglycan and protein degradation, aggrecan and CHAD were analyzed by immunoblotting in extracts of the cultured discs. The profile of aggrecan showed little change after 8 days of culture in control discs. Of particular note is the absence of G1 region (MW 60 to 80 kDa) accumulation, which would be indicative of proteolysis. Thus, proteoglycan loss in the control cultures is probably due to passive diffusion rather than an active catabolic process. In contrast, there was extensive degradation of aggrecan following trypsin treatment, with the accumulation of fragments representing free G1 regions (Fig. 7–9a). In comparison to aggrecan, CHAD was not affected to the same extent by the trypsin treatment (Fig. 7–9b). There was a 25 % depletion in CHAD, but there was no evidence for the accumulation of degradation products. These results suggest that while aggrecan has undergone extensive degradation and loss following

trypsin treatment, the collagen network and its associated CHAD remain relatively intact. Such ECM changes are a feature of early disc degeneration.

TGF $\beta$  is known to stimulate proteoglycan synthesis in connective tissue cells [58], and was used to validate that the trypsin-treated discs can be used to evaluate a repair response following injection of a bio-active substance. TGF $\beta$  or buffer alone was injected into the center of the disc, together with radio-labeled sulfate and soya bean trypsin inhibitor, 1 week after trypsin-induced degeneration. The amount of newly synthesized proteoglycans 72 h after injection nearly doubled in TGF $\beta$ -treated discs ( $p = 0.02$ ) (Fig. 7–10) in comparison to discs treated with buffer alone.

## 7.5 Discussion

Maintenance of the IVD matrix is orchestrated by its sparse cell population that controls the balance between anabolic and catabolic processes. This balance may be perturbed towards catabolic degeneration with age, as cell number and nutrition decline, and cell senescence increases [103, 113, 179]. Degeneration may also be enhanced by genetic differences, high magnitude or frequency loading of the disc, as well as by trauma to the disc [76, 118]. Independent of cause, once degenerative changes have been established, the adult IVD seems incapable of intrinsic repair. It is also not clear if repair can be induced by supplementation with anabolic agents in degenerate human discs. However, promising results have been demonstrated in discs from small animals using growth factor supplementation [38, 127]. Unlike humans, the discs of smaller animals maintain their notochordal cells throughout life, and these cells respond well to growth factors by the production of proteoglycans and the down-regulation of cytokines [129]. While promising results demonstrating an

increase in proteoglycan production and mRNA expression have been demonstrated in isolated human disc cells [82], it is important to verify the findings in a system where the cells are in their native three-dimensional environment. As in vivo work in the human is not feasible, and large animals with a disc structure similar to humans are expensive and difficult to maintain, the availability of an intact organ culture system applicable to human discs would seem ideal.

The objective of this study was to develop a whole disc organ culture system using bovine IVDs. Such discs are of similar structure to humans and possess the same barriers to nutrient diffusion, but have the advantage of being readily available and not having variable degrees of degeneration. The bovine discs were isolated using three different techniques, and were cultured without external load. We chose to develop a system where no external load is being applied, as the frequency and magnitude of optimal loading might differ for the different isolation techniques further complicating the comparison. Cell survival was not drastically changed in discs isolated without any cartilaginous or bony endplates over a 2 week period, but their enormous swelling and severe deformation made them unsuitable for studying repair. On the other hand, discs cultured with intact bony endplates preserved their integrity and shape, but cell survival was compromised and most of the cells were dead after 10 days in culture, also making it impossible to study repair in this system. In contrast, discs isolated with intact cartilaginous endplates overcame these shortcomings, as both disc integrity and cell viability were maintained. It is likely that with the bony endplate present nutrient supply to the cells in the center of the disc is severely impaired, but that retention of only the non-calcified cartilaginous

endplate allows adequate nutrition to be maintained. While the discs maintained their gross morphology with the cartilaginous endplates present, their weight did increase by up to 20%. However, the expected increase in disc height with such limited swelling is within the reported diurnal variation range [175]. This may be a major contributor to the retention of cell viability, and may ensure that normal cell metabolism is maintained.

Organ cultures of whole bovine discs have been reported previously using the BEP and NEP methods [115]. The discs were maintained under a constant load to negate the effects of swelling, and cultures were maintained for 7 days. At the end of this time the majority of cells in the BEP discs were dead, whereas good cell viability was obtained for the NEP discs. The difference between the two isolation techniques presumably reflects the decreased nutrition to the discs when the bony endplate remains intact. The work also illustrates that the NEP method of isolation may be of value if the resulting discs are maintained under load; however, additional studies have shown that the type of loading is important if cell death is to be avoided [105]. The BEP isolation method has been shown to be of use for viable organ culture when the discs were obtained from sheep that were heparinized prior to slaughter [48, 93]. Presumably, heparinization prevented blood clot formation in the capillary channels that are present in the endplate, and so improved nutrient flow. This technique would not however be a feasible option for bovine discs obtained from the abattoir, and this is by far the most convenient source for large animal discs in large quantity. The use of the CEP isolation technique avoids the need for heparinization to improve nutrient supply to the disc, and also avoids the need for the use of loading devices



to prevent excessive swelling that is inherent to the NEP method, as the CEP discs are being contained by the intact cartilage endplates which limit swelling. However, the CEP discs are also amenable to cyclic and higher static loading should this be desired.

Roberts et al. [183] have previously described a technique for developing an explant model of disc degeneration in the bovine caudal disc that would be suitable for testing injectable nucleus pulposus replacements. In this work 100 times more trypsin compared to our study was used and cell viability was not assessed. This resulted in a depletion of the entire matrix and cells in the center of the discs, and created a cavity where cell-containing scaffolds can be injected. This model would probably compare to late stages of disc degeneration and the method would be of limited use to study the effect of bioactive substances on cells already present in the disc. The model that we have developed represents an earlier stage of disc degeneration where existing cells can be stimulated to replace the proteoglycan content that is initially lost.

Currently, treatment of symptomatic disc degeneration often involves surgical intervention and long-term rehabilitation, and is only an option at late stages of degeneration [35, 55, 131]. As surgical intervention involves removal of the diseased intervertebral disc and fusing the adjacent vertebral bone, it leads to a loss of mobility of that joint, which can often result in degeneration at adjacent disc levels. New biological therapies targeted to intervertebral discs to prevent or retard degenerative changes and to promote repair could potentially alleviate or at least delay

the need for surgical intervention. Biological treatment is most likely to be a feasible therapeutic option in early stages of disc degeneration, characterized by loss of proteoglycans but the maintenance of a relatively intact collagen network. In the present study, this type of early degenerative change was induced in normal bovine discs by injecting trypsin into their centers. As this induced degeneration occurs with the long-term retention of cell viability, and preserves metabolically active cells, it represents an ideal system in which to study subsequent repair induced by growth factors. In the present study TGF $\beta$  was injected into the trypsin-treated discs and proteoglycan synthesis was increased, demonstrating the feasibility of studying repair in this system. TGF $\beta$  was used to establish a proof of principle as it is known to induce proteoglycan synthesis in disc cells [187], but it may not be the most appropriate agent for therapeutic use in humans. An unloaded system was used for the present study and this is a valid first screening step as it allows for many replicates to be run simultaneously. Although, the application of physiological load would likely enhance matrix synthesis and thereby the repair response, any substance able to increase synthesis in an unloaded system could be considered as a suitable candidate to further test in a more complex loaded system and finally in a living animal.

## **7.6 Acknowledgments**

This work was supported by financial support from AOSpine grant number AOSBR-07-07, the Canadian Arthritis Network and the Shriners of North America.

## **7.7 Conflict of interest**

None.

## **7.8 Figures**

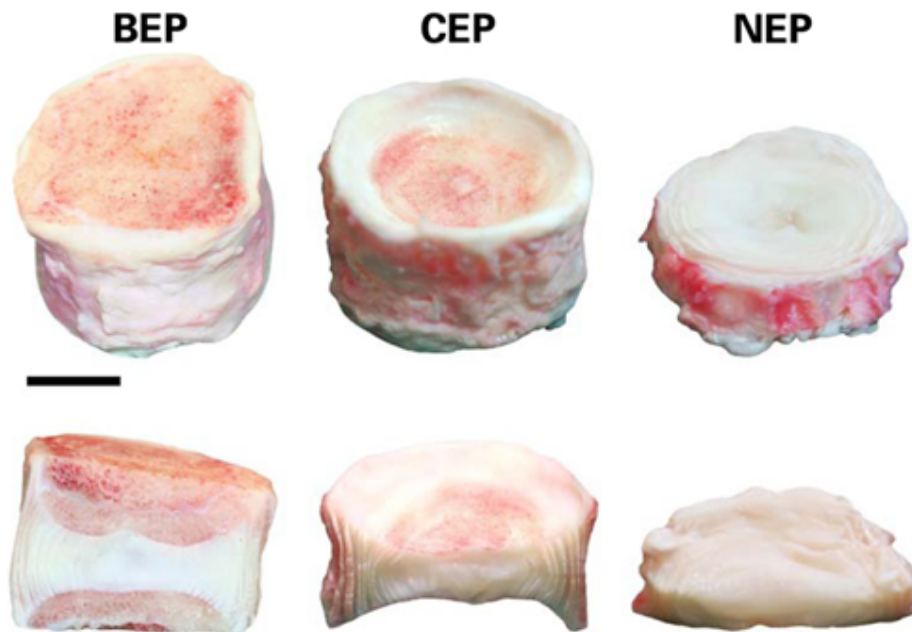
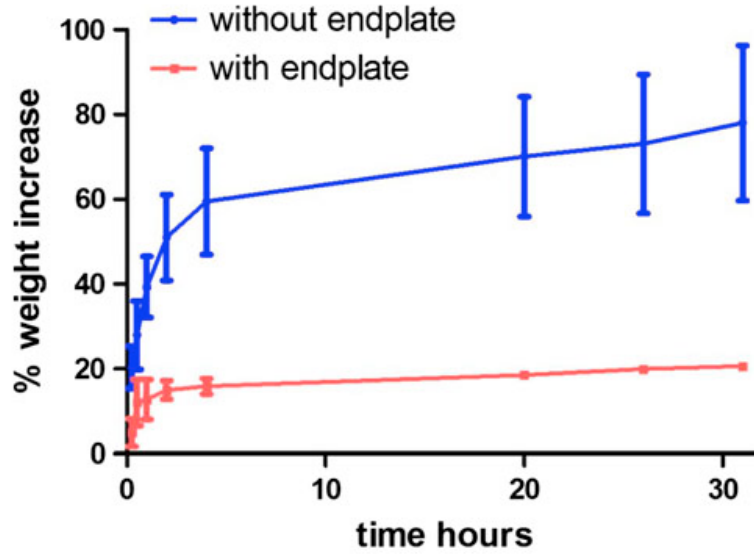
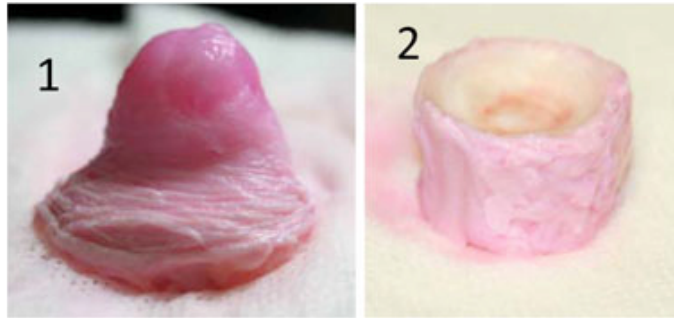


Figure 7-1: Appearance of the IVDs isolated by three different methods. Images of the intact discs (*top row*) and of disc cut sagittally (*bottom row*) are shown. BEP disc retaining cartilage endplates plus adjacent vertebral bone, CEP disc retaining only cartilage endplates, and NEP disc without endplates. The scale bar represents 1 cm.



(a)



(b)

Figure 7-2: Comparison of swelling capacity and deformation of CEP and NEP isolated discs. (a) CEP and NEP isolated discs were placed in culture medium and their weights were measured and plotted as % increase in weight over time ( $n = 4$ , *error bars* indicate standard deviation). CEP and NEP discs were compared at each time point using an unpaired  $t$  test, and  $p$  values  $< 0.01$  were obtained at all time points relative to time 0. (b) Deformation was compared between discs isolated by the NEP (1) and CEP (2) methods at 30 h.

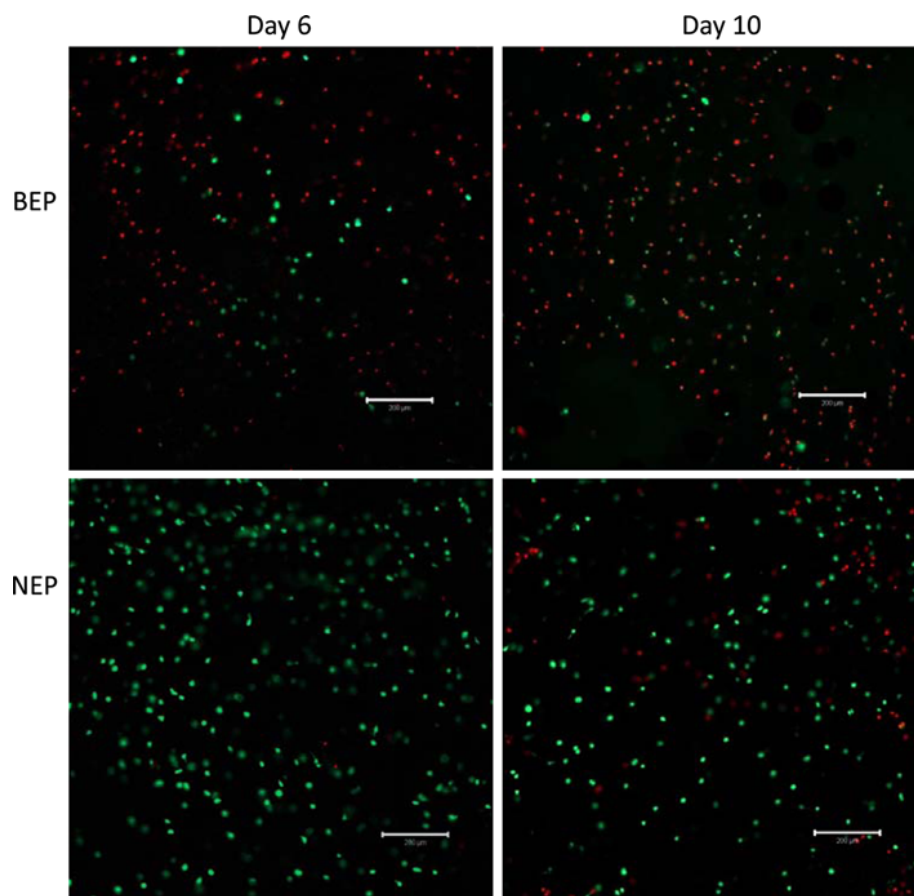


Figure 7-3: Cell survival in the NP of BEP and NEP isolated discs. Cell viability was measured in a 1 mm thick tissue section after incubation in serum-free medium containing fluorescent dyes (Live/Dead<sup>®</sup>, Invitrogen). Live (*green*) and dead (*red*) cells were visualized using an inverted confocal laser scanning microscope after 6 or 10 days of culture ( $n = 4$ ). The scale bars represent 200  $\mu\text{m}$ .

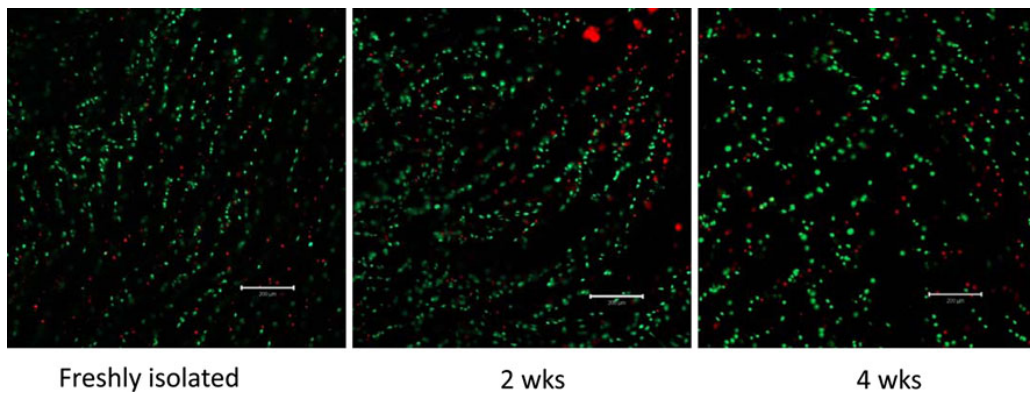


Figure 7-4: Cell survival in the NP of CEP isolated discs. Cell viability was determined in a 1-mm-thick tissue section after incubation in serum-free medium containing fluorescent dyes (Live/Dead<sup>®</sup>, Invitrogen). Live (*green*) and dead (*red*) cells were visualized using an inverted confocal laser scanning microscope in freshly isolated discs and in discs cultured for 2 and 4 weeks ( $n = 4$ ). The scale bars represent 200  $\mu\text{m}$ .

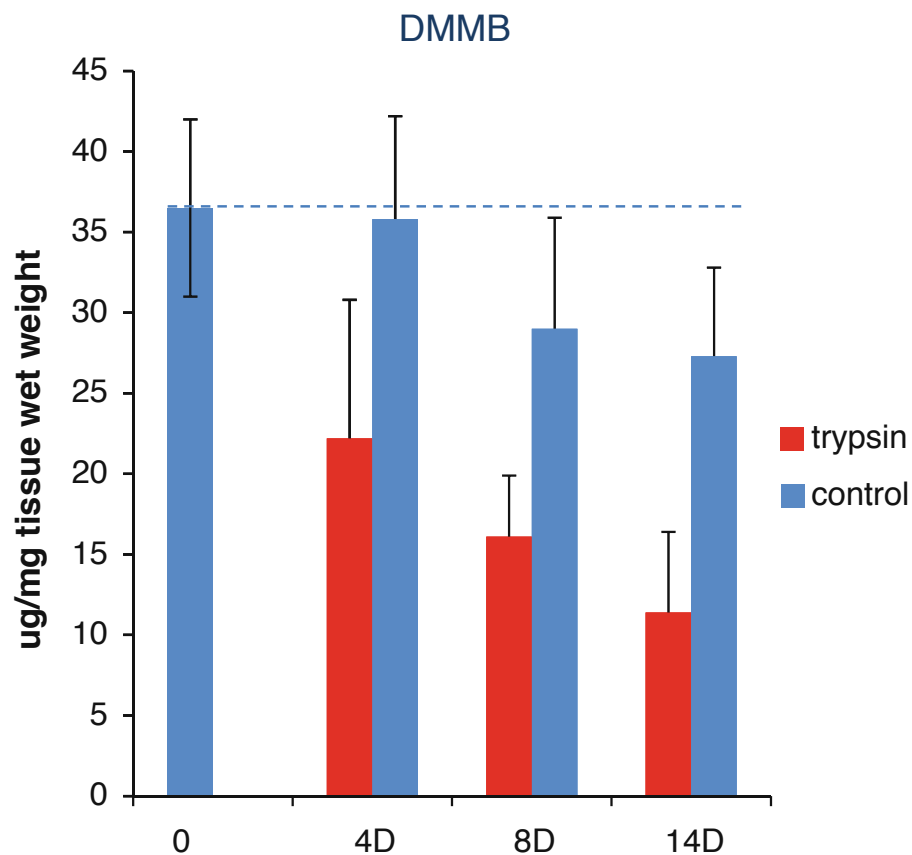


Figure 7–5: Glycosaminoglycan content in CEP discs with or without trypsin treatment. Sulfated GAGs were quantified after trypsin or buffer alone was injected into the center of the disc. GAG content was measured in NP tissue of freshly isolated discs (0) and in discs 4, 8 and 14 days after injection ( $n = 8$ , *error bars* indicate standard deviation). Multivariate linear models were used to assess the effects of treatment,  $p$  values  $< 0.001$  in trypsin-treated sample and  $> 0.05$  in control samples, compared to time 0.

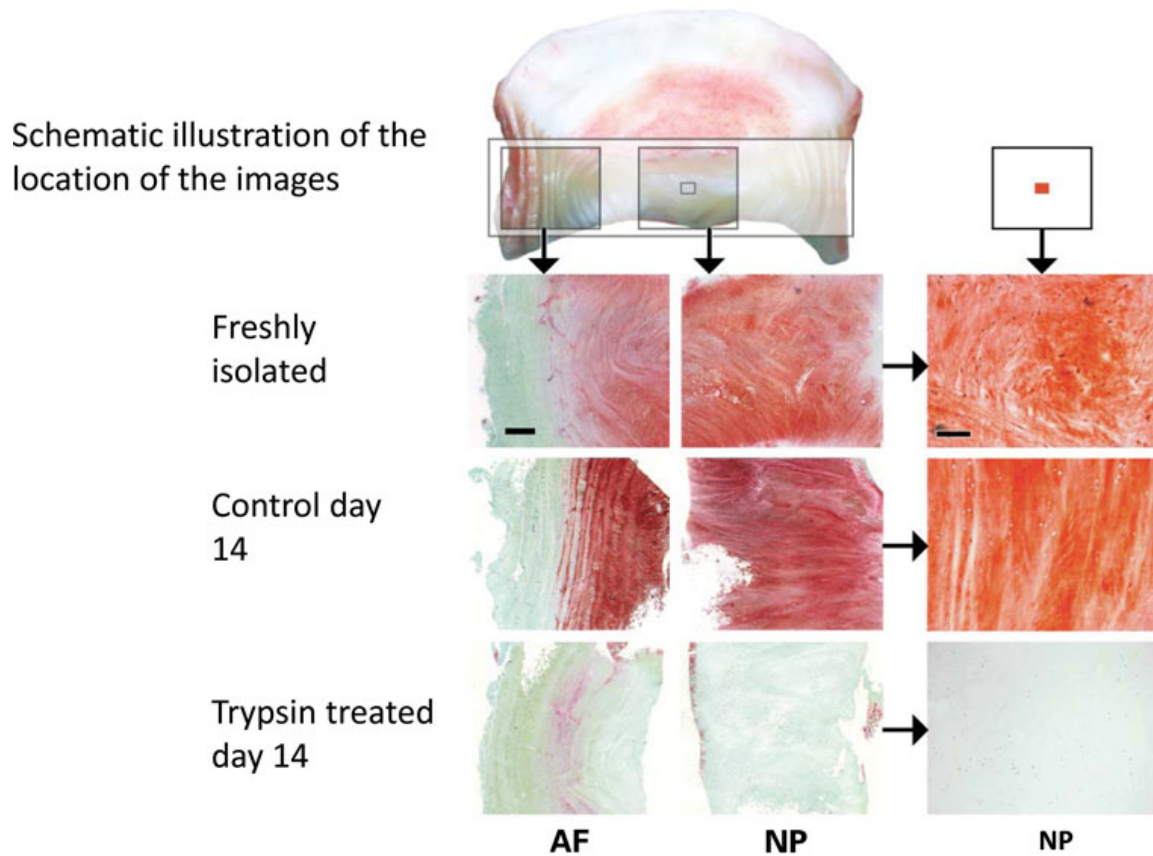


Figure 7–6: Hematoxylin–Safranin O-fast green stained disc sections. Sagittal sections of AF and NP from freshly isolated discs and trypsin- or buffer-injected CEP discs at day 14 are shown. The *scale bars* represent 2 mm for the left hand sections and 200  $\mu\text{m}$  for other sections.



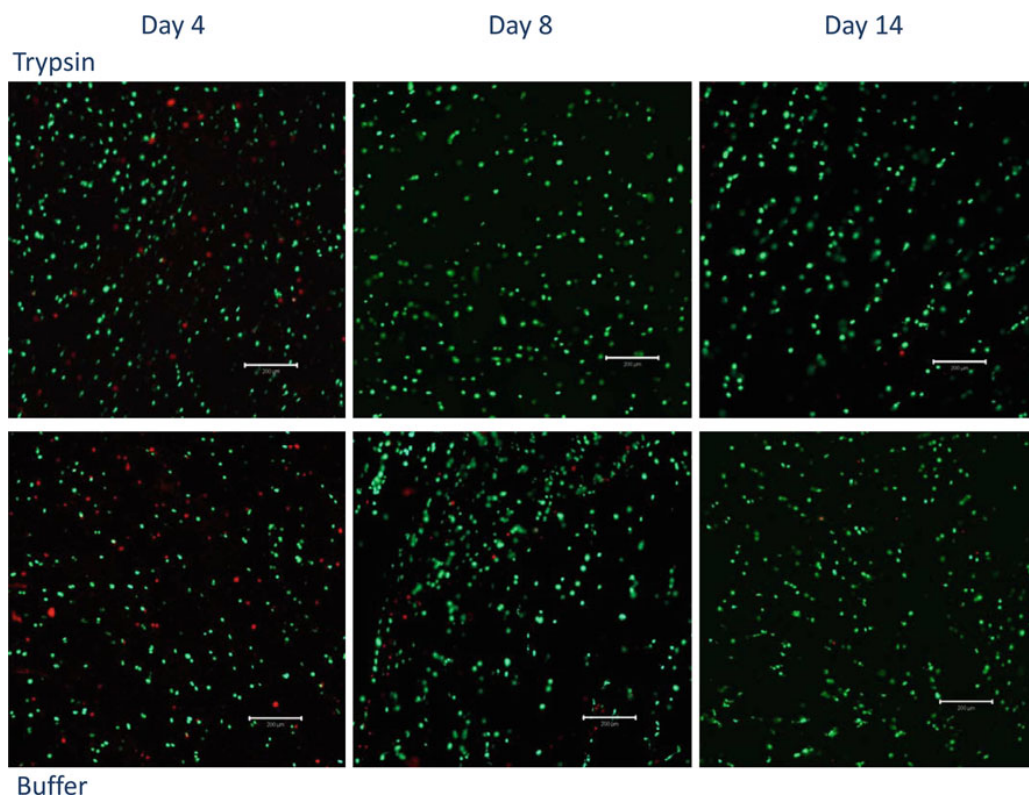


Figure 7–7: Cell viability in trypsin and buffer injected CEP discs. Cell viability was evaluated using fluorescent dyes (Live/Dead<sup>®</sup>, Invitrogen), and live (*green*) and dead (*red*) cells were visualized using an inverted confocal laser scanning microscope in trypsin- and control-injected discs at 4, 8 and 14 days after treatment. The *scale bars* represent 200 μm.

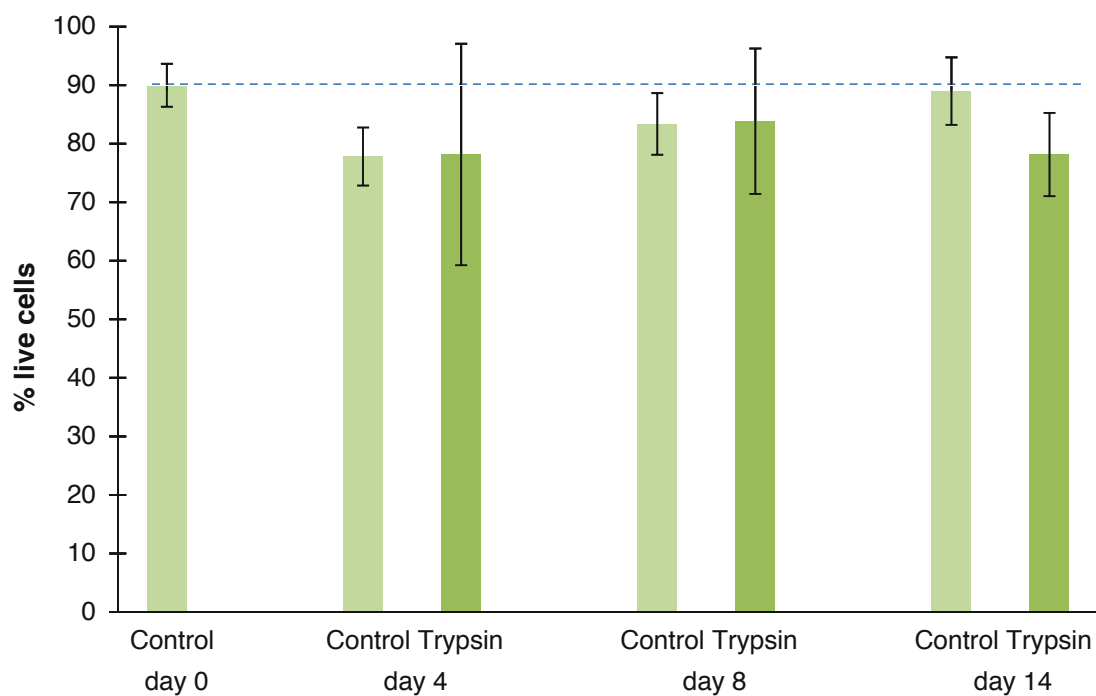


Figure 7–8: Cell viability in trypsin and buffer injected CEP discs. The proportion of live to dead cells was quantified separately in 5 selected, 6  $\mu\text{m}$  sections using the CellC software. Cell viability was calculated as a live to dead cell ratio and presented as % live cells ( $n = 8$ , *error bars* indicate standard deviation). Multivariate linear models were used to assess the effects of treatment, no significant difference was found compared to the control day 0,  $p > 0.05$ ).

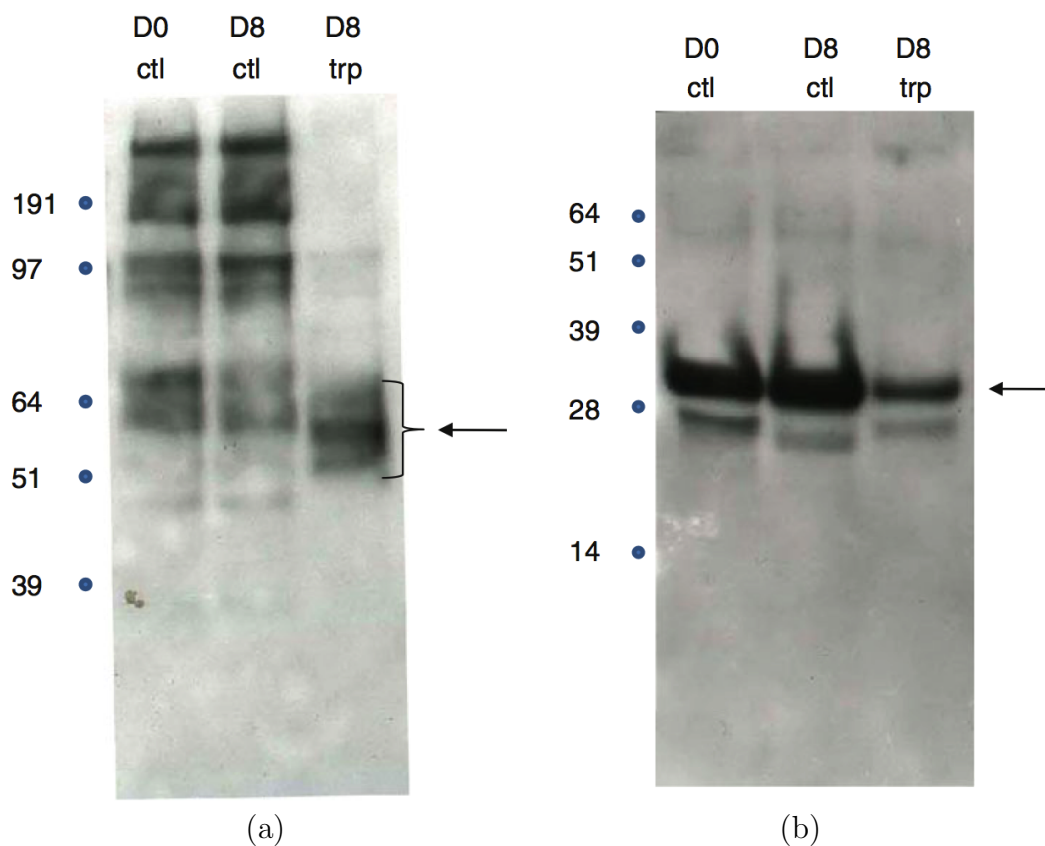


Figure 7-9: ECM and proteoglycan degradation caused by a single trypsin injection. Proteoglycan and protein degradation were analyzed by SDS-PAGE and western blotting using antibodies recognizing aggrecan (a) and CHAD (b). Pooled extract from 8 discs was analyzed in freshly isolated NP tissue (*ctl*), as well as in NP tissue 8 days after trypsin (*D8 trp*) or buffer injection (*D8 ctl*). Fragments representing free aggrecan G1 region or intact CHAD are indicated with an *arrow*.

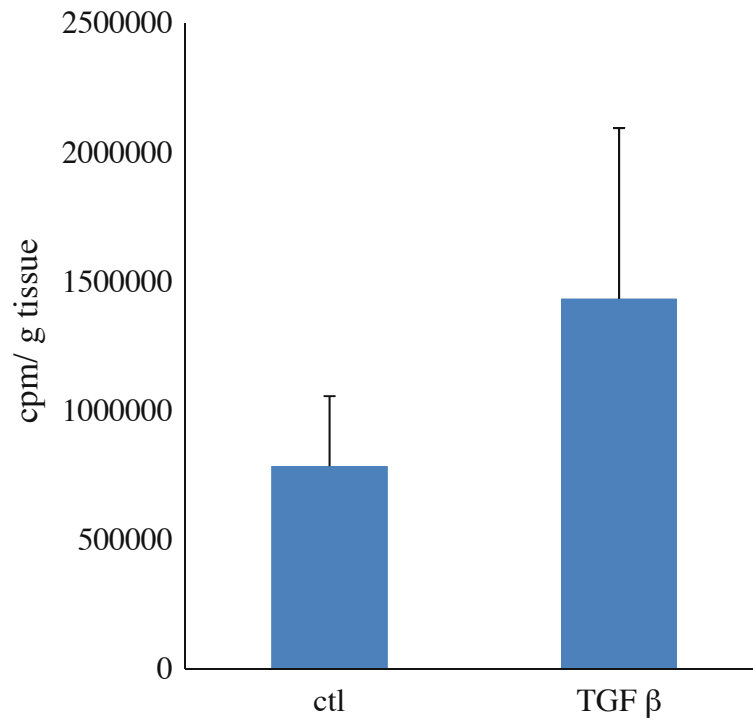


Figure 7–10: Proteoglycan synthesis in trypsin and buffer-injected CEP discs following TGF $\beta$  injection. Incorporation of radiolabeled sulfate was quantified 72 h after injection of 30 ng TGF $\beta$  (TGF  $\beta$ ) or buffer alone (*ctl*). Sulfate incorporation is indicated as cpm per gram wet weight tissue ( $n = 7$  TGF $\beta$  injected and  $n = 8$  control discs per group, *error bars* indicate standard deviation). An unpaired  $t$  test gave a  $p$  value of 0.02.

## **CHAPTER 8**

### **Discussion and Concluding Remarks**

The objective of this thesis was to combine engineering design and experimental techniques to start the development of a bovine coccygeal in-vitro organ culture model, an in-vitro organ culture model that would be a valuable tool used to further understand disc degeneration and to test new techniques of regeneration. When the thesis research was first proposed in 2003 there were very few in-vitro organ culture models for the intervertebral disc. Furthermore, most of them employed static mechanical or osmolaric chemical loading to stimulate the disc and used small sized, such as rabbit and mouse discs, for culture [59, 115]. Despite dynamic loading to be pinpointed as necessary stimulation to maintain proper disc function, many groups had either not developed this capability with the bioreactors or determined that it required too much effort to achieve such a model. In the following years, several groups have continued to develop such a model; however, until recently, successful cultures of bovine coccygeal discs have been limited to one week of viability with static loading [106]. It is the work that was begun in the thesis that allowed for such a model to be achieved through the continued work of Haglund [56].

#### **8.1 Bioreactor Design**

The first part of the thesis was used to develop an in-vitro environment for bovine coccygeal discs. This entailed designing the culturing system that enabled controlled axial mechanical stimulation to the discs. A control program, integrated

electronics and measurement transducers was assembled to make data recording of the disc mechanical response possible. As with all biological experiments, a large number of specimens are required, and for studying the intervertebral disc this was no different. In order to reduce the variability found from animal to animal and the number of animals required, it was logical to have more than one bioreactor unit allowing several discs to be harvested simultaneously. Therefore three bioreactors were built to allow the testing of either three different culturing conditions or to allow for triplicate testing. In the end, the in-vitro environment, bioreactor system, was validated and was shown to be capable of providing discs with an environment mimicking in-vivo physiological type conditions. The bioreactor could operate at 0.1 to 1.0 MPa loads at 0.1 to 1.0 Hz. The system did experience limitations at the low loads of 0.1 MPa and at 1.0 Hz. The difficulty to deliver low amplitude loads was most likely a limitation of the control system design which was a manual closed loop system. At low loads, the friction in the system reduced the axial load to the specimen and could not be corrected. In short, the system would benefit from a closed loop control system to improve the performance at low loading values.

## **8.2 Harvest Methods**

The next part of the thesis was used to determine the best harvesting method to isolate bovine coccygeal disc tissue. Previous studies have limited harvesting to two methods: discs harvested with a thin layer of bony endplate [48, 81, 93, 115] and discs harvested with no endplates [105, 106, 115], both methods having their limitations with no alternative method developed.

The method of leaving the vertebral endplates on the disc tissue is favoured for its mechanical stability, however the formation of blood clots during the harvest have prevented sufficient nutrients to be delivered to the nucleus pulposus of the disc. With smaller IVD tissue, the travel of nutrients across the endplates and into the centre of the disc is not far. However, for larger discs, this distance becomes an increasing limitation. So far, some groups have managed to remove clots and culture ovine discs with endplates in organ culture for up to three weeks [48, 81, 93]. Their method was to dose the animal with heparin, before slaughtering, to harvest the discs. This procedure is only possible in research facilities which house livestock and have access to a veterinarian; furthermore in this particular facility they could use animals that were to be sacrificed for other research purposes. Most research facilities are void of this type of tissue source. Moreover, when we compare the size of caudal ovine discs, which have a reported average disc height of 2.61 mm, to the disc height of bovine coccygeal discs, which is 7.98 mm, the diffusion of nutrients to the centre of the disc is doubled [152].

The second method was to remove the endplates entirely, thereby severing the anchoring of annulus fibres to the endplates, the structural support, altering the biomechanics of the tissue [105, 106, 115]. In order to build a mechanically stimulated IVD in-vitro organ model with large-sized tissue, a harvest method to preserve the mechanical structure of the tissue without sacrificing the nutritional diffusion into the tissue was developed. This method was what we have named as the CEP harvest method. By harvesting the disc tissue with intact bony end plates and drilling it with a high-grade surgical rotary burr, we were able to remove all bony and cartilaginous

material, only to leave a thin cartilaginous layer with the tissue, leaving its natural annular fibre attachments intact.

The results of the harvest method study, comparing previous harvesting methods to the new method showed the tissue harvested with the new method was able to maintain its mechanical structure with dynamic load over a period of one week without completely sacrificing the diffusive properties of the tissue, a primary limitation to large tissues with bony endplates preserved. Furthermore, the results from the one-week viability study comparing discs harvested with our novel method and with discs harvested with endplates, under diurnal loading, showed only a low cell viability for the discs harvested with endplates.

It was through the work of this thesis that a new harvest method was introduced. With this new harvest method, not only was the bovine coccygeal organ culture model realised [56], it also helped to develop both a human [49] and degenerative repair organ culture model [89]. The new method proved to be an interim between both previously presented methods in both mechanical stability and distribution of nutrition to the disc.

### **8.3 First Steps to an In-vitro Organ Culture**

In the later half of the thesis the early development of the organ culture model was pursued. Cell viability and activity for a six-day culture to validate live cells was examined. In this study, live cells were found after a six-day culture with only a slight decrease in cell proliferation and increase in GAG production for the novel harvest method. The study also confirmed the formation of blood clots and an added



diffusion distance contributed by the endplates using the BEP method with low to no cell viability in the nucleus and a decrease of GAG and DNA over the six days.

Preliminary studies under self-confined unloaded conditions of the disc tissue showed successful culturing with almost 80 % viable AF and NP cells for up to six weeks. Based on these preliminary results, an overreaching attempt to push the culture period to six weeks while introducing different loading conditions was tried with failing results. Within the first two weeks almost all discs had lost more than 50 % cell viability. With this level of viability, it was quickly realized that our previous technique used to evaluate cell viability by cell isolation was inadequate. Although this method was an accepted and established method for disc organ culture [59], it was not sufficient due to the low number of cells that remained after two weeks. This was thought as a limitation to the analysis method, regardless of whether the culture protocol itself was the cause for the cell death, which we later discovered was the case. Cell viability measurement method was then changed to laser scanning confocal microscopy, giving the added information of cell viability within the tissue.

Furthermore, biochemical and histological understanding proved to be necessary to understand the effects of mechanical stimulation to disc tissue. Therefore, time was taken to refine both the culturing and analysis methods before a two-week culture study incorporating a more thorough examination of disc response at the molecular level was conducted. Up until this point only the most basic measurements were made, studying GAG, DNA content and metabolic activity with a salt reduction test. With eliminating the cell isolation method, the salt reduction test that was previously used to measure metabolic activity of the cells also needed to be changed. Although

there has been many groups that have measured in detail proteolytic enzymes to mark signs of degeneration in the disc [145, 196, 197, 231], a choice to measure the proteins chondroadherin and fibromodulin was made. Chondroadherin has been suggested to be strongly involved in the regulation of chondrocyte growth and proliferation [201]. Furthermore, different levels of chondroadherin have also been found for the convex versus the concave side of human scoliotic discs [57]. The protein fibromodulin is found to be associated with age-related changes in the disc tissue [206]. In human intervertebral discs, fibromodulin abundance decreases in the nucleus pulposus with age [206]. Furthermore, in the annulus fibrosus, fibromodulin exhibits structural changes with age, losing its keratan sulfate [206]. Rather than looking at different degradation enzymes, the idea was to look at two proteins which may be able to suggest whether the disc, after mechanical stimulation and culture, was healthy, showing signs of accelerated aging or abnormal pathology.

Despite taking the time to revise the methodology for the final two-week, mechanically loaded cultures, the oversight of the bioreactor–“new harvest method” interface led to cell death at the annulus fibrosus of the axially loaded discs and sporadic and inconsistent results. It was with the change of cell viability measurement methodology to laser scanning confocal microscopy that the large amount of cell-death in the annulus could be seen. This result led to the conclusion that the internal loading mechanics of the disc was not replicated with the current bioreactor system. If the previous methods of keeping or eliminating the entire endplate would have been used, this would not have occurred. With this new method of polishing

down the endplate and leaving the cartilaginous layer, in bovine coccygeal discs, non-uniform concave surfaces were created at the endplates.

Stress profilometry is a known method for studying the pressure profile across the intervertebral disc [134]. Previous studies have used this method to characterize and compare the different loading patterns within healthy and degenerative discs. Healthy discs have a uniform load, whereas, depending on the grade of degeneration, degenerated discs show not only irregular loading peaks but also higher loads at the annulus and lower loads at the nucleus [1]. Using the stress profilometry of a healthy bovine coccygeal disc with endplates as the control, the bioreactor interface with the new harvest method can be optimized by exploring different interface shapes until a similar stress profilometry is achieved. This, however, was beyond the scope of the thesis and was not pursued.

It was also during the two-week experiments that the platens of the tissue-loading platen interface, over time, had accumulated debris. This accumulation may have reduced the nutrients available to the tissue during the culturing period. Although the use of porous platens as the disc interface have been presented as a suitable material [115], whether the platens were hydrophilic or hydrophobic was never mentioned. Hydrophilic platens were chosen in the bioreactor to encourage fluid and nutrient flow to the disc tissue, since hydrophilic material wet on fluid contact. However, it was also because of the hydrophilic properties of the platens that drew filtered deposits into its pores. Further understanding of hydrophilic and hydrophobic filters shows that hydrophobic platens would have, although not wet on

direct solution contact, wicked the solution through the platen, which was what was required for the application.

The results of the two-week study reconfirmed the difficulties, at that time (2007), in establishing a dynamic loading, in-vitro intervertebral disc culture model for bovine coccygeal discs, as found by many groups, to analyse the influence between mechanical load and the behaviour of the disc at the cellular level. With the shortcomings of the bioreactor identified, stepping back to validate the culturing methods without the bioreactor seemed like the next logical step.

#### **8.4 One Application of the New Harvest Method**

Despite the setback with the bioreactor development, a separate study showed how the novel culture method could help establish a degeneration-repair model which could be an important tool for the examination of disc regeneration therapies [89]. With the development of the novel harvest method, culturing the disc with only a self-confined loading which would be in the range of 0.1 to 0.3 MPa was a new possibility. Although GAG results of our two-week study showed that self-confined discs lost more than 50 % of their initial GAG, it was unknown whether the drastic loss of GAG was contributed by a learning curve in culturing disc tissue. Furthermore, it was felt that, as long as the control values for the model were monitored at the same time points, it would still be a valid model depending on the application. As a final study, the IVD organ culture model was applied towards the development of a degeneration-repair model. The goal of the study was to test the feasibility of developing a reproducible degeneration model in which to study disc repair. A previous group has also tried to establish such a model using trypsin and papain as

digestive enzymes, although no cell viability was measured [183]. The idea behind developing such a model is to be able to test different types of regeneration type therapies. In this study the organ culturing methodology was validated when discs harvested with the cartilaginous endplates maintained high cell viability and GAG levels. With the model that was developed, only a low amount of trypsin was required to develop an early stage degeneration model. Because of the high level of live cells remaining after two weeks, it can be a very good model to test regeneration techniques that stimulate proteoglycan production.

## **8.5 Clinical Significance**

How does the development of this in-vitro organ culture model fit into the understanding and treatment development of intervertebral disc tissue? Even after thirty years of dedicated research into the area of intervertebral disc tissue, with the discoveries of new biological materials and new diagnostic instruments to analyse tissue, such as MRI, the disc still remains poorly understood. The gold standard of treatment for a degenerated disc is in fact still disc fusion, despite hundreds of implant companies with their expensive mechanical prototypes.

The first part of this thesis began work to develop an in-vitro environment that could be applied towards the development of an in-vitro disc organ culture model. With the goals of more biological disc replacements, the environment had the aim to serve also as a testing platform for biological materials with the potential of cell seeding.

Through the work of the thesis, the largest contribution was the development of a novel harvest method which could later be applied to a degeneration-repair in-vitro organ culture model. The technique is a promising isolation method to further develop the in-vitro organ culture model. The harvested tissue has shown mechanical stability and adequate diffusion of nutrients to the centre of the disc. Although the dynamically loaded bovine coccygeal disc model was never realised, it is off to a good start.

## 8.6 Future Work

The work presented in this thesis was only the beginning work to the development of a bovine coccygeal in-vitro organ culture model that will hopefully become instrumental in discovering and studying biological repair techniques to delay disc degeneration disease progression. Establishing an in-vitro organ culture model is complex. At the time at which this work was completed in 2007, the following was still remaining in the realization of the model:

1. **Improving the interface between harvested disc tissue and fluid-exchanging interface plates.** The current design of the bioreactor did not take into account the concave nature of bovine coccygeal discs. As a result, during the long-term mechanical loading, there was high number of cell death in the annulus fibrosus. A stress profilometry study can be made to compare the load distribution of a healthy coccygeal disc with endplates with discs harvested with the CEP method in the bioreactor chamber to optimise the loading platen-disc interface. Furthermore, a more thorough analysis of the fluid interface exchange at the interface platen surface and the disc can also be made.

Because of the requirement of the disc to receive nutrients by diffusion through surrounding fluid, particularly at the endplates, it would be important to confirm that adequate nutrition is made available to the cultured tissue. The wet test that was used to validate this exchange interface in the bioreactor system did not account for clogging of the endplates over time. Perhaps a different material other than hydrophilic interface plates can be used to avoid this clogging phenomenon. Further work in this area would be useful to bring the organ culture system to the next level.

This suggested work was carried out after 2007 by Haglund et al. [56]. The changes that were made after carrying out a stress profilometry study allowed for a successful bovine coccygeal organ culture model to be established.

2. **Long-term studies using different mechanical loading patterns (frequency, load, amplitude and duration).** The current thesis uses only one frequency, load and amplitude combination that was derived from the findings of current literature to simulate the physiological-like loading of the disc. However, this combination of values requires further study. The “correct” parameters have yet to be established, and whether a special combination of values will lead to regeneration of the disc is still in question. To date, this work is still in the future plans.
3. **Further development of the repair-degeneration model.** The thesis presented a small study into the application of the IVD organ culture model towards the development of a repair-degeneration model. Further validation and quantification of this model is certainly required. It would be of clinical

interest to further develop such a model and use it to test various regeneration treatment strategies. To date, this work is currently in progress by Haglund.

## 8.7 Epilogue

The thesis work began in 2003 with the aim of developing and validating an in-vitro organ culture model, allowing for axial dynamic load stimulation, using bovine coccygeal discs. At that time a few groups were working in parallel on such a model. By 2007, a working, axially loaded organ culture model using bovine coccygeal discs was not realised. The amount of work required was not foreseen. The bioreactor, although having initially met the design requirements that were set out, met new design requirements that were discovered along the way. Without meeting these new requirements it was not possible to move forward on the development of the organ culture model without improving the system. However, on the other hand, with a newly established harvest method for bovine coccygeal discs, another organ culture model could be realised. It took another four years, hard work and the continued dedication of Haglund and group to finally realise the model in 2011. The fruits of the early development work which was conducted in this thesis was finally documented in a publication [56]. In 2009 another group, who was also working in parallel, presented a dynamic axially loaded organ culture model using ovine discs with intact endplates [93]. To date, there have only been two systems that have been presented but the likelihood of more models in the future is high.



## CHAPTER 9

### Conclusion

#### 9.1 Summary

The objective of this thesis was to combine engineering design and experimental techniques to start the development of a bovine coccygeal in-vitro organ culture model. An in-vitro organ culture model that would be a valuable tool used to further understand disc degeneration and to test new techniques of regeneration. When the thesis research was first proposed in 2003 there were very few in-vitro organ culture models for the intervertebral disc. Furthermore most of them employed static mechanical or osmolaric chemical loading to stimulate the disc and used small sized; such as rabbits and mice disc, for culture. Despite dynamic loading to be pinpointed as necessary stimulation to maintain proper disc function, many groups had either not developed this capability with the bioreactors or determined that it required too much effort to achieve such a model. In the following years, several groups have continued to develop such a model, however, until recently, successful culture of bovine coccygeal discs have been limited to one week of viability with static loading [106]. It is the work that was begun in the thesis that allowed for such a model to be achieved through the continued work of Haglund [56].

The first part of the thesis was used to develop in in-vitro environment for bovine coccygeal discs. This entailed designing the culturing system that enabled controlled axial mechanical stimulation to the discs. A control program, integrated electronics

and measurement transducers was assembled to make data recording of the disc mechanical response possible. In the end, the in-vitro environment, bioreactor system, was validated and was shown to be capable of providing discs with an environment mimicking in-vivo physiological type conditions. However, with all biological experiments, a large number of specimens are required in a study, and for studying the intervertebral disc this was no different. In order to be able to compare specimens within on bovine coccygeal disc to reduce variability from animal to animal it was logical to have more than one bioreactor unit. Therefore a total of three were assembled to allow the testing of either three different culturing conditions or to allow for triplicate testing.

The next part of the thesis was used to determine the optimal harvesting method to isolate bovine coccygeal disc tissue. Previous studies have limited harvesting method to two methods. Both methods having their limitations with no alternative method developed. The method of leaving the vertebral endplates on the disc tissue is favoured for its mechanical stability, however the formation of blood clots during the harvest have prevented sufficient nutrients to be delivered to the nucleus pulposus of the disc. The alternate method to remove all endplates entirely, thereby severing the anchoring of annulus fibres to the endplates for structural support, altering the biomechanics of the tissue was the second option. It was through the work of this thesis that a new harvest method, CEP, which was to remove the vertebral endplate and cartilaginous endplate with a high-speed cutter leaving a thin layer of cartilaginous behind, was introduced. With this new harvest method not only was the bovine coccygeal organ culture model realized [56], it also helped to realize both a human

[49] and degenerative repair organ culture model [89]. The new method proved to be an interim between both methods in both mechanical stability and distribution of nutrition to the disc.

In the later half of the thesis the early development of the organ culture model was pursued. The response of the tissue at the cellular level was examined. Cell viability and activity for a six-day culture to validate live cells was examined. In this study, live cells were found after a six-day culture with only a slight decrease in cell proliferation and increase in GAG production for the novel harvest method. The study also confirmed the blood clots and added diffusion distance contributed by the endplates using the BEP method with low to no cell viability in the nucleus and a decrease of GAG and DNA over the six days.

In our next steps, an overreaching attempt to push the culture period to six weeks while introducing different loading conditions was tried with failing results. It was quickly realized that our previous technique used to evaluate cell viability by cell isolation was inadequate. Furthermore, biochemical and histological understanding proved to be necessary to understand the effects of mechanical stimulation to disc tissue. Therefore, time was taken to refine both the culturing and analysis methods before a two-week culture study incorporating a more thorough examination of disc response at the molecular level was conducted. The results of the study showed active viable cells in discs for all loading conditions, supporting the hypothesis that mechanical load could possibly extend disc culture for longer culture periods. However, shortcomings of the bioreactor system and the model were also identified. The

second study reconfirmed the difficulties, at that time (2007), in establishing an dynamic loading, in-vitro intervertebral disc culture model for bovine coccygeal discs, as found by many groups, to analyze the influence between mechanical load and the behaviour of the disc at the cellular level. Despite the set back with the bioreactor development, a separate study showed how the novel culture method could help establish an degeneration-repair model which could be an important tool for the examination of disc regeneration therapies [89].

## 9.2 Future Work

The work presented in this thesis was only the beginning work to the development of a bovine coccygeal in-vitro organ culture model that will hopefully become instrumental in discovering and studying biological repair techniques to delay disc degeneration disease progression. Establishing an in-vitro organ culture model is complex. At the time at which this work was completed in 2007, the following was still remaining in the realization of the model:

1. **Improving the interface between harvested disc tissue and fluid-exchanging interface plates.** The current design of the bioreactor did not take into account the concave nature of bovine coccygeal discs. As a result, during the long-term mechanical loading, there was high number of cell death in the annulus fibrosus. A stress profilometry study can be made to compare the load distribution of a healthy coccygeal disc with endplates with discs harvested with the CEP method in the bioreactor chamber to optimise the loading platen-disc interface. Furthermore, a more thorough analysis of the fluid interface exchange at the interface platen surface and the disc can also be made.

Because of the disc requirement to receive nutrients by diffusion through surrounding fluid, particularly at the endplates, it would be important to confirm that adequate nutrition is made available to the cultured tissue. The wet test that was used to validate this exchange interface in the bioreactor system did not account for clogging of the endplates over time. Perhaps a different material other than hydrophilic interface plates can be used to avoid this clogging phenomenon. Further work in this area would be useful to bring the organ culture system to the next level.

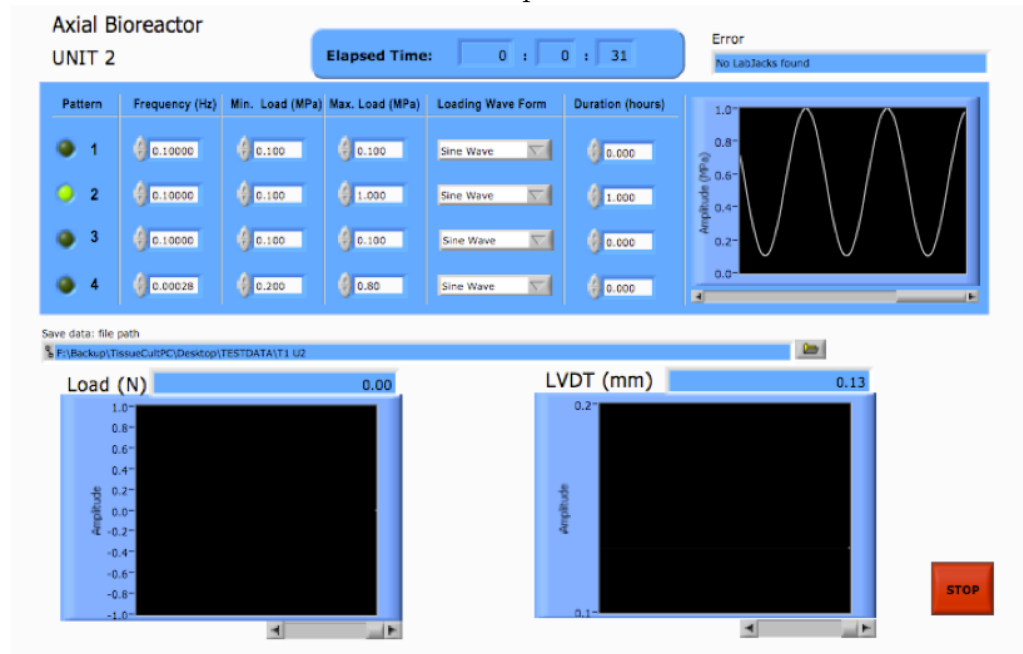
2. **Long-term studies using different mechanical loading patterns (frequency, load, amplitude and duration).** The current thesis uses only one frequency, load and amplitude combination that was derived from the findings of current literature to simulate the physiological-like loading of the disc. However, this combination of values requires further study. The “correct” parameters have yet to be established and whether a special combination of values will lead to regeneration of the disc is still in question.
3. **Further development of the repair-degeneration model.** The thesis presented a small study into the application of the IVD organ culture model towards the development of a repair-degeneration model. Further validation and quantification of this model is certainly required. It would be of clinical interest to further develop such a model and use it to test various regeneration treatment strategies.

## APPENDIX A

### Bioreactor: Labview Code and Bill of Materials

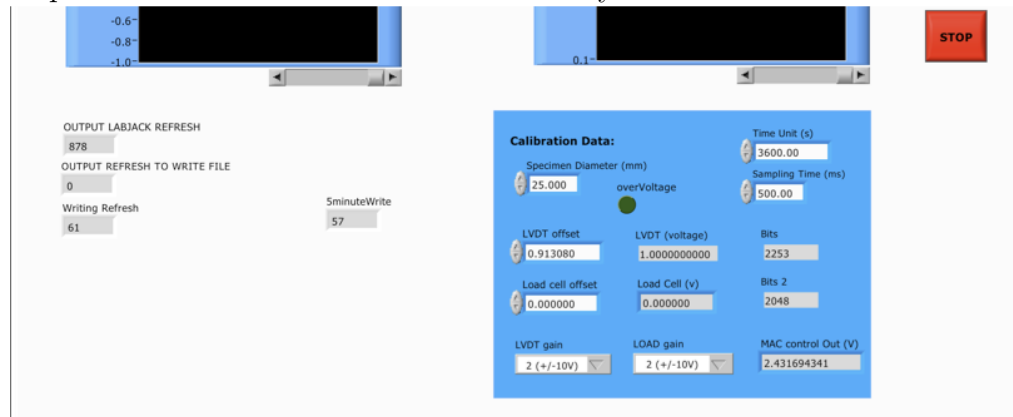
#### A.1 Labview Code

All devices were electronically controlled using a data acquisition board (Labjack U12, Labjack, Colorado, USA) and a custom program written with Labview (National Instruments, Texas, USA). The custom program was designed to allow for dynamic cyclic load ranging from 0.01 to 1.0 Hz. It was also designed to deliver: ramp, square wave, sinusoidal and triangle wave loading patterns. The user interface allowed for four different consecutive patterns to run.



The applied load and displacement readings were displayed in graph and numerical format instantaneously.

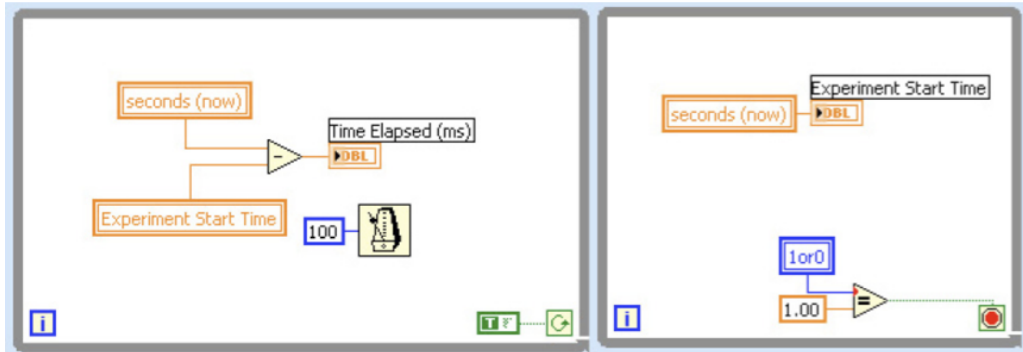
A calibration panel was created so that the specimen cross-sectional diameter could be entered. Furthermore the important calibration parameters of the load and displacement transducers could be manually controlled.



Behind the user interface the program contained the following functions or loops:

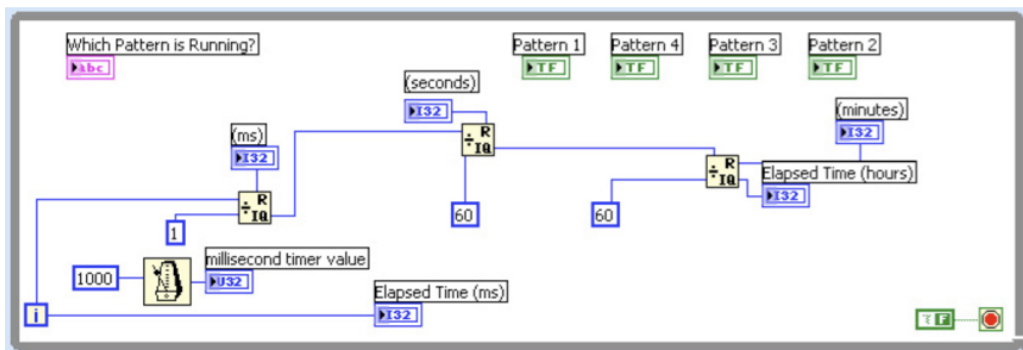
### A.1.1 Block Clock

An independent clock was written to keep the time of the experiment.



### A.1.2 Pattern Display

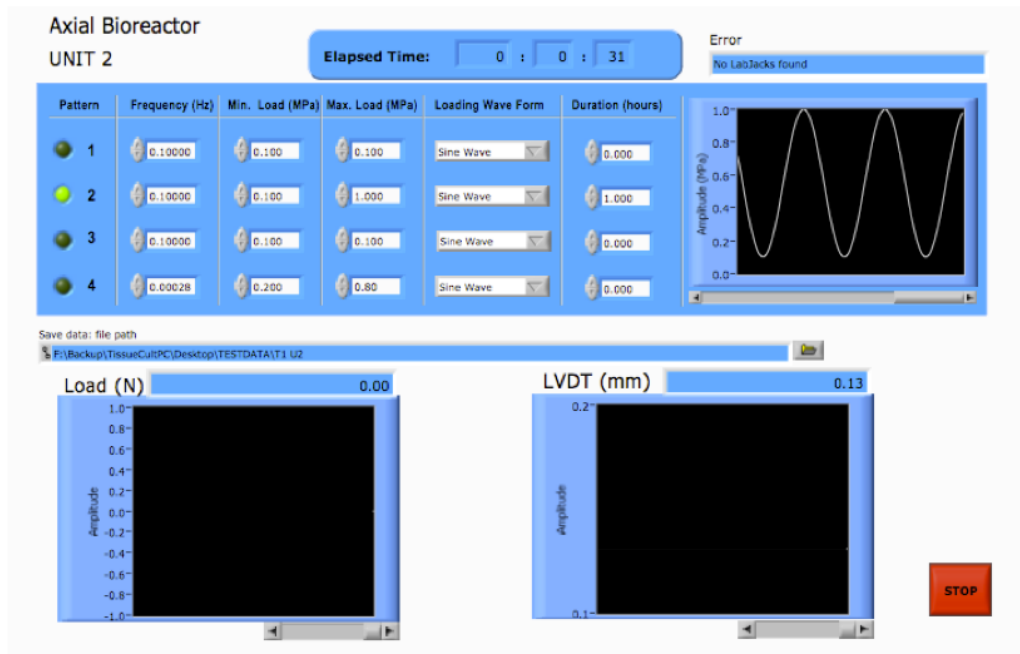
Using the “Elapsed Time” variable, the loading pattern could be indicated and displayed on the front panel.





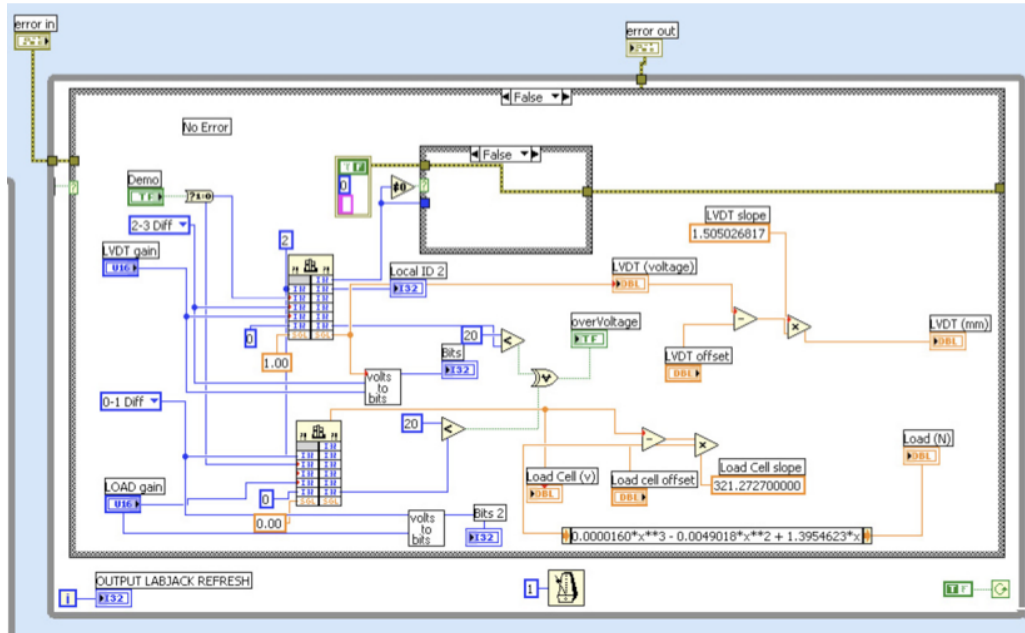
### A.1.3 Data Sampling Counter

A structure was created for a running timer for data writing that was set in reference to the sampling time. Sampling time was dictated by the frequency of the load, ensuring enough data points to capture the load waveform.



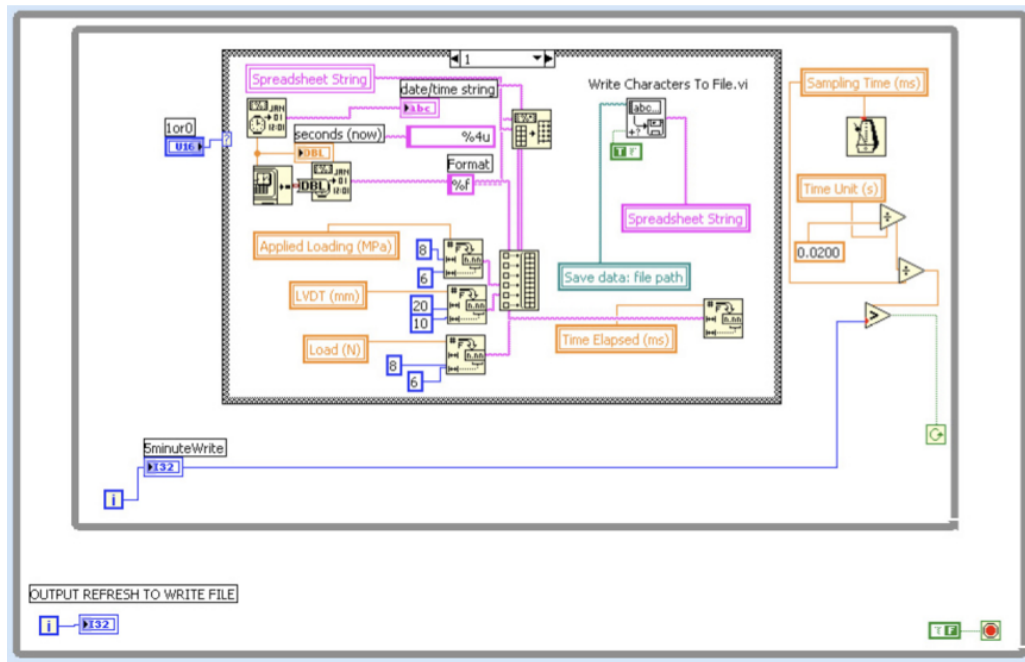
#### A.1.4 Data Input

The data was collected from the Labjack as analog signals and translated according to the technical specifications of the measurement devices into values.



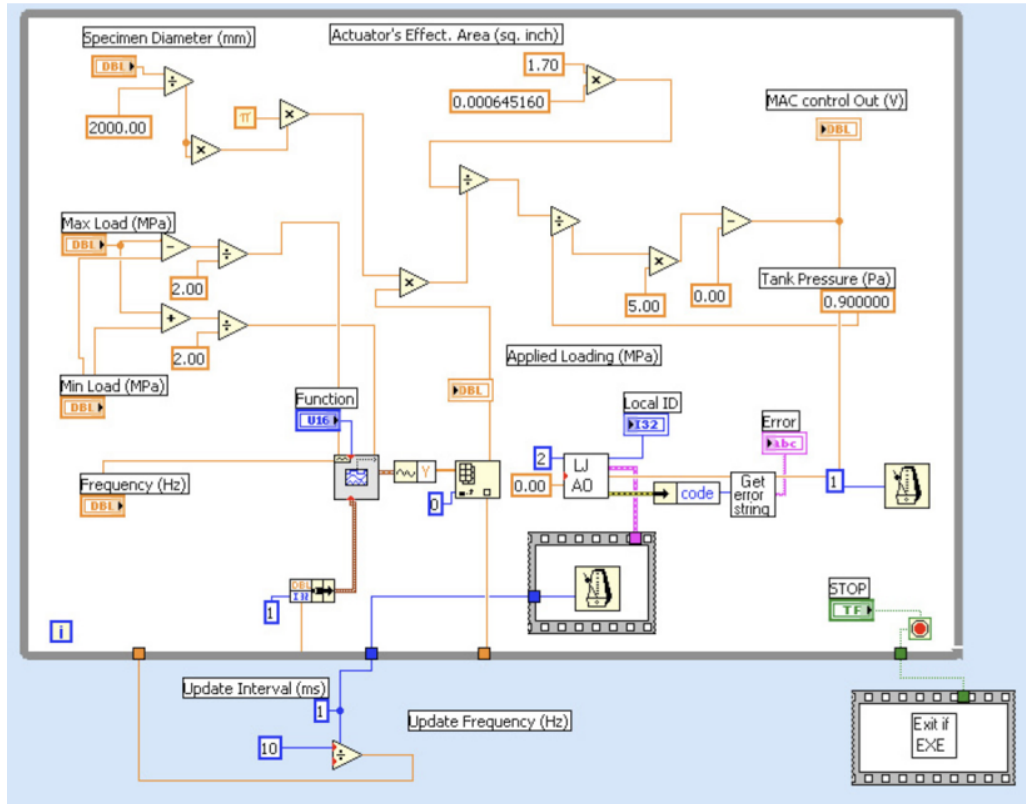
### A.1.5 Data Write

A function was written to record the applied load, actual load from the load transducer and displacement into an .xls data file which was controlled by the set sampling time. The location of the saved file could be set in the front panel of the user interface.



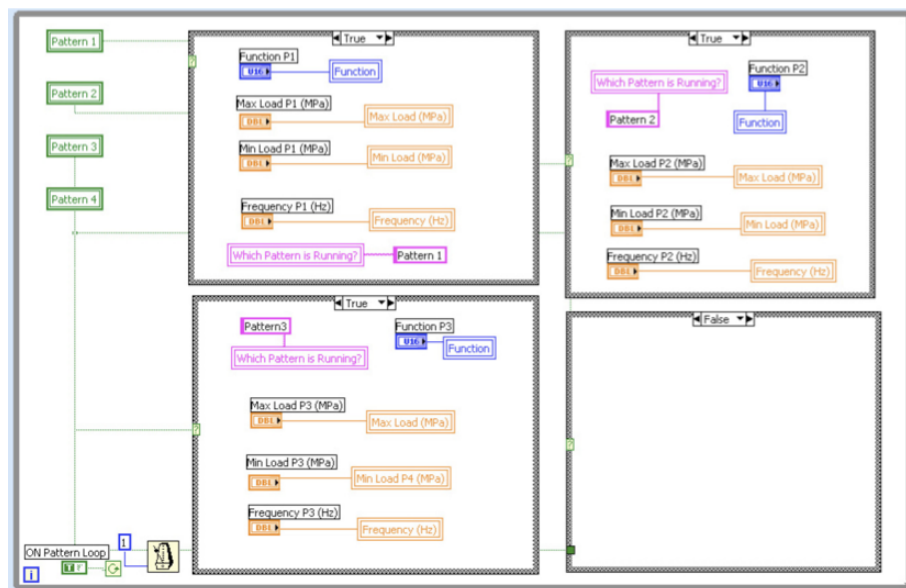
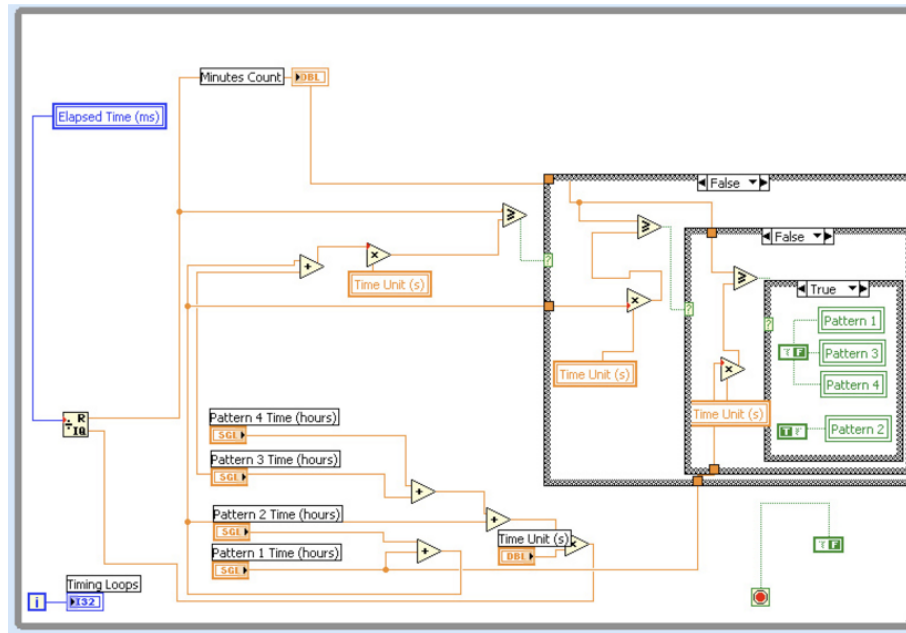
### A.1.6 Applied Load

Taking the user entered specimen diameter, an analog signal was sent through the Labjack to the pneumatic air valve to deliver a load to the specimen.



### A.1.7 Applied Loading Pattern

The user dictated the loading pattern in the front panel. The different loading pattern signals were determined using several true-false structures.



## A.2 Bill of Materials

### Transducers

Linear variable displacement transducer, Omegadyne LD400-5  
Load cell, Omegadyne LC703-300  
Rolling diaphragm actuator, Illinois Pneumatics, Uni-block cylinder 1.7 DAS-1BC  
Proportional air valve, Norgren, VP50 series VP5008PK111H00  
In-line air filter, 15-125PSI, SMC, AQD30-N02DE-Z

### Electronics

2  $\times$  INA114AP instrument amplifiers  
1  $\times$  49 k $\Omega$   $\pm$ 1 % resistor  
1  $\times$  249  $\Omega$   $\pm$ 1 % resistor  
1  $\times$  Enclosure for DAQ board and circuit components  
4  $\times$  10  $\mu$ F capacitors  
1  $\times$  3M terminal strip (923269-ND)  
1  $\times$  USB data acquisition board, Labjack, U12  
1  $\times$  Power supply +24V +12V -12V +5V, Power One, MAP55-4001  
4  $\times$  Female 5-pin connectors

### Machined Components

Stainless steel bioreactor frame  
4  $\times$  10-32 bolts (mount actuator to frame)  
1  $\times$  Polycarbonate bioreactor chamber  
1  $\times$  Polycarbonate piston arm  
1  $\times$  Teflon top interface plate  
1  $\times$  Teflon bottom interface plate  
2  $\times$  45 mm diameter  $\times$  1/8", 70  $\mu$ m pore size hydrophilic polyethylene platens,  
Scientific Commodities, BB2062-70AL (18"  $\times$  18" sheets)  
1  $\times$  LVDT loading plate  
1  $\times$  Polycarbonate load cell – piston arm connector  
1  $\times$  Polycarbonate load cell – actuator connector

### Fluid System

1  $\times$  Masterflex L/S Standard drive system, HV-07553-70  
1  $\times$  Masterflex L/S 12-Channel, 8-roller pump head, HV-07519-25  
1  $\times$  Masterflex tubing cartridge, L/S 14, 07519-85

## APPENDIX B

### MATLAB Routines

One component of the bioreactor system was to collect axial compression force and displacement of the organ culture specimen into a data file with respect to the loading scheme and time. Labview wrote the data files into raw text files. MATLAB routines were used to fit the data to a one-dimensional biphasic model.

The following assumptions were taken for the model that was used to fit the data:

- The intervertebral disc is homogenous, uniform soft tissue with a solid and fluid phase.
- The disc tissue was fully saturated at the onset of loading.
- The structural part of the disc tissue and water are incompressible.
- The compression and flow are one-dimensional (vertical).
- Strains are relatively small.
- Darcy's law is valid at all hydraulic gradients.
- The coefficient of permeability,  $\kappa$ , and the coefficient of volume compressibility, in this case, the aggregate modulus,  $H_A$ , remains constant throughout the process.
- There is a unique relationship, independent of time, between void ratio and effective stress.
- The disc itself, ignoring the initial lateral bulge, has a confined structural shape.

Reducing the linear biphasic equations of Mow [144] to a parabolic partial differential equation [205] for the displacement of the solid matrix, the equation becomes

$$\frac{du}{dt} - H_A \kappa \frac{d^2 u}{dz^2} = 0 \quad (\text{B.1})$$

where  $H_A$  is the aggregate compressive modulus.

The initial and boundary conditions for cyclic compressive loading were:

$$u(0, t) = 0, \quad t \geq 0 \quad (\text{B.2})$$

$$u(z, 0) = 0, \quad 0 \leq z \leq h \quad (\text{B.3})$$

$$H_A \frac{du}{dz} \Big|_{z=h} = -\sigma_0(1 - \cos \omega t), \text{ at } z = h \quad (\text{B.4})$$

where  $h$  is half of the initial tissue thickness,  $\sigma_0$  is the median magnitude of the cyclic load and  $\omega$  is the loading frequency. The solution for the equation then becomes

$$\begin{aligned} u(z, t) = & -\frac{\sigma_0}{H_A} z(1 - \cos \omega t) \\ & + \frac{2\sigma_0}{H_A h} \sum_{n=1}^{\infty} \left[ \sin \mu_n h \sin \mu_n z \frac{\omega}{\mu_n^2 (\alpha_n^2 + \omega^2)} \right. \\ & \left. \times \{ \omega \exp(\alpha_n t) - \alpha_n \sin \omega t - \omega \cos \omega t \} \right] \end{aligned} \quad (\text{B.5})$$

where

$$\mu_n = (n - 0.5) \frac{\pi}{h} \quad (\text{B.6})$$

and

$$\alpha_n = -\mu_n^2 H_A \kappa. \quad (\text{B.7})$$



The characteristic diffusion time of the tissue can be quantified as

$$\tau = \frac{4h^2}{\pi^2 H_A \kappa} . \quad (\text{B.8})$$

At the equilibrium of tissue displacement to the exerted load, the fluid flow out of the tissue has reached a steady state and therefore the applied stress  $\sigma_0$  is carried entirely by the solid matrix of the tissue. The aggregate modulus  $H_A$  represents the intrinsic confined compressive modulus of the tissue's solid skeleton and can be calculated as

$$H_A = \frac{\sigma_0 h}{z_\infty} \quad (\text{B.9})$$

where  $z_\infty$  is the median equilibrated displacement of the tissue.

The solution at the surface of the intervertebral disc tissue , where  $z = h$ , gave

$$u(h, t) = -\frac{\sigma_0}{H_A} \left[ h - \frac{2h}{\pi^2} 4 \sin \frac{\pi}{2} e^{\left[ \frac{-H_A \kappa}{4h^2} \right] \pi^2 t} \right] . \quad (\text{B.10})$$

## B.1 Routine 1

`Plotting_data.m` is the main routine used to implement the model fit on collected load and displacement from the organ culture system.

```

1 % Plotting_data.m
2 %
3 % load data from folder with recorded load and displacement
4 % fit data to model
5 % measurements to determine mechanical properties of axial loaded tissue
6 %
7 clear variables;
```

```

8  close all;
9
10 baseDir = '.';
11
12 expDir = fullfile(baseDir,sprintf('/EXP%d',1));
13 % loading data file from directory EXP1
14 data = readDataset(expDir, 'cep');
15 % call on function readDataset.m to read cep.mat data of EXP1
16
17 [x1, y1, x2, y2] = getDatasets(data.seconds,data.lvd);
18 % finding creep and relaxation start and end periods in data
19 % function getDatasets.m
20
21 [chunks, xf, yf, yMax, yMin] = filterDatasets(x1, y1); %Creep
22 % call of function filterDatasets.m to filter data for creep cycle
23
24 %[chunks, xf, yf] = filterDatasets(x2, y2); %Relax
25 % alternately, above call of function filterDatasets.m to filter data for
26 % relaxation/recovery cycle
27
28 [dt, du, tau2, delta_02, t02, u02] = fitDataset(xf,yf);
29 % call of function fitDataset.m to fit data to a model
30 % returning variables dt:
31
32 if 1
33 noPlots = length(chunks);
34 figure;
35
36 % plotting returned variables to see trend over each relaxation or creep
37 % cycle
38 subplot(3,1,1);

```

```

39 plot([tau2{:}],',.-');
40 ylabel('tau');
41 subplot(3,1,2);
42 plot([delta_02{:}],',.-');
43 ylabel('delta0');
44 subplot(3,1,3);
45 plot([u02{:}] ./ u02{1} * 100 - 100,',.-');
46 ylabel('u0');
47 
48 % assignment of results into variable array
49 variable(1,:)=tau2{:}]
50 variable(2,:)=delta_02{:}]
51 variable(3,:)=t02{:}]
52 variable(4,:)=yMax{:}]
53 variable(5,:)=yMin{:}]
54 variable(6,:)=variable(4,:)-variable(5,:)
55 variable=variable'
56 
57 end
58 end

```

## B.2 Routine 2

readDataset.m is called by the main routine Plot\_data.m to read in data to be analyzed.

```

1 % readDataset.m
2 % function used to read data x.mat file
3 % in directory
4 

```

```

5 function data = readDataset(dataDir,expType)
6
7 dataFile = fullfile(dataDir,sprintf('%s.mat',expType));
8 data = load(dataFile);

```

### B.3 Routine 3

`getDatasets.m` is another function called by the main routine `Plot_data.m` to search for the beginning and end of all creep and relaxation cycles in the data.

```

1 % getDatasets.m
2 % searching for creep and relaxation cycles in the dataset
3 %
4 function [x1, y1, x2, y2] = getDatasets(xi,yi);
5
6 nIntervals = round(xi(end));
7
8 x1 = {};
9 y1 = {};
10 x2 = {};
11 y2 = {};
12
13 for ni = 1:nIntervals
14
15 %nIntervals marks the number of days
16
17     xx1 = ni-1 + 0;
18     % the creep cycle
19
20     xx2 = ni-1 + 0.5;

```

```

21 % the change from creep to recovery
22
23 xx3 = ni-1 + 1;
24 % the recovery cycle
25
26 idx1 = find((xi >= xx1) & (xi < xx2));
27 x1{ni} = xi(idx1);
28 y1{ni} = yi(idx1);
29 idx2 = find((xi >= xx2) & (xi < xx3));
30 x2{ni} = xi(idx2);
31 y2{ni} = yi(idx2);
32
33 end

```

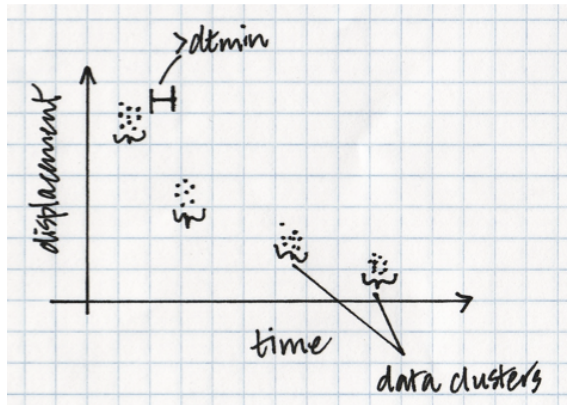
#### B.4 Routine 4

`filterDataset.m` is a function called by the main routine `Plot_data.m`. The routine uses a threshold to average the recorded data points for each creep or relaxation cycle. In the end, a total of twelve data points for each cycle is returned.

```

1 % filterDataset.m
2 % function to separate data into load cycle chunks
3 % distinguishing data from creep and relaxation loading cycles

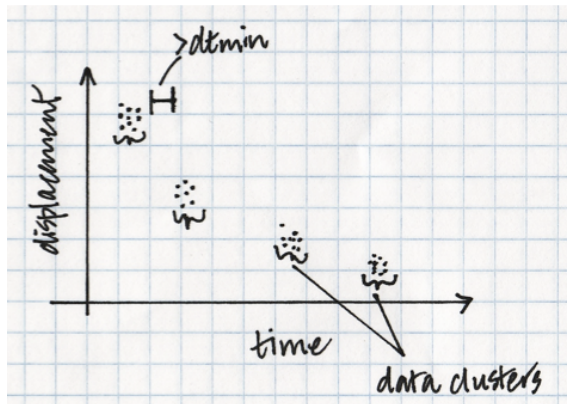
```



```

4 function [ chunks, xf, yf, yMax, yMin ] = filterDataset(x1, y1)
5
6 dtmin = 0.01;
7 % threshold value to distinguish time difference between cluster points in one cycle

```



```

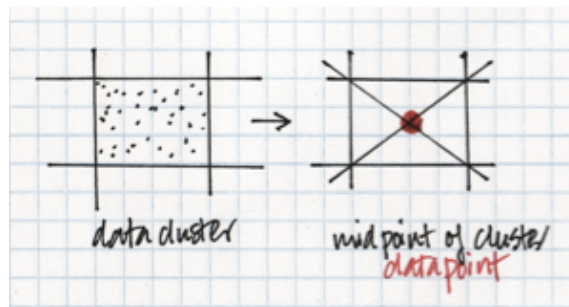
8 chunks = {};
9
10 n = 1;
11
12 chunks{n}.x = [];

```

```

13 chunks{n}.y = [];
14
15 xf = [];
16 yf = [];
17
18 for i=1:length(x1)-1
19
20     x = x1(i);
21     y = y1(i);
22
23     chunks{n}.x = [ chunks{n}.x x ];
24     chunks{n}.y = [ chunks{n}.y y ];
25
26     % averaging of clusters
27     % new points are created { which takes the midpoint
28     % of the cluster of data points

```



```

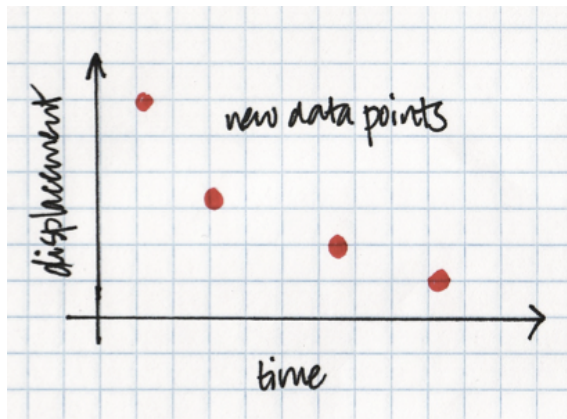
29     if x1(i+1) - x1(i) > dtmin
30
31         chunks{n}.xMin = min(chunks{n}.x);
32         chunks{n}.xMax = max(chunks{n}.x);
33         chunks{n}.yMin = min(chunks{n}.y);
34         chunks{n}.yMax = max(chunks{n}.y);

```

```

35
36     xf = [ xf ((chunks{n}.xMin + chunks{n}.xMax) / 2) ];
37     yf = [ yf ((chunks{n}.yMin + chunks{n}.yMax) / 2) ];
38
39     n = n + 1;
40     chunks{n}.x = [];
41     chunks{n}.y = [];
42     end
43
44 end
45
46 chunks{n}.x = [ chunks{n}.x x1(end) ];
47 chunks{n}.y = [ chunks{n}.y y1(end) ];

```



```

48 chunks{n}.xMin = min(chunks{n}.x);
49 chunks{n}.xMax = max(chunks{n}.x);
50 chunks{n}.yMin = min(chunks{n}.y);
51 chunks{n}.yMax = max(chunks{n}.y);
52
53 xf = [ xf (chunks{n}.xMin + chunks{n}.xMax) / 2 ];

```



```

54 yf = [ yf (chunks{n}.yMin + chunks{n}.yMax) / 2 ];
55
56 yMax=[ chunks{n}.yMax ];
57 yMin=[ chunks{n}.yMin ];

```

## B.5 Routine 5

`fitDataset.m` this function begins the data fit to a model, first by assigning return variables.

```

1 % fitDataset.m
2 % function to assign important variables to be returned with implementation
3 % of model fit.
4
5 function [dt, du, tau, delta_0, t0, u0] = fitDataset(x, y)
6
7 dt = {};
8 du = {};
9 tau = {};
10 delta_0 = {};
11 t0 = {};
12 u0 = {};
13
14 % call for function exponentialFit2.m to fit data
15 % log over all cycles, choosing all creep or choosing all recovery cycles
16
17 for i=1:length(x)
18     xx = x{i};
19     yy = y{i};
20

```

```

21 [dt{i}, du{i}, tau{i}, delta_0{i}, t02{i}, u0{i}] = exponentialFit2(xx,yy);
22
23 end

```

## B.6 Routine 6

exponentialFit2.m finds and shifts the starting point of each cycle,  $x_0$  and  $y_0$ , to 0.

```

1 % exponentialFit2.m
2 % normalize x and y start value to 0 so that the relax or creep cycle can
3 % be fit with model fit

```

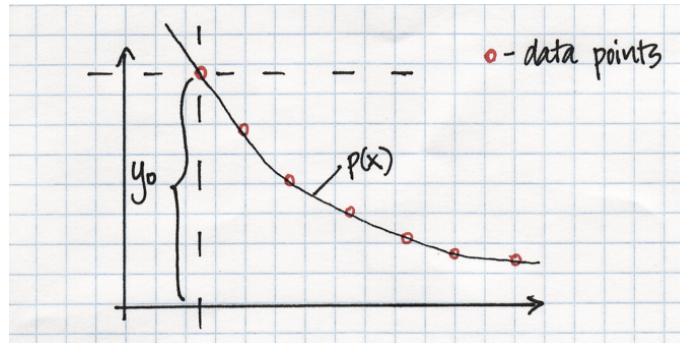


Figure B-1: Illustration of polynomial fit on data set to interpolate  $y_0$  for  $y$  shift

```

4 function [xshift, yshift, tau, delta_0, t02, u0] = exponentialFit(x, y)
5
6 xshift = -floor(2 * x(1)) / 2; % round to next multiple of 0.5
7
8 xfit = x + xshift; % shift dataset to the origin

```

```

9
10 %using a cubic polynomial fit p(x) on the data to interpolate y0
11 [p, s, mu] = polyfit(xfit,y,3);
12 y0 = polyval(p, 0, [], mu)
13 yshift = -y0;
14 yfit = y + yshift;
15
16 if yfit(2) - yfit(1) > 0
17     beta0 = [1 -yfit(end) 0]; % recovery type
18 else
19     beta0 = [1 yfit(end) 0]; % creep type
20 end
21
22 %%%
23 fig = figure;
24 hold on;
25 plot(xfit,yfit,'ro');
26 axis tight;
27 set(gca,'xlimmode','manual','ylimmode','manual');
28 %%%
29
30 % call on function to fit data to model calling of the function
31 % fitFun2.m
32 % call of function selectData.m to eliminate outliers in rawdata
33
34 while true % infinite loop
35
36     % call on selectData.m
37     [xfit2, yfit2] = selectData(fig, xfit, yfit);
38     % selection and deselection of data points for fitting
39     disp('Fitting ...')

```

```

40 % call of fitFun2.m, nonlinear function with initial guess
41 [beta,r,j] = nlinfit(xfit2,yfit2,@fitFun2,beta0);
42 % where beta, r and j return the fitted parameters
43
44 xx = linspace(0,0.5,100);
45
46 % plot results of raw data and fit
47 plot(xx,fitFun2(beta, xx),'k--');
48
49 % print data fit parameters also on plot
50 title(sprintf('tau = %.3f, delta0 = %.3f, Deltat = %.3f',
51             beta(1), beta(2) - yshift, beta(3)));
52
53 [d1, d2, button] = ginput(1); %mouse input for refit or next dataset fit
54 if button == 3; break; end % right mouse button to end fit
55
56 k = ginput(1);
57 if isempty(k); break; end
58
59 end
60
61 % returning model fit parameters, tau, delta_0, t02 and u0 to workspace
62
63 tau = beta(1);
64 delta_0 = beta(2) - yshift; %shift back to real data
65 t02 = -beta(3); %dx
66 u0 = fitFun2(beta, t02) - yshift; % displacement, shift back to real data

```

## B.7 Routine 7

`fitFun2.m` collects is a subroutine function called by the nonlinear fit function `exponentialFit2.m` to finally fit data with the model.

```
1 % fitFun2.m
2 % defined model function using summations
3
4 function u = fitFun2(c, t, varargin)
5 % where t is the value used to evaluate the fit function and varargin
6 % is an optional parameter which is not used
7
8 % the fit parameters
9 tau = c(1);
10 delta_0 = c(2);
11 dx = c(3);
12
13 nMax = 1000; % number of summands
14
15 if nargin > 2
16     nMax = varargin{1};
17 end
18
19 n = (0 : nMax);
20 oddCoef = ((2 * n + 1).^2);
21
22 nx = length(t);
23 u = zeros(nx, 1);
24
25 for i=1:nx
26     summands = exp(-oddCoef * (t(i) + dx) / tau) ./ oddCoef;
```

```

27     u(i,1) = delta_0 * (1 - 8 / pi^2 * sum(summands));
28 end

```

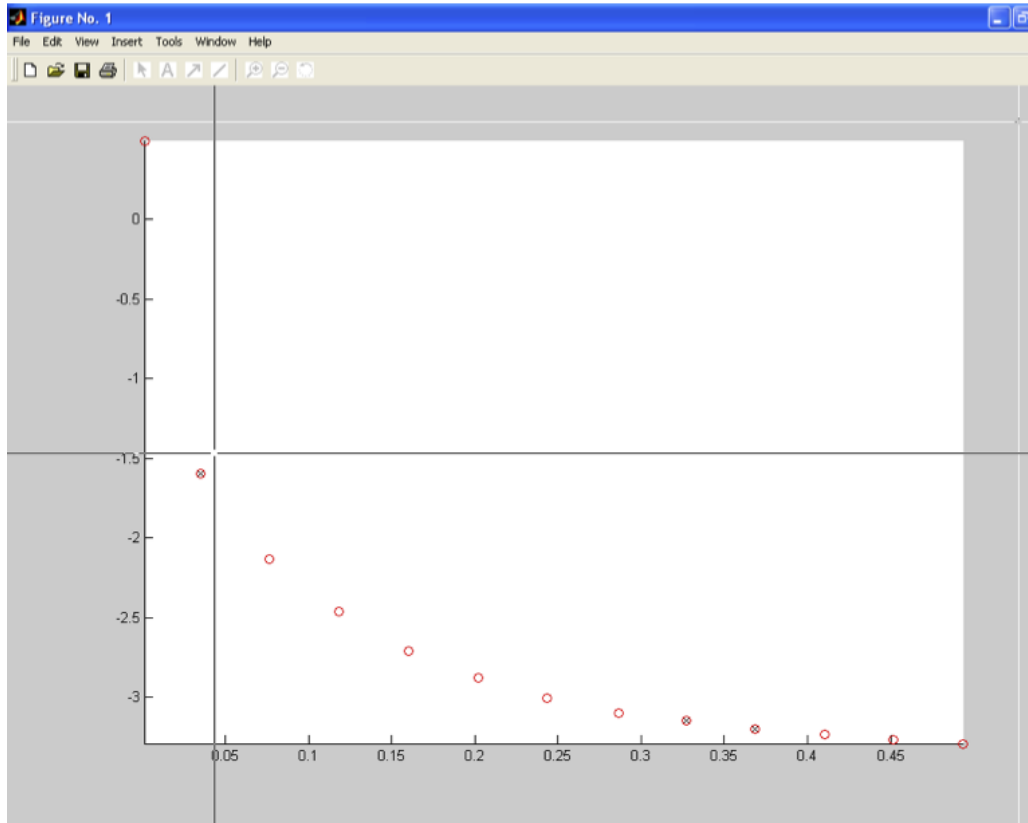


Figure B-2: Figure generated by routine with cross-hair function to select and de-select data point outliers.

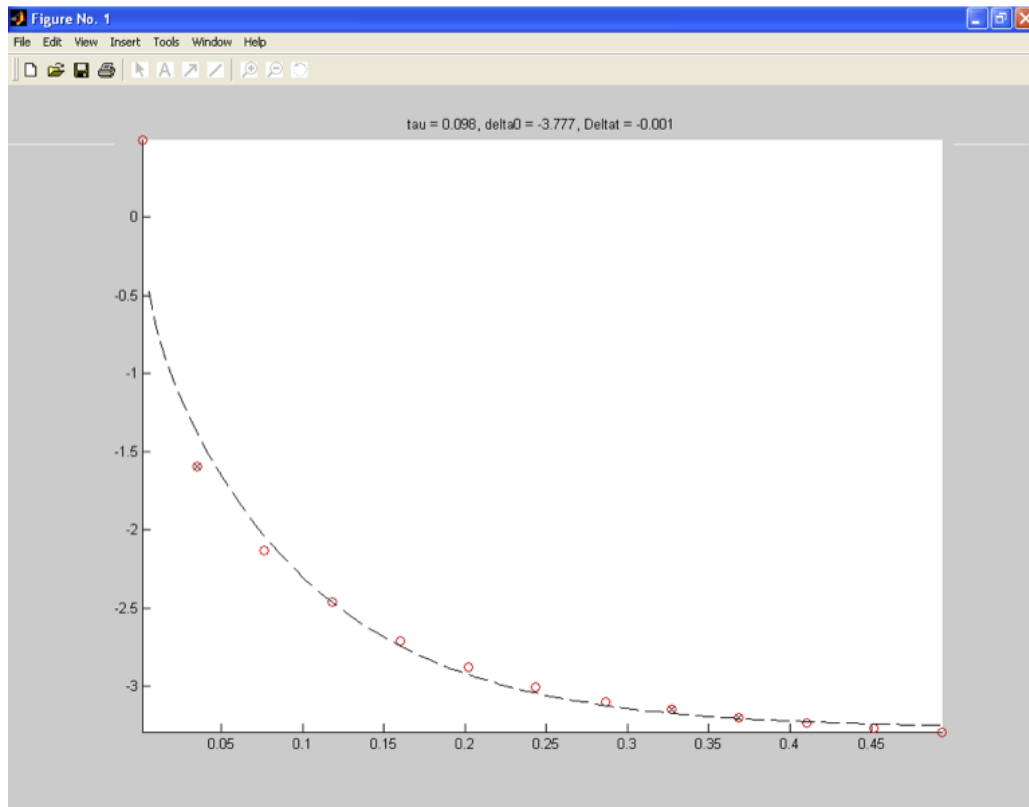


Figure B-3: Data fit of one creep cycle with fitted variables  $\tau$ ,  $\delta a_0$  and  $\Delta t$  returned with figure plot.

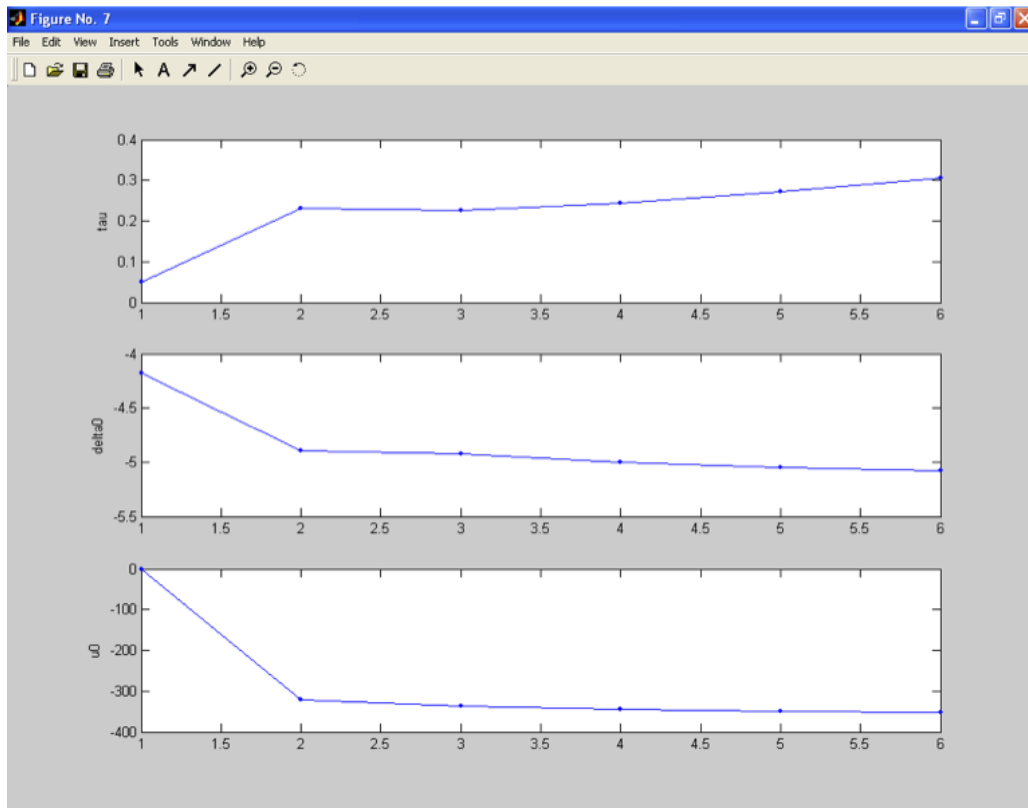


Figure B-4: Plot of fit variables  $\tau$ ,  $\delta a_0$  and  $u_0$  for all six creep or recovery cycles.

Array Editor: variable

File Edit View Web Window Help

Numeric format: shortG Size: 6 by 6

	1	2	3	4	5	6
1	0.050845	-4.1776	0.0021261	-4.3505	-4.6959	0.34539
2	0.23098	-4.8942	0.027896	-4.5709	-4.9163	0.34539
3	0.22512	-4.9207	0.027589	-4.6297	-4.9751	0.34539
4	0.24402	-4.9976	0.027891	-4.6959	-5.0266	0.33069
5	0.27198	-5.0544	0.028512	-4.7106	-5.0706	0.36009
6	0.30672	-5.0779	0.028794	-4.7253	-5.0413	0.316

Figure B-5: Variable output in workspace of MATLAB which gives the fitted and calculated fit variables.



## APPENDIX C

### Preliminary Experiments for Long-Term Culture

In the previous chapter, the culture of intervertebral disc explants for a period of six days was established and the optimal harvesting method was determined. However, an organ model with a validated culture viability period of six days only limits the studies that can be conducted with such an in-vitro model. Our goal is to develop bridging technology for a disc model between cadaver and in-vivo animal models, more specifically a large in-vitro organ culture model to further disc mechanobiology understanding and one that can be used as a tool to test and develop biological regenerative techniques. Such a model would require discs to be cultured for a longer period, in the range of two to six weeks. With a six week model, for example, degeneration of the disc can be induced in the first two weeks and the regenerative treatment can be studied in the following four weeks.

Delivering adequate nutrients to the cells of the intervertebral disc is the common difficulty in developing large disc organ culture models [69]. Without external mechanical stimulation, the disc is supplied preferably by small molecule nutrients and only through diffusion, as the disc is avascular [223]. When the disc is small, the diffusion distance in comparison is much shorter and therefore this difficulty is overcome. However, for large discs additional stimulation to induce convection of nutrients becomes critical [42, 230], especially with large molecule nutrients such as glucose [42, 223]. This chapter presents a study that extends the culture period of the

organ culture model with the use of mechanical stimulation, which has been shown to be effective in increasing nutrient transport to the disc [42, 230]. The developed study examines the effects of three different mechanical stimulations: static loading, dynamic loading and naturally confined loading through swelling. Organ culture cell viability was followed for two, four and six weeks. The objective of the study was to test the hypothesis that mechanical stimuli could help extend the time in which intervertebral discs remain viable in-vitro. The effects of the different mechanical stimuli were compared using cell viability, GAG content and total DNA analysis.

### **C.1 Preliminary Studies**

Prior to this study, preliminary pilot studies were conducted on freshly harvested CEP disc tissue, cultured with the bioreactor system with naturally confined loading conditions through swelling for two and four weeks to determine feasible culture periods. The cultured discs were able to survive after two weeks in these culture conditions. The cell analysis method was previously presented in Chapter 5. Cells were isolated from the tissue with proteinase-K and collagenase-P digestion and stained with a live/dead kit to determine cell viability. Furthermore, the isolated cells were cultured in standard cell culture flasks for an additional week. After the one week of culture, cell attachment and proliferation was also evident. Based on these positive results, the study to extend the culture to six weeks was carried out.

### **C.2 Tissue Preparation**

Discs were harvested from (within four hours of death) bovine coccygeal tails (Abattoir B Poirier, Montreal, Quebec, Canada), freshly and under sterile conditions. A total of sixty discs were harvested using the CEP method (an  $n = 6$  for

three different culture periods; two, four and six weeks and three different mechanical loading stimulations as well as a set of control samples). The experiment was conducted over eight weeks. A plan detailing the order in which discs were harvested and designated for the different culturing conditions allowed, despite the long culture period and limited number of bioreactors being available, to conduct the series within the shortest period of time.

An equal number of discs from the same tail were assigned to the different loading groups to eliminate variability of cell metabolism between subjects. Groups were composed to include similar numbers of disc levels [242]). Disc heights, diameters and weights were measured and recorded. After harvest, the explants were rinsed three times in Hank's balanced salt solution containing 100 U/ml penicillin, 100 µg/ml streptomycin, and 250 µg/ml fungizone. The explants were then transferred into the sterile culture chambers and cultured in Dulbecco's modified Eagle medium with 5 % fetal calf serum, 0.1 % ascorbic acid, 100 µg/ml streptomycin, 100 U/ml penicillin, 250 µg/ml fungizone, HEPES buffer and 2 mM Glutamax. The explants were all cultured in a 37 °C controlled incubator offering 5 % CO<sub>2</sub> and 95 % humidity.

### **C.3 Mechanical Stimulation**

Three different loading conditions were tested: dynamic diurnal, static diurnal and naturally confined loading through swelling. For both dynamic diurnal and static diurnal loading conditions, explants were placed into the custom-built polycarbonate culture chambers of the bioreactor system. The chambers were designed to circulate media well to the top and bottom surfaces of the disc while allowing for radially unconfined uni-axial compression.

For static diurnal loading, linear springs were used to deliver a constant compression force calculated to provide 0.5 MPa for eight hours, followed by a resting load equivalent to 0.1 MPa of stress for sixteen hours. For dynamic diurnal loading, a pneumatically driven actuator on the bioreactor loading-frame allowed the explants to be dynamically compressed using a sinusoidal profile of  $0.45 \pm 0.35$  MPa at 0.3 Hz for eight hours, followed by a static recovery load of 0.1 MPa for sixteen hours. Bioreactors used for dynamic loading are shown in Figure 6–1.

The pressures measured in human lumbar intervertebral disc at L4–L5 are reported to be 0.5 MPa for relaxed standing and 1.1 MPa for flexed forward standing [237]. The natural disc swelling pressure is reported to be in the range of 0.1 to 0.3 MPa [221]. The protocol of 0.8 MPa for the highest loads and 0.1 MPa for lowest load is chosen to match this physiological range.

For the naturally confined loading through swelling discs, explants were placed into modified glass culture chambers with constant media circulation provided by a peristaltic pump. Control discs were also isolated with the same isolation technique and analyzed freshly after harvest.

#### **C.4 Measurement of Cell Viability**

At the end of the culture period, a  $3\text{ mm} \times 3\text{ mm} \times 3\text{ mm}$  piece of annulus fibrosus and nucleus pulposus tissue each was isolated from all discs. The isolated tissue samples were weighed and digested in 0.1 % pronase for one hour. The solution was centrifuged and was followed by digestion in 0.025 % collagenase overnight. The digestive enzymes were removed and the cells were isolated using cycles of washing with Hank’s balanced salt solution followed by centrifuging. The isolated cells were

counted using a Neubauer haemocytometer chamber (Superior, Bad Mergentheim, Germany) and Trypan blue staining. Four counts per sample were averaged and used to seed consistent numbers of cells into a 96-well microassay plate. Each well finally contained 100  $\mu$ l of media and 20 000 cells. The assay plate was incubated at 37 °C for thirty minutes allowing cells to sink to the bottom of the well plate.

After the incubation, 50  $\mu$ l of Ethidium Homodimer-1/Calcein AM (EthD-1, 2  $\mu$ M / calcein AM, 1.6  $\mu$ M) from a Live/Dead® cell viability kit (Invitrogen, Basel, Switzerland) was administered to each well. This was followed by a thirty-minute incubation period. The stained samples were imaged with a confocal microscope. (Leica, DM Ill filters: IS S450-490nm and N2.1 S515-560nm). Five high-resolution digital photographs using both filters were taken from each well at set locations spread over the well. Total live/dead cell counts were obtained using image analysis software (CellC, Tampere University of Technology, Tampere, Finland).

Discs cultured for four weeks with static diurnal load or dynamic diurnal load showed a lack of cells. Low cell numbers were noticed at the first stage of quantification involving the haemocytometer and Trypan blue staining. As a result of the low cell numbers, live/dead staining could not be performed.

## **C.5 Discussion**

The six-week culture period was driven by the aim to develop a degeneration/regeneration model allowing the inducement of degeneration and/or trauma followed by a period of two to four more weeks to assess methods of repair/regeneration. To carry out the study, more culture chambers were manufactured to allow for each of the different loading conditions running in parallel with discs of the same animal.

The discs were randomly assigned to the different loading conditions and different culture times to eliminate a possible bias. The studies entailed harvesting nine discs in one harvesting period. The overall experiment lasted eight weeks to complete six samples per test condition (loading method, culture time). Starting at four weeks using cell isolation with pronase and collagenase needed for live/dead staining became difficult. The experimental results were inconclusive and therefore the cell viability measurement method needed to be revised for subsequent experiments.

## **C.6 Summary**

The study presented in this chapter extended the culture period to six weeks along with the introduction of mechanical stimulation; the latter has been reported to be a strong influence on disc cells [79, 117, 121, 204, 214]. The first four-week cell viability results lead to a revision of the analysis methods used to determine mechanical stimulation effects and to validate cell viability in the in-vitro organ culture model. The revised methods for cell-viability measurements, protocols for histological evaluation and biochemistry analysis are expected to increase the relevancy and accuracy of results in subsequent studies. The study of the influence of mechanical load for a shorter culture term, but employing the revised analysis methods, would be the next logical step.

## References

- [1] M. A. Adams and P. J. Roughley. “What is intervertebral disc degeneration, and what causes it?” In: *Spine* 31.18 (2006), pp. 2151–61.
- [2] D. J. Aguiar, S. L. Johnson, and T. R. Oegema. “Notochordal cells interact with nucleus pulposus cells: regulation of proteoglycan synthesis”. In: *Experimental Cell Research* 246.1 (1999), pp. 129–37.
- [3] S. H. Ahn, P. N. Teng, and C. Niyibizi. “The effects of BMP-12 and BMP-2 on proteoglycan and collagen synthesis in nucleus pulposus cells from human degenerated discs”. In: *ISSLS 29th Annual Meeting Proceeding*, 49. 2002.
- [4] K. Akeda, H. S. An, R. Pichika, M. Attawia, E. J. Thonar, M. E. Lenz, A. Uchida, and K. Masuda. “Platelet-rich plasma (PRP) stimulates the extracellular matrix metabolism of porcine nucleus pulposus and annulus fibrosus cells cultured in alginate beads”. In: *Spine* 31.9 (2006), pp. 959–66.
- [5] M. Alini, S. M. Eisenstein, K. Ito, C. Little, A. A. Kettler, K. Masuda, J. Melrose, J. Ralphs, I. Stokes, and H. J. Wilke. “Are animal models useful for studying human disc disorders/degeneration?” In: *Eur Spine J* 17.1 (2008), pp. 2–19.
- [6] M. Alini, W. Li, P. Markovic, M. Aebi, R. C. Spiro, and P. J. Roughley. “The potential and limitations of a cell-seeded collagen/hyaluronan scaffold

- to engineer an intervertebral disc-like matrix”. In: *Spine* 28.5 (2003), 446–54; discussion 453–446–54; discussion 453.
- [7] M. Alini, P. J. Roughley, J. Antoniou, T. Stoll, and M. Aebi. “A biological approach to treating disc degeneration: not for today, but maybe for tomorrow”. In: *Eur Spine J* 11 Suppl 2 (2002), S215–20.
  - [8] D. B. Allan and G. Waddell. “An historical perspective on low back pain and disability”. In: *Acta Orthop Scand Suppl* 234 (1989), pp. 1–23.
  - [9] H. S. Amonoo-Kuofi. “Morphometric changes in the heights and anteroposterior diameters of the lumbar intervertebral discs with age”. In: *J Anat* 175 (1991), pp. 159–68.
  - [10] H. S. An and K. Masuda. “Relevance of in vitro and in vivo models for intervertebral disc degeneration”. In: *J Bone Joint Surg Am* 88 Suppl 2 (2006), pp. 88–94.
  - [11] J. Antoniou, T. Steffen, F. Nelson, N. Winterbottom, A. P. Hollander, R. A. Poole, M. Aebi, and M. Alini. “The human lumbar intervertebral disc: evidence for changes in the biosynthesis and denaturation of the extracellular matrix with growth, maturation, ageing, and degeneration”. In: *J Clin Invest* 98.4 (1996), pp. 996–1003.
  - [12] I. Barbosa, S. Garcia, V. Barbier-Chassefiere, J. P. Caruelle, I. Martelly, and D. Papy-Garcia. “Improved and simple micro assay for sulfated glycosaminoglycans quantification in biological extracts and its use in skin and muscle tissue studies”. In: *Glycobiology* 13.9 (2003), pp. 647–53.



- [13] H. K. Beard, S. Roberts, and J. P. O'Brien. "Immunofluorescent staining for collagen and proteoglycan in normal and scoliotic intervertebral discs". In: *J Bone Joint Surg Br* 63B.4 (1981), pp. 529–34.
- [14] Helge Bertram, Eric Steck, Gerald Zimmerman, Bohua Chen, Claus Carstens, Andreas Nerlich, and Wiltrud Richter. "Accelerated intervertebral disc degeneration in scoliosis versus physiological ageing develops against a background of enhanced anabolic gene expression". In: *Biochem Biophys Res Commun* 342.3 (2006), pp. 963–72.
- [15] E. J. Blain. "Mechanical regulation of matrix metalloproteinases". In: *Front Biosci* 12 (2007), pp. 507–27.
- [16] N. Boos, S. Weissbach, H. Rohrbach, C. Weiler, K. F. Spratt, and A. G. Nerlich. "Classification of age-related changes in lumbar intervertebral discs: 2002 Volvo Award in basic science". In: *Spine* 27.23 (2002), pp. 2631–44.
- [17] P. Bornstein. "Cell-matrix interactions: the view from the outside". In: *Methods Cell Biol* 69 (2002), pp. 7–11.
- [18] L. M. Boyd and A. J. Carter. "Injectable biomaterials and vertebral endplate treatment for repair and regeneration of the intervertebral disc". In: *Eur Spine J* 15 Suppl 3 (2006), S414–21–S414–21.
- [19] D. Brickley-Parsons and M. J. Glimcher. "Is the chemistry of collagen in intervertebral discs an expression of Wolff's Law? A study of the human lumbar spine". In: *Spine* 9.2 (1984), pp. 148–63.

- [20] S. B. Bruehlmann, J. B. Rattner, J. R. Matyas, and N. A. Duncan. “Regional variations in the cellular matrix of the annulus fibrosus of the intervertebral disc”. In: *J Anat* 201.2 (2002), pp. 159–71.
- [21] J. A. Buckwalter. “Aging and degeneration of the human intervertebral disc”. In: *Spine* 20.11 (1995), pp. 1307–14.
- [22] W. F. Butler and P. Ghosh. “Comparative anatomy and development of the mammalian disc”. In: *The biology of the intervertebral disc*. Boca Raton, FL: CRC, 1988, pp. 83–108.
- [23] K. Buttner-Janzen, S. Hahn, K. Schikora, and H. D. Link. “[Basic principles of successful implantation of the SB Charite model LINK intervertebral disk endoprosthesis]”. In: *Orthopade* 31.5 (2002), pp. 441–53.
- [24] J. P. Callaghan and S. M. McGill. “Intervertebral disc herniation: studies on a porcine model exposed to highly repetitive flexion/extension motion with compressive force”. In: *Clin Biomech (Bristol, Avon)* 16.1 (2001), pp. 28–37.
- [25] L. Camper, D. Heinegard, and E. Lundgren-Akerlund. “Integrin  $\alpha 2 \beta 1$  is a receptor for the cartilage matrix protein chondroadherin”. In: *J Cell Biol* 138.5 (1997), pp. 1159–67.
- [26] S. C. Chan, S. J. Ferguson, and B. Gantenbein-Ritter. “The effects of dynamic loading on the intervertebral disc”. In: *Eur Spine J* 20.11 (2011), pp. 1769–812.
- [27] W. H. Chen, W. C. Lo, J. J. Lee, C. H. Su, C. T. Lin, H. Y. Liu, T. W. Lin, W. C. Lin, T. Y. Huang, and W. P. Deng. “Tissue-engineered intervertebral disc

- and chondrogenesis using human nucleus pulposus regulated through TGF-beta1 in platelet-rich plasma”. In: *J Cell Physiol* 209.3 (2006), pp. 744–54.
- [28] J. J. Costi, T. C. Hearn, and N. L. Fazzalari. “The effect of hydration on the stiffness of intervertebral discs in an ovine model”. In: *Clin Biomech (Bristol, Avon)* 17.6 (2002), pp. 446–55.
- [29] G. Crevensten, A. J. Walsh, D. Ananthakrishnan, P. Page, G. M. Wahba, J. C. Lotz, and S. Berven. “Intervertebral disc cell therapy for regeneration: mesenchymal stem cell implantation in rat intervertebral discs”. In: *Ann Biomed Eng* 32.3 (2004), pp. 430–4.
- [30] G. Cs-Szabo, P. J. Roughley, A. H. Plaas, and T. T. Glant. “Large and small proteoglycans of osteoarthritic and rheumatoid articular cartilage”. In: *Arthritis Rheum* 38.5 (1995), pp. 660–8.
- [31] B. W. Cunningham, G. L. Lowery, H. A. Serhan, A. E. Dmitriev, C. M. Orbegoso, P. C. McAfee, R. D. Fraser, R. E. Ross, and S. S. Kulkarni. “Total disc replacement arthroplasty using the AcroFlex lumbar disc: a non-human primate model”. In: *Eur Spine J* 11 Suppl 2 (2002), S115–23–S115–23.
- [32] C. N. Demers, J. Antoniou, and F. Mwale. “Value and limitations of using the bovine tail as a model for the human lumbar spine”. In: *Spine* 29.24 (2004), pp. 2793–9.
- [33] A. Di Martino, A. R. Vaccaro, J. Y. Lee, V. Denaro, and M. R. Lim. “Nucleus pulposus replacement: basic science and indications for clinical use”. In: *Spine* 30.16 Suppl (2005), S16–22–S16–22.

- [34] J L DiFabio, R H Pearce, B Caterson, and H Hughes. “The heterogeneity of the non-aggregating proteoglycans of the human intervertebral disc”. In: *Biochem J* 244.1 (1987), pp. 27–33.
- [35] A. D. Diwan, H. K. Parvataneni, S. N. Khan, H. S. Sandhu, F. P. Girardi, and Jr. Cammisa F. P. “Current concepts in intervertebral disc restoration”. In: *Orthop Clin North Am* 31.3 (2000), pp. 453–64.
- [36] K. D. van den Eerenbeemt, R. W. Ostelo, B. J. van Royen, W. C. Peul, and M. W. van Tulder. “Total disc replacement surgery for symptomatic degenerative lumbar disc disease: a systematic review of the literature”. In: *Eur Spine J* 19.8 (2010), pp. 1262–80.
- [37] D. M. Elliott and J. J. Sarver. “Young investigator award winner: validation of the mouse and rat disc as mechanical models of the human lumbar disc”. In: *Spine* 29.7 (2004), pp. 713–22.
- [38] M. B. Ellman, H. S. An, P. Muddasani, and H. J. Im. “Biological impact of the fibroblast growth factor family on articular cartilage and intervertebral disc homeostasis”. In: *Gene* 420.1 (2008), pp. 82–9.
- [39] R. J. Errington, K. Puustjarvi, I. R. White, S. Roberts, and J. P. Urban. “Characterisation of cytoplasm-filled processes in cells of the intervertebral disc”. In: *J Anat* 192 ( Pt 3) (1998), pp. 369–78.
- [40] S. Etebar and D. W. Cahill. “Risk factors for adjacent-segment failure following lumbar fixation with rigid instrumentation for degenerative instability”. In: *J Neurosurg* 90.2 Suppl (1999), pp. 163–9.

- [41] D. R. Eyre. “Collagen: structure and synthesis [proceedings]”. In: *Scott Med J* 22.1 (1977), pp. 85–85.
- [42] S. J. Ferguson, K. Ito, and L. P. Nolte. “Fluid flow and convective transport of solutes within the intervertebral disc”. In: *J Biomech* 37.2 (2004), pp. 213–21.
- [43] S. J. Ferguson and T. Steffen. “Biomechanics of the aging spine”. In: *Eur Spine J* 12 Suppl 2 (2003), S97–S103–S97–S103.
- [44] B. P. Flynn, A. P. Bhole, N. Saeidi, M. Liles, C. A. Dimarzio, and J. W. Ruberti. “Mechanical strain stabilizes reconstituted collagen fibrils against enzymatic degradation by mammalian collagenase matrix metalloproteinase 8 (MMP-8)”. In: *PLoS One* 5.8 (2010), e12337.
- [45] B. J. Freeman and J. Davenport. “Total disc replacement in the lumbar spine: a systematic review of the literature”. In: *Eur Spine J* 15 Suppl 3 (2006), S439–47–S439–47.
- [46] S. L. Frick, E. N. Hanley, R. A. Meyer, W. K. Ramp, and T. M. Chapman. “Lumbar intervertebral disc transfer. A canine study”. In: *Spine* 19.16 (1994), 1826–34; discussion 1834–5–1826–34; discussion 1834–5.
- [47] T. Ganey, J. Libera, V. Moos, O. Alasevic, K. G. Fritsch, H. J. Meisel, and W. C. Hutton. “Disc chondrocyte transplantation in a canine model: a treatment for degenerated or damaged intervertebral disc”. In: *Spine* 28.23 (2003), pp. 2609–20.
- [48] B. Gantenbein, T. Grunhagen, C. R. Lee, C. C. van Donkelaar, M. Alini, and K. Ito. “An in vitro organ culturing system for intervertebral disc explants

- with vertebral endplates: a feasibility study with ovine caudal discs”. In: *Spine* 31.23 (2006), pp. 2665–73.
- [49] R. Gawri, F. Mwale, J. Ouellet, P. J. Roughley, T. Steffen, J. Antoniou, and L. Haglund. “Development of an organ culture system for long-term survival of the intact human intervertebral disc”. In: *Spine (Phila Pa 1976)* 36.22 (2011), pp. 1835–42.
- [50] G. Ghiselli, J. C. Wang, N. N. Bhatia, W. K. Hsu, and E. G. Dawson. “Adjacent segment degeneration in the lumbar spine”. In: *J Bone Joint Surg Am* 86-A.7 (2004), pp. 1497–503.
- [51] P. Gillet. “The fate of the adjacent motion segments after lumbar fusion”. In: *J Spinal Disord Tech* 16.4 (2003), pp. 338–45.
- [52] K J Gooch, T Blunk, D L Courter, A L Sieminski, G Vunjak-Novakovic, and L E Freed. “Bone morphogenetic proteins-2, -12, and -13 modulate in vitro development of engineered cartilage”. In: *Tissue Eng* 8.4 (2002), pp. 591–601. DOI: 10.1089/107632702760240517.
- [53] H. E. Gruber, E. C. Fisher, B. Desai, A. A. Stasky, G. Hoelscher, and E. N. Hanley. “Human intervertebral disc cells from the annulus: three-dimensional culture in agarose or alginate and responsiveness to TGF-beta1”. In: *Exp Cell Res* 235.1 (1997), pp. 13–21.
- [54] H. E. Gruber, J. A. Ingram, K. Leslie, H. J. Norton, and E. N. Hanley. “Cell shape and gene expression in human intervertebral disc cells: in vitro tissue engineering studies”. In: *Biotech Histochem* 78.2 (2003), pp. 109–17.

- [55] R. D. Guyer, K. T. Foley, F. M. Phillips, and P. A. Ball. “Minimally invasive fusion: summary statement”. In: *Spine (Phila Pa 1976)* 28.15 Suppl (2003), S44.
- [56] L. Haglund, J. Moir, L. Beckman, K. R. Mulligan, B. Jim, J. A. Ouellet, P. Roughley, and T. Steffen. “Development of a bioreactor for axially loaded intervertebral disc organ culture”. In: *Tissue Eng Part C Methods* 17.10 (2011), pp. 1011–9.
- [57] L. Haglund, J. Ouellet, and P. Roughley. “Variation in chondroadherin abundance and fragmentation in the human scoliotic disc”. In: *Spine (Phila Pa 1976)* 34.14 (2009), pp. 1513–8.
- [58] T E Hardingham, M T Bayliss, V Rayan, and D P Noble. “Effects of growth factors and cytokines on proteoglycan turnover in articular cartilage”. In: *Br J Rheumatol* 31 Suppl 1 (1992), pp. 1–6.
- [59] D. Haschtmann, J. V. Stoyanov, L. Ettinger, L. P. Nolte, and S. J. Ferguson. “Establishment of a novel intervertebral disc/endplate culture model: analysis of an ex vivo in vitro whole-organ rabbit culture system”. In: *Spine* 31.25 (2006), pp. 2918–25.
- [60] D. Hastreiter, R. M. Ozuna, and M. Spector. “Regional variations in certain cellular characteristics in human lumbar intervertebral discs, including the presence of alpha-smooth muscle actin”. In: *J Orthop Res* 19.4 (2001), pp. 597–604.

- [61] S. E. Haynesworth, M. A. Baber, and A. I. Caplan. “Cell surface antigens on human marrow-derived mesenchymal cells are detected by monoclonal antibodies”. In: *Bone* 13.1 (1992), pp. 69–80.
- [62] S. E. Haynesworth, J. Goshima, V. M. Goldberg, and A. I. Caplan. “Characterization of cells with osteogenic potential from human marrow”. In: *Bone* 13.1 (1992), pp. 81–8.
- [63] Sarah Kathleen Heathfield, Christine Lyn Le Maitre, and Judith Alison Hoyland. “Caveolin-1 expression and stress-induced premature senescence in human intervertebral disc degeneration”. In: *Arthritis Res Ther* 10.4 (2008), R87. DOI: 10.1186/ar2468.
- [64] T. F. Heathfield, P. Onnerfjord, L. Dahlberg, and D. Heinegard. “Cleavage of fibromodulin in cartilage explants involves removal of the N-terminal tyrosine sulfate-rich region by proteolysis at a site that is sensitive to matrix metalloproteinase-13”. In: *J Biol Chem* 279.8 (2004), pp. 6286–95.
- [65] E. Hedbom and D. Heinegard. “Interaction of a 59-kDa connective tissue matrix protein with collagen I and collagen II”. In: *J Biol Chem* 264.12 (1989), pp. 6898–905.
- [66] H. Hedlund, S. Mengarelli-Widholm, D. Heinegard, F. P. Reinholt, and O. Svensson. “Fibromodulin distribution and association with collagen”. In: *Matrix Biol* 14.3 (1994), pp. 227–32.
- [67] A. P. Hollander, T. F. Heathfield, J. J. Liu, I. Pidoux, P. J. Roughley, J. S. Mort, and A. R. Poole. “Enhanced denaturation of the alpha (II) chains of



- type-II collagen in normal adult human intervertebral discs compared with femoral articular cartilage”. In: *J Orthop Res* 14.1 (1996), pp. 61–6.
- [68] S. Holm, A. K. Holm, L. Ekstrom, A. Karladani, and T. Hansson. “Experimental disc degeneration due to endplate injury”. In: *J Spinal Disord Tech* 17.1 (2004), pp. 64–71.
- [69] H. A. Horner and J. P. Urban. “2001 Volvo Award Winner in Basic Science Studies: Effect of nutrient supply on the viability of cells from the nucleus pulposus of the intervertebral disc”. In: *Spine* 26.23 (2001), pp. 2543–9.
- [70] D. W. Hukins, M. C. Kirby, T. A. Sikoryn, R. M. Aspden, and A. J. Cox. “Comparison of structure, mechanical properties, and functions of lumbar spinal ligaments”. In: *Spine (Phila Pa 1976)* 15.8 (1990), pp. 787–95.
- [71] D. W. L. Hukins. “Collagen Orientation”. In: *Connective tissue matrix*. London: Macmillan, 1984, pp. 211–239.
- [72] M. D. Humzah and R. W. Soames. “Human intervertebral disc: structure and function”. In: *Anat Rec* 220.4 (1988), pp. 337–56.
- [73] C. J. Hunter, J. R. Matyas, and N. A. Duncan. “Cytomorphology of notochordal and chondrocytic cells from the nucleus pulposus: a species comparison”. In: *J Anat* 205.5 (2004), pp. 357–62.
- [74] C. J. Hunter, J. R. Matyas, and N. A. Duncan. “The notochordal cell in the nucleus pulposus: a review in the context of tissue engineering”. In: *Tissue Eng* 9.4 (2003), pp. 667–77.
- [75] Christopher J Hunter, John R Matyas, and Neil A Duncan. “The functional significance of cell clusters in the notochordal nucleus pulposus: survival and

- signaling in the canine intervertebral disc”. In: *Spine (Phila Pa 1976)* 29.10 (2004), pp. 1099–104.
- [76] W. C. Hutton, Y. Toribatake, W. A. Elmer, T. M. Ganey, K. Tomita, and T. E. Whitesides. “The effect of compressive force applied to the intervertebral disc in vivo. A study of proteoglycans and collagen”. In: *Spine* 23.23 (1998), pp. 2524–37.
- [77] W. C. Hutton, S. T. Yoon, W. A. Elmer, J. Li, H. Murakami, A. Minamide, and T. Akamaru. “Effect of tail suspension (or simulated weightlessness) on the lumbar intervertebral disc: study of proteoglycans and collagen”. In: *Spine* 27.12 (2002), pp. 1286–90.
- [78] J. C. Iatridis, K. Godburn, K. Wuertz, M. Alini, and P. J. Roughley. “Region-dependent aggrecan degradation patterns in the rat intervertebral disc are affected by mechanical loading in vivo”. In: *Spine (Phila Pa 1976)* 36.3 (2011), pp. 203–9.
- [79] J. C. Iatridis, J. J. MacLean, P. J. Roughley, and M. Alini. “Effects of mechanical loading on intervertebral disc metabolism in vivo”. In: *J Bone Joint Surg Am* 88 Suppl 2 (2006), pp. 41–6.
- [80] J C Iatridis, P L Mente, I A Stokes, D D Aronsson, and M Alini. “Compression-induced changes in intervertebral disc properties in a rat tail model”. In: *Spine (Phila Pa 1976)* 24.10 (1999), pp. 996–1002.

- [81] S. Illien-Junger, B. Gantenbein-Ritter, S. Grad, P. Lezuo, S. J. Ferguson, M. Alini, and K. Ito. “The combined effects of limited nutrition and high-frequency loading on intervertebral discs with endplates”. In: *Spine (Phila Pa 1976)* 35.19 (2010), pp. 1744–52.
- [82] Y. Imai, K. Miyamoto, H. S. An, E. J. Thonar, G. B. Andersson, and K. Masuda. “Recombinant human osteogenic protein-1 upregulates proteoglycan metabolism of human annulus fibrosus and nucleus pulposus cells”. In: *Spine (Phila Pa 1976)* 32.12 (2007), 1303–9; discussion 1310.
- [83] H. Ishihara, D. S. McNally, J. P. Urban, and A. C. Hall. “Effects of hydrostatic pressure on matrix synthesis in different regions of the intervertebral disk”. In: *J Appl Physiol* 80.3 (1996), pp. 839–46.
- [84] T. Ishii, H. Tsuji, A. Sano, Y. Katoh, H. Matsui, and N. Terahata. “Histochemical and ultrastructural observations on brown degeneration of human intervertebral disc”. In: *J Orthop Res* 9.1 (1991), pp. 78–90.
- [85] M R Jahnke and C A McDevitt. “Proteoglycans of the human intervertebral disc. Electrophoretic heterogeneity of the aggregating proteoglycans of the nucleus pulposus”. In: *Biochem J* 251.2 (1988), pp. 347–56.
- [86] M. C. Jensen, M. N. Brant-Zawadzki, N. Obuchowski, M. T. Modic, D. Malkasian, and J. S. Ross. “Magnetic resonance imaging of the lumbar spine in people without back pain”. In: *N Engl J Med* 331.2 (1994), pp. 69–73.
- [87] B. Jim, O. Arlet, L. Beckman, and T. Steffen. “The influence of harvesting methods for the development of an in-vitro intervertebral disc model”. In: vol. 10 S3. In Proceedings of the European Cells and Materials VI /SRN I

- Spinal Motion Segment: From Basic Science to Clinical Application. European Cells and Materials, 2005.
- [88] B. Jim, S. J. Ferguson, and T. Steffen. “Bovine Coccygeal Disc Organ Culture Model – Improved Cell Viability & Activity Using a Novel Disc Preparation Method”. In: *34th Annual Meeting of The International Society for the Study of the Lumbar Spine*. 2007.
  - [89] B. Jim, T. Steffen, J. Moir, P. Roughley, and L. Haglund. “Development of an intact intervertebral disc organ culture system in which degeneration can be induced as a prelude to studying repair potential”. In: *Eur Spine J* 20.8 (2011), pp. 1244–54.
  - [90] W. E. Johnson, H. Evans, J. Menage, S. M. Eisenstein, A. El Haj, and S. Roberts. “Immunohistochemical detection of Schwann cells in innervated and vascularized human intervertebral discs”. In: *Spine* 26.23 (2001), pp. 2550–7.
  - [91] B. Johnstone and M. T. Bayliss. “The large proteoglycans of the human intervertebral disc. Changes in their biosynthesis and structure with age, topography, and pathology”. In: *Spine* 20.6 (1995), pp. 674–84.
  - [92] J G de Jong, W M Heijs, and R A Wevers. “Mucopolysaccharidoses screening: dimethylmethylene blue versus alcian blue”. In: *Ann Clin Biochem* 31 ( Pt 3) (1994), pp. 267–71.
  - [93] S. Junger, B. Gantenbein-Ritter, P. Lezuo, M. Alini, S. J. Ferguson, and K. Ito. “Effect of limited nutrition on in situ intervertebral disc cells under simulated-physiological loading”. In: *Spine (Phila Pa 1976)* 34.12 (2009), pp. 1264–71.

- [94] A. M. Kaigle, S. H. Holm, and T. H. Hansson. “1997 Volvo Award winner in biomechanical studies. Kinematic behavior of the porcine lumbar spine: a chronic lesion model”. In: *Spine* 22.24 (1997), pp. 2796–806.
- [95] M. Karlsson and S. Bjornsson. “Quantitation of proteoglycans in biological fluids using Alcian blue”. In: *Methods Mol Biol* 171 (2001), pp. 159–73.
- [96] M. Kasra, V. Goel, J. Martin, S. T. Wang, W. Choi, and J. Buckwalter. “Effect of dynamic hydrostatic pressure on rabbit intervertebral disc cells”. In: *J Orthop Res* 21.4 (2003), pp. 597–603.
- [97] M. Kasra, W. D. Merryman, K. N. Loveless, V. K. Goel, J. D. Martin, and J. A. Buckwalter. “Frequency response of pig intervertebral disc cells subjected to dynamic hydrostatic pressure”. In: *J Orthop Res* 24.10 (2006), pp. 1967–73.
- [98] A. Katsuura and S. Hukuda. “Experimental study of intervertebral disc allografting in the dog”. In: *Spine* 19.21 (1994), pp. 2426–32.
- [99] L. I. Kauppila. “Ingrowth of blood vessels in disc degeneration. Angiographic and histological studies of cadaveric spines”. In: *J Bone Joint Surg Am* 77.1 (1995), pp. 26–31.
- [100] A. Kettler and H. J. Wilke. “Review of existing grading systems for cervical or lumbar disc and facet joint degeneration”. In: *Eur Spine J* 15.6 (2006), pp. 705–18.
- [101] S. N. Khan and A. J. Stirling. “Controversial topics in surgery: degenerative disc disease: disc replacement. Against”. In: *Ann R Coll Surg Engl* 89.1 (2007), pp. 6–11.

- [102] Ki-Won Kim, Kee-Yong Ha, Jun-Seok Lee, Suk-Woo Nam, Young-Kyun Woo, Tae-Hong Lim, and Howard S. An. “Notochordal cells stimulate migration of cartilage end plate chondrocytes of the intervertebral disc in in vitro cell migration assays”. In: *The Spine Journal: Official Journal of the North American Spine Society* (2008).
- [103] D. Kletsas. “Senescent cells in the intervertebral disc: numbers and mechanisms”. In: *Spine J* 9.8 (2009), pp. 677–8.
- [104] T. Kluba, T. Niemeyer, C. Gaissmaier, and T. Grunder. “Human annulus fibrosis and nucleus pulposus cells of the intervertebral disc: effect of degeneration and culture system on cell phenotype”. In: *Spine* 30.24 (2005), pp. 2743–8.
- [105] C. L. Korecki, J. J. MacLean, and J. C. Iatridis. “Characterization of an in vitro intervertebral disc organ culture system”. In: *Eur Spine J* 16.7 (2007), pp. 1029–37.
- [106] C. L. Korecki, J. J. MacLean, and J. C. Iatridis. “Dynamic compression effects on intervertebral disc mechanics and biology”. In: *Spine (Phila Pa 1976)* 33.13 (2008), pp. 1403–9.
- [107] M. W. Kroeber, F. Unglaub, H. Wang, C. Schmid, M. Thomsen, A. Nerlich, and W. Richter. “New in vivo animal model to create intervertebral disc degeneration and to investigate the effects of therapeutic strategies to stimulate disc regeneration”. In: *Spine* 27.23 (2002), pp. 2684–90.
- [108] M. E. Kunkel, A. Herkommer, M. Reinehr, T. M. Bockers, and H. J. Wilke. “Morphometric analysis of the relationships between intervertebral disc and

- vertebral body heights: an anatomical and radiographic study of the human thoracic spine”. In: *J Anat* (2011).
- [109] M. K. Kwan, W. M. Lai, and V. C. Mow. “A finite deformation theory for cartilage and other soft hydrated connective tissues–I. Equilibrium results”. In: *J Biomech* 23.2 (1990), pp. 145–55.
  - [110] N. E. Lane, M. C. Nevitt, H. K. Genant, and M. C. Hochberg. “Reliability of new indices of radiographic osteoarthritis of the hand and hip and lumbar disc degeneration”. In: *J Rheumatol* 20.11 (1993), pp. 1911–8.
  - [111] T. Larsson, Y. Sommarin, M. Paulsson, P. Antonsson, E. Hedbom, M. Wendel, and D. Heinegard. “Cartilage matrix proteins. A basic 36-kDa protein with a restricted distribution to cartilage and bone”. In: *J Biol Chem* 266.30 (1991), pp. 20428–33.
  - [112] C. L. Le Maitre, A. J. Freemont, and J. A. Hoyland. “Accelerated cellular senescence in degenerate intervertebral discs: a possible role in the pathogenesis of intervertebral disc degeneration”. In: *Arthritis Res Ther* 9.3 (2007), R45–R45.
  - [113] Christine Lyn Le Maitre, Anthony John Freemont, and Judith Alison Hoyland. “Accelerated cellular senescence in degenerate intervertebral discs: a possible role in the pathogenesis of intervertebral disc degeneration”. In: *Arthritis Res Ther* 9.3 (2007), R45. DOI: 10.1186/ar2198.

- [114] C. R. Lee, S. Grad, J. J. Maclean, J. C. Iatridis, and M. Alini. “Effect of mechanical loading on mRNA levels of common endogenous controls in articular chondrocytes and intervertebral disk”. In: *Anal Biochem* 341.2 (2005), pp. 372–5.
- [115] C. R. Lee, J. C. Iatridis, L. Poveda, and M. Alini. “In vitro organ culture of the bovine intervertebral disc: effects of vertebral endplate and potential for mechanobiology studies”. In: *Spine* 31.5 (2006), pp. 515–22.
- [116] D. A. Lee and D. L. Bader. “Compressive strains at physiological frequencies influence the metabolism of chondrocytes seeded in agarose”. In: *J Orthop Res* 15.2 (1997), pp. 181–8.
- [117] J. C. Lotz, O. K. Colliou, J. R. Chin, N. A. Duncan, and E. Liebenberg. “Compression-induced degeneration of the intervertebral disc: an in vivo mouse model and finite-element study”. In: *Spine* 23.23 (1998), pp. 2493–506.
- [118] J. C. Lotz, A. H. Hsieh, A. L. Walsh, E. I. Palmer, and J. R. Chin. “Mechanobiology of the intervertebral disc”. In: *Biochem Soc Trans* 30.Pt 6 (2002), pp. 853–8.
- [119] K. D. Luk, D. K. Ruan, D. H. Chow, and J. C. Leong. “Intervertebral disc autografting in a bipedal animal model”. In: *Clin Orthop Relat Res* 337 (1997), pp. 13–26.
- [120] J. Luo, M. H. Sun, Q. Kang, Y. Peng, W. Jiang, H. H. Luu, Q. Luo, J. Y. Park, Y. Li, R. C. Haydon, and T. C. He. “Gene therapy for bone regeneration”. In: *Curr Gene Ther* 5.2 (2005), pp. 167–79.



- [121] J. J. MacLean, C. R. Lee, M. Alini, and J. C. Iatridis. “The effects of short-term load duration on anabolic and catabolic gene expression in the rat tail intervertebral disc”. In: *J Orthop Res* 23.5 (2005), pp. 1120–7.
- [122] J. J. MacLean, C. R. Lee, S. Grad, K. Ito, M. Alini, and J. C. Iatridis. “Effects of immobilization and dynamic compression on intervertebral disc cell gene expression in vivo”. In: *Spine* 28.10 (2003), pp. 973–81.
- [123] B. A. Maldonado and T. R. Oegema. “Initial characterization of the metabolism of intervertebral disc cells encapsulated in microspheres”. In: *J Orthop Res* 10.5 (1992), pp. 677–90.
- [124] B. Mansson, C. Wenglén, M. Mörgelin, T. Saxne, and D. Heinegård. “Association of chondroadherin with collagen type II”. In: *J Biol Chem* 276.35 (2001), pp. 32883–8. DOI: 10.1074/jbc.M101680200.
- [125] F. Marchand and A. M. Ahmed. “Investigation of the laminate structure of lumbar disc annulus fibrosus”. In: *Spine (Phila Pa 1976)* 15.5 (1990), pp. 402–10.
- [126] A. Maroudas, R. A. Stockwell, A. Nachemson, and J. Urban. “Factors involved in the nutrition of the human lumbar intervertebral disc: cellularity and diffusion of glucose in vitro”. In: *J Anat* 120.Pt 1 (1975), pp. 113–30.
- [127] K. Masuda. “Biological repair of the degenerated intervertebral disc by the injection of growth factors”. In: *Eur Spine J* 17 Suppl 4 (2008), pp. 441–51.
- [128] K. Masuda, Y. Imai, M. Okuma, C. Muehleman, K. Nakagawa, K. Akeda, E. Thonar, G. Andersson, and H. S. An. “Osteogenic protein-1 injection into a

- degenerated disc induces the restoration of disc height and structural changes in the rabbit anular puncture model”. In: *Spine* 31.7 (2006), pp. 742–54.
- [129] Koichi Masuda and Howard S An. “Prevention of disc degeneration with growth factors”. In: *Eur Spine J* 15 Suppl 3 (2006), S422–32. DOI: 10.1007/s00586-006-0149-1.
  - [130] R. L. Mauck, B. A. Byers, X. Yuan, and R. S. Tuan. “Regulation of cartilaginous ECM gene transcription by chondrocytes and MSCs in 3D culture in response to dynamic loading”. In: *Biomech Model Mechanobiol* 6.1-2 (2007), pp. 113–25.
  - [131] H. M. Mayer, K. Wiechert, A. Korge, and I. Qose. “Minimally invasive total disc replacement: surgical technique and preliminary clinical results”. In: *Eur Spine J* 11 Suppl 2 (2002), S124–30.
  - [132] I W McLean and P K Nakane. “Periodate-lysine-paraformaldehyde fixative. A new fixation for immunoelectron microscopy”. In: *J Histochem Cytochem* 22.12 (1974), pp. 1077–83.
  - [133] D. W. McMillan, G. Garbutt, and M. A. Adams. “Effect of sustained loading on the water content of intervertebral discs: implications for disc metabolism”. In: *Ann Rheum Dis* 55.12 (1996), pp. 880–7.
  - [134] D. S. McNally, M. A. Adams, and A. E. Goodship. “Development and validation of a new transducer for intradiscal pressure measurement”. In: *J Biomed Eng* 14.6 (1992), pp. 495–8.
  - [135] J. Melrose, S. Roberts, S. Smith, J. Menage, and P. Ghosh. “Increased nerve and blood vessel ingrowth associated with proteoglycan depletion in an ovine

- anular lesion model of experimental disc degeneration”. In: *Spine* 27.12 (2002), pp. 1278–85.
- [136] J. Melrose, S. Smith, and P. Ghosh. “Differential expression of proteoglycan epitopes by ovine intervertebral disc cells”. In: *J Anat* 197 ( Pt 2) (2000), pp. 189–98.
- [137] J. Melrose, S. M. Smith, R. C. Appleyard, and C. B. Little. “Aggrecan, versican and type VI collagen are components of annular translamellar crossbridges in the intervertebral disc”. In: *Eur Spine J* 17.2 (2008), pp. 314–24.
- [138] J. Melrose, S. M. Smith, E. S. Fuller, A. A. Young, P. J. Roughley, A. Dart, and C. B. Little. “Biglycan and fibromodulin fragmentation correlates with temporal and spatial annular remodelling in experimentally injured ovine intervertebral discs”. In: *Eur Spine J* 16.12 (2007), pp. 2193–205.
- [139] S. K. Mirza. “Point of view: Commentary on the research reports that led to Food and Drug Administration approval of an artificial disc”. In: *Spine* 30.14 (2005), pp. 1561–4.
- [140] K. Miyamoto, K. Masuda, J. G. Kim, N. Inoue, K. Akeda, G. B. Andersson, and H. S. An. “Intradiscal injections of osteogenic protein-1 restore the viscoelastic properties of degenerated intervertebral discs”. In: *Spine J* 6.6 (2006), pp. 692–703.
- [141] H. Mizuno, A. K. Roy, C. A. Vacanti, K. Kojima, M. Ueda, and L. J. Bonassar. “Tissue-engineered composites of anulus fibrosus and nucleus pulposus for intervertebral disc replacement”. In: *Spine* 29.12 (2004), 1290–7; discussion 1297–8–1290–7; discussion 1297–8.

- [142] H. Mizuno, A. K. Roy, V. Zaporozhan, C. A. Vacanti, M. Ueda, and L. J. Bonassar. “Biomechanical and biochemical characterization of composite tissue-engineered intervertebral discs”. In: *Biomaterials* 27.3 (2006), pp. 362–70.
- [143] M. Mizuno, R. Fujisawa, and Y. Kuboki. “Bone chondroadherin promotes attachment of osteoblastic cells to solid-state substrates and shows affinity to collagen”. In: *Calcif Tissue Int* 59.3 (1996), pp. 163–7.
- [144] V. C. Mow, S. C. Kuei, W. M. Lai, and C. G. Armstrong. “Biphasic creep and stress relaxation of articular cartilage in compression? Theory and experiments”. In: *J Biomech Eng* 102.1 (1980), pp. 73–84.
- [145] F. Mwale, K. Masuda, R. Pichika, L. M. Epure, T. Yoshikawa, A. Hemmad, P. J. Roughley, and J. Antoniou. “The efficacy of Link N as a mediator of repair in a rabbit model of intervertebral disc degeneration”. In: *Arthritis Res Ther* 13.4 (2011), R120.
- [146] A. Nachemson, T. Lewin, A. Maroudas, and M. A. Freeman. “In vitro diffusion of dye through the end-plates and the annulus fibrosus of human lumbar intervertebral discs”. In: *Acta Orthop Scand* 41.6 (1970), pp. 589–607.
- [147] M. Nagae, T. Ikeda, Y. Mikami, H. Hase, H. Ozawa, K. Matsuda, H. Sakamoto, Y. Tabata, M. Kawata, and T. Kubo. “Intervertebral disc regeneration using platelet-rich plasma and biodegradable gelatin hydrogel microspheres”. In: *Tissue Eng* 13.1 (2007), pp. 147–58.
- [148] P. J. Neame, Y. Sommarin, R. E. Boynton, and D. Heinegard. “The structure of a 38-kDa leucine-rich protein (chondroadherin) isolated from bovine cartilage”. In: *J Biol Chem* 269.34 (1994), pp. 21547–54.

- [149] K. Nishimura and J. Mochida. “Percutaneous reinsertion of the nucleus pulposus. An experimental study”. In: *Spine* 23.14 (1998), 1531–8; discussion 1539–1531–8; discussion 1539.
- [150] R. P. Nockels. “Dynamic stabilization in the surgical management of painful lumbar spinal disorders”. In: *Spine* 30.16 Suppl (2005), S68–72–S68–72.
- [151] T. Nomura, J. Mochida, M. Okuma, K. Nishimura, and K. Sakabe. “Nucleus pulposus allograft retards intervertebral disc degeneration”. In: *Clin Orthop Relat Res* 389 (2001), pp. 94–101.
- [152] G. D. O’Connell, E. J. Vresilovic, and D. M. Elliott. “Comparison of animals used in disc research to human lumbar disc geometry”. In: *Spine* 32.3 (2007), pp. 328–33.
- [153] Jr. Oegema T. R. “The role of disc cell heterogeneity in determining disc biochemistry: a speculation”. In: *Biochem Soc Trans* 30.Pt 6 (2002), pp. 839–44.
- [154] T. R. Oegema, S. L. Johnson, D. J. Aguiar, and J. W. Ogilvie. “Fibronectin and its fragments increase with degeneration in the human intervertebral disc”. In: *Spine* 25.21 (2000), pp. 2742–7.
- [155] M. Okuma, J. Mochida, K. Nishimura, K. Sakabe, and K. Seiki. “Reinsertion of stimulated nucleus pulposus cells retards intervertebral disc degeneration: an in vitro and in vivo experimental study”. In: *J Orthop Res* 18.6 (2000), pp. 988–97.
- [156] A. van Ooij. “Analysis of porous ingrowth in intervertebral disc prostheses: a nonhuman primate model”. In: *Spine* 28.19 (2003), pp. 2304–2304.

- [157] H. Oshima, H. Ishihara, J. P. Urban, and H. Tsuji. “The use of coccygeal discs to study intervertebral disc metabolism”. In: *J Orthop Res* 11.3 (1993), pp. 332–8.
- [158] G. Paesold, A. G. Nerlich, and N. Boos. “Biological treatment strategies for disc degeneration: potentials and shortcomings”. In: *Eur Spine J* 16.4 (2007), pp. 447–68.
- [159] R. Paul, R. C. Haydon, H. Cheng, A. Ishikawa, N. Nenadovich, W. Jiang, L. Zhou, B. Breyer, T. Feng, P. Gupta, T. C. He, and F. M. Phillips. “Potential use of Sox9 gene therapy for intervertebral degenerative disc disease”. In: *Spine* 28.8 (2003), pp. 755–63.
- [160] C. A. Pezowicz, P. A. Robertson, and N. D. Broom. “Intralamellar relationships within the collagenous architecture of the annulus fibrosus imaged in its fully hydrated state”. In: *J Anat* 207.4 (2005), pp. 299–312.
- [161] C. W. Pfirrmann, A. Metzdorf, M. Zanetti, J. Hodler, and N. Boos. “Magnetic resonance classification of lumbar intervertebral disc degeneration”. In: *Spine* 26.17 (2001), pp. 1873–8.
- [162] F. Postacchini, M. Bellocci, and M. Massobrio. “Morphologic changes in annulus fibrosus during aging. An ultrastructural study in rats”. In: *Spine* 9.6 (1984), pp. 596–603.
- [163] K. Puustjarvi, M. Lammi, H. Helminen, R. Inkinen, and M. Tammi. “Proteoglycans in the intervertebral disc of young dogs following strenuous running exercise”. In: *Connect Tissue Res* 30.3 (1994), pp. 225–40.

- [164] P. P. Raj. “Intervertebral disc: anatomy-physiology-pathophysiology-treatment”. In: *Pain Pract* 8.1 (2008), pp. 18–44.
- [165] S. Rajasekaran, J. N. Babu, R. Arun, B. R. Armstrong, A. P. Shetty, and S. Murugan. “ISSLS prize winner: A study of diffusion in human lumbar discs: a serial magnetic resonance imaging study documenting the influence of the endplate on diffusion in normal and degenerate discs”. In: *Spine* 29.23 (2004), pp. 2654–67.
- [166] F. Ramirez and D. B. Rifkin. “Cell signaling events: a view from the matrix”. In: *Matrix Biol* 22.2 (2003), pp. 101–7.
- [167] F. Rannou, S. Poiraudau, V. Foltz, M. Boiteux, M. Corvol, and M. Revel. “Monolayer anulus fibrosus cell cultures in a mechanically active environment: local culture condition adaptations and cell phenotype study”. In: *J Lab Clin Med* 136.5 (2000), pp. 412–21.
- [168] J. A. Reinecke, P. Wehling, P. Robbins, C. H. Evans, M. Sager, G. Schulze-Allen, and H. Koch. “[In vitro transfer of genes in spinal tissue]”. In: *Z Orthop Ihre Grenzgeb* 135.5 (1997), pp. 412–6.
- [169] D. K. Resnick and W. C. Watters. “Lumbar disc arthroplasty: a critical review”. In: *Clin Neurosurg* 54 (2007), pp. 83–7.
- [170] P. A. Revell, E. Damien, L. Di Silvio, N. Gurav, C. Longinotti, and L. Ambrosio. “Tissue engineered intervertebral disc repair in the pig using injectable polymers”. In: *J Mater Sci Mater Med* 18.2 (2007), pp. 303–8.

- [171] A. T. Reza and S. B. Nicoll. “Hydrostatic pressure differentially regulates outer and inner annulus fibrosus cell matrix production in 3D scaffolds”. In: *Ann Biomed Eng* 36.2 (2008), pp. 204–13.
- [172] P. E. Riches, N. Dhillon, J. Lotz, A. W. Woods, and D. S. McNally. “The internal mechanics of the intervertebral disc under cyclic loading”. In: *J Biomech* 35.9 (2002), pp. 1263–71.
- [173] M. V. Risbud, T. J. Albert, A. Guttapalli, E. J. Vresilovic, A. S. Hillibrand, A. R. Vaccaro, and I. M. Shapiro. “Differentiation of mesenchymal stem cells towards a nucleus pulposus-like phenotype in vitro: implications for cell-based transplantation therapy”. In: *Spine* 29.23 (2004), pp. 2627–32.
- [174] M. V. Risbud, M. W. Izzo, C. S. Adams, W. W. Arnold, A. S. Hillibrand, E. J. Vresilovic, A. R. Vaccaro, T. J. Albert, and I. M. Shapiro. “An organ culture system for the study of the nucleus pulposus: description of the system and evaluation of the cells”. In: *Spine* 28.24 (2003), 2652–8; discussion 2658–9–2652–8; discussion 2658–9.
- [175] N. Roberts, D. Hogg, G. H. Whitehouse, and P. Dangerfield. “Quantitative analysis of diurnal variation in volume and water content of lumbar intervertebral discs”. In: *Clin Anat* 11.1 (1998), pp. 1–8.
- [176] S. Roberts, M. A. Bains, A. Kwan, J. Menage, and S. M. Eisenstein. “Type X collagen in the human intervertebral disc: an indication of repair or remodelling?” In: *Histochem J* 30.2 (1998), pp. 89–95.
- [177] S. Roberts, B. Caterson, J. Menage, E. H. Evans, D. C. Jaffray, and S. M. Eisenstein. “Matrix metalloproteinases and aggrecanase: their role in disorders



- of the human intervertebral disc”. In: *Spine (Phila Pa 1976)* 25.23 (2000), pp. 3005–13.
- [178] S. Roberts, S. M. Eisenstein, J. Menage, E. H. Evans, and I. K. Ashton. “Mechanoreceptors in intervertebral discs. Morphology, distribution, and neuropeptides”. In: *Spine* 20.24 (1995), pp. 2645–51.
- [179] S Roberts, E H Evans, D Kletsas, D C Jaffray, and S M Eisenstein. “Senescence in human intervertebral discs”. In: *Eur Spine J* 15 Suppl 3 (2006), S312–6. DOI: 10.1007/s00586-006-0126-8.
- [180] S. Roberts, H. Evans, J. Trivedi, and J. Menage. “Histology and pathology of the human intervertebral disc”. In: *J Bone Joint Surg Am* 88 Suppl 2 (2006), pp. 10–4.
- [181] S. Roberts, J. Menage, V. Duance, S. Wotton, and S. Ayad. “1991 Volvo Award in basic sciences. Collagen types around the cells of the intervertebral disc and cartilage end plate: an immunolocalization study”. In: *Spine* 16.9 (1991), pp. 1030–8.
- [182] S. Roberts, J. Menage, and S. M. Eisenstein. “The cartilage end-plate and intervertebral disc in scoliosis: calcification and other sequelae”. In: *J Orthop Res* 11.5 (1993), pp. 747–57.
- [183] S. Roberts, J. Menage, S. Sivan, and J. P. Urban. “Bovine explant model of degeneration of the intervertebral disc”. In: *BMC Musculoskelet Disord* 9 (2008), p. 24.

- [184] S. Roberts, J. Menage, and J. P. Urban. “Biochemical and structural properties of the cartilage end-plate and its relation to the intervertebral disc”. In: *Spine* 14.2 (1989), pp. 166–74.
- [185] S Roberts, J P Urban, H Evans, and S M Eisenstein. “Transport properties of the human cartilage endplate in relation to its composition and calcification”. In: *Spine (Phila Pa 1976)* 21.4 (1996), pp. 415–20.
- [186] L Rosenberg. “Chemical basis for the histological use of safranin O in the study of articular cartilage”. In: *J Bone Joint Surg Am* 53.1 (1971), pp. 69–82.
- [187] P. Roughley, C. Hoemann, E. DesRosiers, F. Mwale, J. Antoniou, and M. Alini. “The potential of chitosan-based gels containing intervertebral disc cells for nucleus pulposus supplementation”. In: *Biomaterials* 27.3 (2006), pp. 388–96.
- [188] P. J. Roughley. “Biology of intervertebral disc aging and degeneration: involvement of the extracellular matrix”. In: *Spine* 29.23 (2004), pp. 2691–9.
- [189] P. J. Roughley, M. Alini, and J. Antoniou. “The role of proteoglycans in aging, degeneration and repair of the intervertebral disc”. In: *Biochem Soc Trans* 30.Pt 6 (2002), pp. 869–74.
- [190] P. J. Roughley, R. J. White, G. Cs-Szabo, and J. S. Mort. “Changes with age in the structure of fibromodulin in human articular cartilage”. In: *Osteoarthritis Cartilage* 4.3 (1996), pp. 153–61.
- [191] D. Sakai, J. Mochida, T. Iwashina, A. Hiyama, H. Omi, M. Imai, T. Nakai, K. Ando, and T. Hotta. “Regenerative effects of transplanting mesenchymal

- stem cells embedded in atelocollagen to the degenerated intervertebral disc”. In: *Biomaterials* 27.3 (2006), pp. 335–45.
- [192] D. Sakai, J. Mochida, T. Iwashina, T. Watanabe, T. Nakai, K. Ando, and T. Hotta. “Differentiation of mesenchymal stem cells transplanted to a rabbit degenerative disc model: potential and limitations for stem cell therapy in disc regeneration”. In: *Spine* 30.21 (2005), pp. 2379–87.
- [193] D. Sakai, J. Mochida, Y. Yamamoto, T. Nomura, M. Okuma, K. Nishimura, T. Nakai, K. Ando, and T. Hotta. “Transplantation of mesenchymal stem cells embedded in Atelocollagen gel to the intervertebral disc: a potential therapeutic model for disc degeneration”. In: *Biomaterials* 24.20 (2003), pp. 3531–41.
- [194] J. J. Sarver and D. M. Elliott. “Altered disc mechanics in mice genetically engineered for reduced type I collagen”. In: *Spine* 29.10 (2004), pp. 1094–8.
- [195] M. L. Schollum, P. A. Robertson, and N. D. Broom. “ISSLS prize winner: microstructure and mechanical disruption of the lumbar disc annulus: part I: a microscopic investigation of the translamellar bridging network”. In: *Spine (Phila Pa 1976)* 33.25 (2008), pp. 2702–10.
- [196] C. A. Seguin, R. M. Pilliar, J. A. Madri, and R. A. Kandel. “TNF-alpha induces MMP2 gelatinase activity and MT1-MMP expression in an in vitro model of nucleus pulposus tissue degeneration”. In: *Spine (Phila Pa 1976)* 33.4 (2008), pp. 356–65.
- [197] S. Seki, Y. Asanuma-Abe, K. Masuda, Y. Kawaguchi, K. Asanuma, C. Muehleman, A. Iwai, and T. Kimura. “Effect of small interference RNA (siRNA) for

- ADAMTS5 on intervertebral disc degeneration in the rabbit anular needle-puncture model”. In: *Arthritis Res Ther* 11.6 (2009), R166.
- [198] J. Selinummi, J. Seppala, O. Yli-Harja, and J. A. Puhakka. “Software for quantification of labeled bacteria from digital microscope images by automated image analysis”. In: *Biotechniques* 39.6 (2005), pp. 859–63.
- [199] L. A. Setton and J. Chen. “Cell mechanics and mechanobiology in the intervertebral disc”. In: *Spine* 29.23 (2004), pp. 2710–23.
- [200] L. A. Setton and J. Chen. “Mechanobiology of the intervertebral disc and relevance to disc degeneration”. In: *J Bone Joint Surg Am* 88 Suppl 2 (2006), pp. 52–7.
- [201] Z. Shen, S. Gantcheva, B. Mansson, D. Heinegard, and Y. Sommarin. “Chondroadherin expression changes in skeletal development”. In: *Biochem J* 330 (Pt 1) (1998), pp. 549–57.
- [202] A. H. Siddiqui, M. Z. Rafique, M. N. Ahmad, and M. U. Usman. “Role of magnetic resonance imaging in lumbar spondylosis”. In: *J Coll Physicians Surg Pak* 15.7 (2005), pp. 396–9.
- [203] J. W. Stevens, G. L. Kurriger, A. S. Carter, and J. A. Maynard. “CD44 expression in the developing and growing rat intervertebral disc”. In: *Developmental Dynamics: An Official Publication of the American Association of Anatomists* 219.3 (2000), pp. 381–90.
- [204] I. A. Stokes and J. C. Iatridis. “Mechanical conditions that accelerate intervertebral disc degeneration: overload versus immobilization”. In: *Spine* 29.23 (2004), pp. 2724–32.

- [205] J K Suh, Z Li, and S L Woo. “Dynamic behavior of a biphasic cartilage model under cyclic compressive loading”. In: *J Biomech* 28.4 (1995), pp. 357–64.
- [206] R. Sztrolovics, M. Alini, J. S. Mort, and P. J. Roughley. “Age-related changes in fibromodulin and lumican in human intervertebral discs”. In: *Spine (Phila Pa 1976)* 24.17 (1999), pp. 1765–71.
- [207] R. Sztrolovics, M. Alini, P. J. Roughley, and J. S. Mort. “Aggrecan degradation in human intervertebral disc and articular cartilage”. In: *Biochem J* 326 ( Pt 1) (1997), pp. 235–41.
- [208] T. K. Taylor, J. Melrose, D. Burkhardt, P. Ghosh, L. E. Claes, A. Kettler, and H. J. Wilke. “Spinal biomechanics and aging are major determinants of the proteoglycan metabolism of intervertebral disc cells”. In: *Spine* 25.23 (2000), pp. 3014–20.
- [209] J. P. Thompson, T. R. Oegema, and D. S. Bradford. “Stimulation of mature canine intervertebral disc by growth factors”. In: *Spine* 16.3 (1991), pp. 253–60.
- [210] J. P. Thompson, R. H. Pearce, M. T. Schechter, M. E. Adams, I. K. Tsang, and P. B. Bishop. “Preliminary evaluation of a scheme for grading the gross morphology of the human intervertebral disc”. In: *Spine* 15.5 (1990), pp. 411–5.
- [211] S. Tim Yoon, K. Su Kim, J. Li, J. Soo Park, T. Akamaru, W. A. Elmer, and W. C. Hutton. “The effect of bone morphogenetic protein-2 on rat intervertebral disc cells in vitro”. In: *Spine* 28.16 (2003), pp. 1773–80.

- [212] H. Towbin, T. Staehelin, and J. Gordon. “Electrophoretic transfer of proteins from polyacrylamide gels to nitrocellulose sheets: procedure and some applications”. In: *Proc Natl Acad Sci U S A* 76.9 (1979), pp. 4350–4.
- [213] L. T. Twomey and J. R. Taylor. “Age changes in lumbar vertebrae and intervertebral discs”. In: *Clin Orthop Relat Res* 224 (1987), pp. 97–104.
- [214] F. Unglaub, H. Lorenz, A. Nerlich, W. Richter, and M. W. Kroeber. “[Stimulation of degenerative changes in the intervertebral disc through axial compression. Radiologic, histologic and biomechanical research in an animal model]”. In: *Z Orthop Ihre Grenzgeb* 141.4 (2003), pp. 412–7.
- [215] J. Urban, D. Chan, and G. Schreiber. “A rat serum glycoprotein whose synthesis rate increases greatly during inflammation”. In: *J Biol Chem* 254.21 (1979), pp. 10565–8.
- [216] J. Urban, S. Roberts, and J. Ralphs. “The Nucleus of the Intervertebral Disc from Development to Degeneration”. In: *American Zoologist* 40.1 (2000), pp. 53–61.
- [217] J. P. Urban. “[Role of mechanical constraints in the maintenance and degradation of articular cartilage]”. In: *Rev Prat* 50.16 Suppl (2000), pp. 9–12.
- [218] J. P. Urban. “The chondrocyte: a cell under pressure”. In: *Br J Rheumatol* 33.10 (1994), pp. 901–8.
- [219] J. P. Urban. “The role of the physicochemical environment in determining disc cell behaviour”. In: *Biochem Soc Trans* 30.Pt 6 (2002), pp. 858–64.

- [220] J. P. Urban, S. Holm, A. Maroudas, and A. Nachemson. “Nutrition of the intervertebral disc: effect of fluid flow on solute transport”. In: *Clin Orthop Relat Res* 170 (1982), pp. 296–302.
- [221] J. P. Urban and J. F. McMullin. “Swelling pressure of the lumbar intervertebral discs: influence of age, spinal level, composition, and degeneration”. In: *Spine* 13.2 (1988), pp. 179–87.
- [222] J. P. Urban and S. Roberts. “Degeneration of the intervertebral disc”. In: *Arthritis Res Ther* 5.3 (2003), pp. 120–30.
- [223] J. P. Urban, S. Smith, and J. C. Fairbank. “Nutrition of the intervertebral disc”. In: *Spine* 29.23 (2004), pp. 2700–9.
- [224] M. R. Urban, J. C. Fairbank, S. R. Bibby, and J. P. Urban. “Intervertebral disc composition in neuromuscular scoliosis: changes in cell density and glycosaminoglycan concentration at the curve apex”. In: *Spine* 26.6 (2001), pp. 610–7.
- [225] A. R. Vaccaro and M. G. Fehlings. “The applicability of clinical equipoise and sham surgery in patients with symptomatic lumbar radiculopathy due to a herniated disc: the SPORT trial”. In: *Spine* 32.19 (2007), pp. 2039–40.
- [226] G. Vadala, G. A. Sowa, and J. D. Kang. “Gene therapy for disc degeneration”. In: *Expert Opin Biol Ther* 7.2 (2007), pp. 185–96.
- [227] T. Videman, M. C. Battie, L. E. Gibbons, K. Maravilla, H. Manninen, and J. Kaprio. “Associations between back pain history and lumbar MRI findings”. In: *Spine* 28.6 (2003), pp. 582–8.

- [228] C. J. Wallach, S. Sobajima, Y. Watanabe, J. S. Kim, H. I. Georgescu, P. Robbins, L. G. Gilbertson, and J. D. Kang. “Gene transfer of the catabolic inhibitor TIMP-1 increases measured proteoglycans in cells from degenerated human intervertebral discs”. In: *Spine* 28.20 (2003), pp. 2331–7.
- [229] R. Walmsley. “The development and growth of the intervertebral disc”. In: *Edinburgh Med J* 60.8 (1953), pp. 341–64.
- [230] A. J. Walsh and J. C. Lotz. “Biological response of the intervertebral disc to dynamic loading”. In: *J Biomech* 37.3 (2004), pp. 329–37.
- [231] B. A. Walter, C. L. Korecki, D. Purmessur, P. J. Roughley, A. J. Michalek, and J. C. Iatridis. “Complex loading affects intervertebral disc mechanics and biology”. In: *Osteoarthritis Cartilage* (2011).
- [232] D. L. Wang, S. D. Jiang, and L. Y. Dai. “Biologic response of the intervertebral disc to static and dynamic compression in vitro”. In: *Spine* 32.23 (2007), pp. 2521–8.
- [233] J. C. Wang, J. M. Kabo, P. M. Tsou, L. Halevi, and A. N. Shamie. “The effect of uniform heating on the biomechanical properties of the intervertebral disc in a porcine model”. In: *Spine J* 5.1 (2005), pp. 64–70.
- [234] J. Y. Wang, A. E. Baer, V. B. Kraus, and L. A. Setton. “Intervertebral disc cells exhibit differences in gene expression in alginate and monolayer culture”. In: *Spine* 26.16 (2001), 1747–51; discussion 1752–1747–51; discussion 1752.
- [235] P. Wehling, K. P. Schulitz, P. D. Robbins, C. H. Evans, and J. A. Reinecke. “Transfer of genes to chondrocytic cells of the lumbar spine. Proposal for a



- treatment strategy of spinal disorders by local gene therapy”. In: *Spine* 22.10 (1997), pp. 1092–7.
- [236] A. A. White and M. M. Panjabi. *Clinical Biomechanics of the Spine*. JB Lippincott Company, 1990.
  - [237] H. Wilke, P. Neef, B. Hinz, H. Seidel, and L. Claes. “Intradiscal pressure together with anthropometric data—a data set for the validation of models”. In: *Clin Biomech (Bristol, Avon)* 16 Suppl 1 (2001), S111–26–S111–26.
  - [238] H. J. Wilke, P. Neef, M. Caimi, T. Hoogland, and L. E. Claes. “New in vivo measurements of pressures in the intervertebral disc in daily life”. In: *Spine (Phila Pa 1976)* 24.8 (1999), pp. 755–62.
  - [239] H. J. Wilke, A. Rohlmann, S. Neller, F. Graichen, L. Claes, and G. Bergmann. “ISSLS prize winner: A novel approach to determine trunk muscle forces during flexion and extension: a comparison of data from an in vitro experiment and in vivo measurements”. In: *Spine* 28.23 (2003), pp. 2585–93.
  - [240] H. J. Wilke, F. Rohlmann, C. Neidlinger-Wilke, K. Werner, L. Claes, and A. Kettler. “Validity and interobserver agreement of a new radiographic grading system for intervertebral disc degeneration: Part I. Lumbar spine”. In: *Eur Spine J* 15.6 (2006), pp. 720–30.
  - [241] H. J. Wilke, H. Schmidt, K. Werner, W. Schmolz, and J. Drumm. “Biomechanical evaluation of a new total posterior-element replacement system”. In: *Spine* 31.24 (2006), 2790–6; discussion 2797–2790–6; discussion 2797.
  - [242] M. A. Wiseman, H. L. Birch, M. Akmal, and A. E. Goodship. “Segmental variation in the in vitro cell metabolism of nucleus pulposus cells isolated

- from a series of bovine caudal intervertebral discs”. In: *Spine* 30.5 (2005), pp. 505–11.
- [243] S. H. Yang, P. Q. Chen, Y. F. Chen, and F. H. Lin. “An in-vitro study on regeneration of human nucleus pulposus by using gelatin/chondroitin-6-sulfate/hyaluronan tri-copolymer scaffold”. In: *Artif Organs* 29.10 (2005), pp. 806–14.
- [244] J. Yu, U. Tirlapur, J. Fairbank, P. Handford, S. Roberts, C. P. Winlove, Z. Cui, and J. Urban. “Microfibrils, elastin fibres and collagen fibres in the human intervertebral disc and bovine tail disc”. In: *J Anat* 210.4 (2007), pp. 460–71.
- [245] J. Yu, P. C. Winlove, S. Roberts, and J. P. Urban. “Elastic fibre organization in the intervertebral discs of the bovine tail”. In: *J Anat* 201.6 (2002), pp. 465–75.
- [246] Y. Zhang, H. S. An, S. Song, M. Toofanfard, K. Masuda, G. B. Andersson, and E. J. Thonar. “Growth factor osteogenic protein-1: differing effects on cells from three distinct zones in the bovine intervertebral disc”. In: *Am J Phys Med Rehabil* 83.7 (2004), pp. 515–21.
- [247] Y. Zhang, H. S. An, E. J. Thonar, S. Chubinskaya, T. C. He, and F. M. Phillips. “Comparative effects of bone morphogenetic proteins and sox9 over-expression on extracellular matrix metabolism of bovine nucleus pulposus cells”. In: *Spine* 31.19 (2006), pp. 2173–9.
- [248] Y. G. Zhang, X. Guo, P. Xu, L. L. Kang, and J. Li. “Bone mesenchymal stem cells transplanted into rabbit intervertebral discs can increase proteoglycans”. In: *Clin Orthop Relat Res* 430 (2005), pp. 219–26.